Fahrtbericht SO-147 Peru-Auftrieb

BMBF-Forschungsvorhaben
03G0147A

Cruise Report SO-147 Peru-Upwelling

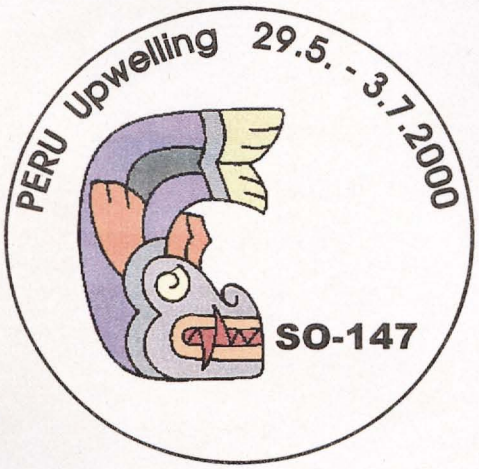

Valparaiso 29.05.2000 -
Callao 03.07.2000

BGR Bundesanstalt für Geowissenschaften und Rohstoffe

Bundesanstalt für Geowissenschaften und Rohstoffe
Federal Institute for Geoscience and Natural Resources

BGR
Hannover

SO 147
PERU-Auftrieb

BMBF-Forschungsvorhaben 03G0147A

Fahrtbericht

Projektleiter: Dr. H. R. Kudraß

Auftraggeber: Bundesministerium für Bildung und Forschung (BMBF)

Archiv Nr.: 0120607
Tagebuch Nr.: 11 672/00
Dezember 2000, BGR Hannover

Contents

Zusammenfassung

Kudrass, H.R.

Das Projekt Peru-Auftrieb besteht aus Teilprojekten mehrerer mariner Forschungsgruppen (BGR/Hannover, Geomar/Kiel, IfG/Mainz, INI/Rostock, ICBM/Oldenburg, MPI Mikrobiologie/Bremen), die über vielfältige methodische Ansätze eng miteinander verbunden sind. Die multidisziplinären Untersuchungen der einzelnen Teilprojekte ergänzen sich so, dass ein umfassendes Bild der Variabilität des Auftriebs vor Peru in Zeit und Raum erarbeitet werden kann. Der Schwerpunkt der gemeinsamen Untersuchungen zielt darauf ab, die bakteriell gesteuerten geochemischen Prozesse in der anoxisch/suboxischen Wasser-Sediment-Grenzschicht zu verstehen, den Abbau und die Veränderung der organischen Substanzen zu untersuchen, die daraus resultierenden Flüsse von Methan, Schwefel und Phosphat unter in-situ Bedingungen und Langzeitexperimenten zu erfassen.
Die Kenntnis der rezenten Auftriebsprozesse und deren Auswirkungen auf das Sediment, wird es in einem zweiten Schritt erlauben, die zeitliche und räumliche Variabilität des Auftriebs seit dem letzten Hochglazial paläoklimatisch zu deuten. Dabei soll der multidisziplinäre Ansatz mit seismischen, sedimentologischen, geochemischen und mikropaläontologisch stratigraphischen Methoden dazu dienen, eine möglichst hoch aufgelöste Zeitreihe der Akkumulationsmuster, des terrigenen Eintrages, der Fixierung von C_{org}, Opal, Karbonat und Phosphat im Sediment zu erhalten, um letztlich zu rekonstruieren, wie der Auftrieb vor Peru auf global klimatische Veränderungen reagiert und diese durch Rückkopplung selbst beeinflußt hat (Abb.1).

Folgende Detailziele ergeben sich aus diesem Ansatz:

- Hochauflösende Entschlüsselung der Geschichte des Klimaphänomens „El Nino" während des Holozäns und des Hochglazials
- Bedingungen der Phosphoritentstehung, und ihre Verbreitung im Auftriebsgebiet vor Peru
- Rolle der vor Peru auftretenden Schwefelbakterien (Thioploca, Beggiatoa), im Kohlenstoff-, Stickstoff- und Schwefelkreislauf.

Die Fahrt begann am 29. Mai 2000 im Hafen von Valparaiso/Chile, wo SONNE nach der Werftüberholung aufgerüstet wurde. Nach einer sechstägigen Überfahrt mit teilweiser bathymetrischer Vermessung des nördlichen Chile-Tiefsee-Grabens und dem gescheiterten Versuch ein verlorengegangenes Side-Scan Sonar zu bergen wurde am 04.Juni 2000 Callao erreicht. Nach der Einschiffung der beiden peruanischen Gastwissenschaftler begannen die vielfältigen Untersuchungen im Arbeitsgebiet am 5. Juni und endeten am 1. Juli 2000.

Schematisches Phosphorbudget

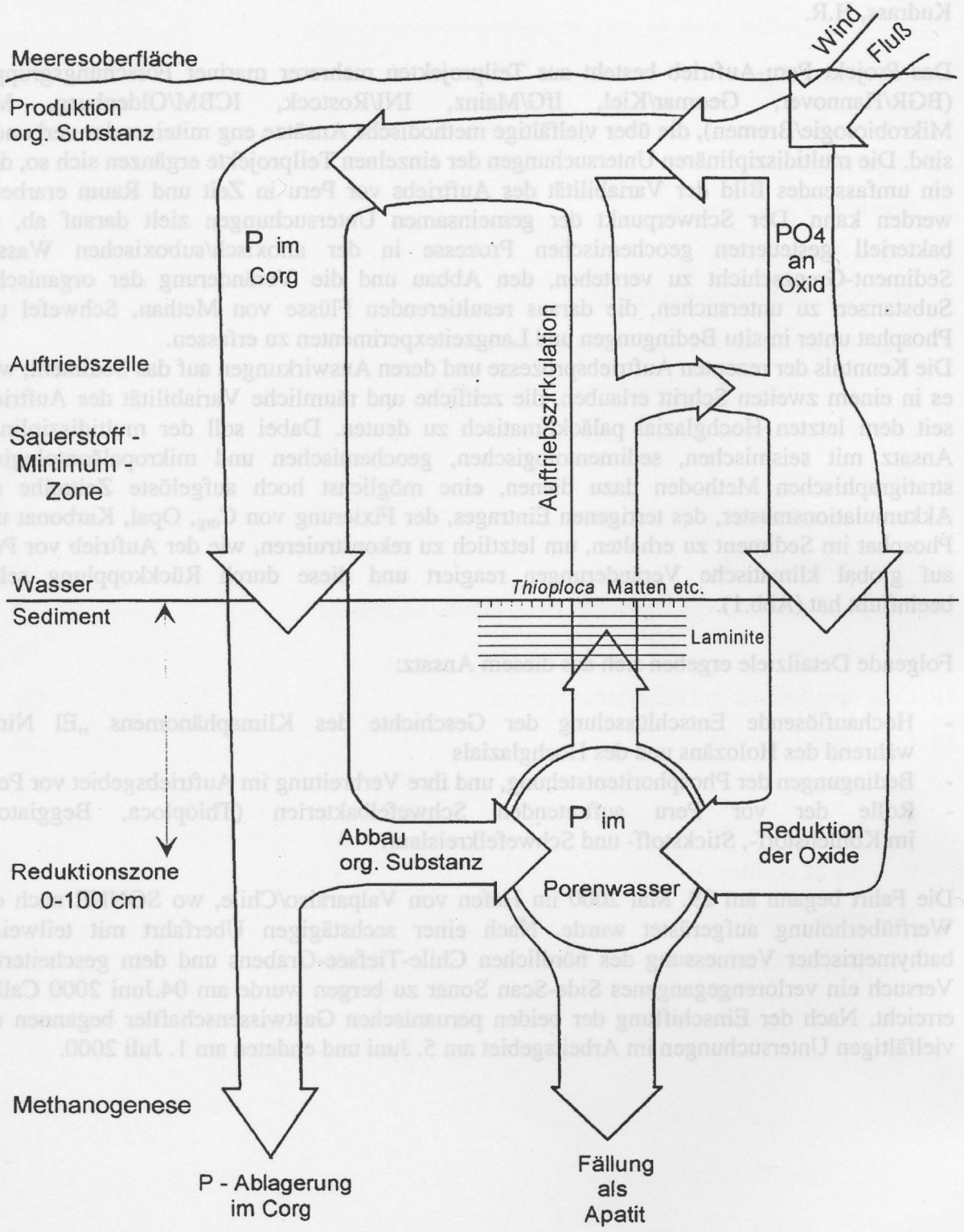

Abb. 1: Schematisches Phosphorbudget in Auftriebsregionen: Es gibt die Beziehungen zwischen terrigenem P-Eintrag (Wind/Flüsse), Nutzung durch die marine Lebewelt, Einbettung im Sediment und diagenetische Remobilisierung wieder.

Dabei wurden folgende Methoden und Geräte der Vermessung und Probenahme eingesetzt:
- bathymetrisches Vermessungssystem Hydrosweep
- hochauflösende Sedimentecholotsysteme SEL-96, SES-2000 (INI/Rostock)
- seilgeführte Kernnahme-Geräte (Kolbenlot, Kastenlot der BGR)
- Oberflächenbeprobung mit Multicorer (GEOMAR), Kastengreifer (BGR)
- Video-kontrollierter Hydraulikgreifer,
- Fernseh/Foto-Schlitten
- Multisonde (Leitfähigkeit, Temperatur, Dichte, Sauerstoff) und Wasserschöpfer
-Multisensor-Core-Logger (BGR)
-Spektrometer (IfG/Mainz)
-Porenwasserpresse und Ionenchromatograph (BGR)
-Porenwasserpresse und Spektrophotometer (ICBM)
-Sauerstoff-, pH- und Redox-Mikrosensoren (MPI)

Insgesamt wurden 6000 km flachseismische Profile mit den beiden im Hydrographenschacht eingebauten Sedimentecholoten SEL und SES vermessen. Die dabei gleichzeitig laufende bathymetrische Fächerlot-Vermessung mit Differential GPS Navigation resultierte nur in einem kleinen Gebiet in einer flächendeckenden Dichte, aber auch die einzelnen Tiefenprofile werden die vorhandenen groben Tiefenkarten des oberen Kontinentalhanges und Schelfs deutlich verbessern. Die sehr hoch auflösenden seismischen Profile gaben beste Hinweise für geeignete Beprobungspunkte, vor allem um möglichst ungestörte Sequenzen für die paläoklimatische Analysen zu gewinnen.

Auf 143 Stationen wurden Sedimentproben mit dem Multicorer, dem Kolbenlot und dem Kastenlot gewonnen. Der längste Kolbenlotkern ist fast 19 m lang Die Probennahme wurde durch sechs Photoschlittenprofile in verschiedenen Wassertiefen ergänzt. Mit sieben CTD Profilen wurden die hydrographische Bedingungen erfaßt.

Alle gewonnen Kerne wurden an Bord mit dem Multi-Sensor-Core-Logger und spektralanalytisch vermessen. Fast 700 Proben von Porenwasser, vor allem aus den Multicorern, wurden in der Kühlkammer gepreßt und sofort mit dem Ionenchromatographen und dem Spektrophotometer anaylsiert. Die mikrobiologischen Proben wurden teils konserviert und teils verschiedenen Experimenten unterworfen.

Darüber hinaus wurden zwei Experimentiertürme geborgen, die vor 8 Jahren mit zahlreichen Karbonatproben vor Peru ausgesetzt wurden. Das Probenmaterial wurde konserviert und soll Aufschluss über frühdiagenetische Veränderungen bei der Phosphoritbildung geben.

Die hohe organische Produktion in der Auftriebszelle und deren absinkende Abfallprodukte verbrauchen den Sauerstoff in den unteren Wasserstockwerken. Unterhalb des produktiven, 16-20 ° C warmen Oberflächenwassers gehen an einer Sprungschicht bei etwa 30 m Wassertiefe die Sauerstoffgehalte auf unter 0,5 mg/l zurück. Diese Sauerstoff-Minimum-Zone dehnt sich bis zu Wassertiefen von ca. 600 m aus.

Nach der Strukturanalyse ist der Schelf und der obere Kontinentalhang vor Chimbote prinzipiell von dem Rest des Arbeitsgebietes unterschieden. Eine fast 100 km breite Schelfplattform, die aus leicht verfalteten und gekappten, vermutlich tertiären terrigenen Flachwassersedimenten mit Sand-Ton-Wechsellagerungen besteht, bricht an einem markanten Schelfknick bei rund 200 m zu einem steilen Kontinentalhang ab. Im Küstensaum lagert in Wassertiefen von 165 m bis 115 m eine übereinander gestapelte Abfolge von Deltasequenzen diskordant über dem gefalteten „Basement". Eine cm- bis dm-dicke polymikte

Phosphoritkruste mit vielen Walknochen, großen Haifischzähnen, gut gerundeten Geröllen und Glaukonitsand überdeckt die Diskordanzfläche auf dem äußeren Schelf. Speziell die großen Haifischzähne deuten auf ein hohes Alter hin, sie können aber auch aus dem unterlagernden Sedimenten aufgearbeitet sein.

Im südlich anschließendem Arbeitsgebiet bis zur Halbinsel von Pisco neigt sich ein schmaler Schelf ohne deutlich erkennbare Schelfkante langsam in den oberen Kontinentalhang. Bis auf einige aufragende Inseln stehen hier jungquartäre Sedimente in fast kontinuierlichen Lagen an. Der lagige Aufbau ist jedoch von einer Vielzahl von Erosionsdiskordanzen gegliedert. Eine kontinuierliche vermutlich holozäne Abfolge ist nur in Wassertiefen zwischen 100 und 400 m zu erwarten. In größeren Wassertiefen bestimmen vom peruanischen Unterstrom gebildete Mudwaves die Ablagerung, in kleineren Wassertiefen fehlen die jüngsten Sedimente. Ausnahmen bilden einige Halbinseln, in deren nördlichen Strömungsschatten direkt unter Küste 10-20 m mächtige holozäne laminierte und feingeschichtete Flachwassersedimente vermessen und beprobt worden sind. Eine weitere Ausnahme bildet eine über 25 m mächtige Schlicklinse, die einer Schelfuntiefen nördlich vorgelagert ist und in der eine von drei Diskordanzen unterbrochene 19 m lange Abfolge von feingeschichteten Diatomeenschlämmen gekernt wurde.

Generell bestehen die Sedimente auf dem äußeren Schelf aus Corg-reichen, feingeschichteten Diatomeenschlämmen, deren Lamination wahrscheinlich durch eine Kombination von variabler, auftriebsgesteuerter Diatomeenproduktion und lateraler Verlagerung im südwärts gerichteten Unterstrom entstanden ist.
Die Reflexionsspektren des Sediments lassen sich aus der Mischung von drei Frequenzbanden erklären, die der organischen Substanz (vom Chlorophyll abstammende Phäopigmente) und terrigenen Komponenten zugeordnet werden. Die hochfrequenten Variationen ermöglichen eine vorläufige Korrelation der langen Kerne. Damit hat sich diese neue Methode zur schnellen detailierten Kernanalyse bestens bewährt.

Die Meeresbodenoberfläche unter der oberen Sauerstoffminimum-Zone ist von auffällig weißen, cm-dick verfiltzten Matten von filamentösen Schwefelbakterien der Gattung *Thioploca* und *Beggiatoa* bedeckt, wobei in 150 m Wassertiefe die größte, bakterielle Biomasse nachgewiesen wurde. *Thioploca* Filamente reichen bis 28 cm unter die Sedimentoberfläche. Am oberen Ende der Sauerstoffmimimumzone werden ehemals flächendeckenden Bakterienmatten streckenweise erodiert und als leicht transportierbare Rollen vom Gezeitenstrom verlagert.
Nach den geochemischen Untersuchungen am Porenwasser nehmen in den meisten Kernen die Sulfatgehalte mit zunehmender Kernteufe ab, während die Phosphatgehalte direkt an der Oberfläche den geringen Meerwassergehalten bei 0,3 entsprechen und nach unten bis zu 7 mg/l ansteigen.

Abstract

Kudrass, H.R.

The SONNE expedition of the SO 147 project "PERU UPWELLING" was performed between the 29th of May and the 3rd of July 2000. The cruise started in Valparaiso/Chile with a bathymetric survey of the Chile deep-sea trench and ended in the harbour of Callao/Peru. For almost four weeks seismic profiling, photographic survey, and sampling concentrated on the shelf and upper continental slope in three areas off central Peru between Chimbote and Pisco.

We used two high-resolution sediment echosounders to investigate the architecture of the surface sediments. Along 6000 km-long profiles the linear echosounder SEL-96 was run with 5 kHz. The new parametric echosounder SES-2000 successfully operated with a 10 kHz frequency. It achieved a penetration of up to 60 m with a vertical resolution of 6 to 12 cm. Reflection data of the two systems were recorded for later processing. On board we used the colour prints of both systems to choose appropriate sampling positions. At 143 sites the hydraulic grab sampler, the multicorer, the box corer, the gravity corer, and the piston corer were employed. At 35 coring stations we recovered an accumulated length of 155 m. In addition, we surveyed the sea floor along 10 profiles with the television and the stereographic colour camera. The CTD sonde was used seven times to determine the hydrographic parameters and to sample specific water layers.
The high productivity of the upwelling and the rich flux of settling dead organic matter from the oxygenated 30 m-thick surface water cause an oxygen minimum zone which extends up to 600 m water depth. However, at several locations near the shelf edge we observed in the center of the oxygen minimum zone jelly fish, many crabs and fishes indicating a probably turbulent mixture of oxygen-rich surface waters.

Based on the submarine morphology, the survey area consists of two types. In the northern area off Chimbote a 100 km-broad rather deep shelf with about 130 m water depth extends right to the shelf break. This shelf is formed by numerous sandy outcrops of probably Tertiary age which are partly covered by a discontinuous layer of fine muddy sand. At that shelf the hydraulic television guided grab sampler mostly recovered massive dm-thick phosphoritic crusts. Especially, erosional surfaces are covered by this crust consisting of a polymict breccia consisting of whale bones, large shark teeth, phosphoritic rubble and, occasionally, well rounded igneous rock pebbles. The components are partly cemented by mm-thick layers of black shiny phosphorite which sometimes covers serpulid worm tubes and mollusc shells. Dark green glauconitic sand is also often encrusted. The large shark teeth are certainly of Tertiary age and may be residual components from the underlying sediment.

The shelf of the central ad southern areas is comparatively narrow. It is only some 10 km wide and slowly bends into the upper continental slope. At the transition between the two shelf types a stacked sequences of three deltaic sequences lying between 160 m and 125 m water depths forms the inner shelf. In the transition zone, small synsedimentary normal faults dissect the Late Pleistocene sediments of the outer shelf and upper slope. Apart from some isolated basement highs and some islands the shelf and upper slope is covered by a well layered sequence. Close inspection indicates, however, numerous small internal erosional discordances, even in the centre of the Holocene deposition between 100 m and 400 m. In deeper water mud waves have formed under the influence of the Peruvian undercurrent, in more shallow water the Holocene sediments are missing. Only in some sheltered sections near headlands and around the islands at the outer shelf west off Callao a thick probably Holocene sequence is deposited. In one depocenter a 19 m-long sequence of finely laminated

diatomaceous ooze was recovered. Similar sequences with distinct terrigenous clay-silt-layers at the top and base of 10 m-long cores were deposited at a few places of the sheltered inner shelf.

Generally the sediments of the outer shelf consist of organic rich, finely laminated diatomaceous ooze. The lamination seems to be caused by a combination of the changing productivity of variable upwelling and changing intensity of the undercurrent. The onboard mm-spaced reflectance measurements of the cores identify several end members of the absorption band, which could be used for a first correlation of cores.

The sea floor under the oxgen minimum zone is widely covered by white, cm-thick filaments of the sulfur bacteria *Beggiatoa* and *Thioploca*. The highest density of the bacteria was observed at about 150 m water depth probably corresponding to the highest recent sedimentation rate. *Thioploca* filaments extend up to 28 cm into the sediments. In shallower water depth some of the microbial mats were eroded and transported as rolls by currents.

The sulfur bacteria profoundly change the porewater chemistry in the surface sediments. More than 700 pore water samples have been collected under cold-room conditions and were immediately analysed in an ion-chromatograph. In most cores sulphate concentration decreases with depth in core while the sulphide concentration increases. Concentrations of chloride and bromide continually decrease in some cores whereas phosphate concentrations generally increase with depth.

1. Objectives

Kudrass, H.R.

The PERU UPWELLING project (PERU AUFTRIEB) consists of six interfaced subprojects which are supported and carried out by six partners (BGR/Hannover, GEOMAR/Kiel, IfG/Mainz, ICBM/Oldenburg, MPI Mikrobiologie/Bremen, INI/Rostock). The combined multidisciplinary approach aims to establish a comprehensive model of the microbiological, sedimentary, and geochemical processes forming the sediments of the high-productivity zone of the Peru upwelling.

The joint investigations focussed on the bacterial controlled geochemical processes at the oxic/anoxic water-sediment-interface, on the early diagenetic modification of the organic material and on the fluxes of methane, sulphur, and phosphor. The understanding of the presently active processes and the resulting sedimentary products will be used to interpret the variations of the sedimentary upwelling record during the Last Glacial and the Holocene. Especially, the El-Nino variability should be traced in different time intervals using seismic, sedimentological, geochemical and micropaleontological methods. The terrigenous input related to extreme La-Nina conditions will be used to correlate the marine record with the continental climatic variation.

Based on these overall objectives, the project is focussed on three targets:

- establish a high-resolution record of the paleoceanographic variations of the upwelling and related continental run off for the last Glacial and the Holocene,
- define the conditions of diagenetic formation of phosphorit, and
- determine the influence of the sulphur bacteria on the interface flux of sulphur, nitrogen and carbon.

2. Narrative Cruise Report

Kudrass, H.R.

The SO 147 cruise started at the 29 of May 2000 in the harbour of Valparaiso / Chile. During the first two days four containers of equipment were loaded onboard. Installation of the scientific laboratories was continuing when RV SONNE left the harbour at the 30 of May at 1 pm. The ship sailed northwest and after crossing the former CONDOR-area (SONNE-cruise) and reaching the deep-sea trench a long northward 810 nm-long bathymetric profile was mapped. This swath mapping was interrupted by a search for a lost Side Scan Sonar off the Mejillones Peninsula in 3500 m water depth (23° 21,3´ S ; 70° 56,5´W). Unfortunately we could not relocate the instrument and the attached 4400 m wire. After a 6 hour-long visual inspection of the most prospective profile with the TV camera of the hydraulic grab we abandoned the search and continued the bathymetric profiling of the northern Chile trench. During this survey and the following transit to Peru the installation of the laboratories was finished and in several meetings the scientific background of the project and the distribution policy of data between the individual subprojects were discussed.

At the 4 of June at 5 pm the ship reached the harbour of Callao and at the following day our Chilean counterparts and the rest of the scientific crew came onboard. In addition, a photographer and a scientist from BGR who had taken numerous shots from the SONNE left the ship. The photographs will be processed and compiled to allow a virtual access to the

vessel on the world-wide web. With completion of the crew SONNE left the harbour at the same day and reached some hours later the survey area at the inner shelf.
For next six weeks we concentrated our investigations in three areas. We started in the central region north of Callao. During the transit from Chile two sediment echosounders of the University of Rostock had been installed in the central moon pool and before arrival at Callao had become operational. These two systems delivered records with the same penetration of the uppermost sediment cover, but with a higher lateral resolution than the hull-mounted PARASOUND. As the PARASOUND and the Rostock systems interfered to some degree, we decided to run the Rostock sediment-echosounders only.
In general, the day-light time was dedicated to sample the sediments. Especially the heavy sampling gear, like the TV-controlled hydraulic grab, the piston and gravity corer were preferentially employed during the 6 am and 8 pm. Sediment-echosounder profiling and long profiles with the photosledge were mainly performed during night time. However, quite often this principle had to be abandoned for an optimal use of ship´s time. The use of sediment sampling gear was also restricted by the speed of the laboratories to handle the incoming material, which generally had to be processed within hours after the recovery. Before sampling or visual inspection the area was explored with the high-resolution seismic system yielding very valuable detailed information on sampling targets.

Sampling of sediment was done for various purposes, multicorer and box spade corer were used for surface sediments, longer sequences were obtained by gravity corer or the piston corer. Consolidated or very sandy sediments were recovered by the hydraulic grab. Occasionally the CTD sonde was employed to measure the oceanographic conditions and to collect water samples with the rosette sampler. These data were needed for correction of the swath echosounder HYDROSWEEP.

Seismic profiling and sampling continued in the central area north of Callao until the 10 of June and then the center of activity moved northward 10°45´ N. With some long seismic profiles we did a reconnaissance survey of the broad shelf off Chimbote. Sampling in that area was mainly aimed to recover phosphoritic crusts from the wide-spread discordance and datable sediments from the stacked deltaic sequences of the inner shelf. In addition, some longer cores we sampled to document the paleoceanographic variations at the steep upper continental slope.

At the end of the profiling and sampling survey we recovered within two hours a set of carbonate samples and rocks from 150 m water depth, which have been part of a long-term exposure experiment. The set consisting of a large 1-m high plastic tube with attached samples and a 300-m long rope was caught by a small dragon anchor attached by a 5-m rope to the hydraulic grab. With the aid of the television camera installed in the grab the search anchor was dragged at the surface sediments. Traces of the rope in the surface sediments and additional strain on the wire of the TV grab indicated that the anchor became hooked to the rope. Originally, five experimental sets had been lowered into the oxygen minimum zone and left at the sea floor during the cruise SO 79 in 1992. The first set which was lowered in the muddy sequence north of Callao but could not be relocated at the present cruise. When passing through the central area at the 22 of June we used the successfully employed salvage technique on the second experimental set exposed in the muddy sequence and recovered it within a short period of two hours by slow TV guided bottom profiling.

After the successful recovery of this long-term experimental set and a final photographic survey of the oxygen minimum zone from 100 m to 155 m water depths we left the central survey area and started profiling and sampling of the southern area off Pisco at the 27 of June.

Here we employed the same set of sampling devices as in the central area. Our greatest success was the recovery of a 19-m long piston corer with Late Pleistocene and Holocene laminated sediments from a local depocenter of the central shelf (KL 106). In the southern area we also employed a set of box corers at close distance to recover friable phosphorites in the main depositional center of the outer shelf.

The final activity of the cruise switched back to the central area off Callao, when two German journalists joined the ship at the anchorage of Callao for a two-day visit at the 25 and 26 of June. We completed our bathymetric survey, the profiling and sampling programme in the central area at the 1 of July and reached the harbour of Callao at the 7 pm. Demobilisation of the laboratories and packing, unloading and shipping of equipment and samples continued until the very end of the charter period at the 3rd of July 2000.

3. Cruise Participants

Lückge, A.

SONNE Cruise SO 147 was planned, coordinated and led by the Bundesanstalt für Geowissenschaften und Rohstoffe (BGR, Hannover), in cooperation with GEOMAR (Kiel), the Institut für Chemie und Biologie des Meeres (ICBM, Universität Oldenburg), the Max-Planck-Institut für marine Mikrobiologie (MPI, Bremen), the Institut für Geowissenschaften (Universität Mainz), Institut für Nachrichtentechnik und Informationselektronik (Universität Rostock) and the Instituto Geologico, Minero y Metalurgico (INGEMMET, Lima). The shipboard scientific party of this cruise included 23 scientists and technicians from Germany and two scientists from Peru (INGEMMET, Lima).

Addresses and E-mail of Shipboard Scientific Participants:

Bundesanstalt für Geowissenschaften und Rohstoffe
Stilleweg 2
30655 Hannover

Dr. KUDRASS, Hermann	kudrass@bgr.de
Dr. WIEDICKE-HOMBACH, Michael	michael.wiedicke@bgr.de
Dr. LÜCKGE, Andreas	a.lueckge@bgr.de
Dr. REINHARDT, Lutz	l.reinhardt@bgr.de
Dr. STRASSBURG, Silke	s.strassburg@bgr.de
BRUNS, Angelika	angelika.bruns@bgr.de
GOERGENS, Rainer	r.goergens@bgr.de
HARAZIM; Bodo	harazim@bgr.de
KOCH, Robert	r.koch@bgr.de
STEINMANN, Dieter	d.steinmann@bgr.de

GEOMAR, Forschungszentrum für marine Geowissenschaften
Wischhof 1 - 3
24148 Kiel

Prof. Dr. DULLO, Christian	cdullo@geomar.de
Dr. BIEBOW, Nicole	nbiebow@geomar.de
Dipl. Geol. WOLF, Anja	awolf@geomar.de

Max-Planck-Institut für marine Mikrobiologie
Celsiusstraße 1
28359 Bremen

Dipl. Geol. KALLMEYER, Jens	jkallmey@mpi-bremen.de
Dipl. Biol. RIECHMANN; Daniela	driechma@mpi-bremen.de
Dipl. Biol. WIERINGA, Elze	ewiering@mpi-bremen.de
KLOCKGETHER, Gabriele	gklockge@mpi-bremen.de

Universität Mainz
Institut für Geowissenschaften
Becherweg 21
35099 Mainz

Dr. REIN, Bert	brein@mail.uni-mainz.de
Dipl. Geol. SCHABER, Katja	Schak021@mail.uni-mainz.de

Universität Oldenburg
Institut für Chemie und Biologie des Meeres
Postfach 2503
26111 Oldenburg

Dr. SCHNETGER, Bernhard	b.schnetger@icbm.de
Dr. DELLWIG, Olaf	olaf.dellwig@icbm.de

Universität Rostock
Institut für Nachrichtentechnik und Informationselektronik
Richard Wagner Straße 31
18119 Rostock

Prof. Dr. WENDT, Gert	gert.wendt@ntie.uni-rostock.de
Dipl. Ing. WUNDERLICH, Jens	jw@jwunder.de

INGEMMET
Instituto Geologico, Minero y Metalurgico
Avenida Canada 1470 San Borja
Lima , Peru

Ing. ZAVALA, Bilberto	bzavala@ingemmet.gob.pe
Ing. VALENZUELA, Germán	valen@ingemmet.gob.pe

Officers and Crew R.V.SONNE

The Officers and Crew of RV SONNE consisted of 30 representatives of Reederei Forschung (RF), of which 2 electronic engineers, 2 systems operators and one fitter were only responsible for scientific tasks.

Andresen, Hartmut	Captain
Bendin, Axel	Chief Mate
Löffler, Jörn	Second Chief Mate
Köthe, Wolfgang	Radio Officer
Boldt, Wieland	Ship's Doctor
Neumann, Peter	Chief Engineer
Guzman, Werner	Second Engineer
Grund, Helmut	Second Engineer
Konrath, Rolf	Electrician
Hofmann, Hilmar	Chief Electronics Technician (WTD)
Vöhrs, Helmut	Electronics Technician (WTD)
Klein, Andreas	Systems Operator (WTD)
Stammer, Kurt	Systems Operator (WTD)
Schymatzek, Peter	Fitter
Teichert, Klaus	Motor Assistant
Isbrecht, Frank	Motor Assistant
v. Arronet, Johannes	Motor Assistant
Blohm, Volker	Motor Assistant
Tiemann, Frank	Chief Cook
Braatz, Willy	Second Cook
Bronn, Johann	Chief Steward
Wege, Andreas	Steward
Eller, Peter	Steward
Mischker, Joachim	Boatswain
Bierstedt, Torsten	Seaman
Kaiser, Reiner	Seaman
Mucke, Peter	Seaman
Reichmacher, Wolfgang	Seaman
Ventz, Günter	Seaman

WTD= Wissenschaftlicher-Technischer Dienst (Scientific-Technical Services of RF).

4. SES / SEL Sedimentechosounder

Wendt, G., Wunderlich, J.

Echosounders for acoustic subbottom profiling generate sound pulses by electrical transducers. The pulses are sent to the sea bottom. Sea bottom and sediment layers reflect the sound waves. These reflections are received by the echosounder device and an echoprint is calculated.

The sound pulse can be generated by two methods, linear or non-linear (parametric) acoustics. Parametric echosounders transmit two signals of slightly different high frequencies at high sound pressures (primary frequencies f_1 and f_2). Because of non-linearities in the sound propagation at high pressures, both signals interact and produce a new lower frequency. As the signal with the difference frequency ($f_2 - f_1$, secondary frequency) is lower, its penetration in the sediments is increased. The primary frequencies are also used for exact determination of water depth even in low-reflectivity soft sediments.

Parametric systems have a small beam width in spite of small transducer dimensions independent of the difference frequency. The beam width only depends on the primary frequency related to the transducer aperture, even for the secondary frequency. There are no significant side lobes and a constant directivity for different secondary frequencies is

achieved. Therefore the insonified area is the same one for different frequencies. The extremely high bandwidth of parametric systems allows to generate very short sound pulses which result in a high vertical resolution.
But there are also some disadvantages using non-linear acoustics. High sound pressures and therefore high transmitting power are required because of significant loss in the signal amplitude for the difference frequency. In deep water the linear system has a better performance.

Echosounding Equipment
During cruise SO-147 two different sediment echosounder systems were used, both developed by the research group of underwater acoustics of the Rostock University:

- a linear sediment echosounder system SEL-96
- a parametric sediment echosounder system SES-2000

Linear Sediment Echosounder System SEL-96
The linear sediment echosounder system SEL-96 was developed by the research project "ASS Ostsee", granted by the German Ministry of Education and Research (BMBF 1994-1997; FKZ: 03G0513A). SEL-96 was optimized for the RV "A. v. Humboldt" of the Baltic Sea Research Institute Warnemuende (IOW). The sound pulse is generated by a magnetostrictive phase-shifted transducer array with 18 separately controlled elements (6 x 3 matrix). Electronic beam stabilizing and steering is possible in both, roll and pitch directions.
Real time signal processing produces echo prints of the sea floor, reflectors in the sediment and buried objects with high two-dimensional resolution. High repetition rates increases the signal to noise ratio by echo stacking and increase the probability to detect small single objects and sediment structures.

Parametric Sediment Echosounder System SES-2000
Based on the successfully introduced sediment echosounder system SES-96 a new parametric echosounder system SES-2000 is under construction. This new system is optimized to detect in shallow water small buried objects and sediment structures with a high three-dimensional resolution. We made some special adaptations for the SO-147 expedition to increase the signal power for greater water depths. Sound pulses are generated by a small piezoceramic phase shifted transducer array with 32 separately controlled elements (32 x 1 matrix). The sound pressure is 247 dB re 1µPa. Electronic beam stabilizing and steering is possible in roll direction.
Focussed signals with a low frequency are transmitted by using the parametric effects of high frequency transmission. Extremely high system bandwidth allows specially formed very short transmission pulses which produce a very high resolution. The high frequent signal from the primary transmitter frequency is processed separately to exactly detect the bottom surface. Real time signal processing produces echo prints of sediment layers and buried objects with high three-dimensional resolution. High repetition rates are used to improve the signal to noise ratio and to raise the degree of probability to find small single objects and small bottom structures. SES-2000 is a flexible echosounder system that can be easily adapted to different tasks and operational areas.

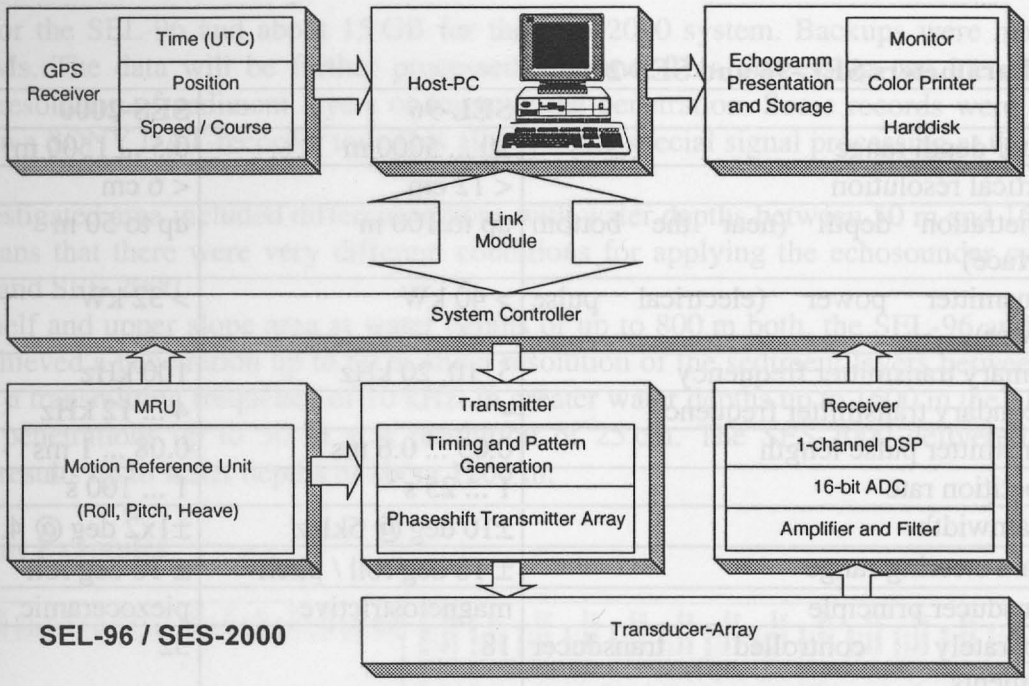

Fig. 4.1: *SEL-96 / SES-2000 system architecture*

System Components

The echosounder systems SEL-96 and SES-2000 consists of a main device, a host PC and a transducer array (Fig. 1 for the general structure). The main device has integrated transmitters, receivers and modules for analog and digital real time signal processsing. Analog to digital converters (ADC) are used for digitizing the receiver signal with 16-bit resolution at sampling rates up to 200 kHz depending on signal bandwidth.

The ship´s information system with GPS data is connected to the serial port of the PC. A special link module connects the echosounder main device to the PC which is used for system controlling and data display. All received data are stored digitally on a harddisk including GPS data and other important system parameters. The echosounder file format is device specific but may be converted into the standard SEG-Y format for post processing using conventional equipment. Analog data storage on DAT-recorder is also possible.

A color echoprint is immediately generated using 12 colors at a logarithmic scale. The echoprint includes all important parameters, e.g. GPS position, course and speed over ground, time (UTC), pulse frequency, pulse length and echo stacking rate. All transmitter and recording parameters are controlled by software, designed for this purpose.

The transducer is an array of several elements that are controlled separately for beam steering and stabilizing. Therefore all the ship movements are detected by a motion reference unit (MRU). This sensor, made by SEATEX (Norway), outputs absolute roll, pitch and yaw, and dynamic heave. Roll and pitch values are used for beam stabilizing in the sediment echosounders. Echoprints are compensated by the MRU heave value.

All the signal and image processing is done in real time but the digitally stored data can also be reprocessed at home to get more information.

Main Parameters SEL-96 and SES-2000

	SEL-96	SES-2000
water depth range	10 ... 5000 m	0.5 ... 1500 m
vertical resolution	< 12 cm	< 6 cm
penetration depth (near the bottom surface)	up to 100 m	up to 50 m
transmitter power (electrical pulse power)	> 40 kW	> 32 kW
primary transmitter frequency	5, 10, 20 kHz	100 kHz
secondary transmitter frequency	-	4 ... 12 kHz
transmitter pulse length	0.05 ... 0.6 ms	0.08 ... 1 ms
repetition rate	1 ... 25 s^{-1}	1 ... 100 s^{-1}
Beamwidth	±10 deg @ 5kHz	±1x2 deg @ 4...12kHz
beam steering range	± 16 deg roll / pitch	± 16 deg roll
transducer principle	magnetostrictive	piezoceramic
separately controlled transducer elements	18	32
Transducers dimensions	ca. 70 x 70 cm^2	ca. 20 x 40 cm^2
Transducer weight (in air, incl. 40m cable)	ca. 350 kg	ca. 70 kg

Results

In the first period of cruise SO-147 (Valparaiso – Lima) the echosounder equipment was installed. The transducers of both echosounders had to be mounted in the hydroacoustical shaft of RV "Sonne". To avoid acoustical disturbances near the linear transducer array of SEL-96 it was necessary to close the shaft by an acoustical window. This carbon fiber window was successful tested at cruise SO 93. The advantage of this thin (only 5 mm) window is the low sound absorption at higher frequencies.

During the first week the echosounders SEL-96 and SES-2000 have been operated simultaneously but asynchroneously to the ship´s PARASOUND-System. Different frequencies were used to reduce disturbances between the echosounders. Later the PARASOUND was switched off to improve the results of SEL-96 and SES-2000.

To get high resolution as well as high penetration the echosounders SEL-96 and SES-2000 operated in parallel, the first one at a low frequency (5 kHz) and the second one at a higher frequency (10 kHz).

The parameters of the motion reference unit (MRU) had to be optimized and to be adapted to the ship behavior to effectively correct roll, pitch and heave motions. The heave compensation algorithm used by the echosounders SEL-96 and SES-2000 was optimized to improve results at greater water depths.

Core stations were used for further signal tests, e.g. testing other transmitting frequencies and pulse lengths.

Profile data with a total length of about 6000 km were produced. Echoprint examples are shown in Fig. 2 to 4. Depth values have been computed from travel times assuming a constant sound velocity of 1500 m/s. Variations of sound velocity due to water temperature, pressure and salinity were not taken into account. The data are plotted time sequentially from the left to the right. Heave components are removed from the echoprints by an enhanced algorithm using the heave data delivered by the motion reference unit (MRU).

All the received signals were stored digitally on harddisk together with the GPS data and system parameters. The total volume of digitally stored echosounding information is about

14 GB for the SEL-96 and about 15 GB for the SES-2000 system. Backups were made on CD-ROMs. The data will be further processed at home. This processing can increase the vertical resolution of sediment layers or improve the penetration. Some records were stored analog on a SONY DAT-recorder too. This allows some special signal processing at the home lab.

The investigated area included different regions with water depths between 50 m and 1600 m. That means that there were very different conditions for applying the echosounder systems SEL-96 and SES-2000.

In the shelf and upper slope area at water depths of up to 800 m both, the SEL-96 and SES-2000, achieved a penetration up to 60 m and a resolution of the sediment layers between 6 to 12 cm at a transmitting frequency of 10 kHz. In greater water depths up to 1600 m the SEL-96 reached penetrations up to 30 m at a resolution of 25 cm. The SES-2000 delivered more detailed results up to water depths of about 1200 m.

Echoprint Examples

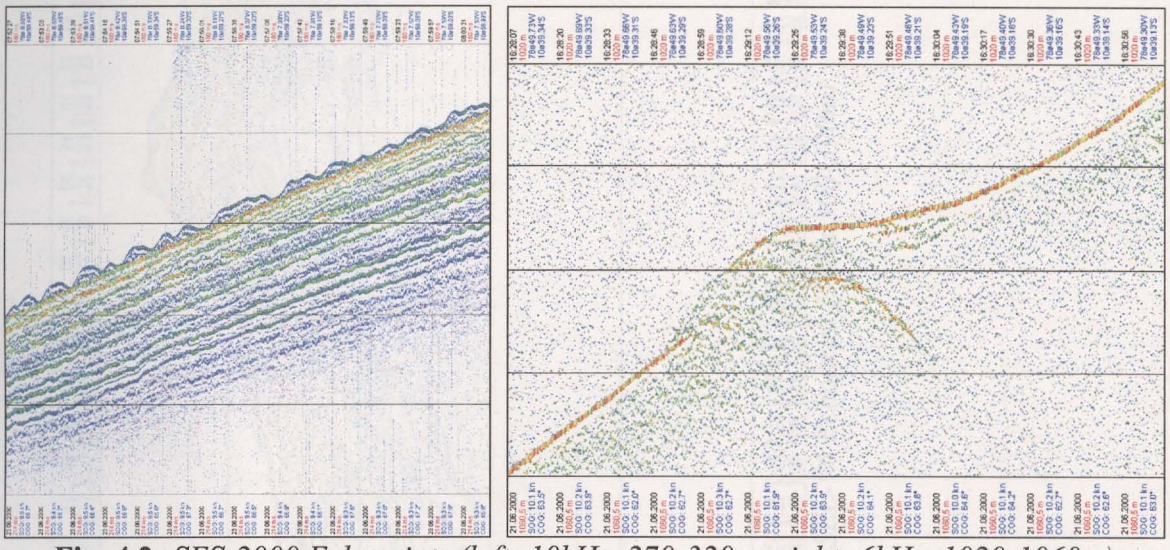

Fig. 4.2: *SES-2000 Echoprints (left: 10kHz, 270-320m; right: 6kHz, 1020-1060m)*

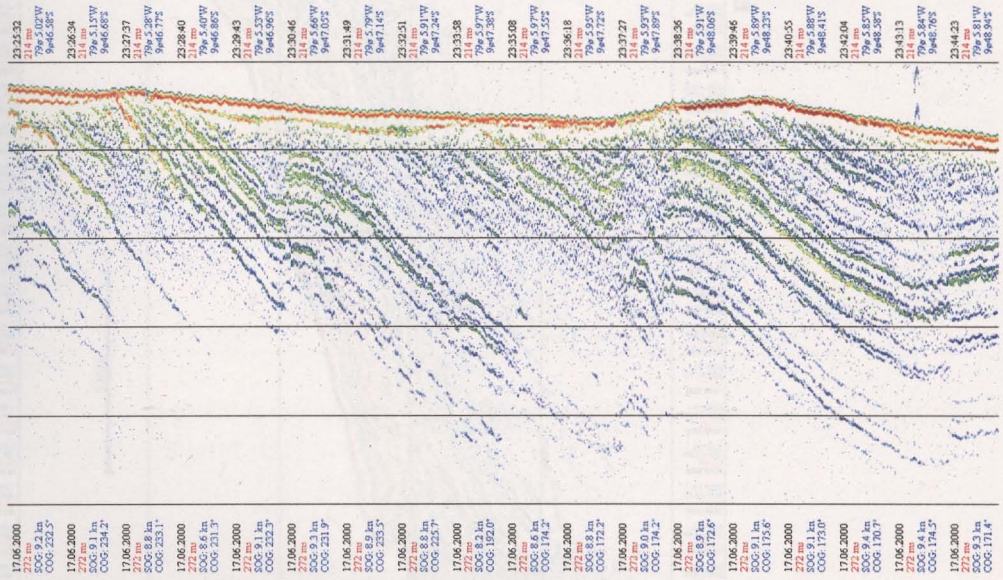

Fig. 4.3: *SEL-96 Echoprint (5kHz,160-205m)*

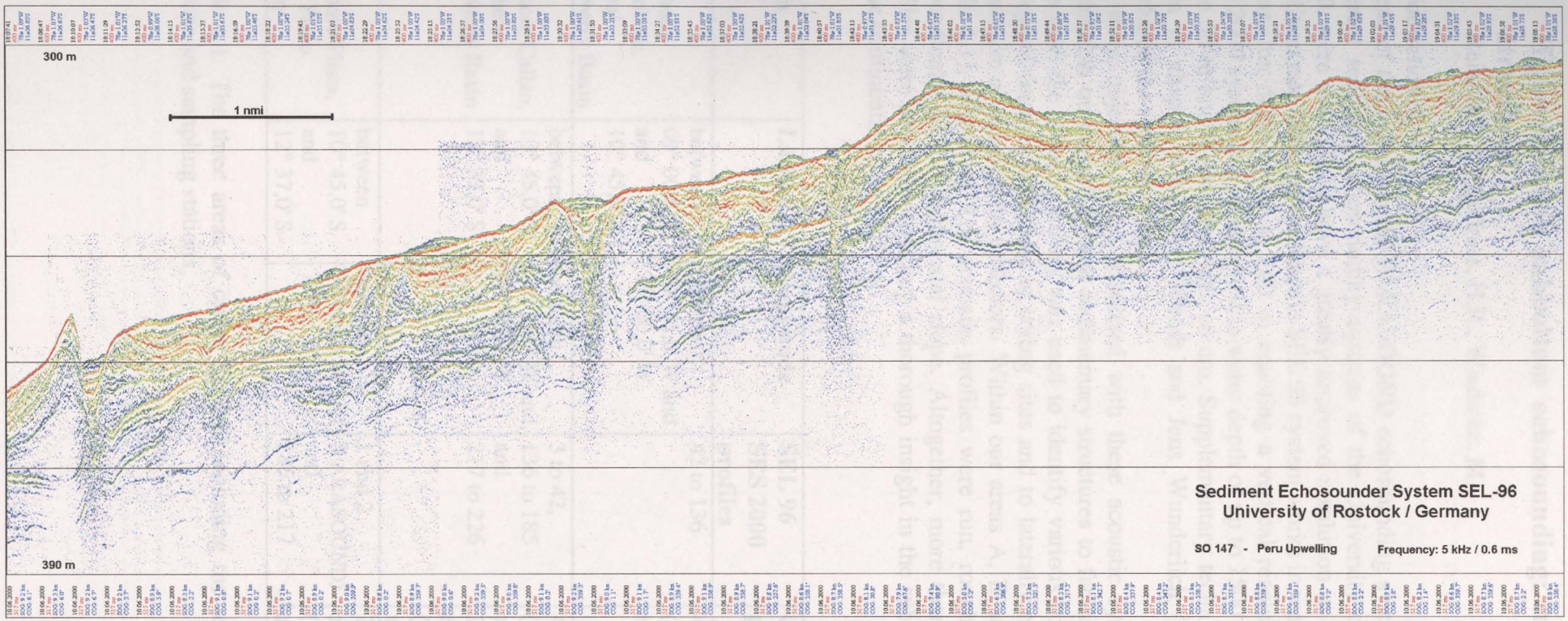

Fig. 4.4: *SEL-96 Echoprint (5kHz,300-390m)*

5. High-resolution subbottom echosounding: inventory of sedimentary structures

Reinhardt, L., Kudrass, H.R., Wiedicke, M.

Introduction

Instead of the hull-mounted PARASOUND echosounding system onboard RV SONNE, two different sediment echosounding systems of the University of Rostock, SEL 96 and SES 2000, were used. They have a greatly improved resolution in shallow water due to a higher repetition rate. The non-parametric SEL 96 system works in water depths up to 5000 m with a penetration depth of up to 100 m enabling a vertical resolution <12 cm. The parametric SES 2000 system can be operated in water depth of up to 1500 m. It achieves a penetration of up to 50 m and a resolution of <6 cm. Supplementary technical details of the systems are given in chapter 4 by Gert Wendt and Jens Wunderlich (University of Rostock), who developed the systems.

The main objective to be addressed with these acoustic systems was to obtain detailed information on the sub-bottom sedimentary structures to facilitate sediment sampling. Apart from that, the acoustic survey was used to identify various echo types and their relation to geological features especially at coring sites and to laterally extrapolate this information by correlation of sub-bottom reflectors. Within our areas A, B, and C (Figs. 5.1, 5.2, 5.3, and Table 5.1), a total of 216 acoustic profiles were run, roughly oriented both parallel and perpendicular to the continental slope. Altogether, more than 6000 km of high-resolution profiles were acquired providing a thorough insight in the sub-bottom sedimentary structure of the continental slope off Peru.

Area	Latitude	Longitude	SEL 96 SES 2000 profiles	Connecting profiles	Stations
A offshore Chimbote, central Salaverry Basin	between 09° 00,0' S and 10° 45,0' S	between 79° 45,0' W and 78° 00,0' W	42 to 136	42 and 136 (connection to area B)	28KG to 92SF
B offshore Callao, southern Salaverry Basin	between 10° 45,0' S and 12° 37,0' S	between 78° 35,0' W and 77° 05,0' W	3 to 42, 136 to 185 and 217 to 226	42 and 136: (connection to area B) 2, 3, 185, 186 and 217 (connection to area C)	2MC to 27KL and 93FS to 118KA
C offshore Pisco, East Pisco Basin	between 10° 45,0' S and 12° 37,0' S	between 78° 35,0' W and 77° 05,0' W	1 and 2 (PARASOUND) and 186 to 217	2 ,3, 185, 186, and 217: (connection to area B)	1MC and 119 to 149 GA

Table 5.1: The three areas of cruise SO-147 including the respective numbers of acoustic profiles and sampling stations.

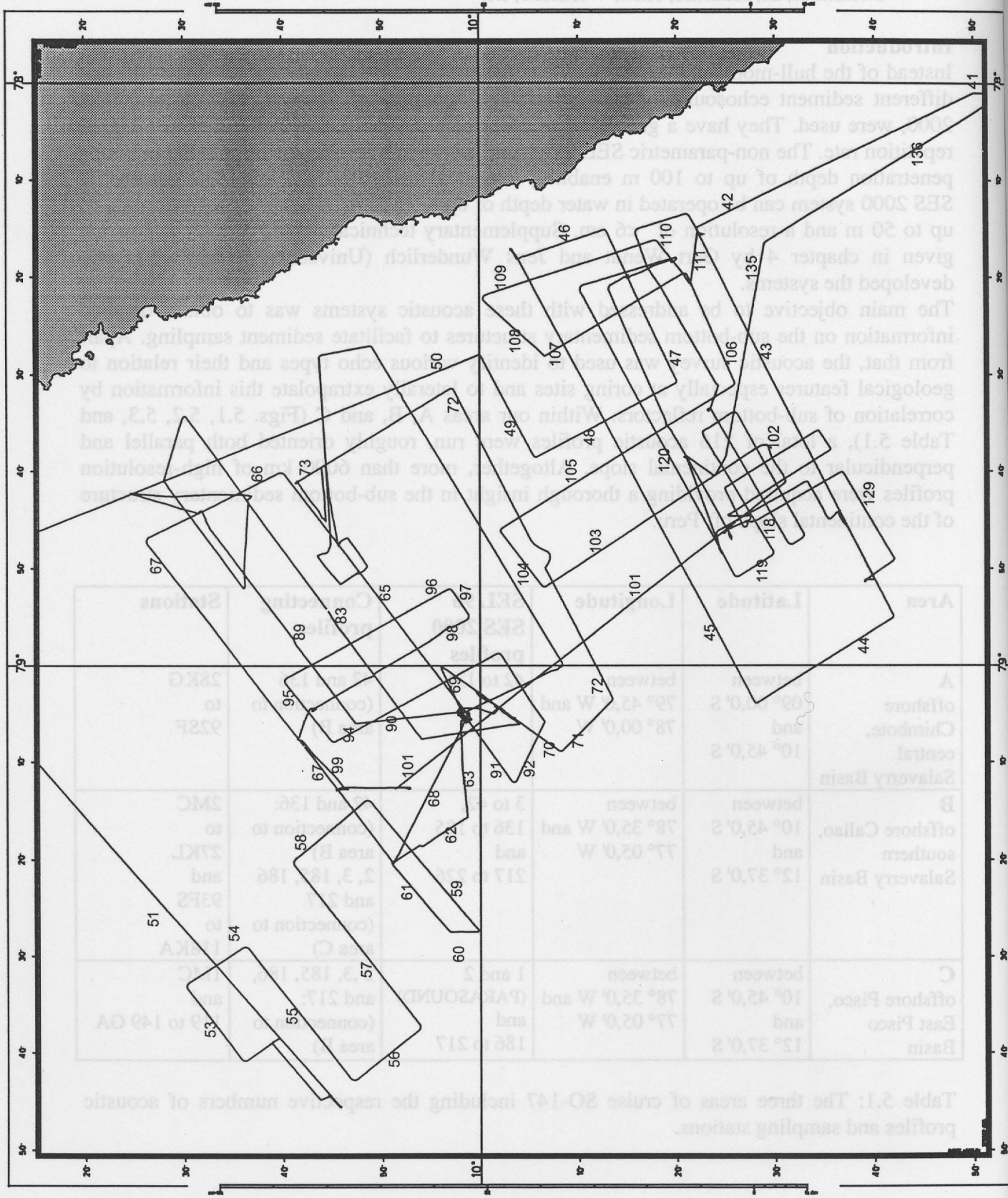

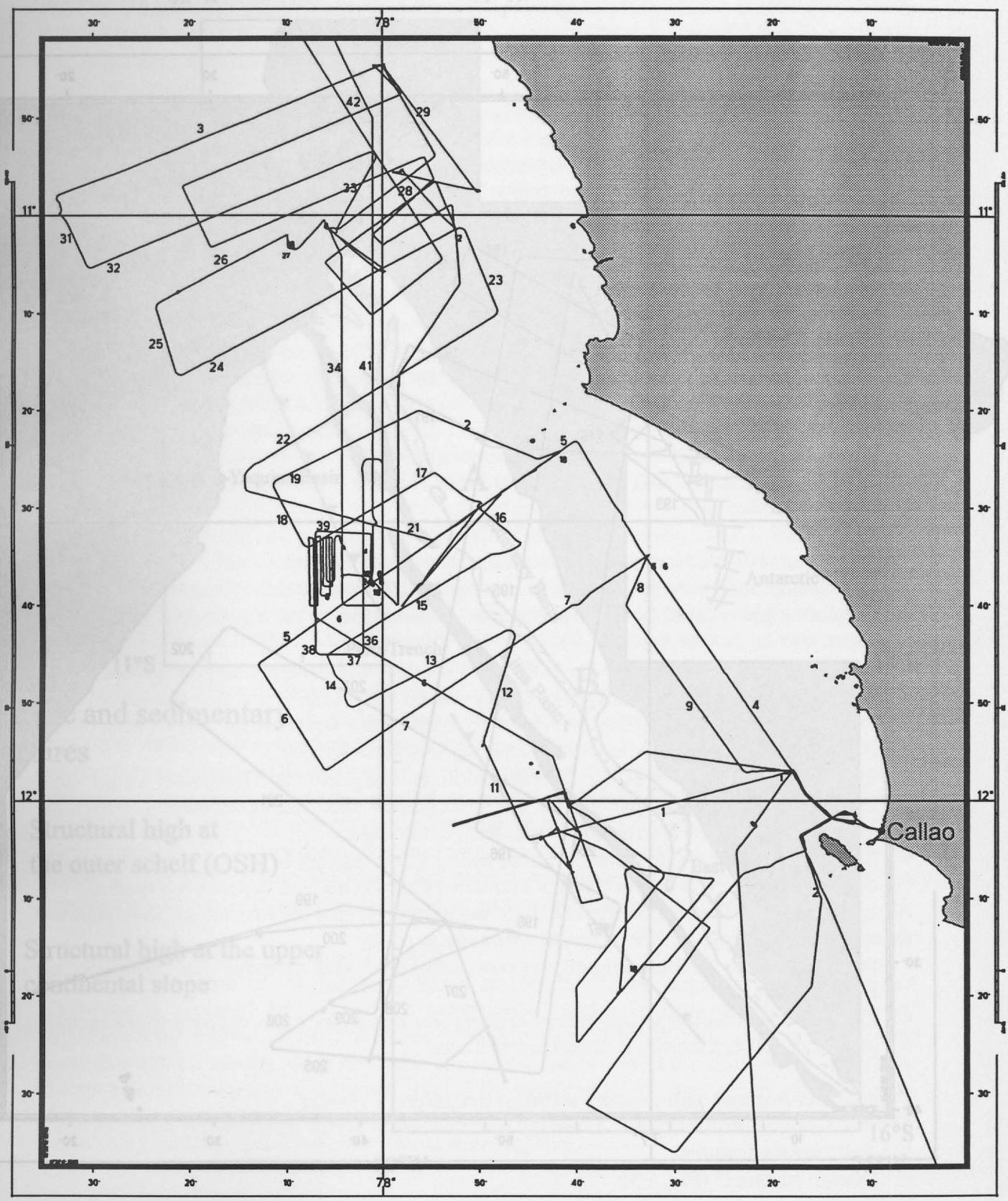

Fig. 5.2: Map of area B, south Salaverry Basin off Callao

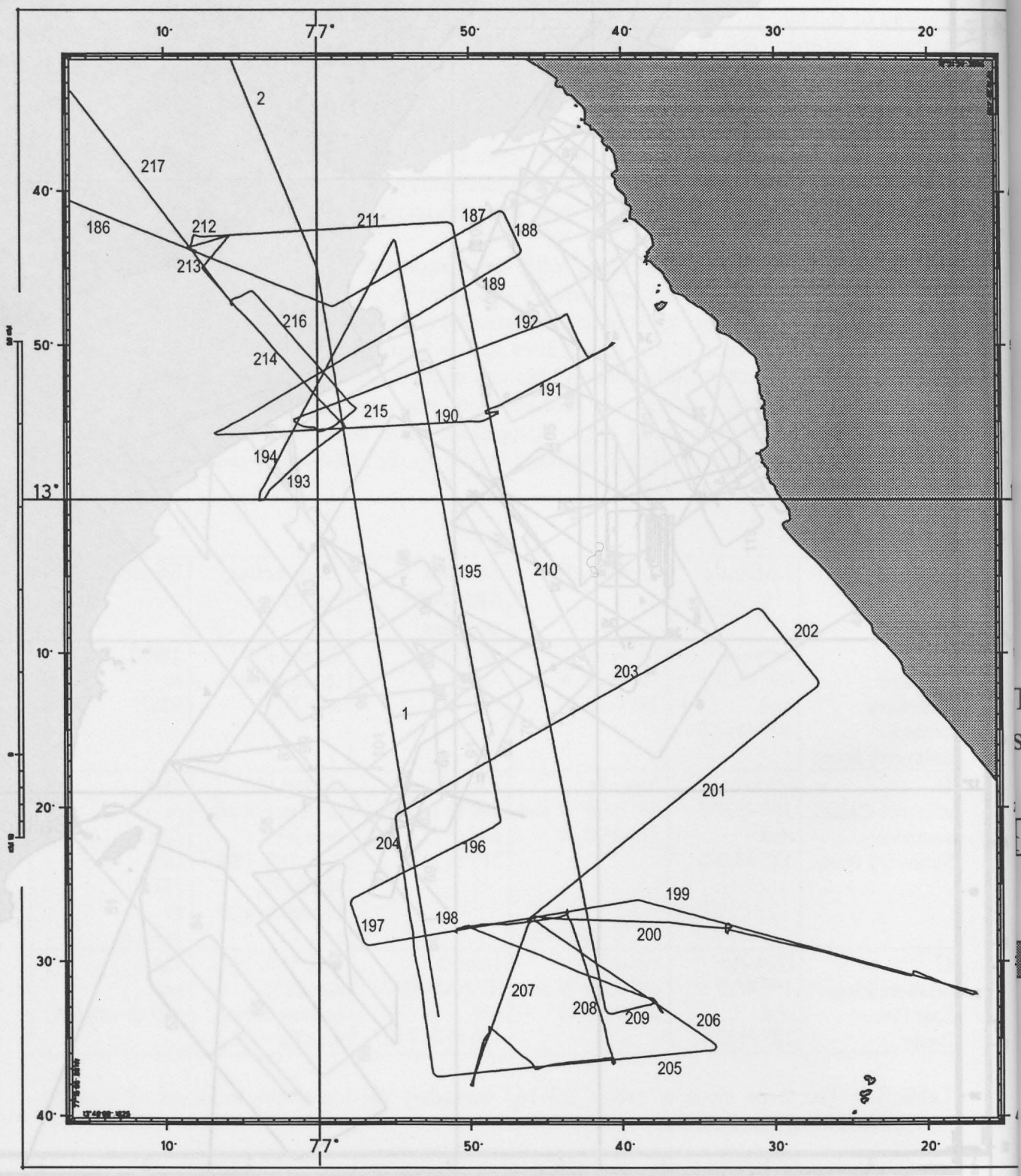

Fig. 5.3: Map of area C, East pisco Basin

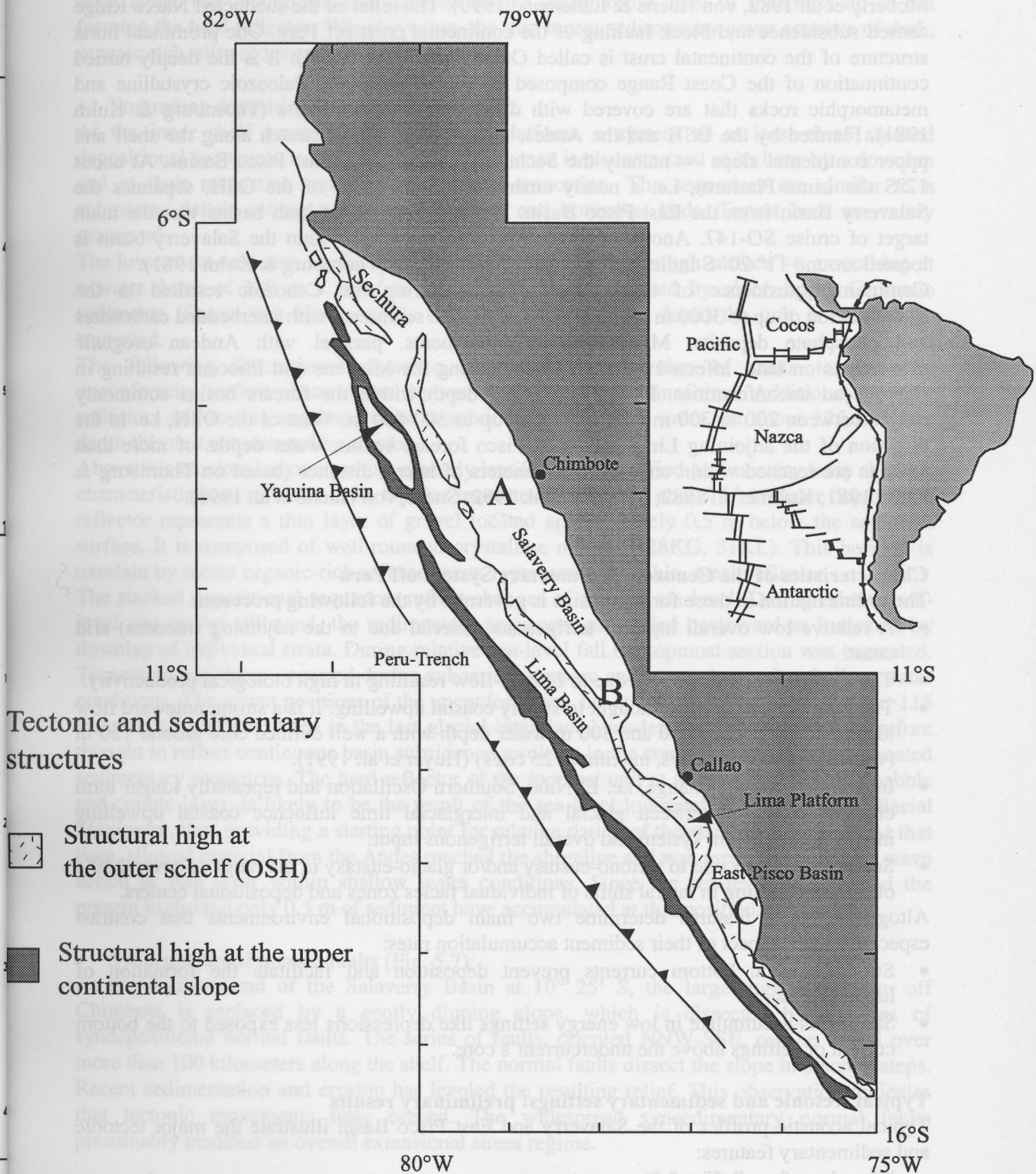

Fig. 5.4: Geological setting of the Peruvian continental margin (adapted from Thornburg & Kulm, 1981).

Tectonic setting

The convergent continental margin off Peru is characterized by tectonic erosion (e.g., Moberly et al. 1982, von Huene & Lallemand 1990). The relief of the subducted Nazca Ridge caused subsidence and block faulting of the continental crust off Peru. One prominent horst structure of the continental crust is called Outer Shelf High (OSH). It is the deeply buried continuation of the Coast Range composed of Precambrian and Paleozoic crystalline and metamorphic rocks that are covered with dislocated Neogene strata (Thornburg & Kulm 1981). Flanked by the OSH and the Andes, three forearc basins stretch along the shelf and upper continental slope — namely the Sechura, Salaverry and East Pisco Basins. At about 12°S the Lima Platform, i.e. a nearly emerging massif block of the OSH, separates the Salaverry Basin from the East Pisco Basin. The sediment fill of both basins was the main target of cruise SO-147. Another structural high of the OSH within the Salaverry basin is located around 11° 20' S indicated by several small islands (Thornburg & Kulm 1981).
Continuing subsidence of these forearc basins during the Cenozoic resulted in the accumulation of up to 3000 m of mainly clastic marine sediments with interbedded carbonates and phosphate deposits. Major tectonic movements, parallel with Andean orogenic movements on land, affected the shelf basins during the Miocene and Pliocene resulting in pronounced unconformities. Present day water depth within the forearc basins commonly ranges between 200 to 300 m and may reach up to 500-600 m. West of the OSH, i.e. in the direction of the adjoining Lima and West Pisco forearc basins, water depths of more than 1500 m are reached within only a few kilometers of lateral distance (based on Thornburg & Kulm 1981; Kulm et al. 1982; Moberly et al. 1982; Suess, von Huene et al. 1990).

Characteristics of the Cenozoic Sedimentary System off Peru

The sedimentation in these forearc basins is governed by the following processes:

- A relative low overall input of terrigenous material due to the adjoining (modern) arid coast.
- The strong coastal upwelling due to Ekman-flow resulting in high biological productivity.
- The Peru Undercurrent is thought to supply coastal upwelling. It is a strong poleward flow located today between 50 and 300 m water depth with a well defined core around 150 m (velocity: around 10 cm/s, maximum 25 cm/s) (Huyer et al. 1991).
- Interannual climate change, i.e. El Niño–Southern Oscillation and repeatedly longer term climatic contrasts between glacial and interglacial time influence coastal upwelling intensity, the current system and overall terrigenous input.
- Sea-level changes due to tectono-eustasy and/or glacio-eustasy in the range of several 10's of meters resulting in lateral shifts of individual facies zones and depositional centers.

Altogether, these features determine two main depositional environments that contrast especially with respect of their sediment accumulation rates:

- Strong oceanic bottom currents prevent deposition and facilitate the formation of hardgrounds.
- Sediments accumulate in low energy settings like depressions less exposed to the bottom current or settings above the undercurrent's core.

Typical tectonic and sedimentary settings: preliminary results

Typical acoustic profiles of the Salaverry and East Pisco Basin illustrate the major tectonic and sedimentary features:

- "Rough surfaces" (Fig. 5.5):

Typical features especially of area A off Chimbote are "rough surfaces" that are characterized by a strong reflector near the surface. A thin layer of recent sediment (indicated by weaker reflectors) overlies the rugged surface. The erosional unconformity has formed on older, often

slightly folded sedimentary units of mostly Miocene/Pliocene age (Suess, von Huene et al. 1990). Accumulation of sediment has been prevented by the high-energy current system. Over wide areas, the unconformity is covered with a phosphoritic crust of thickness up to dm forming the hard reflector. Where present, the thin recent sedimentary cover consists of dark, organic rich, silty sediment.

- Prograding depositional sequences (Fig. 5.6):

At the inner shelf south of the Chimbote platform, a system of at least three stacked depositional sequences is recognized. Each sequence is characterized at its base by a downlap and at their respective tops by an erosional truncation. The sequences are similar to a submarine deltaic setting with topset, foreset, and bottomset beds. Topset beds are rarely preserved.
The lowermost unit rests on the unconformity surface — the "rough surface"— smoothing at a water depth of 180 m a relief of 10 to 15 m that is formed by older, upper Cenozoic sediments (Suess, von Huene et al. 1990). At 160 m water depth the unit is erosionally truncated.
The following depositional sequence shows also a downlap of strata towards the unconformity surface characterized by very well developed clinoforms. Additional stronger reflectors within this sequence allow a subdivision into three units. At about 125 m water depth this unit is truncated by erosion.
Above this erosional unconformity, a nearly lentil-shaped stratified sedimentary body shows a characteristic hard reflector at its top that truncates the strata at about115 m water depth. This reflector represents a thin layer of gravel located approximately 0.5 m below the sediment surface. It is composed of well-rounded crystalline material (28KG, 31KL). This horizon is overlain by recent organic-rich soft sediment, represented by a thin, weak reflector.
The stacked depositional sequences reflect changes of relative sea-level. During relative sea-level rise and/or stillstand, the sedimentary sequences prograded basinward as indicated by downlap of individual strata. During relative sea-level fall the topmost section was truncated. Truncation may have occurred during subaerial exposure and/or erosion under shallow water conditions. The recent positions of the unconformities, i.e. at 160 m, 125 m, and at about 115 m, cannot be accomodated in the last glacial-interglacial sea-level changes and are therefore thought to reflect continuous basin subsidence resulting in the stacked pattern of the truncated sedimentary sequences. The hard reflector of the topmost unit at about 115 m, i.e. the pebble and cobble layer, is likely to be the result of the sea-level lowstand during the Last Glacial Maximum, thus providing a starting point for relative dating of the stacked sequences. At that time, alluvial material from the Andes reached the shoreline and was probably spread by wave action as thin layer within shallow water conditions. Since the sea-level has reached the present highstand only 0.5 m of sediment have accumulated at this position.

- Syndepositional normal faults (Fig. 5.7):

At the southern end of the Salaverry Basin at 10° 25' S, the large rugged platform off Chimbote is replaced by a gently dipping slope, which is dissected by a series of syndepositional normal faults. The series of faults, oriented NNW-SSE, can be traced over more than 100 kilometers along the shelf. The normal faults dissect the slope in discrete steps. Recent sedimentation and erosion has leveled the resulting relief. This observation indicates that tectonic movements have ceased. The widespread synsedimentary normal faults presumably manifest an overall extensional stress regime.

- Mud-waves (Fig. 5.8):

Between 250 m and 400 m water depth, the uppermost sedimentary sheet continuously disintegrates into mud-waves. Below ca. 400 m this unit completely disappears. The mud-

waves are characterized by weak reflections resting commonly on harder continuous reflectors suggesting sand-mud lithology. The mud-waves have a convex upward shape with a maximum thickness of 2 to 3 m, a length of 100's of meters and seem to be N-S oriented. Thus, they are most probably a result of the Peru Undercurrent. Closer video inspection by means of the OFOS system revealed that the mud-waves are covered with a soft, fluffy layer indicating that at the time of inspection no transport of sediment took place.

- Mud-lens near Callao (Fig. 5.9):

Near Callao (77° 39,86' W / 12° 03,00' S) within a water depth of about 180 m, a more than 25 m thick sedimentary body was discovered that we called "mud-lens near Callao". The transparent, bedded sequence onlaps a seismically opaque rugged surface. The mud-lens can be subdivided in at least 4 subordinate sedimentary units, limited by slight discordances. Piston core 106KL (19,34 m length) penetrated the upper two reflectors, i.e., a double reflector between about 4 to 5 m and a single reflector 12 m below the sediment surface. The sequence accumulated in a niche that was less affected by the high-energy undercurrent.

- Channels (Figs. 5.10 and 5.11):

At various positions along the edge of the slope subparallel channels dissect the uppermost continental slope. A detailed survey with closely spaced lines was carried out in area A. For more details see the section 5.5 on bathymetry.

In summary areas A, B, and C are characterized as follows:
Area A (Salaverry basin off Chimbote) is dominated by a widespread, shallow and rugged shelf that is partly covered with a hard phosphoritic crust or gravel. The platform ends at a shelf break at about 150 m water depth. Around 10° 25' S the platform retreats and is replaced by a gently dipping slope formed by a succession of stacked sedimentary sequences. Here, synsedimentary normal faults cut up the slope.
In the northern part of area B (southern end of the Salaverry basin) of gently dipping slope continues. A zone of mud-waves is located here between about 280 m to 400 m water depth. The southern part of area B off Callao is formed by the structural high of the Lima platform creating protected niches enabling the continuous accumulation of laminated Quaternary sediments (e.g. the Callao mud-lens).
Area C in the South (East-Pisco Basin) features a wide shallow shelf with a gentle slope without a pronounced shelf break. Near the coast a wedge of Holocene sandy sediments has accumulated rapidly thinning at about 130 m water depth. The exposed underlying unconformity may be an equivalent of the platform with a phosphoritic crust in area A.

Additional descriptions of individual sampling sites with relation to acoustic facies are given in chapter 12 (ALPAKKA-report).

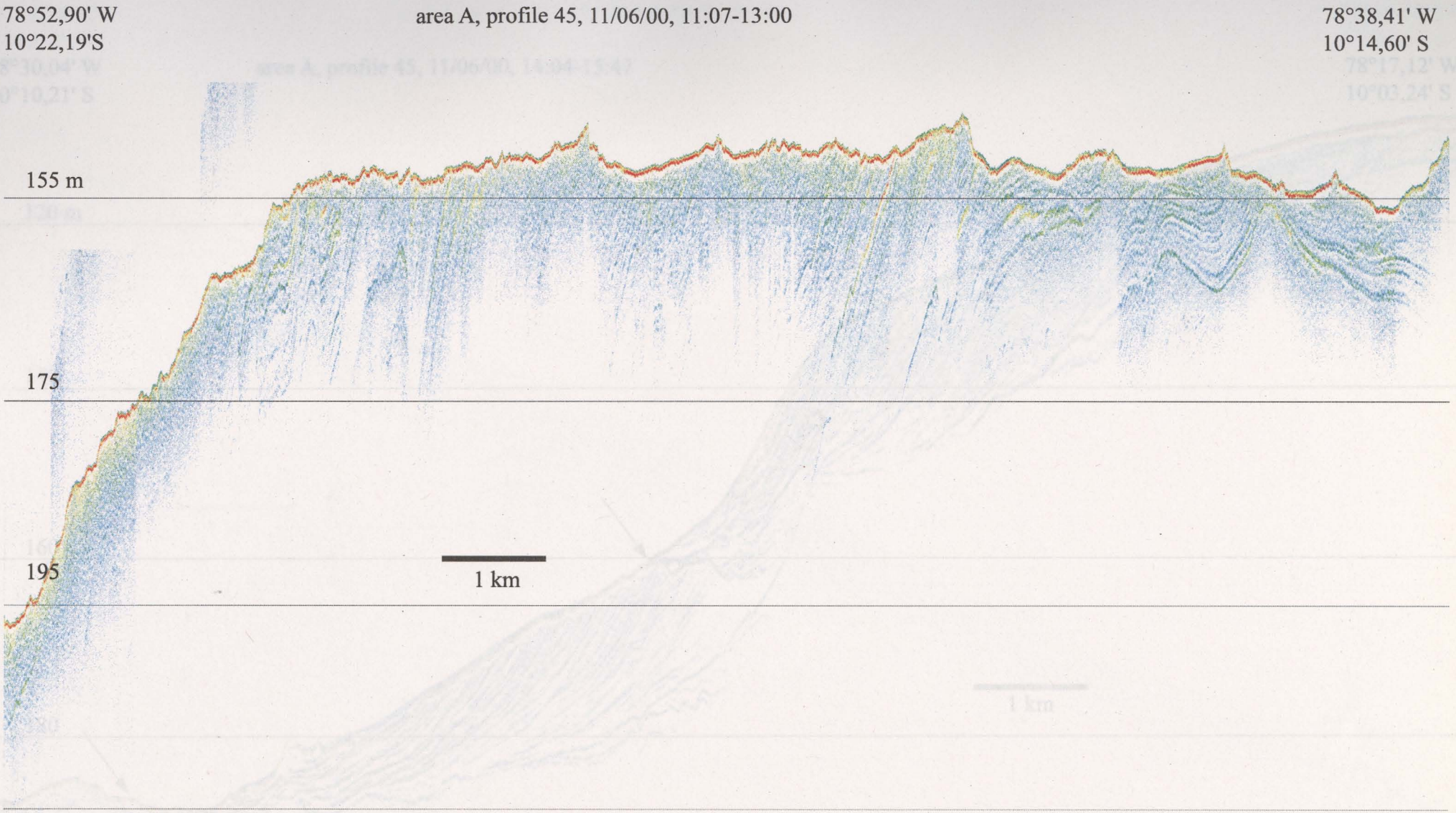

Fig. 5.5: "Rough surfaces"

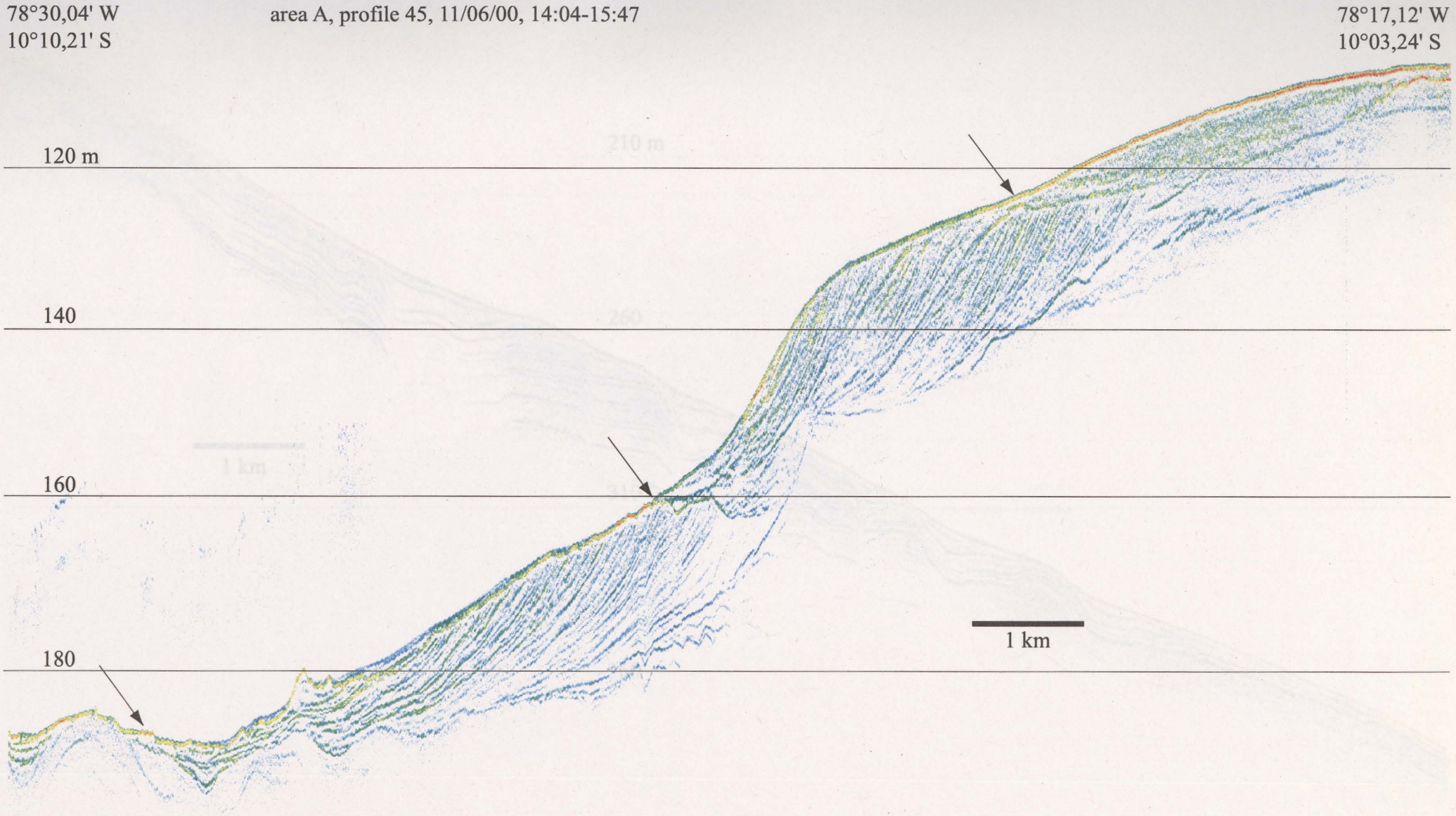

Fig. 5.6: Prograding depositional sequences.

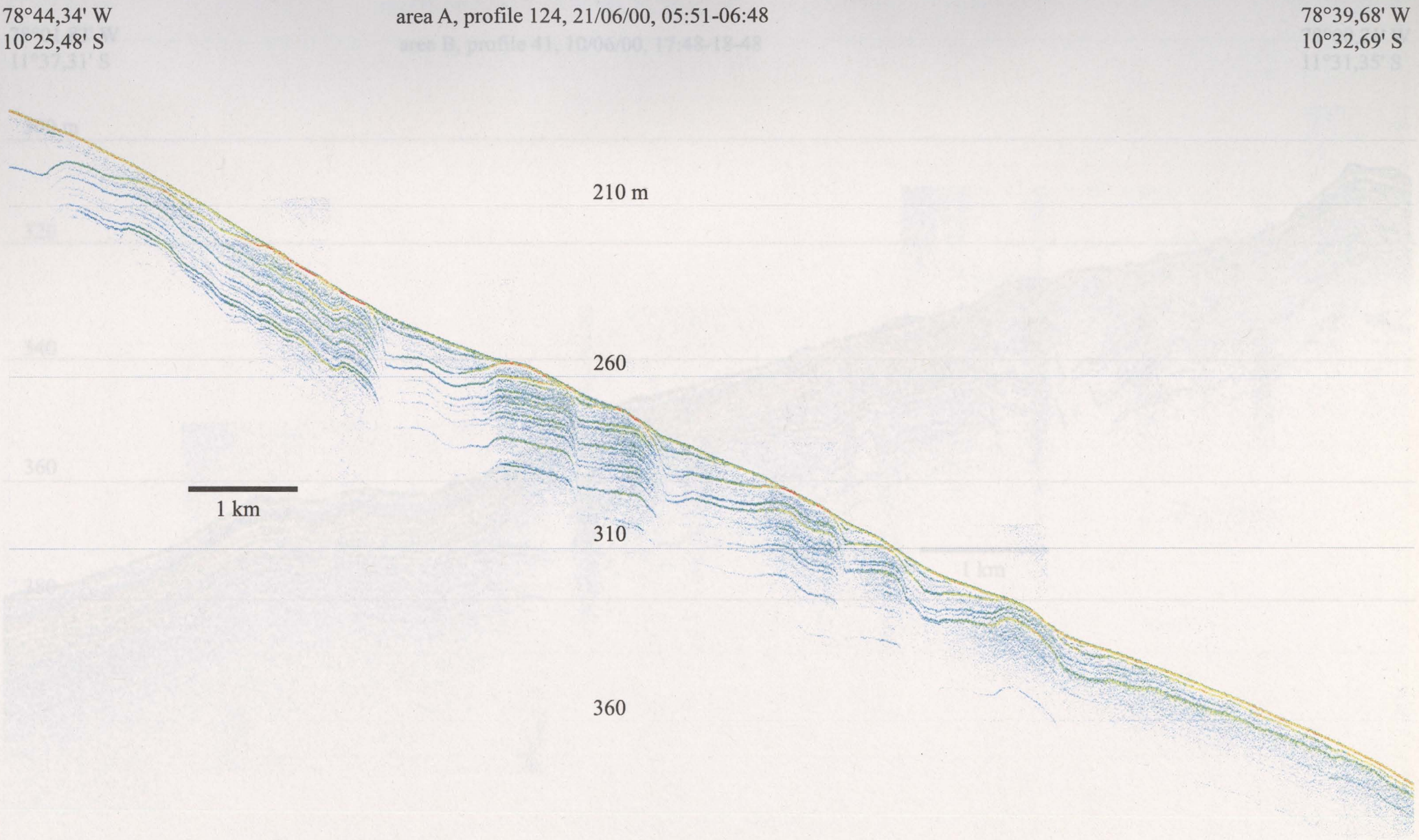

Fig. 5.7: Synsedimentary faults.

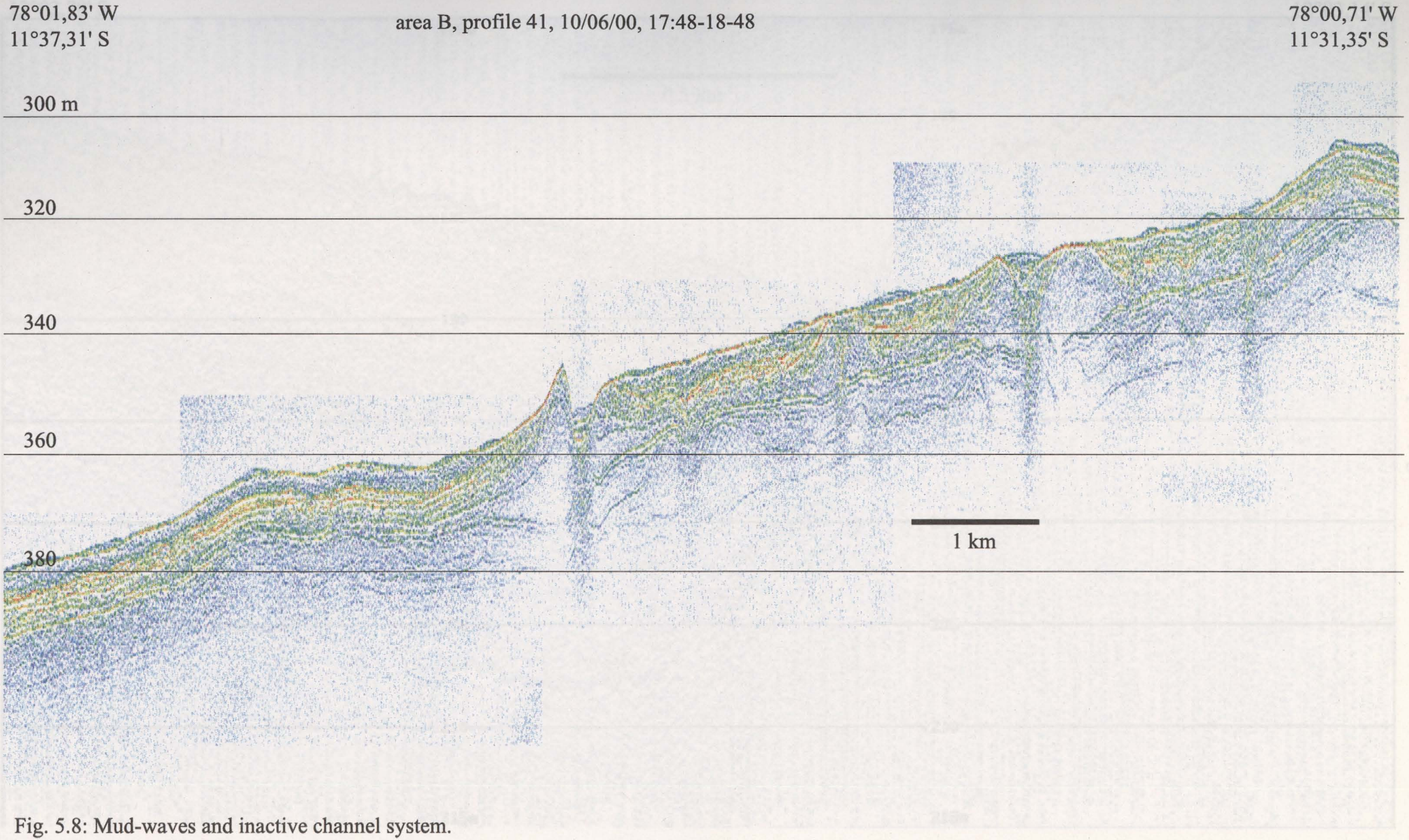

Fig. 5.8: Mud-waves and inactive channel system.

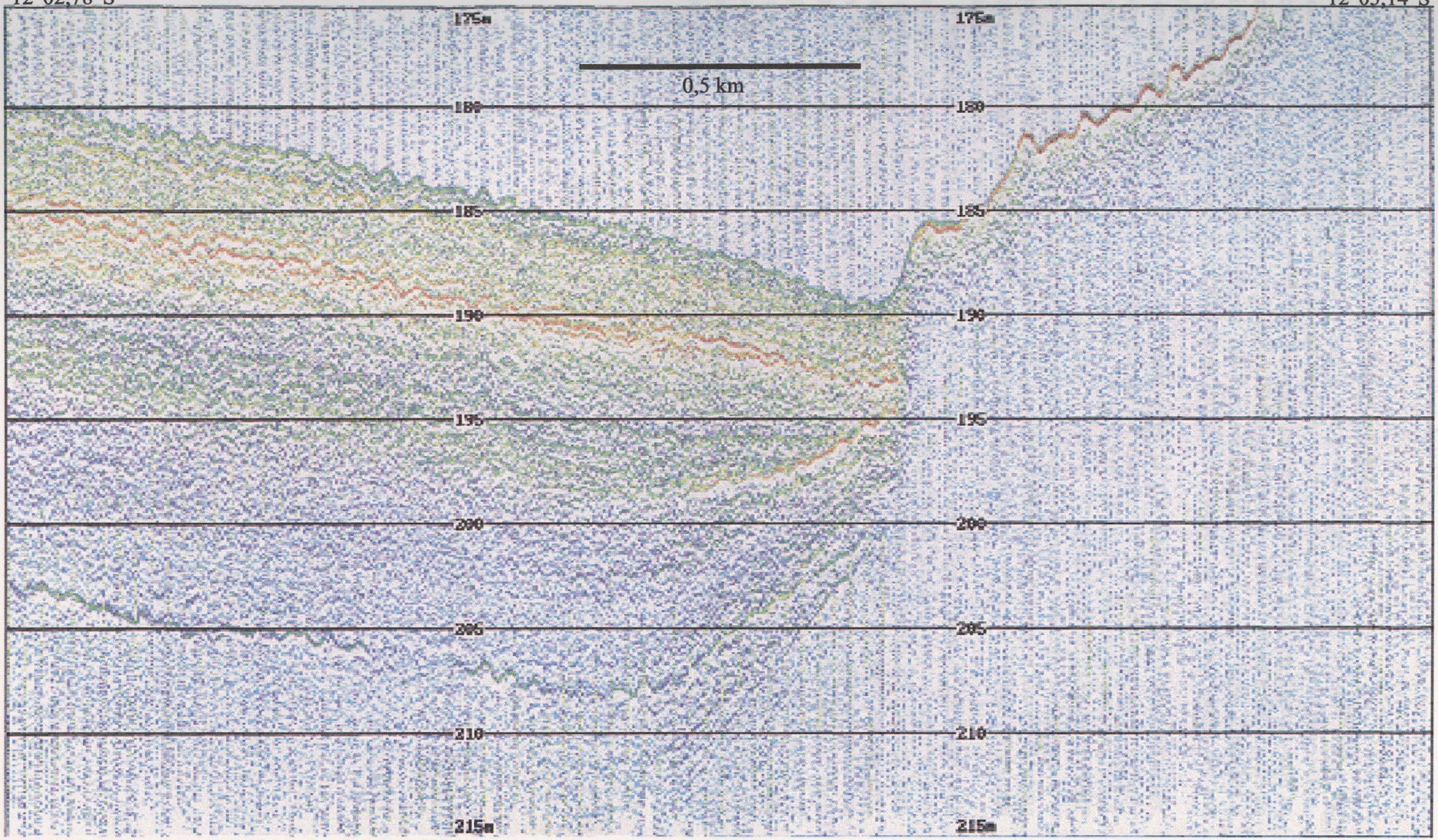

Fig. 5.9: Mud-lens near Callao.

Bathymetric survey by HYDROSWEEP swathmapping

Bathymetric data were continuously recorded along the tracks of cruise SO-147 using the onboard multibeam HYDROSWEEP echosounder system manufactured by Krupp-Atlas-Electronics. Technical details of the automatically calibrating swath mapping system with an operating frequency of 15.5 kHz are given in Grant & Schreiber (1990). Each track covers an area twice as wide as the water depth. All data were stored on magnetic tape. Onboard a bathymetric map could not be produced, as individual sweeps of adjoining tracks did not overlap.

A limited sector in area B at the westward edge of the Salaverry basin was, however, surveyed in greater detail to map the courses of a series of channels that were initially identified on acoustic sub-bottom profiles (Fig. 5.10). Within a rectangle between long. 78° 08' W to 78° 02' W and lat. 11° 32' S to 11° 41' S, 12 closely spaced HYDROSWEEP lines were run resulting in a detailed bathymetric map. Conversion of echo-soundings to a proper depth by complete ray tracing through the different water layers was achieved by using a composite sound velocity profile derived from CTD stations 24MS and 100MS. The total depth range reaches from about 350 m to 610 m (Fig. 5.11).

All 6 individual channels run slightly meandering down the slope. Three of them are well developed and cut into underlying sediments up to 25 m depth. Levees with a height of 5 m are moderately developed. Another three channels of only about 5 m depth are covered with younger sediments (Fig. 5.10), thus being less obvious on the HYDROSWEEP bathymetric map (Fig. 5.11). In general, all channels are running straight. However, some of them are slightly bent, especially the 1st, 2nd, and the 4th channel with some small meanders in their (upper) course. The more-or-less straight course might be due to a relative steep gradient of the slope at the edge of the Salaverry basin towards the adjoining deeper Lima Basin. These conduits for the transport of material seem to be inactive at present time as indicated by various stages of sediment infill. They may have been formed by turbidity currents during a major sea-level fall.

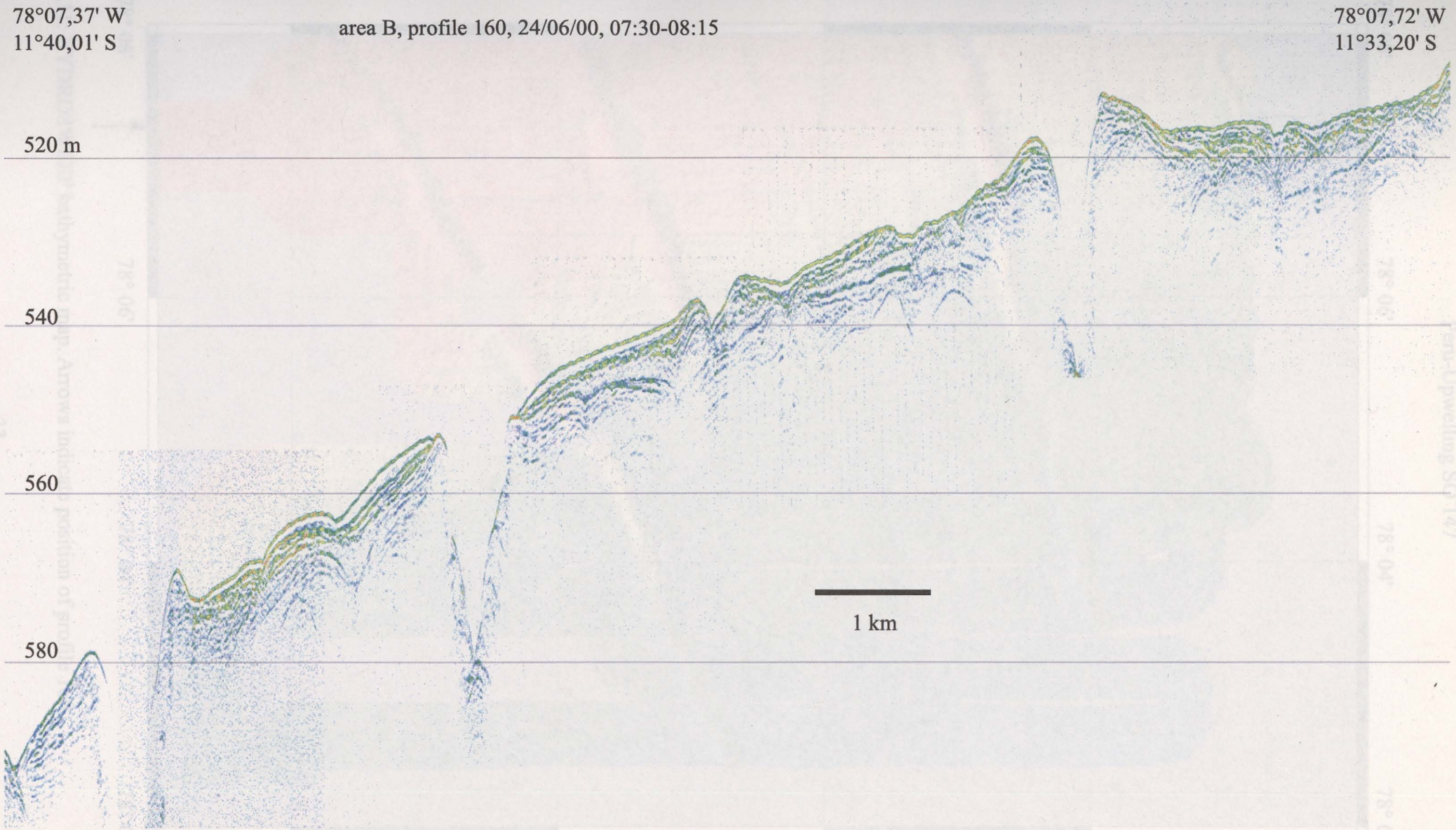

Fig. 5.10: Channel system.

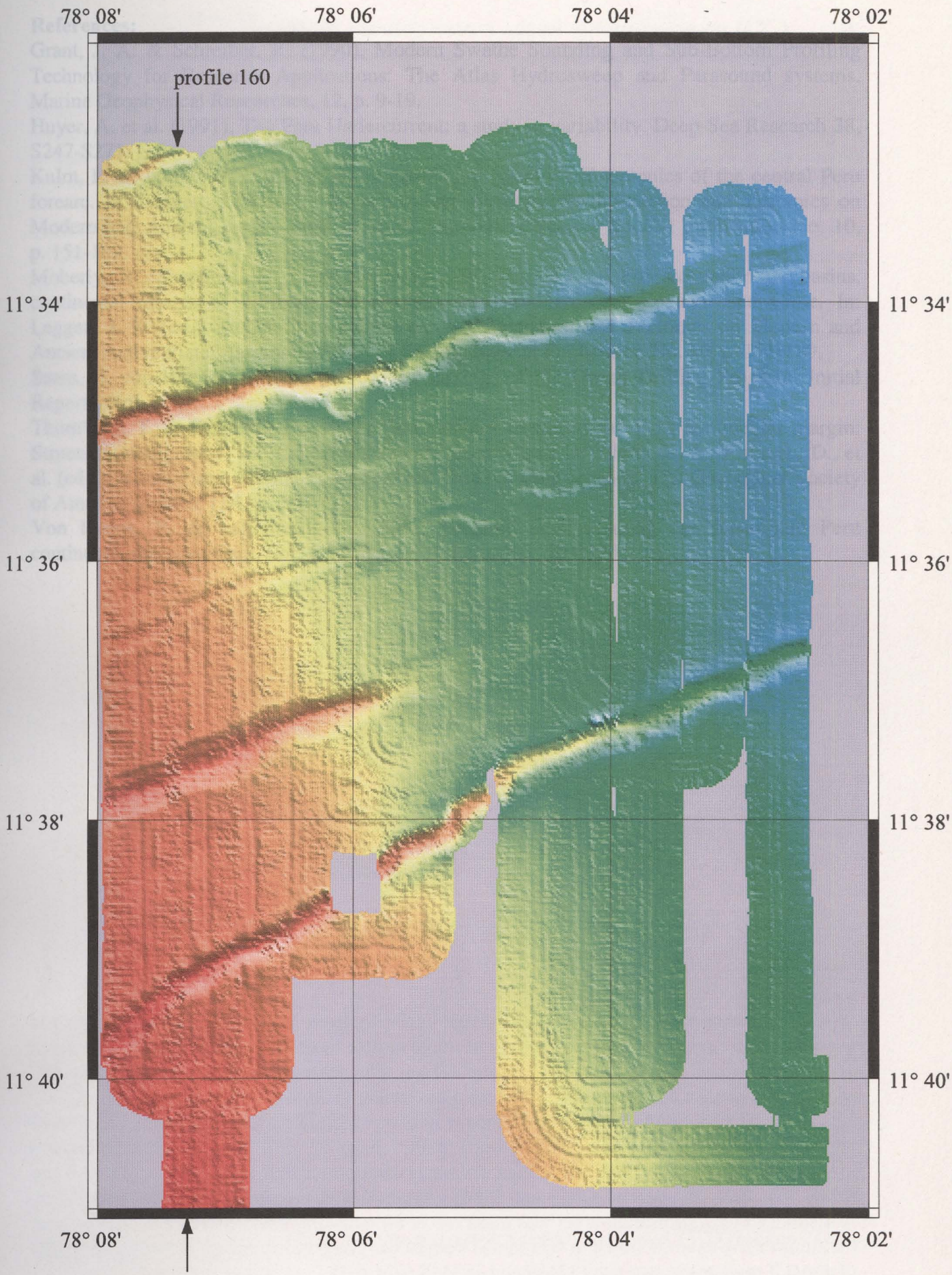

Fig. 5.11: HYDROSWEEP bathymetric map. Arrows indicate position of profile 160.

References:

Grant, J. A. & Schreiber, R. (1990), Modern Swathe Sounding and Sub-Bottom Profiling Technology for Research Applications: The Atlas Hydrosweep and Parasound systems. Marine Geophysical Researches, 12, p. 9-19.

Huyer, A. et al. (1991), The Peru Undercurrent: a study in variability. Deep-Sea Research 38, S247-S271.

Kulm, L. D. et al. (1982), Cenozoic structure, stratigraphy and tectonics of the central Peru forearc. In: Leggett, J. K. (ed.), Trench-forearc Geology: Sedimentation and Tectonics on Modern and Ancient Active Plate Margins. Geological Society Special Publication No. 10, p. 151-169.

Moberly, R., Shepherd, G. L. & Coulbourn, W. T. , (1982), Forearc and other basins, continental margin of northern and southern Peru and adjacent Ecuador and Chile. In: Leggett, J. K. (ed.), Trench-forearc Geology: Sedimentation and Tectonics on Modern and Ancient Active Plate Margins. Geological Society Special Publication No. 10, p. 171-189.

Suess, E. von Huene, R. et al. (1990), Proceedings of the Ocean Drilling Program, Initial Reports, Vol. 112.

Thornburg, T. & Kulm, L. D. (1981): Sedimentary basins of the Peru continental margin: Structure, stratigraphy, and Cenozoic tectonics from 6°S to 16°S latitude. In: Kulm, L. D., et al. (eds.), Nazca Plate: Crustal Formation and Andean Convergence. The Geological Society of America Memoir 154, p. 393-422.

Von Huene, R. & Lallemand, S. (1990), Tectonic erosion along the Japan and Peru continental margins. Geol. Soc. Of America, Bulletin 102, 704-720.

6. CTD measurements in the water column off Peru

Lückge, A., Reinhardt, L.

Measurements of temperature, salinity and oxygen variations as well as changes in density within the oceanic water column are usually carried out by lowering a CTD (chemistry, temperature, density) probe into the water. During cruise SO147 we have used CTD sensors to monitor the distribution of the oxygen minimum zone (OMZ) at 7 sites (Fig. 6.1), as well as to measure temperature and salinity profiles.

Hydrographic parameters (temperature, salinity, oxygen concentration, and density) were measured continuously during lowering and hieving, using the shipboard CTD (SEABIRD SEACAT; SBE 9plus 10500 m, Sea-Bird Electronics Inc.) that was mounted on a rack that also contained twenty four 10 l rosette water bottles (Ocean Test Equipment) for water sampling. CTD stations of cruise SO147 are shown in Figure 6.1.

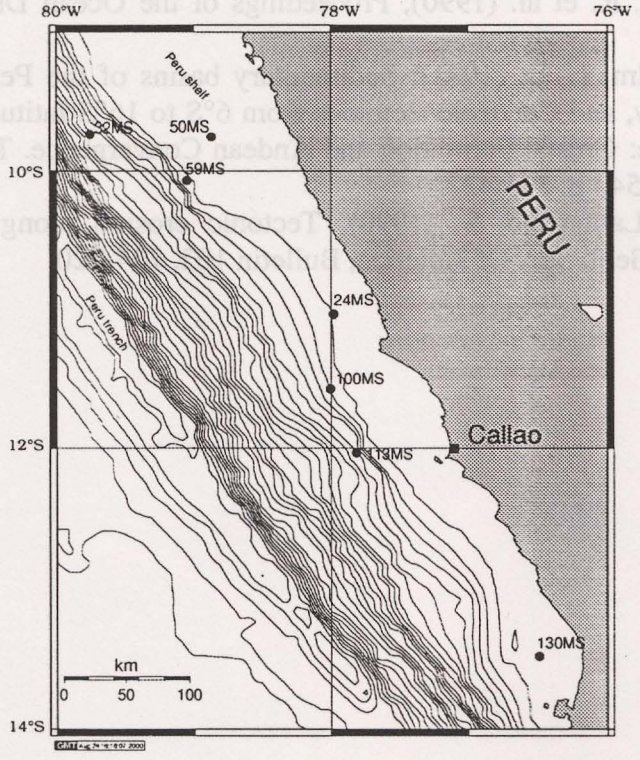

Fig. 6.1: CTD-stations of cruise SO-147 at the shelf and the upper slope off Peru

Results

Surface temperatures (at 1 meter depth) varied generally from 16 to 20°C. Salinity of surface waters was relatively uniform with values of 35.03 to 35.11 salinity units (Fig. 6.2). The depth of the pycnocline varied between 30 and 80 m. The lowest temperatures of about 4°C encountered at sites 32MS and 113MS were measured at 1100 and 1400m respectively.

Maximum oxygen concentrations in surface waters down to 15 m varied generally between 8 and 9 mg/l. These values decreased abruptly within 20 to 30 m at the pycnocline to about 4 mg/l and finally oxygen reaches values distinctly lower than 0.5 mg/l at 35 to 55 m water depth (Fig. 6.2). At stations 32MS and 59MS oxygen depletion is established at about 70 m. A distinct oxygen minimum layer was observed at all sampling stations off Peru. The oxygen minimum zone extends down to 600 m and deeper oxygen concentrations increases to values of about 3 mg/l at the two sites 32MS and 113MS (Fig. 6.2).

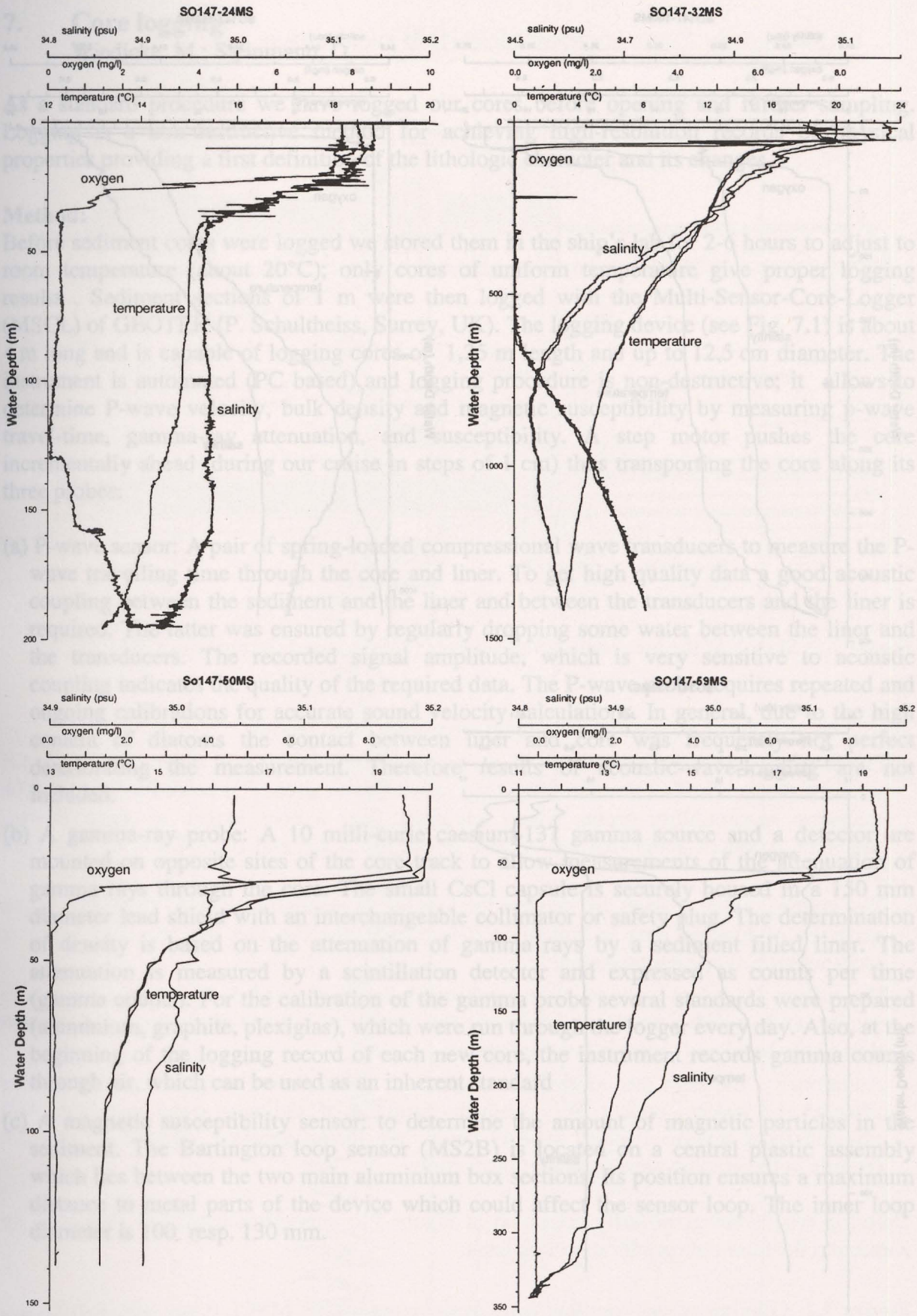

Fig. 6.2: Temperature distribution, salinity and oxygen concentrations at CTD stations 24MS, 32MS, 50MS and 59MS of SO147.

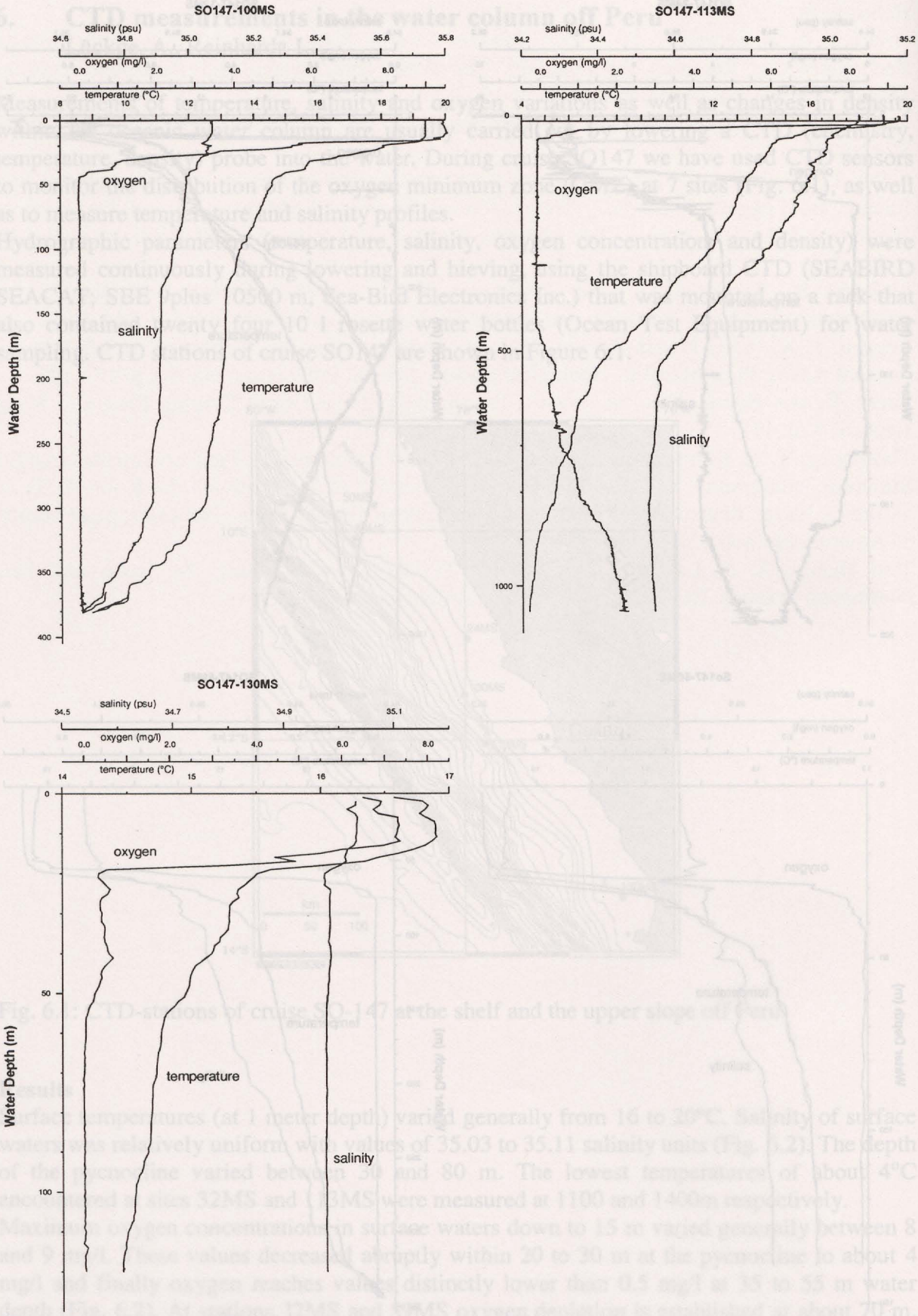

Fig. 6.2 (continued): Temperature distribution, salinity and oxygen concentrations at CTD stations 100MS, 113MS, and 130MS of SO147.

7. Core logging

Wiedicke, M.; Steinmann, D.

As a standard procedure we have logged our cores before opening and further sampling. Logging is a non-destructive method for achieving high-resolution records of physical properties providing a first definition of the lithologic character and its changes.

Method:

Before sediment cores were logged we stored them in the ship's lab for 2-6 hours to adjust to room temperature (about 20°C); only cores of uniform temperature give proper logging results . Sediment sections of 1 m were then logged with the Multi-Sensor-Core-Logger (MSCL) of GEOTEK (P. Schultheiss, Surrey, UK). The logging device (see Fig. 7.1) is about 4 m long and is capable of logging cores of 1,25 m length and up to 12,5 cm diameter. The instrument is automated (PC based) and logging procedure is non-destructive; it allows to determine P-wave velocity, bulk density and magnetic susceptibility by measuring p-wave travel-time, gamma-ray attenuation, and susceptibility. A step motor pushes the core incrementally ahead (during our cruise in steps of 1 cm) thus transporting the core along its three probes:

(a) P-wave sensor: A pair of spring-loaded compressional wave transducers to measure the P-wave travelling time through the core and liner. To get high quality data a good acoustic coupling between the sediment and the liner and between the transducers and the liner is required. The latter was ensured by regularly dropping some water between the liner and the transducers. The recorded signal amplitude, which is very sensitive to acoustic coupling indicates the quality of the required data. The P-wave probe requires repeated and ongoing calibrations for accurate sound velocity calculations. In general, due to the high content of diatoms the contact between liner and core was frequently not perfect deteriorating the measurement. Therefore results of acoustic-wave-logging are not included.

(b) A gamma-ray probe: A 10 milli-curie caesium-137 gamma source and a detector are mounted on opposite sites of the core track to allow measurements of the attenuation of gamma rays through the core. The small CsCl capsule is securely housed in a 150 mm diameter lead shield with an interchangeable collimator or safety plug. The determination of density is based on the attenuation of gamma rays by a sediment filled liner. The attenuation is measured by a scintillation detector and expressed as counts per time (gamma counts). For the calibration of the gamma probe several standards were prepared (aluminium, graphite, plexiglas), which were run through the logger every day. Also, at the beginning of the logging record of each new core, the instrument records gamma counts through air, which can be used as an inherent standard

(c) A magnetic susceptibility sensor: to determine the amount of magnetic particles in the sediment. The Bartington loop sensor (MS2B) is located on a central plastic assembly which lies between the two main aluminium box sections. Its position ensures a maximum distance to metal parts of the device which could affect the sensor loop. The inner loop diameter is 100 resp. 130 mm.

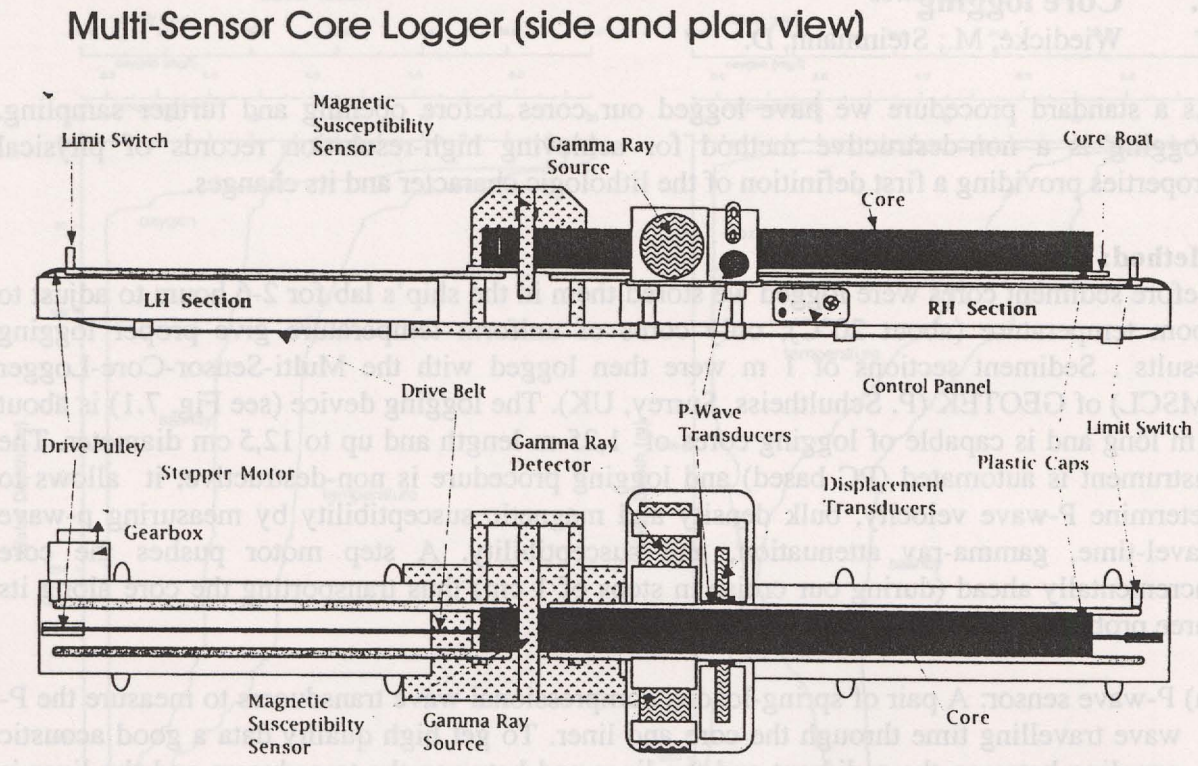

Figure 7.1: Sketch of the multi-sensor core-logger (MSCL) used during cruise SO-147

Additional aspects of importance to logging are briefly listed below:

- The continuity of the measurements along core is slightly interrupted at the ends of the 1m sections despite the fact that the following 1m-section is already in place for logging. The magnetic susceptibility probe, which integrates over a core length of about 15 cm, therefore produces somewhat low values in the top 8 cm and basal 8 cm of each core section.
- The starting point of each 1m section for logging is manually defined. Therefore, depth accuracy of logging data is limited (+ 2-3 cm) despite the fact that the step motor is working with very high precision.
- The cutting procedure tends to cause mechanical disturbances of the sediment core at both section ends which sometimes influences the quality of gamma-attenuation and P-wave data in the basal and topmost few centimetres.
- Additionally, the high gas content of several of the sediment cores of this cruise also affected the gamma counts. Poor acoustic coupling of sediment cores and liner wall affected most p-wave logs of SO-147 cores. We have, therefore, omitted the p-wave records in the graphic presentation of most cores.

Core-log results are graphically presented in Figure 7.2; curves represent raw data with no correction for false data points at section ends.

Figure 7.2: Logging curves resulting from deployment of the MSCL (Core nos. 4, 6,12, 25, 27, 34, 41, 44, 46, 78, 83, 87, 97, 103, 105, 106, 136, 137, 144); for most cores p-wave record is not presented due to poor acoustic coupling of sediment and liner wall.

SO147 04SL

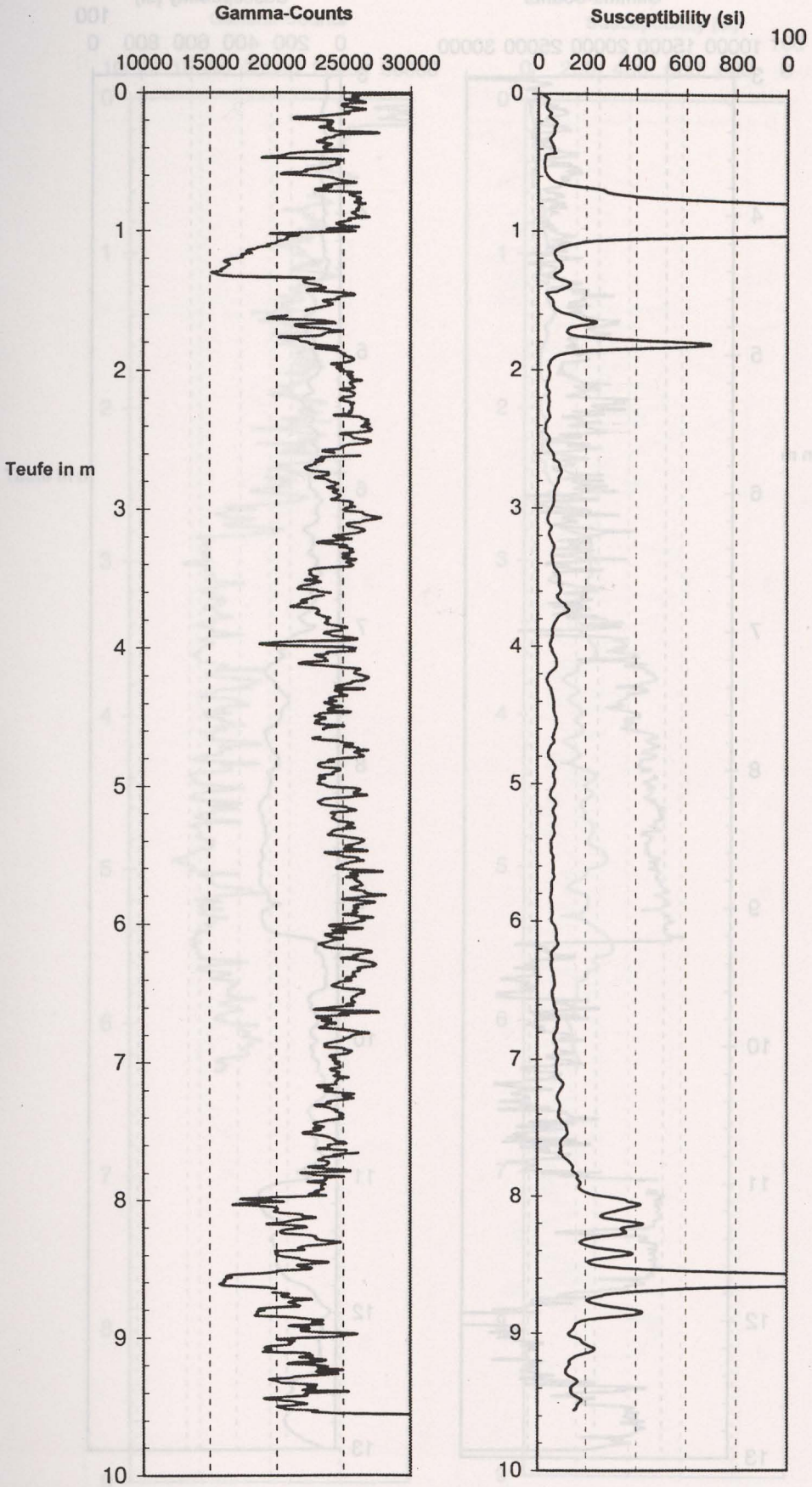
Gamma-Counts
10000 15000 20000 25000 30000
Susceptibility (si)
0 200 400 600 800 100 0
Teufe in m
0
1
2
3
4
5
6
7
8
9
10

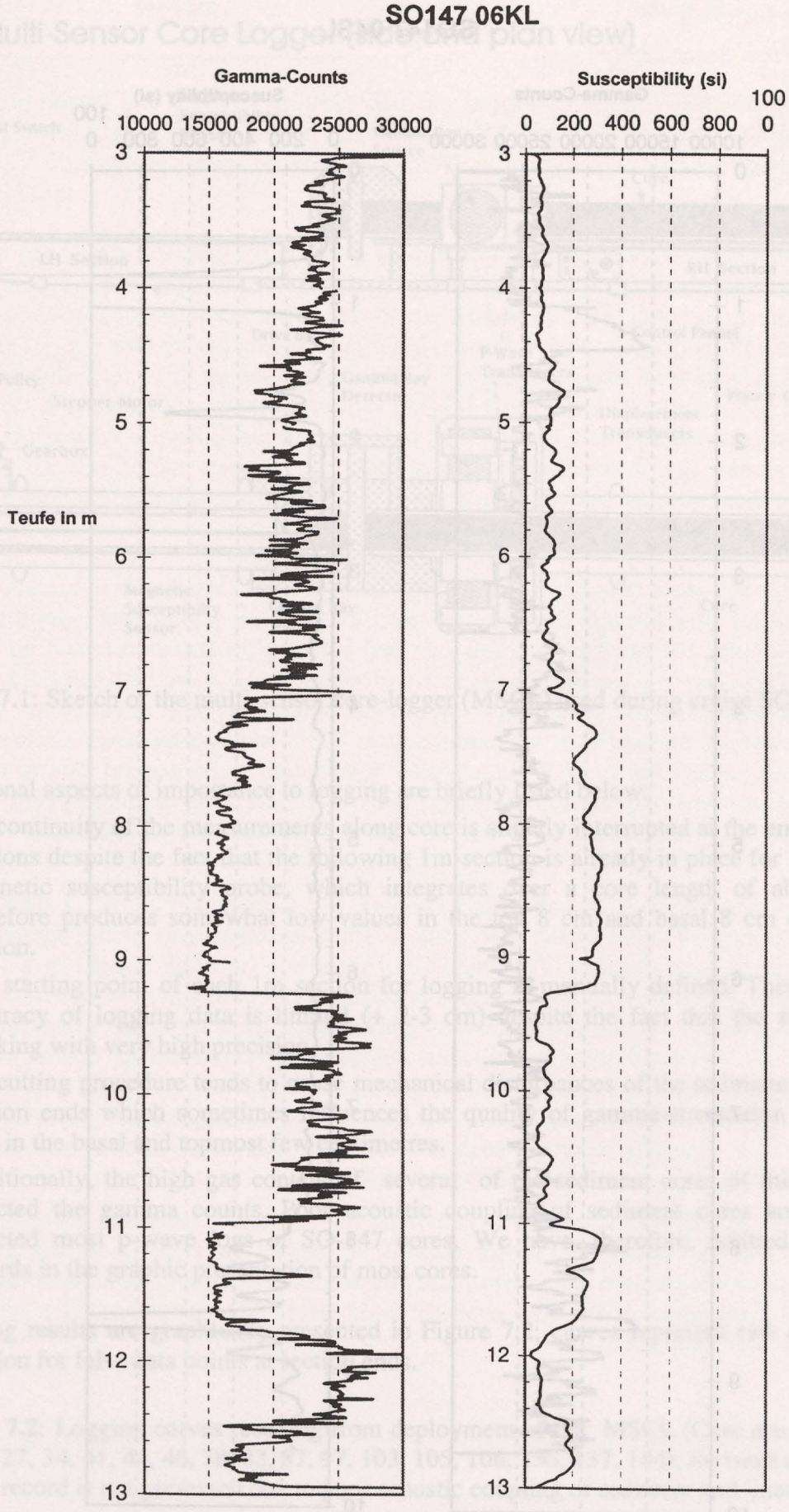
SO147 06KL
Gamma-Counts
10000 15000 20000 25000 30000
Susceptibility (si)
0 200 400 600 800 100 0
Teufe in m
3
4
5
6
7
8
9
10
11
12
13

SO147 12KL

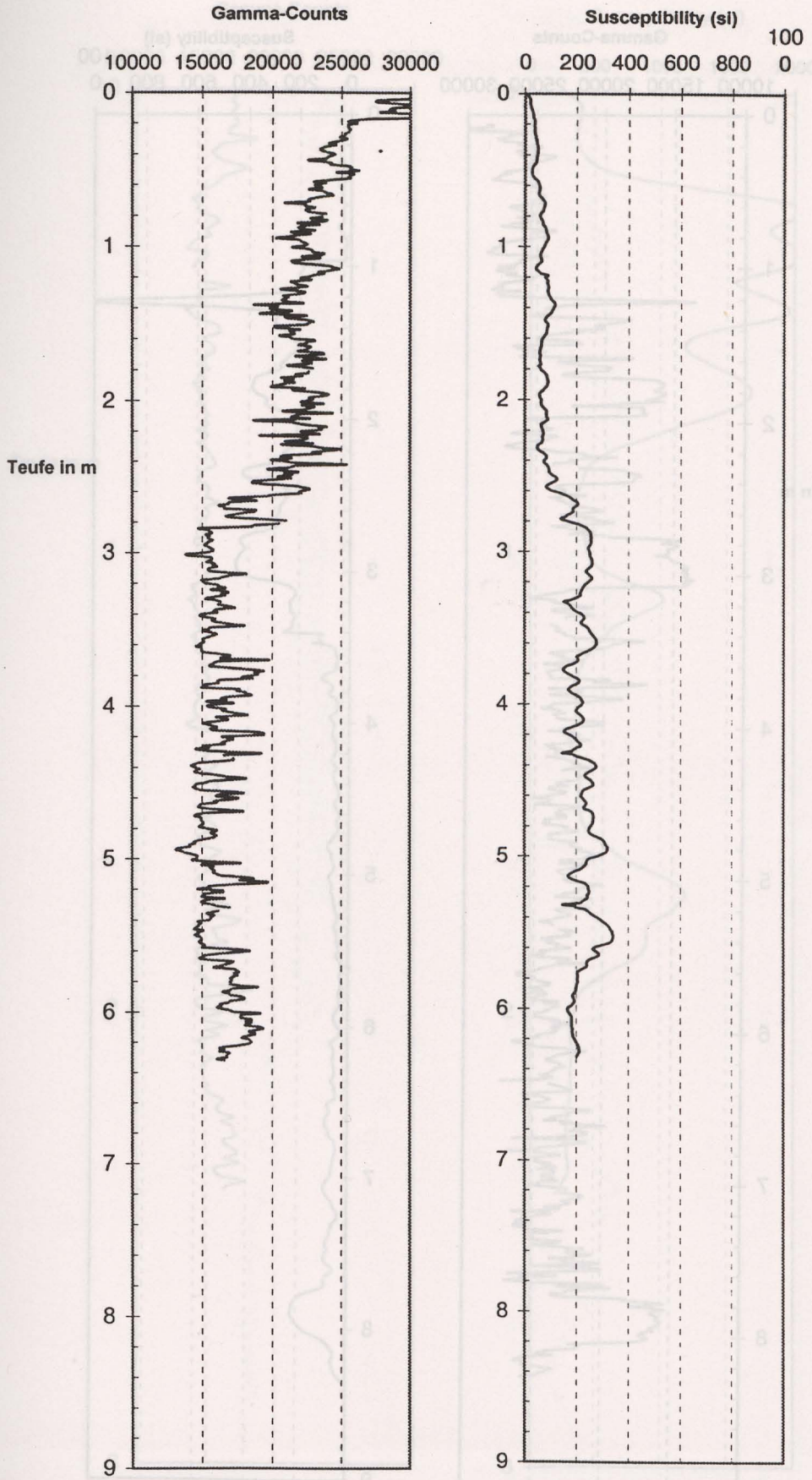
Gamma-Counts
10000 15000 20000 25000 30000
Susceptibility (si)
0 200 400 600 800 100 0
Teufe in m
0
1
2
3
4
5
6
7
8
9

SO147 25SL

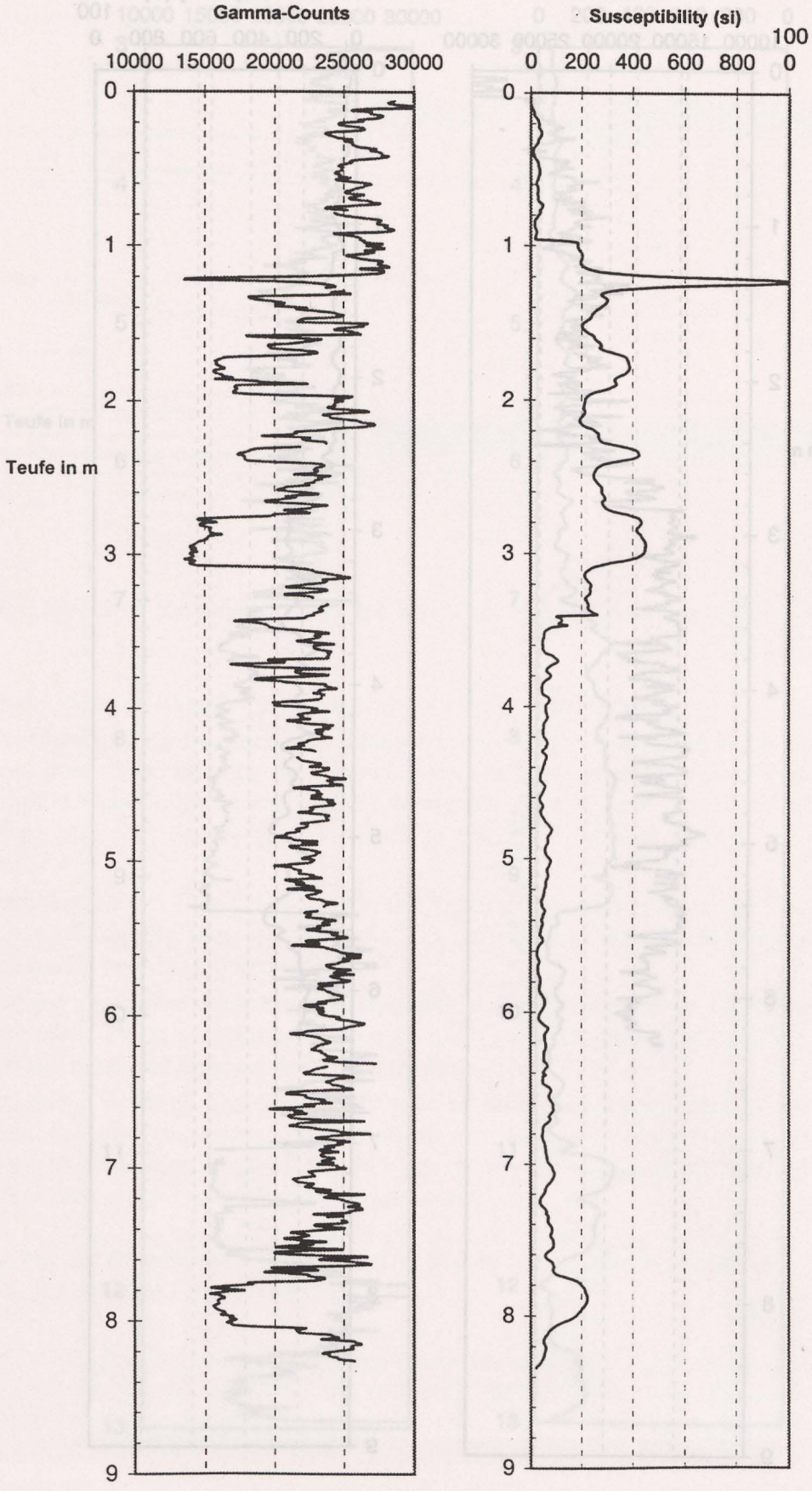
Gamma-Counts
10000 15000 20000 25000 30000
Susceptibility (si)
0 200 400 600 800 100
0
Teufe in m
0
1
2
3
4
5
6
7
8
9

SO147 27KL

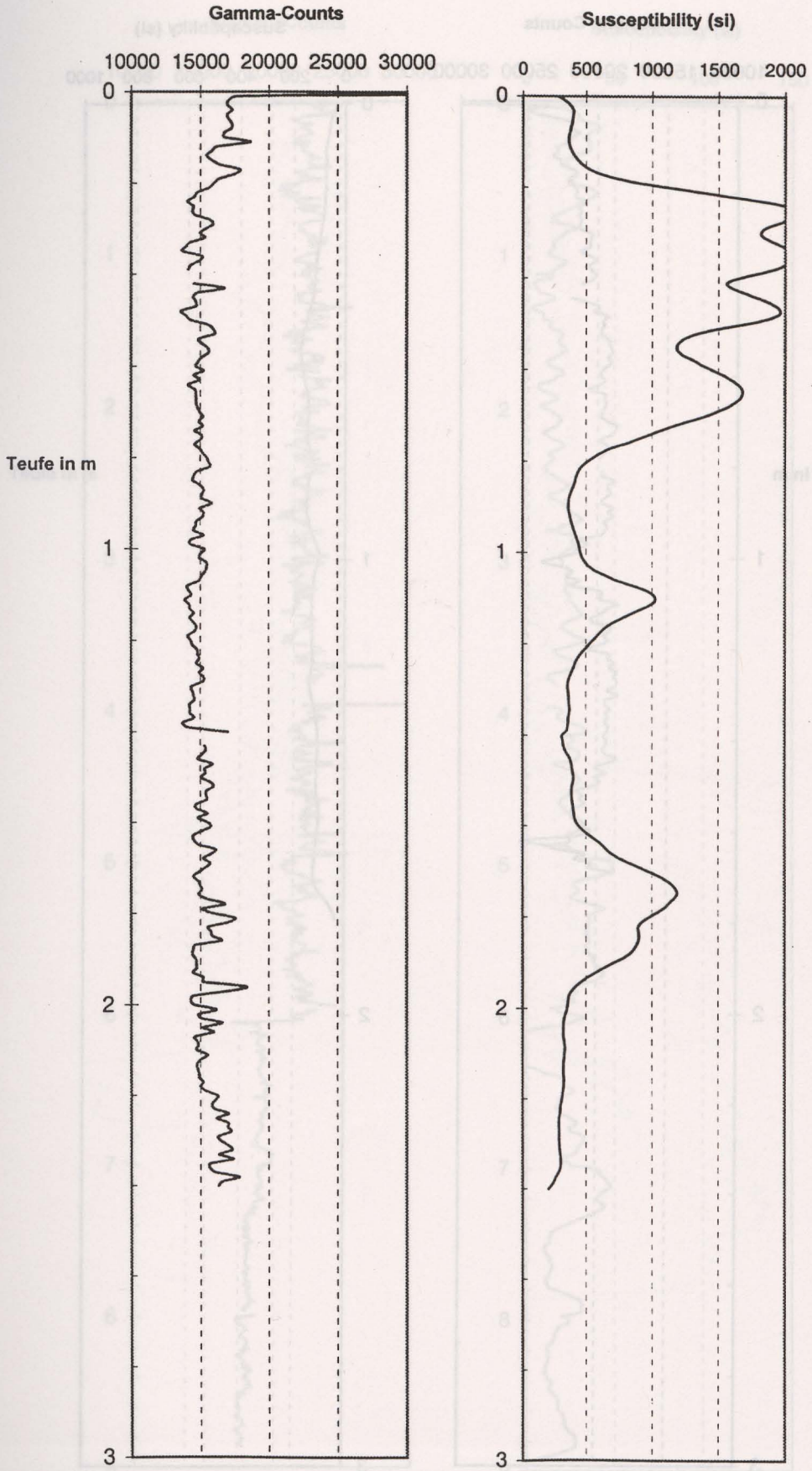
Gamma-Counts
10000 15000 20000 25000 30000
Susceptibility (si)
0 500 1000 1500 2000
Teufe in m
0
1
2
3

SO147 34SL

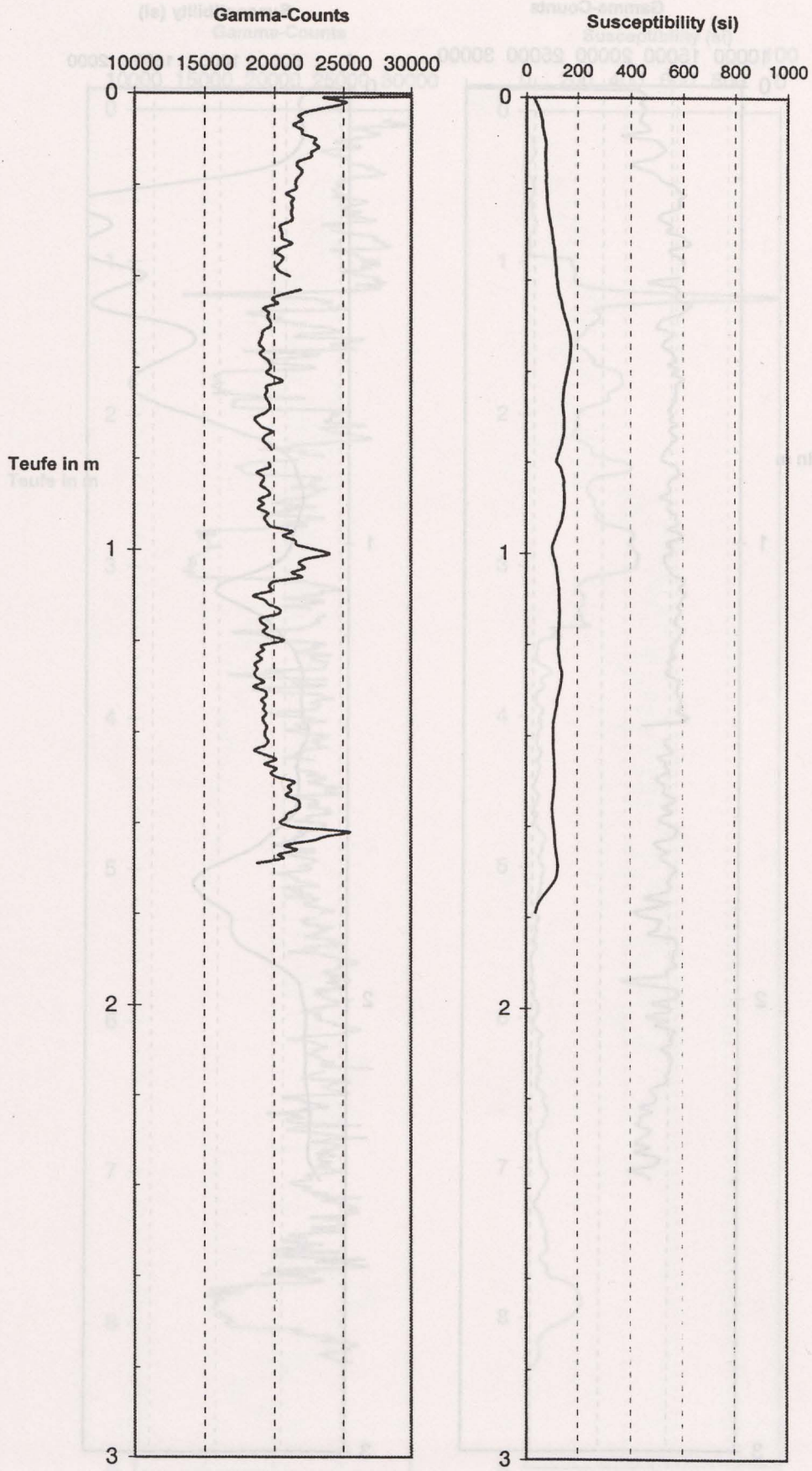
Gamma-Counts
10000 15000 20000 25000 30000
Susceptibility (si)
0 200 400 600 800 1000
Teufe in m
0
1
2
3

SO147 41SL

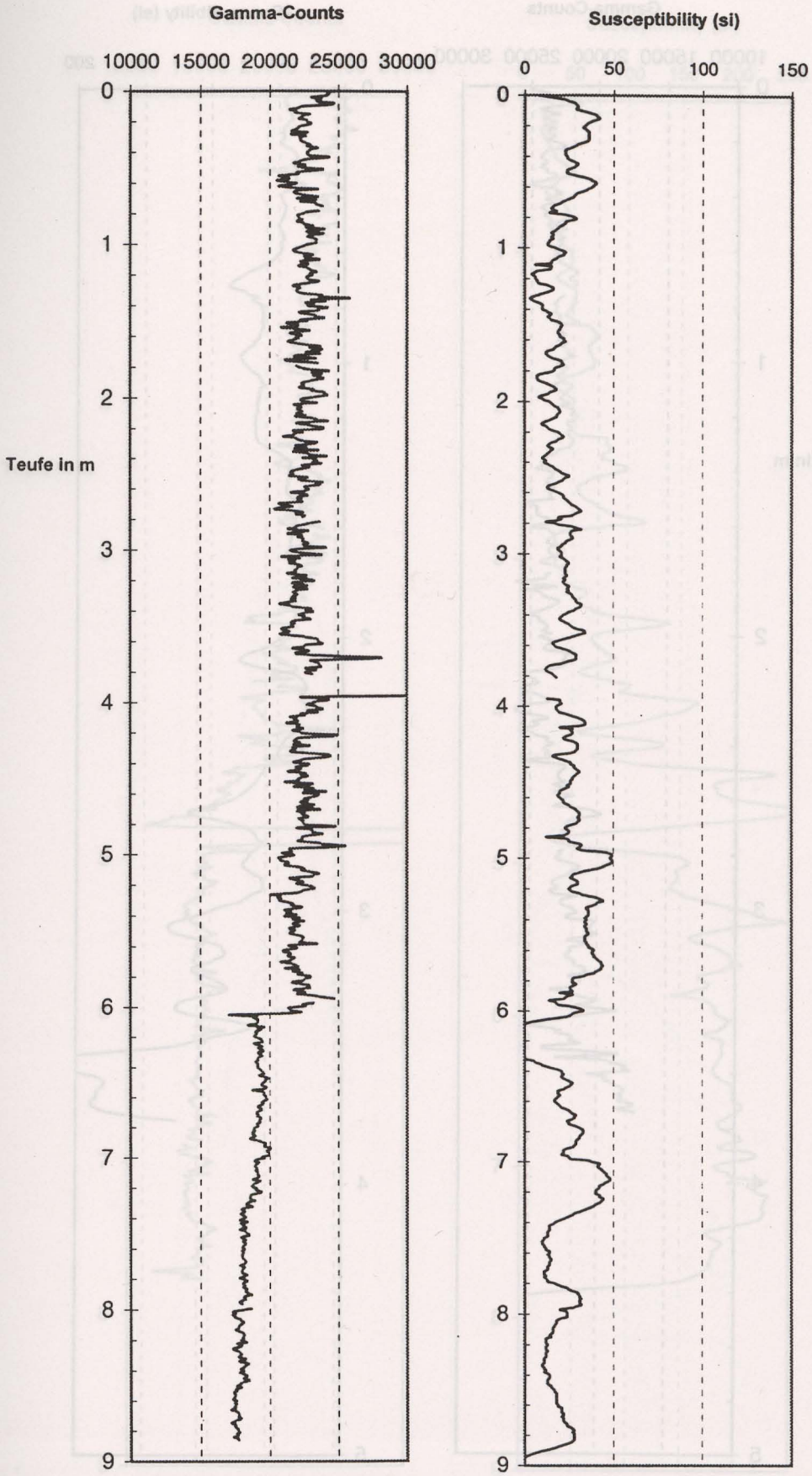
Gamma-Counts
10000 15000 20000 25000 30000
Susceptibility (si)
0 50 100 150
Teufe in m
0
1
2
3
4
5
6
7
8
9

SO147 44SL

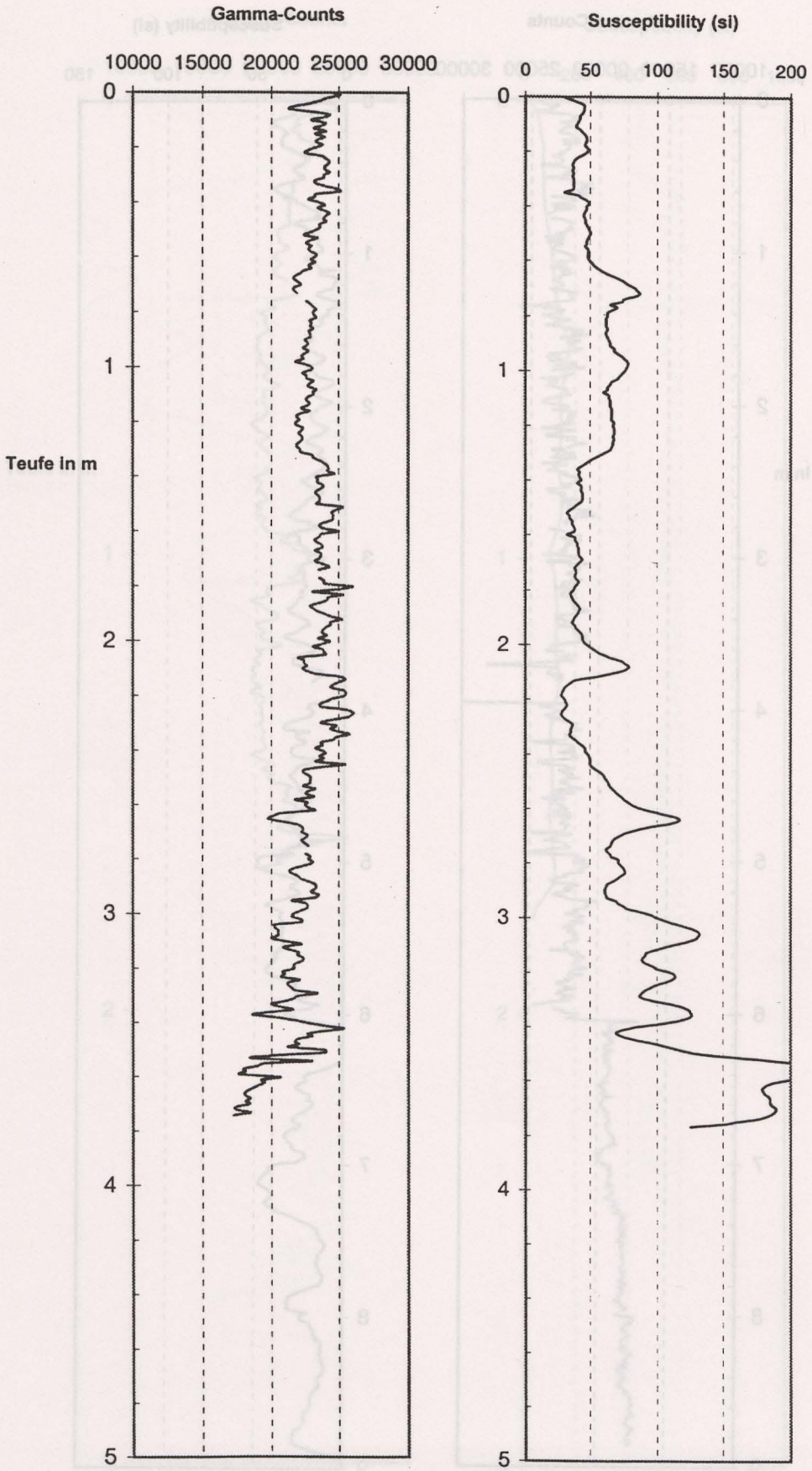
Gamma-Counts
10000 15000 20000 25000 30000
Susceptibility (si)
0 50 100 150 200
Teufe in m
0
1
2
3
4
5

SO147 46KL

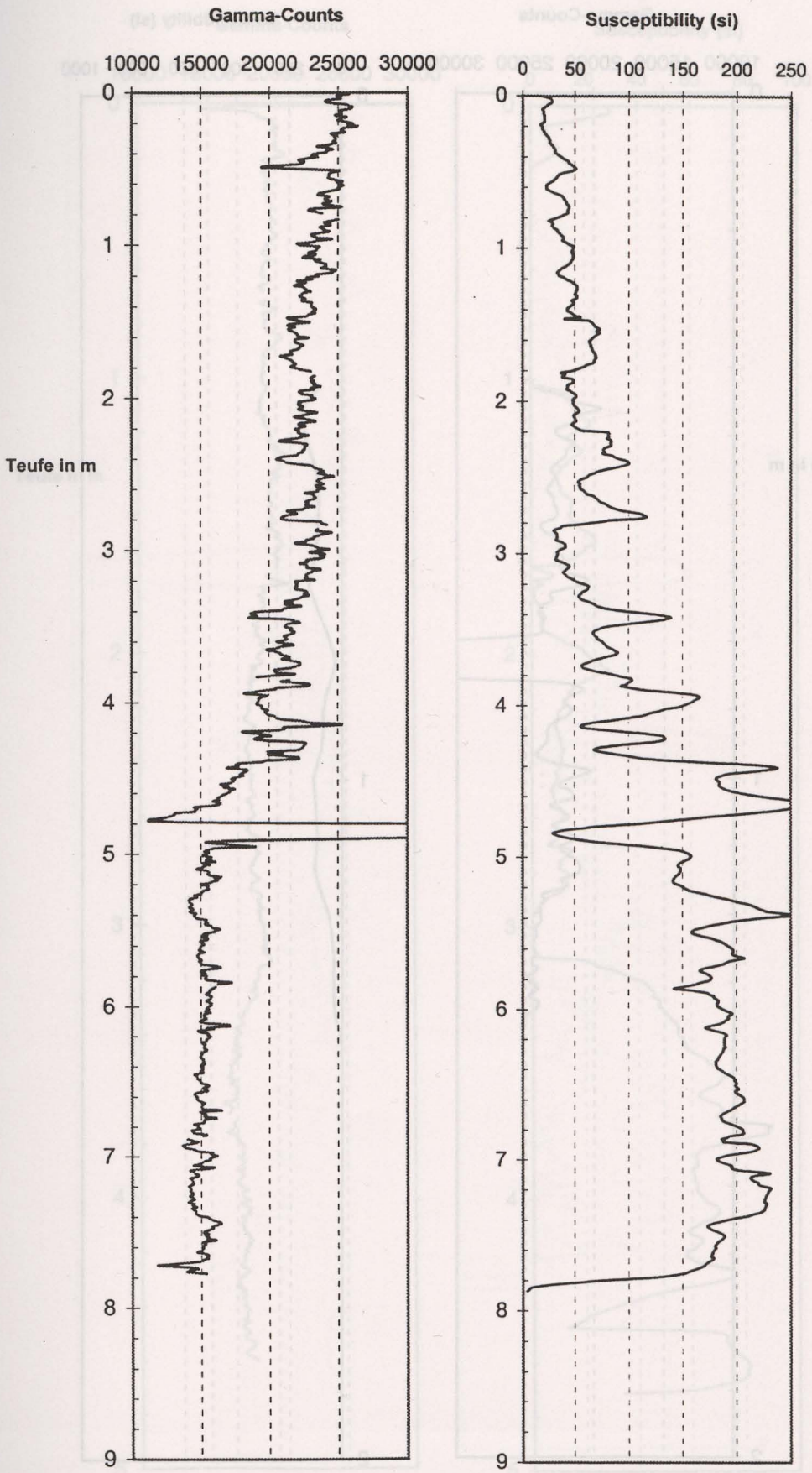
Gamma-Counts
10000 15000 20000 25000 30000
Susceptibility (si)
0 50 100 150 200 250
Teufe in m
0
1
2
3
4
5
6
7
8
9

SO147 78SL

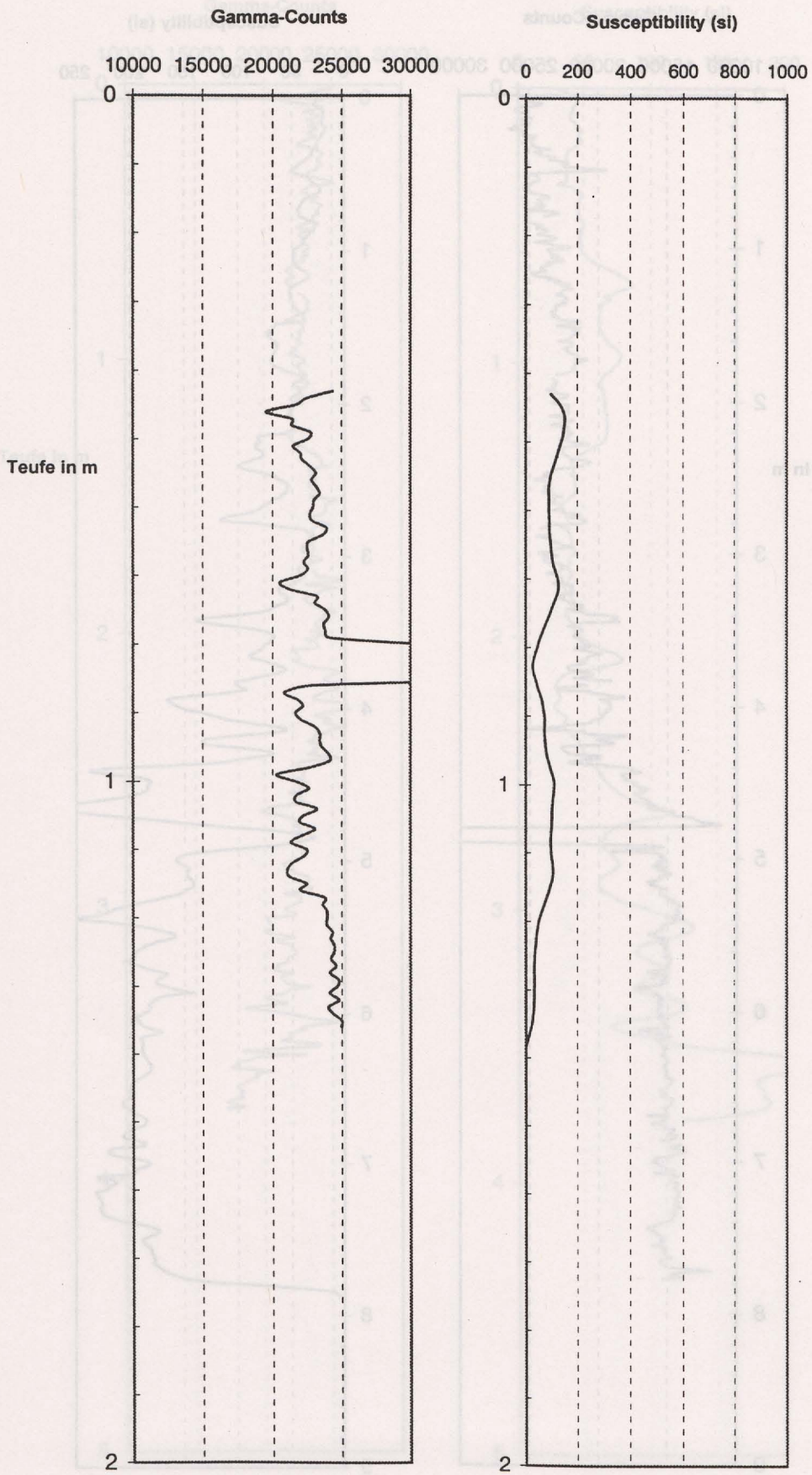
Gamma-Counts
10000 15000 20000 25000 30000
Susceptibility (si)
0 200 400 600 800 1000
Teufe in m
0
1
2
0
1
2

SO147 83SL

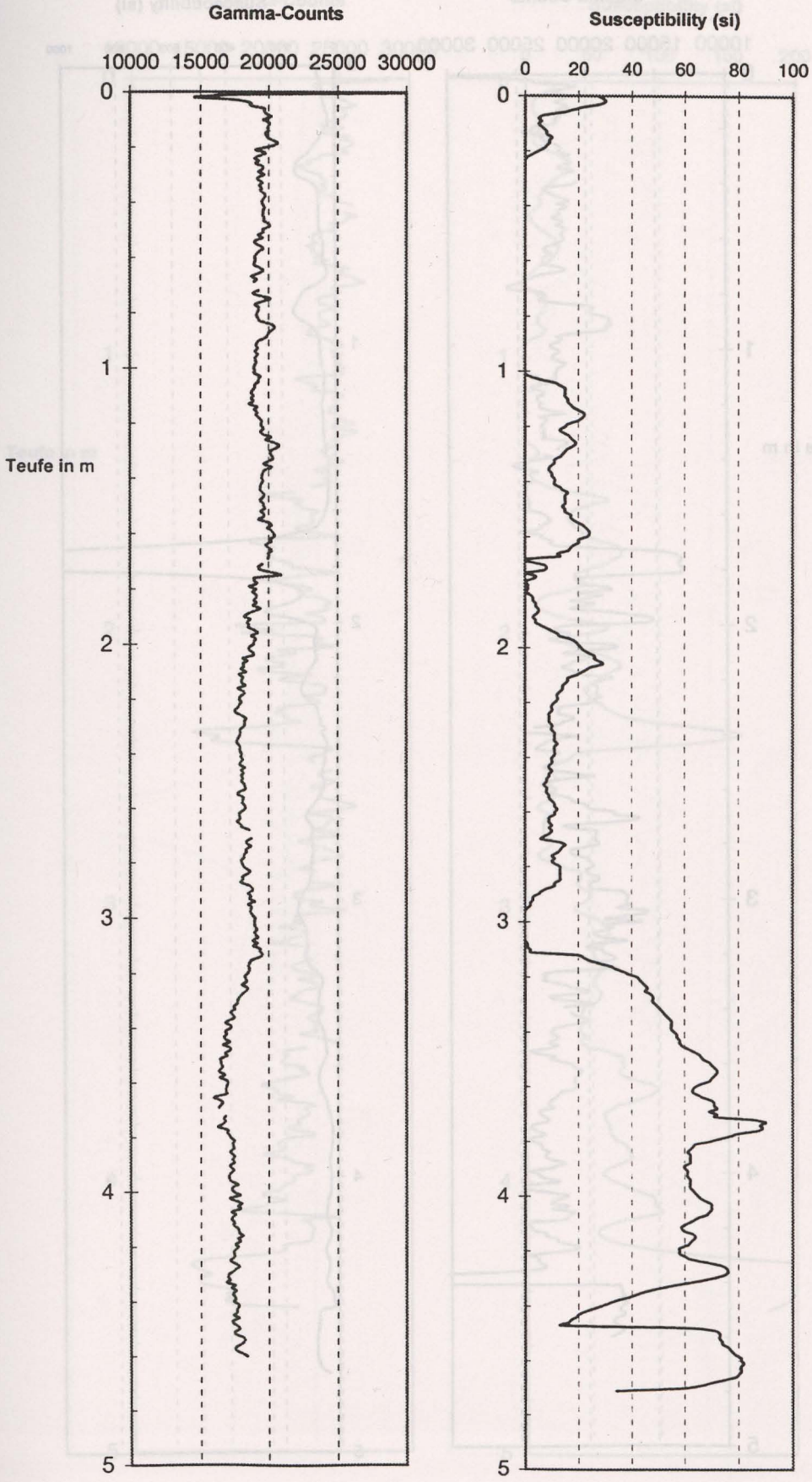
Gamma-Counts
10000 15000 20000 25000 30000
Susceptibility (si)
0 20 40 60 80 100
Teufe in m
0
1
2
3
4
5

SO147 87SL

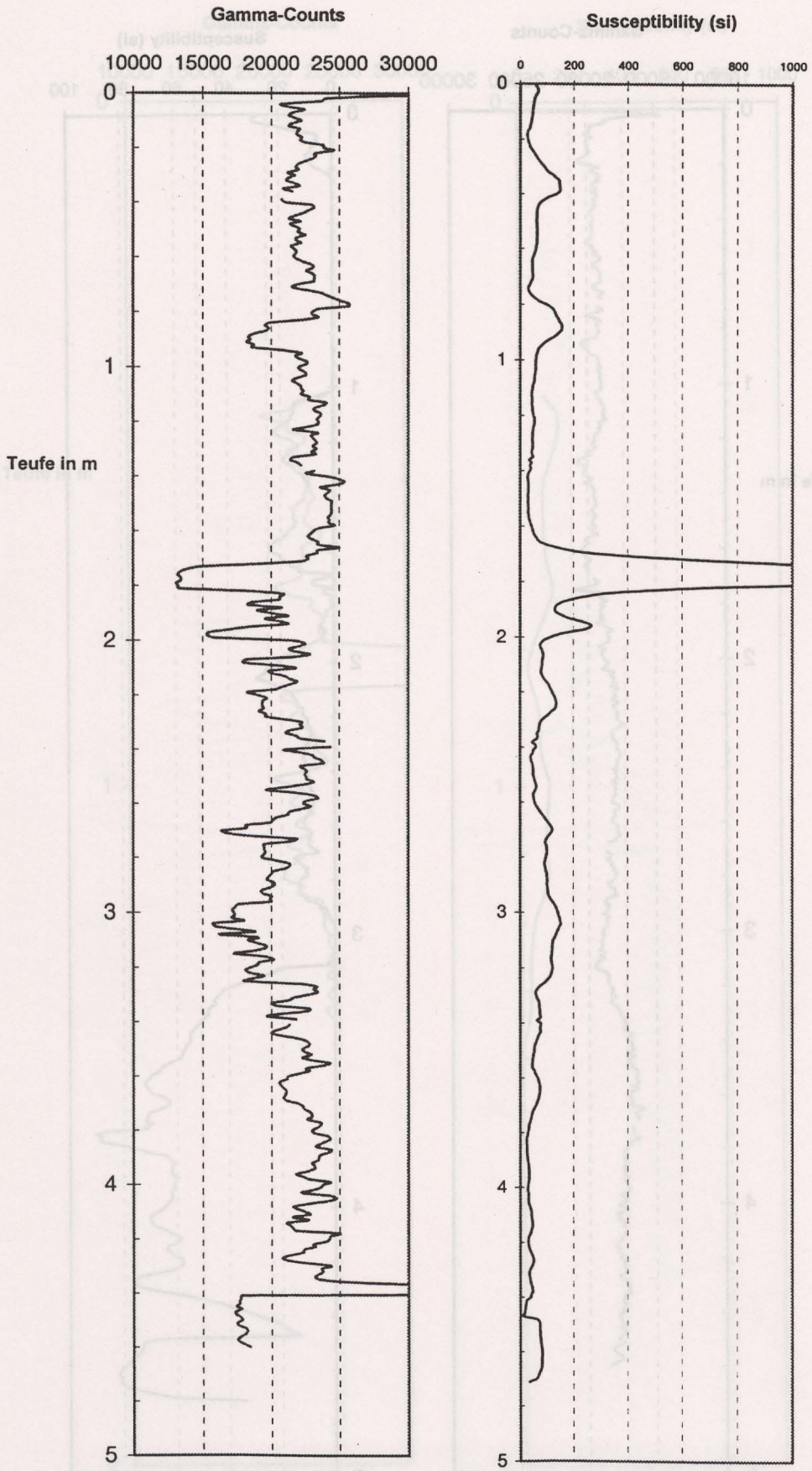
Gamma-Counts
10000 15000 20000 25000 30000
Susceptibility (si)
0 200 400 600 800 1000
Teufe in m
0
1
2
3
4
5

SO147 97SL

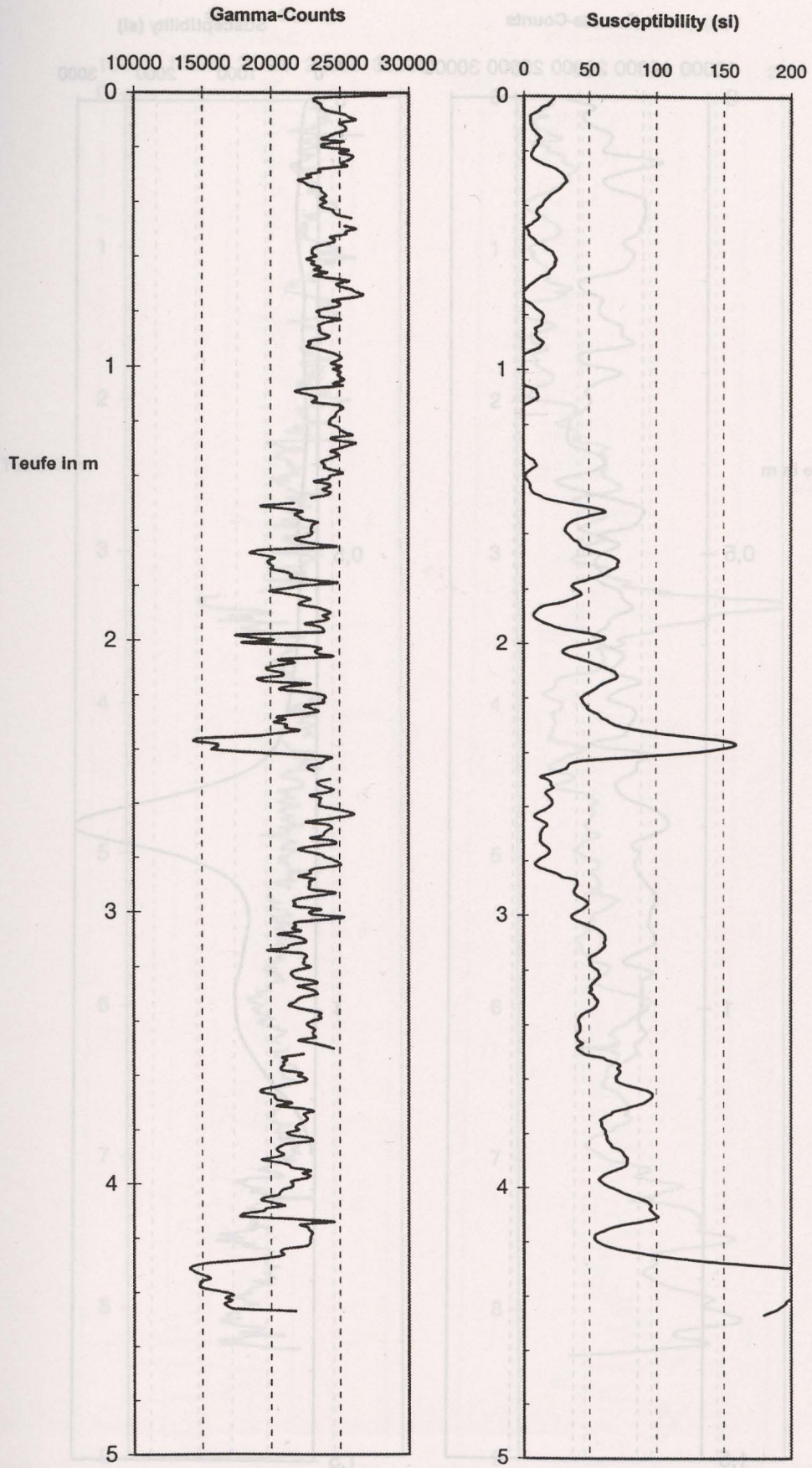
Gamma-Counts
10000 15000 20000 25000 30000
Susceptibility (si)
0 50 100 150 200
Teufe in m
0
1
2
3
4
5

SO147 103SL

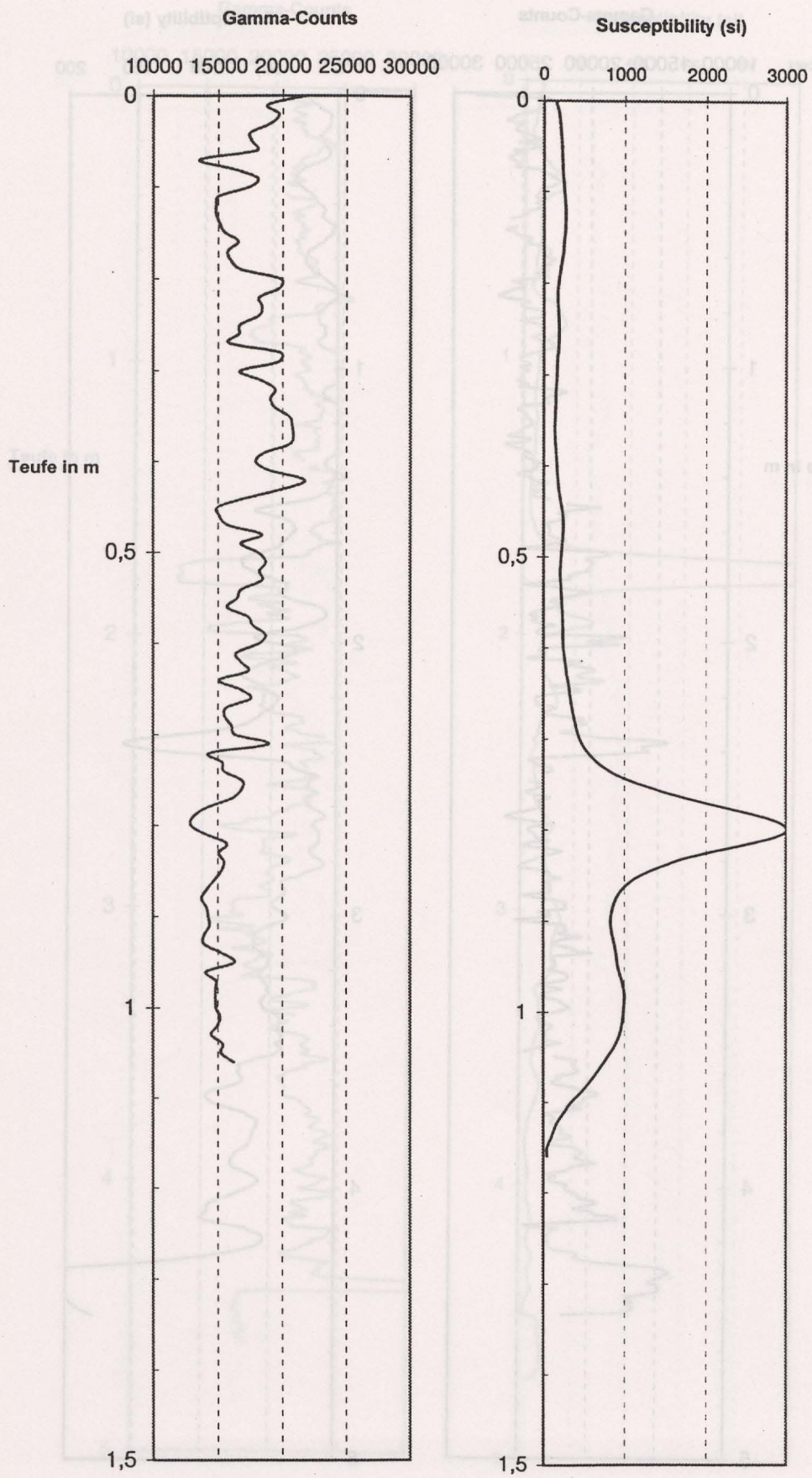
Gamma-Counts
10000 15000 20000 25000 30000
Susceptibility (si)
0 1000 2000 3000
Teufe in m
0
0,5
1
1,5

SO147105SL

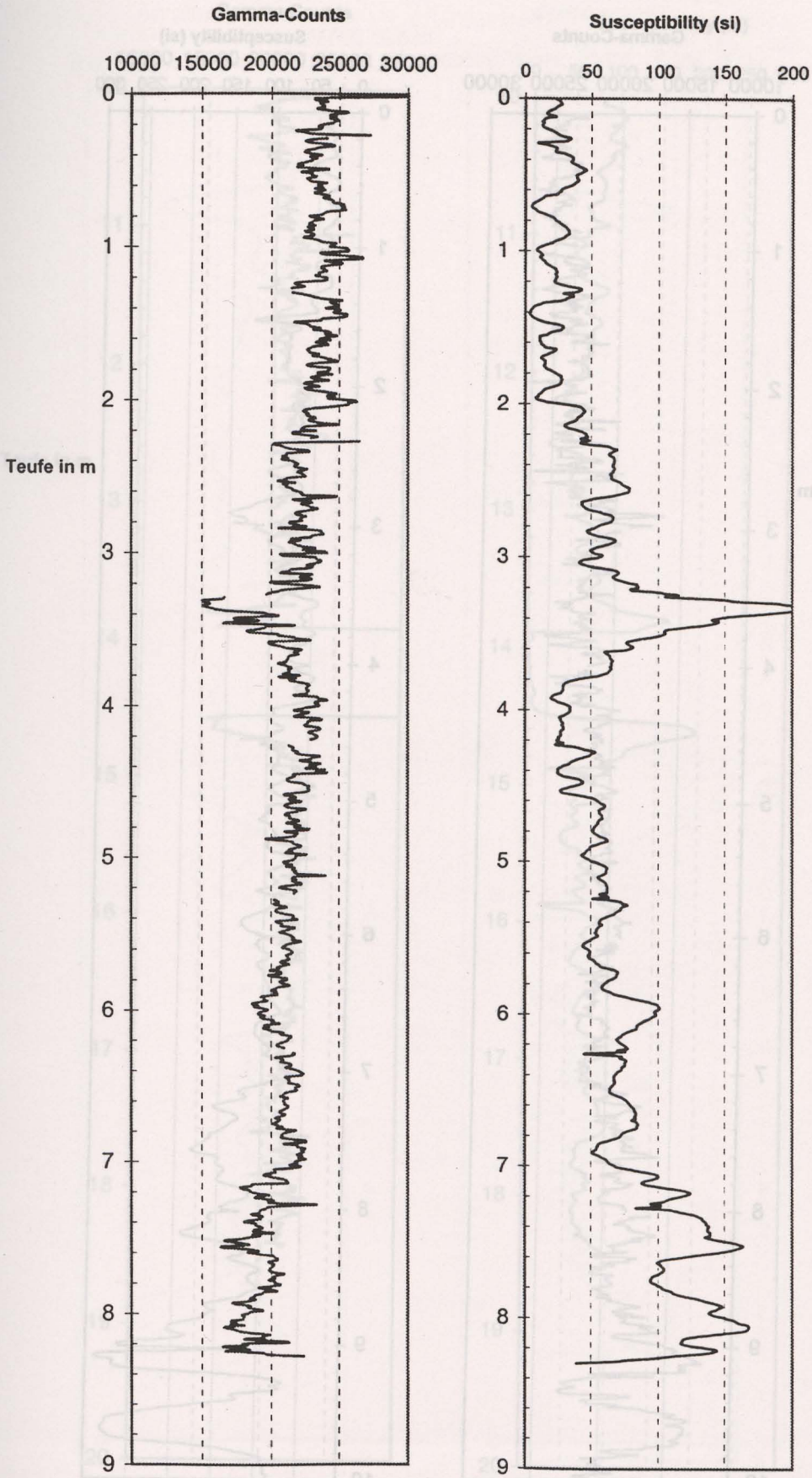
Gamma-Counts
10000 15000 20000 25000 30000
Susceptibility (si)
0 50 100 150 200
Teufe in m
0
1
2
3
4
5
6
7
8
9

SO147106KL

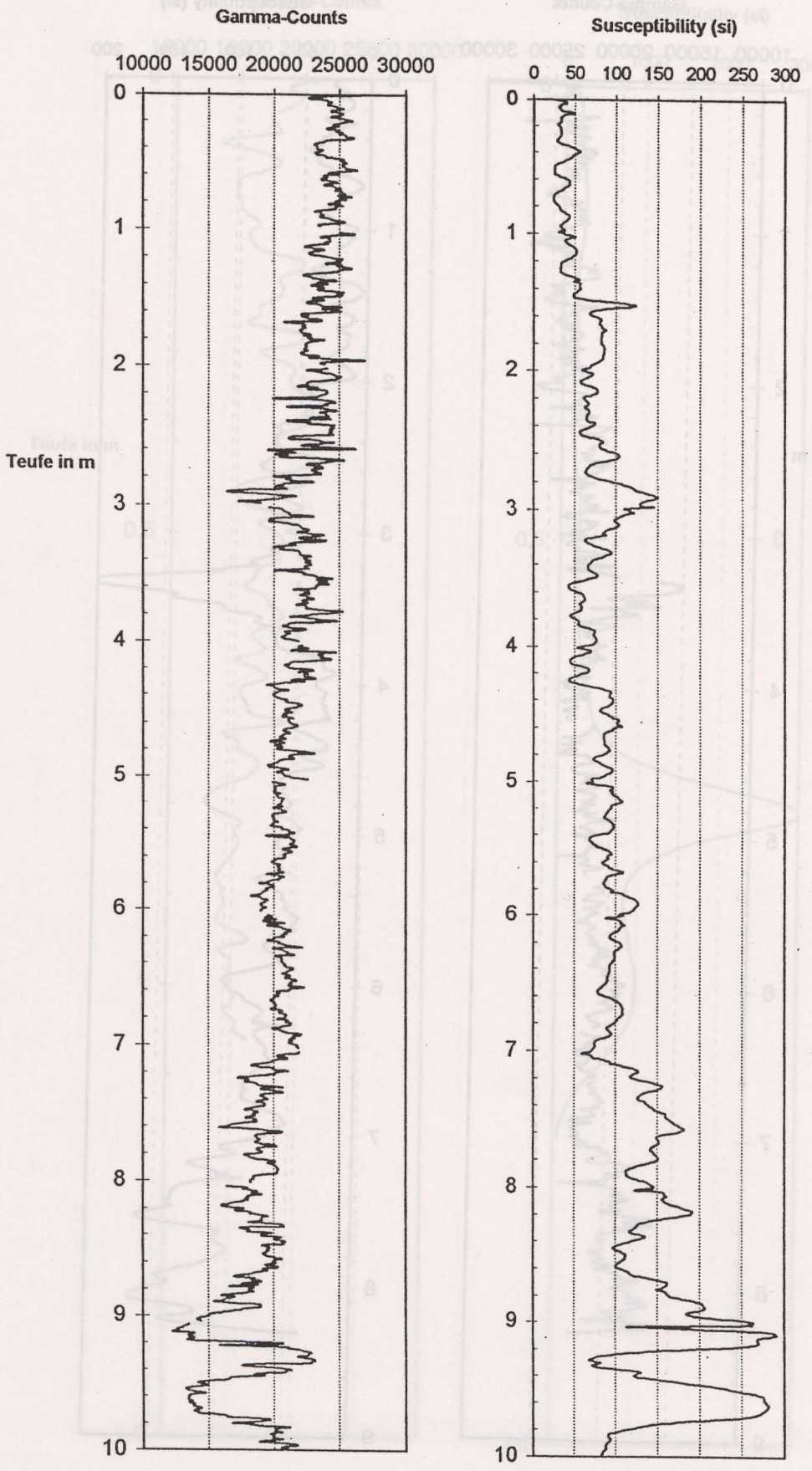
Gamma-Counts
10000 15000 20000 25000 30000
Susceptibility (si)
0 50 100 150 200 250 300
Teufe in m
0
1
2
3
4
5
6
7
8
9
10

SO147106KL

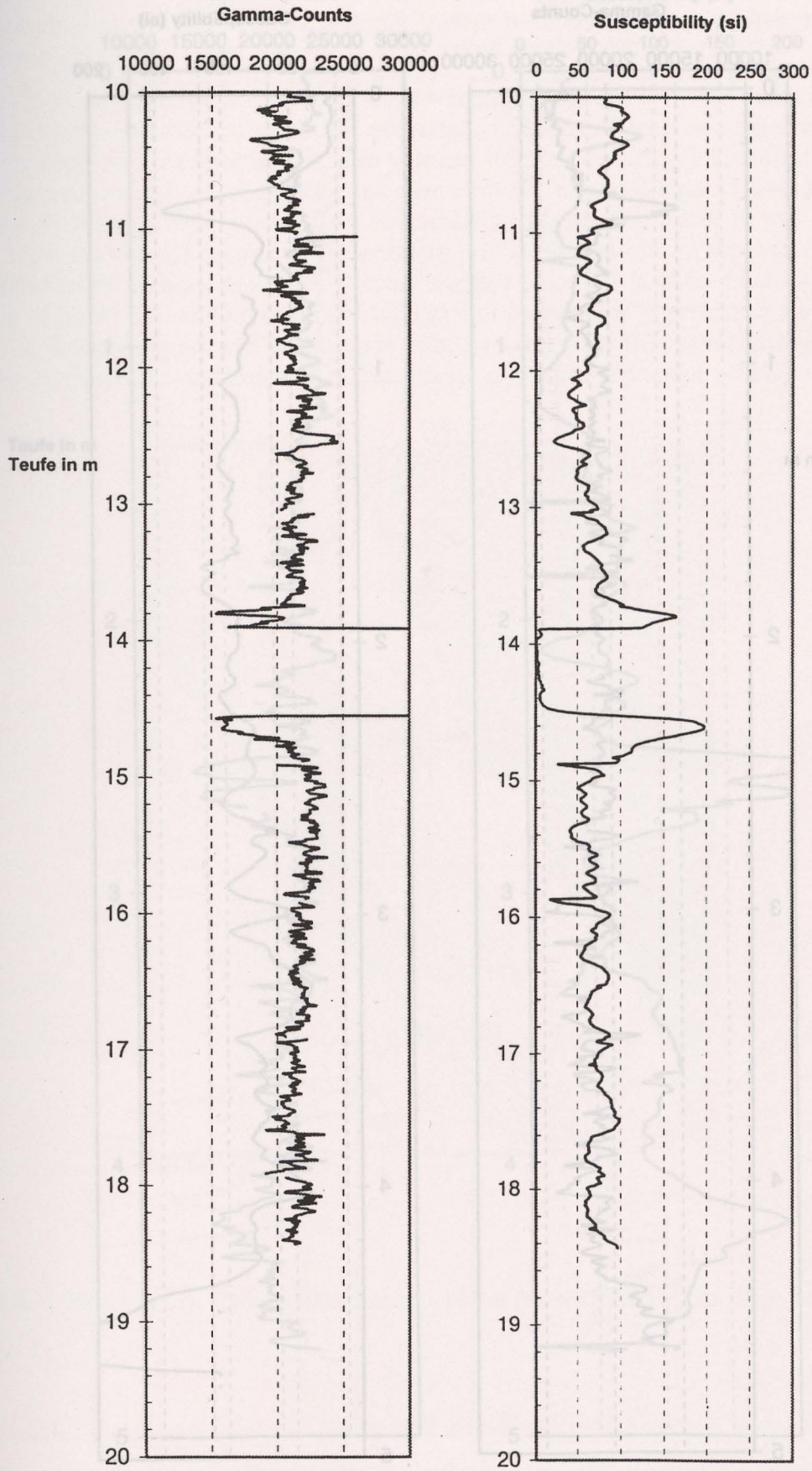
Gamma-Counts
10000 15000 20000 25000 30000
Susceptibility (si)
0 50 100 150 200 250 300
Teufe in m
10
11
12
13
14
15
16
17
18
19
20

SO147 136SL

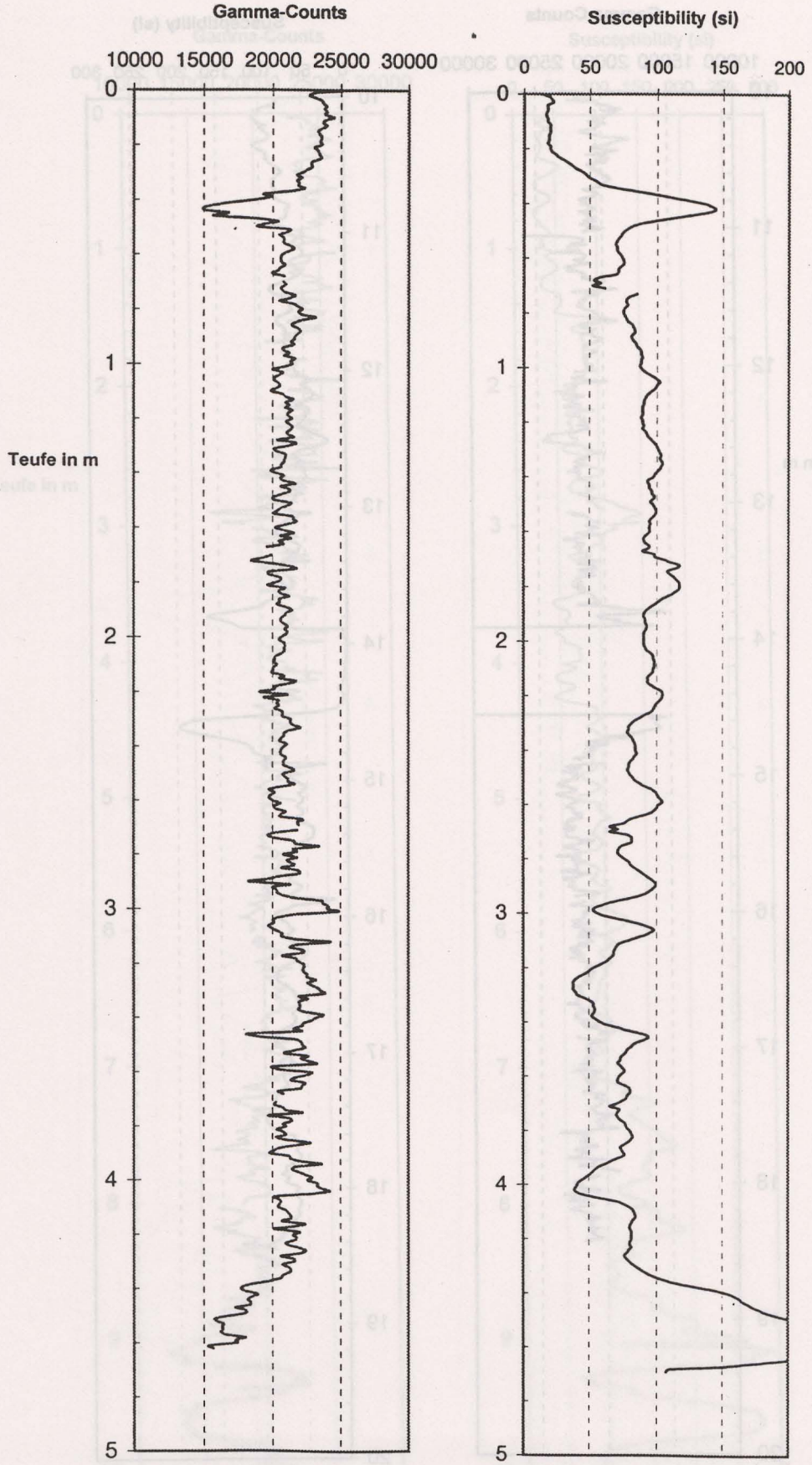
Gamma-Counts
10000 15000 20000 25000 30000
Susceptibility (si)
0 50 100 150 200
Teufe in m
0
1
2
3
4
5

SO147 137SL

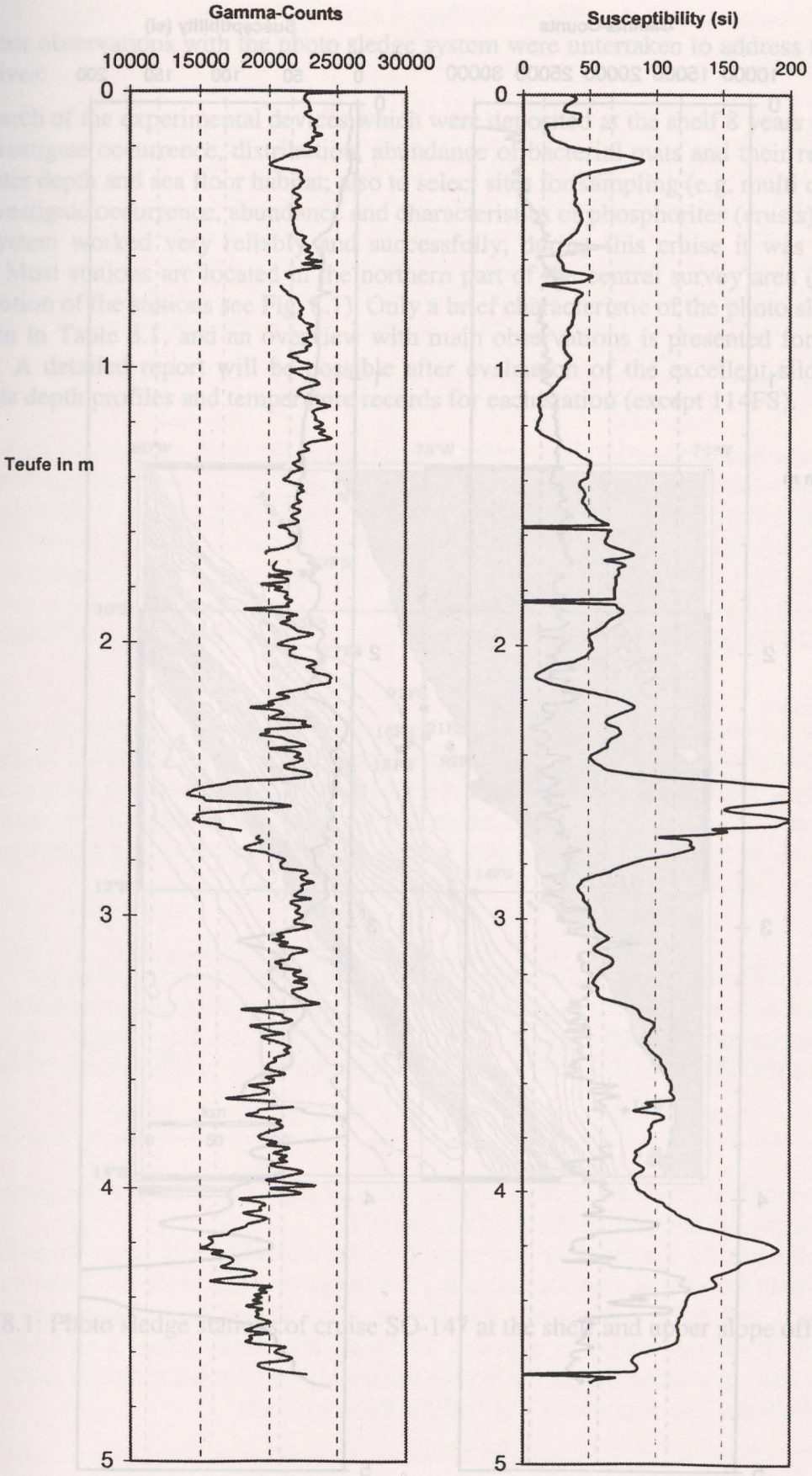
Gamma-Counts
10000 15000 20000 25000 30000
Susceptibility (si)
0 50 100 150 200
Teufe in m
0
1
2
3
4
5

SO147 144SL

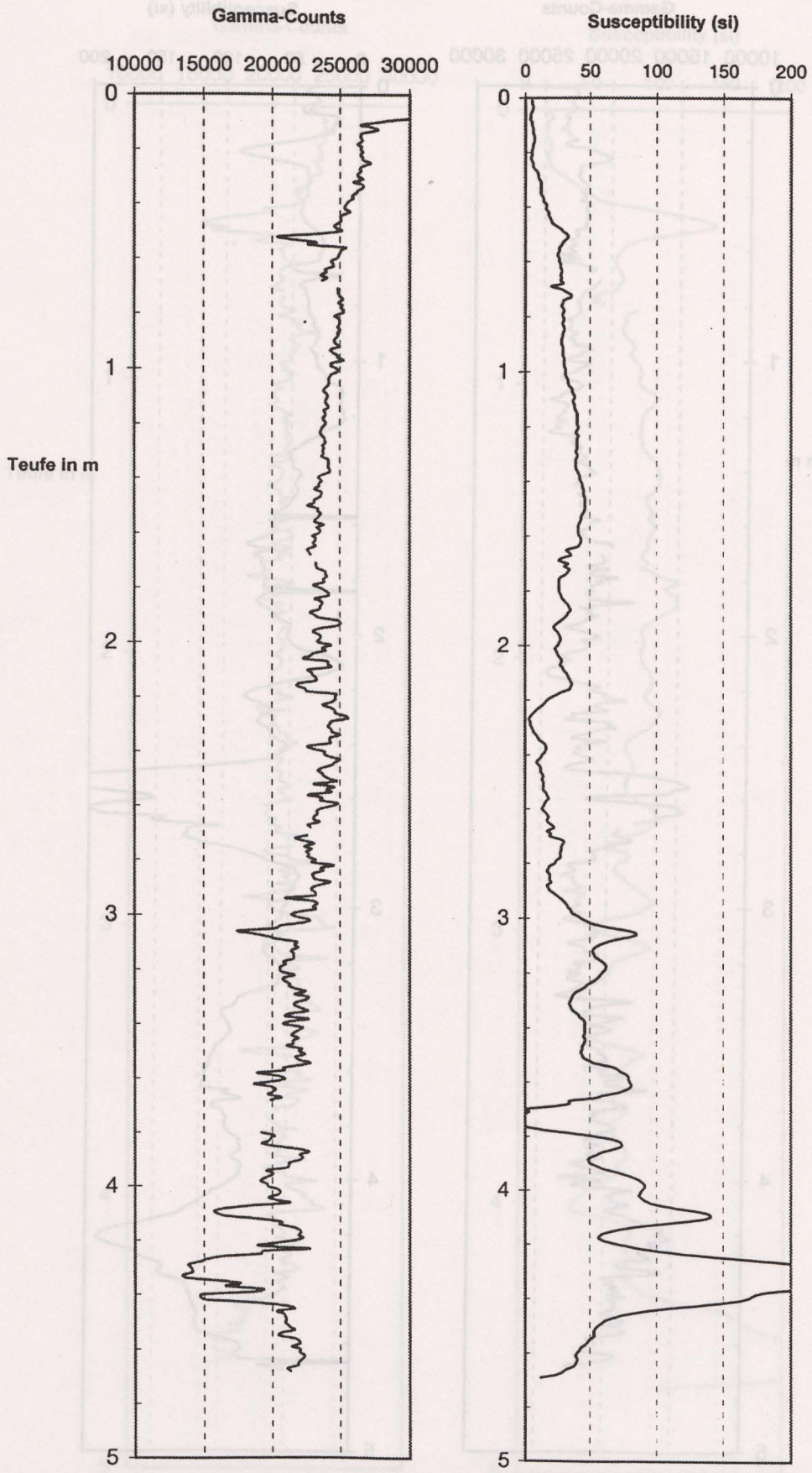
Gamma-Counts
10000 15000 20000 25000 30000
Susceptibility (si)
0 50 100 150 200
Teufe in m
0
1
2
3
4
5

8. Deployment of the photo sledge (OFOS)

Wiedicke, M.

Sea floor observations with the photo sledge system were untertaken to address the following objectives:

- Search of the experimental devices which were deposited at the shelf 8 years ago;
- Investigate occurrence, distribution, abundance of bacterial mats and their relationship to water depth and sea floor habitat; also to select sites for sampling (e.g. multi corer);
- Investigate occurrence, abundance and characteristics of phosphorites (crusts);

The system worked very reliably and successfully; during this cruise it was deployed 10 times. Most stations are located in the northern part of the central survey area (Area A) (for distribution of the stations see Fig. 8.1). Only a brief characteristic of the photo sledge stations is given in Table 8.1, and an overview with main observations is presented for each station below. A detailed report will be possible after evaluation of the excellent slides. Figure 2 presents depth profiles and temperature records for each station (except 114FS).

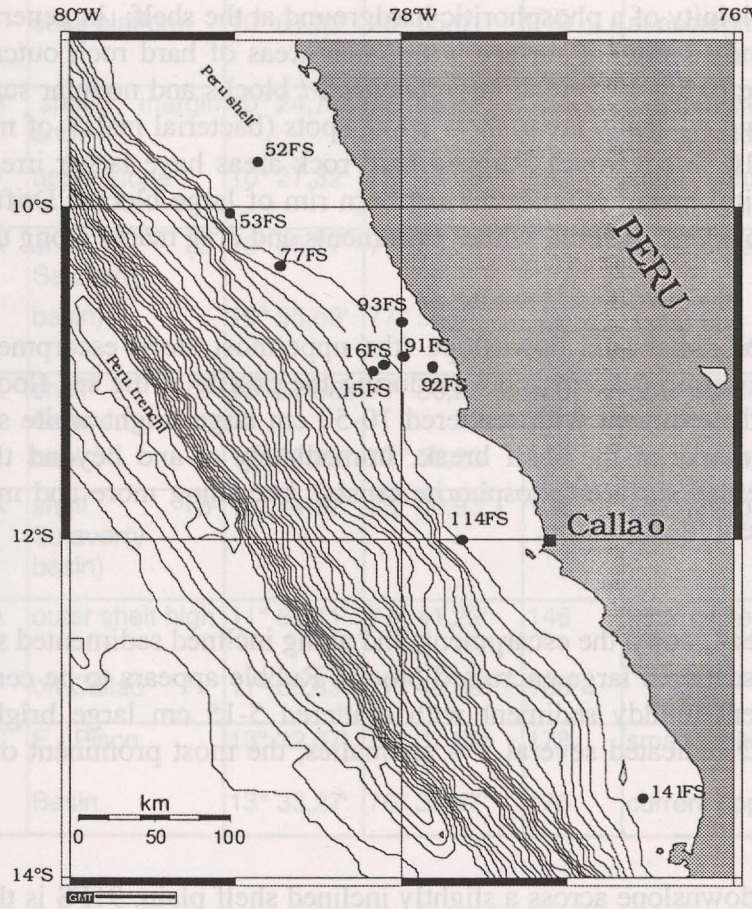

Figure 8.1: Photo sledge stations of cruise SO-147 at the shelf and upper slope off Peru

15FS:
Track across mud waves in water depths of 280-360 m. No obvious difference in the frequency of benthic animals and traces where observed between 'mud wave areas' and inbetween mud waves.

16FS:
Photo profile in search of experimental devices deposited at the shelf 8 years ago (in search of ropes and drag marks; **Experimental Site C**). Sea floor mottled, dark brown thick and soft mud with many white spots (bacterial mats) of 20-30 cm size. Along track alternating sections with many white mats (in places completely covering the sea floor ; > 3 m) and, those with few mats. Larger white mats occasionally have gray coloured central area. Sighting of several lineaments (rope !). Few living long-legged crabs were observed towards the end of the profile. During ascent of the sledge many shrimps were encountered in water depths of about 80 - 50 m.

52FS:
Photo profile in the vicinity of a phosphoritic hardground at the shelf: in general, the seafloor exhibits muddy – sandy sediment surface with patch areas of hard roch outcrops. Outcrops have a rugged surface (0.5 – 1 m) with large boulders / blocks and nodular surface (partially cemented rubble). Muddy- sandy areas show white spots (bacterial mats) of mostly 5-10 cm diameter. (less than 10 % coverage). Rugged hard rock areas have larger irregular confined thicker (=>bright white) mats, often at the northern rim of large blocks. Drifting medusa at the begin of the deployment. Several 'white' lineaments and drag marks along the track.

53FS
Track across the shelf break and downslope (the uppermost steep escarpment): numerous shrimps encountered during descent and also during the profile at the sea floor. At the shelf (plain) muddy – sandy sediment with scattered 10-50 cm large bright white spots (bacterial mats). Several drag marks at the shelf break. Immediately at and beyond the shelf break nodular, rubbly cemented surface (phosphorite crusts), becoming more and more blocky; in parts with thin sediment 'dust' on top.

77FS:
Track across shelf break, down the escarpment, and along inclined sedimented slope:
sanddy surface with scattered large encrusted blocks. Rubble appears to be cemented. At the foot of the escarpment muddy sediment with scattered 5-15 cm large bright white spots (bacterial mats). CTD indicated several T – anomalies, the most prominent one at the shelf break.

91FS:
Photo sledge profile downslope across a slightly inclined shelf plain. 91FS is the deepest part of a composite profile comprising 91FS, 92FS, and 93FS.
Along the entire profile, the sea floor is covered by thick white bacterial mats; when touching the sea floor with the weight used for indicating the sledge distance to the sea floor, the white mats tear open and thick patches of the fibrous material are being suspended and the underlying black sediment layer is exposed. The mats commonly have a nodular surface texture. Very few spots along the profile expose the muddy dark brown sediment surface.
Table 8.1: OFOS stations of cruise SO-147 off the Peruvian coast

	Station No.	Area		Position Latitude (S)	Longitude (W)	Water depth (m)	Remarks
1	**15 FS**	A	shelf (S-Salaverry basin)	11° 03,62'	78° 16,52'	208	mottled surface
				11° 05'	78° 15,00'	115	('black & white')
2	**16 FS**	A	shelf (S-Salaverry basin)	11° 01'	78° 10,00'	159	searching experimental
				11° 02'	78° 09'	79	site C
3	**52 FS**	B	wide shelf platform	9° 47,63'	78° 48,60'	139	sediment with few white mats; towards shelf break knobby crusts
4	**53 FS**	B	slope + shelf break of wide	9° 57,95'	79° 05,03'	172	many shrimps; sediment with few mats;
			shelf platform	10° 01,32'	79° 05,01'	210	at escarpment complete phosph. crusts
5	**77 FS**	B	shelf margin and	10° 24,74'	78° 46,17'	154	T-anomalies; encrusted rubble (escarpment) and
			upper slope	10° 27,32'	78° 45,05'	182	small scattered white bacterial mats (sediment apron)
6	**91 FS**	A	shelf (S-Salaverry basin)	10° 55,57'	77° 58,14'	149	dominantely thick white
				10° 55,63'	77° 58,98'	155	bacterial mats ('snowy landscape')
7	**92 FS**	A	shelf (S-Salaverry basin)	10° 57,60'	77° 50,23'	100	poor visibility,
				10° 57,62'	77° 50,23'	100	many crabs
8	**93 FS**	A	shelf (S-Salaverry basin)	10° 44,62'	78° 00,93'	132	alternating mats and barren areas
9	**114 FS**	A	outer shelf high	11° 59,11'	77° 41,22'	146	thick white mats
			off Callao	11° 59,83'	77° 40,89'	168	
10	**141 FS**	C	E - Pisco	13° 32,67'	76° 37,83'	178	small 'white spots'
			Basin	13° 33,27'	76° 37,47'	176	current ripples

92FS:
The shallowest portion of the composite profile 91FS – 93FS. This was a very brief deployment of the photo sledge. When lowering the instrument the camera encountered numerous swimming up to 10 cm long red crabs in very muddy water. The visibility was so poor that the sea floor could hardly be identified from 2 m above. Crabs occurred down to the very bottom.

93FS:
Intermediate depth section of the composite profile 91FS – 93FS. This track is an interplay of sections with bacterial mats and those without mats: the bacterial mats are commonly thinner than in 91FS, and their texture resembles ripple marks (also indicated by the colour: bright white at 'crests', grey in 'valleys'). Inbetween the areas characterized by these mats are about 5 – 10 m long sections which show soft brown muddy sediment without mats. At a few sites, thin flakes of slightly enrolled mat material indicate mechanical removal of the mats from the sediment surface.

114FS:
Photo profile across the onset of the youngest sediment sequence at the outer shelf off Callao. Sea floor dominantly covered by thick white fibrous mats. We observed places, where the mats have been damaged leaving dm-sized darker spots. Flakes of displaced mats were seen ontop of white mats slowly moving indicating current activity. Mats often display a knobby surface.

141FS:
Photo profile at the shallow shelf area of the East Pisco Basin. Scattered 'white spots' (bacterial mats) of commonly 10-30 cm size on brown muddy sediment; spots often contain gray central area. Some sections of the track with coarser sediment and very few spots. Ripple marks in some areas run oblique to the sledge track.

Figure 8.2 (see the following 5 pages):
Temperature profiles acquired near the sea floor with a CTD probe mounted to the photo sledge are presented for 9 out of 10 deployments (stations 15FS& 16FS, 52FS & 53FS, 77FS & 91FS, 92FS & 93FS and 141FS). Note in particular the temperature 'anomalies' of Station 77FS near the shelf break.

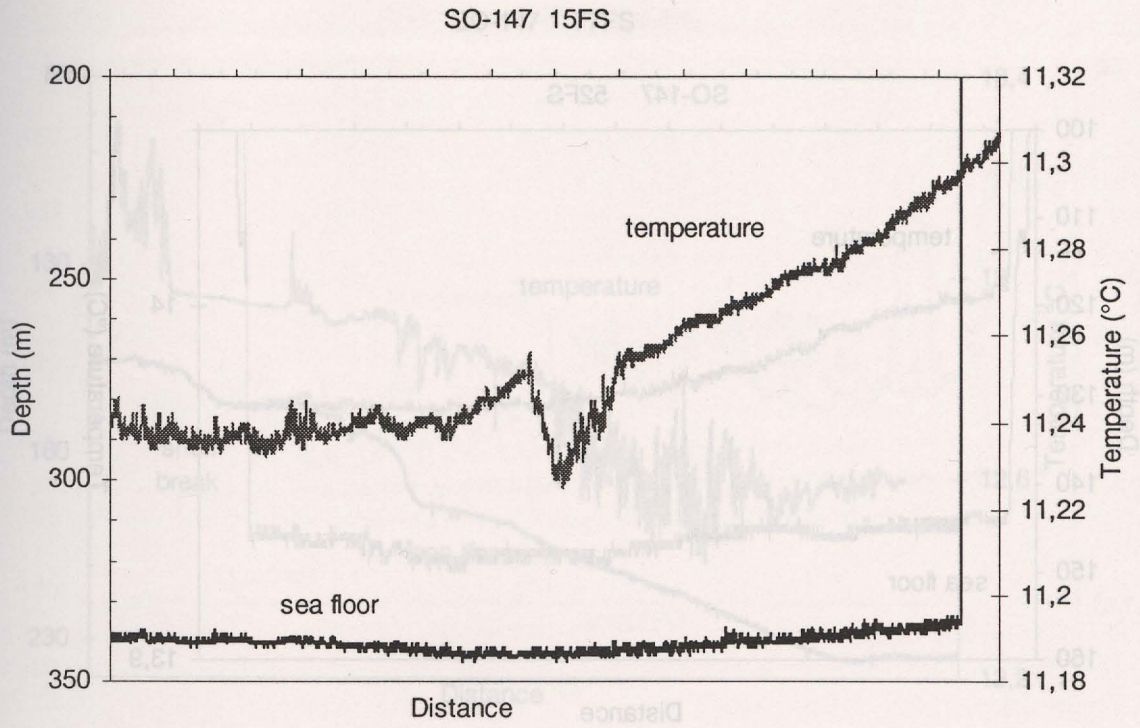
SO-147 15FS
200
250
300
350
Depth (m)
temperature
sea floor
Distance
11,32
11,3
11,28
11,26
11,24
11,22
11,2
11,18
Temperature (°C)

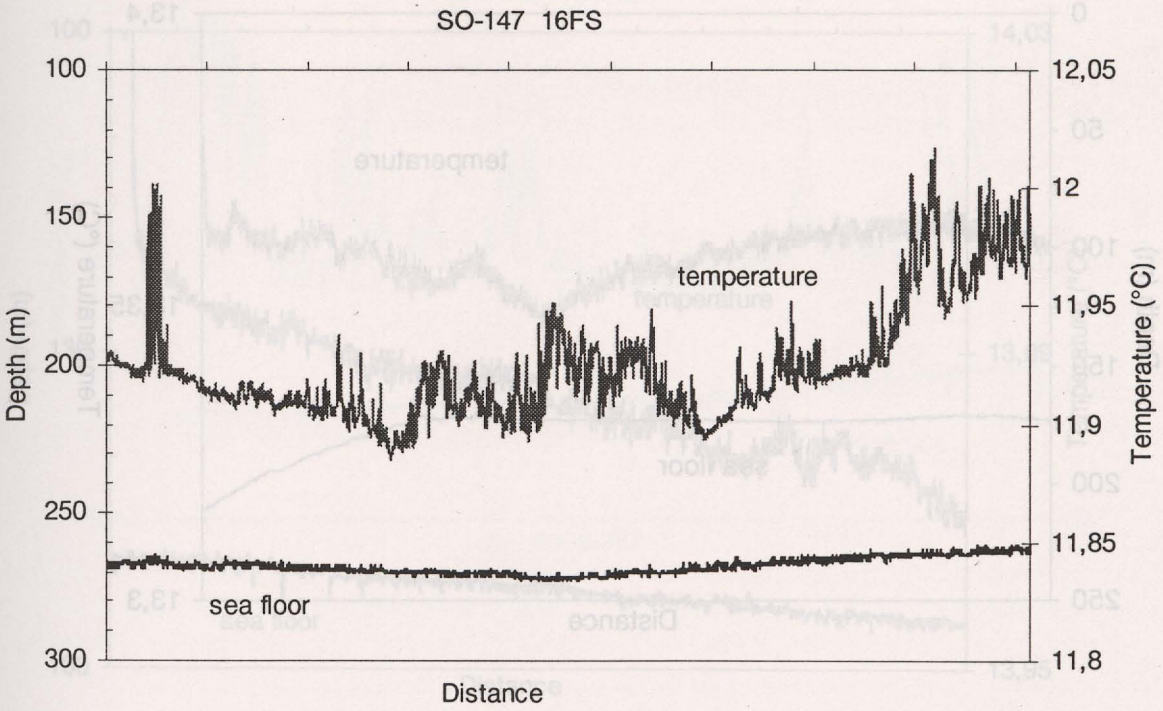
SO-147 16FS
100
150
200
250
300
Depth (m)
temperature
sea floor
Distance
12,05
12
11,95
11,9
11,85
11,8
Temperature (°C)

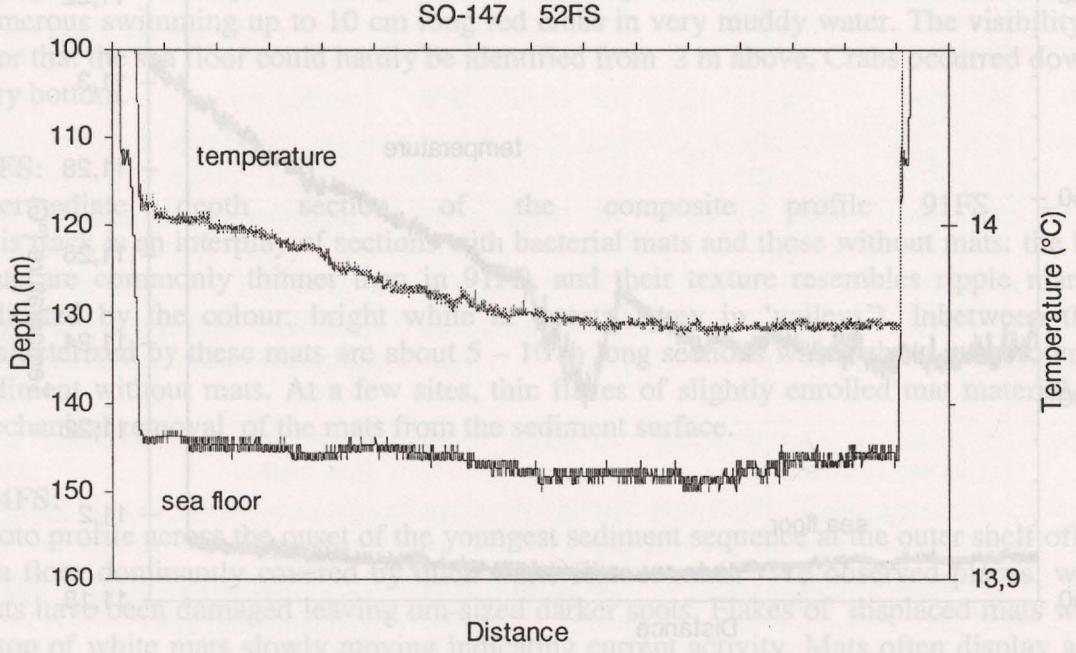
SO-147 52FS
100
110
120
130
140
150
160
Depth (m)
temperature
sea floor
14
13,9
Temperature (°C)
Distance

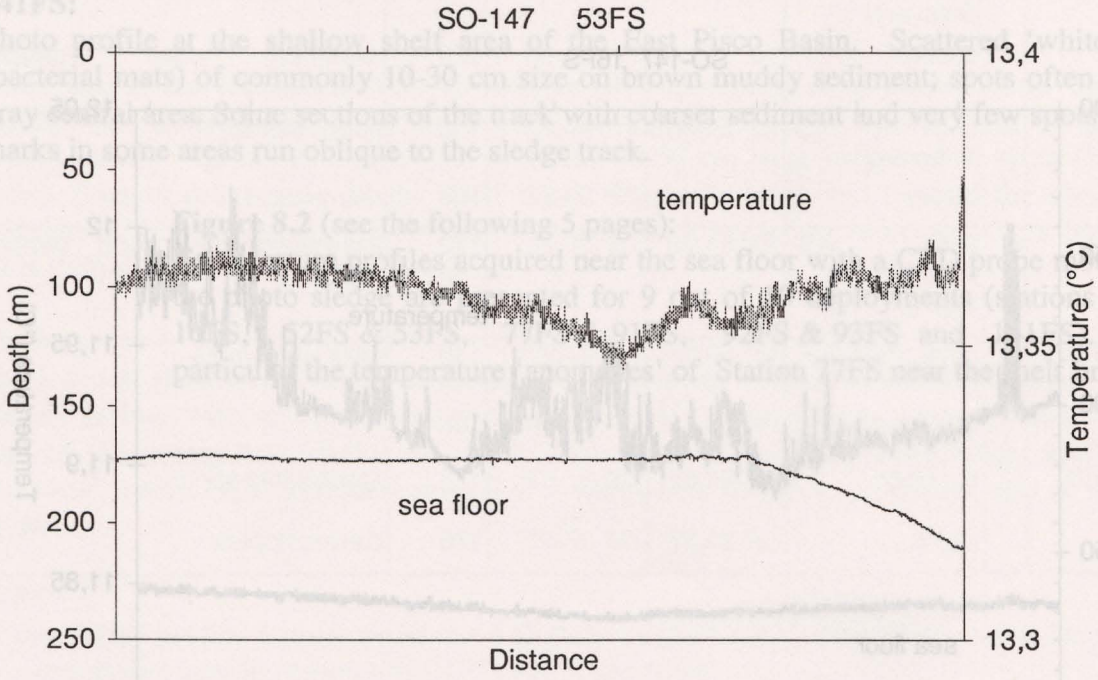
SO-147 53FS
0
50
100
150
200
250
Depth (m)
temperature
sea floor
13,4
13,35
13,3
Temperature (°C)
Distance

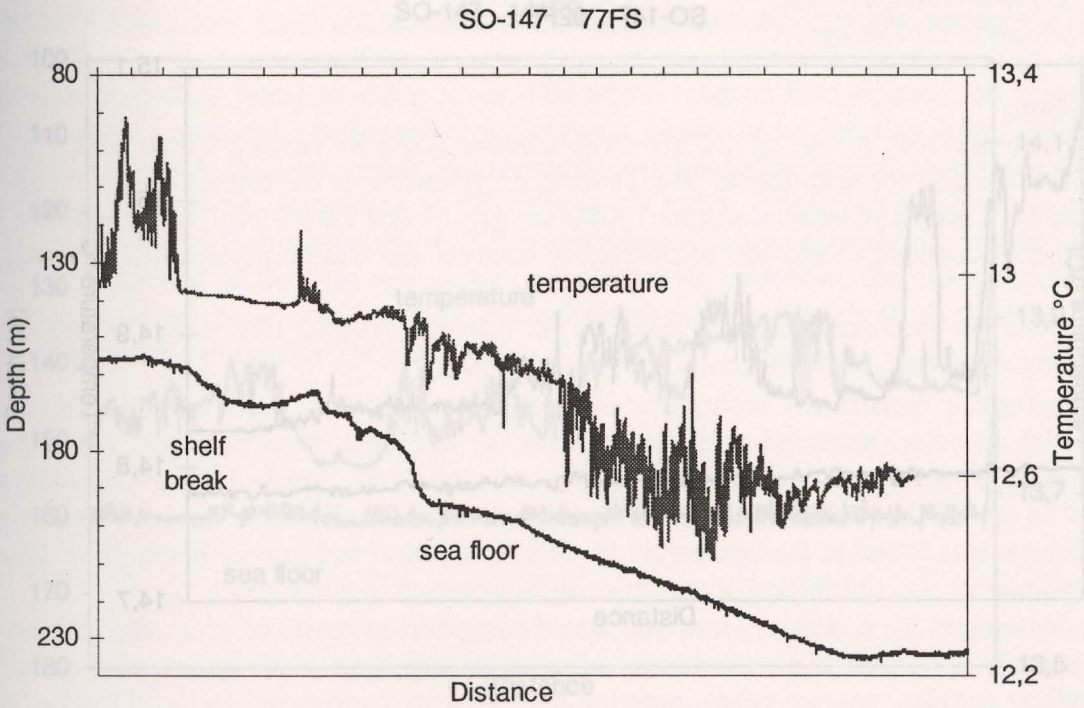
SO-147 77FS
80
130
180
230
Depth (m)
13,4
13
12,6
12,2
Temperature °C
temperature
shelf
break
sea floor
Distance

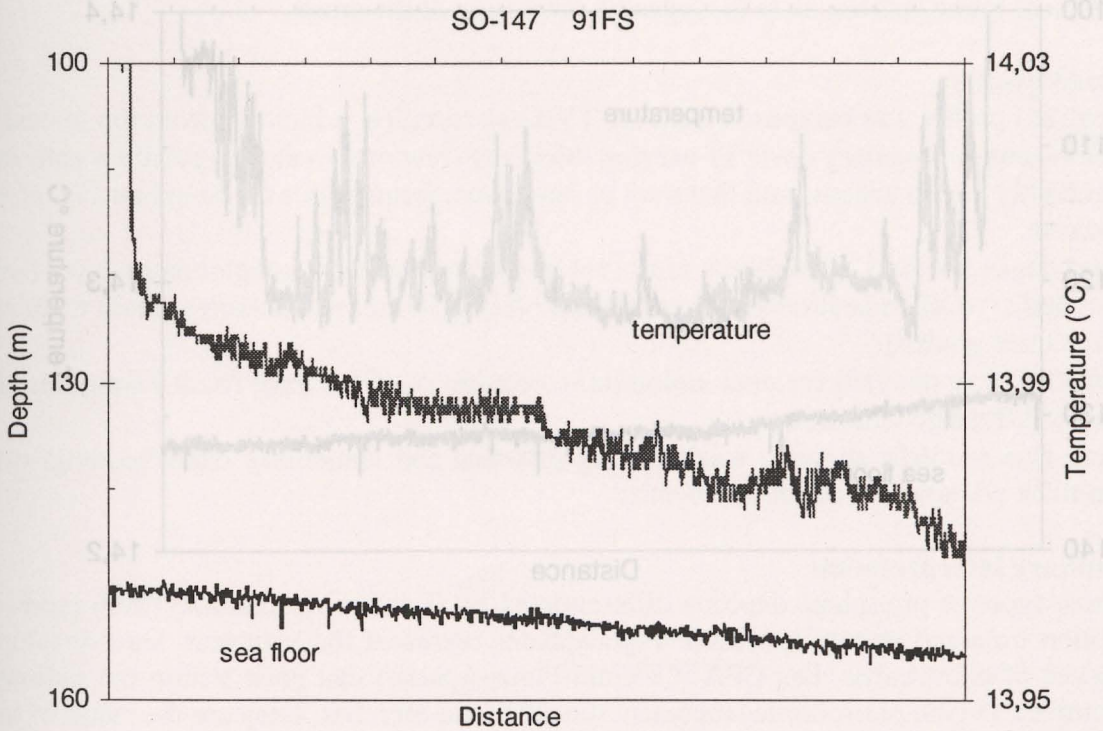
SO-147 91FS
100
130
160
Depth (m)
14,03
13,99
13,95
Temperature (°C)
temperature
sea floor
Distance

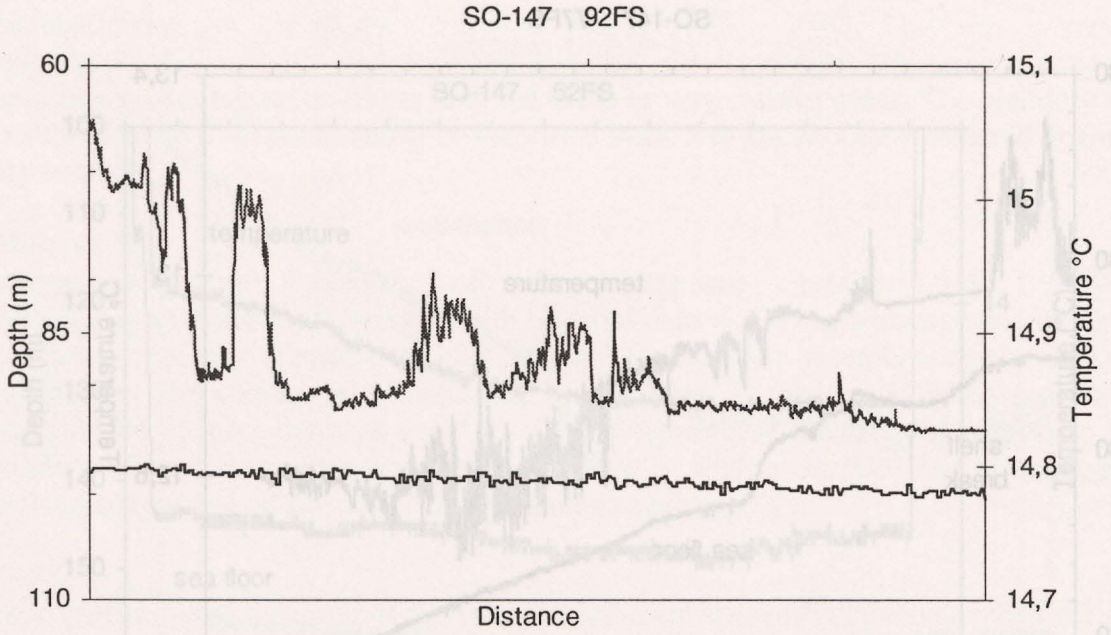
SO-147 92FS
60
85
110
Depth (m)
15,1
15
14,9
14,8
14,7
Temperature °C
Distance

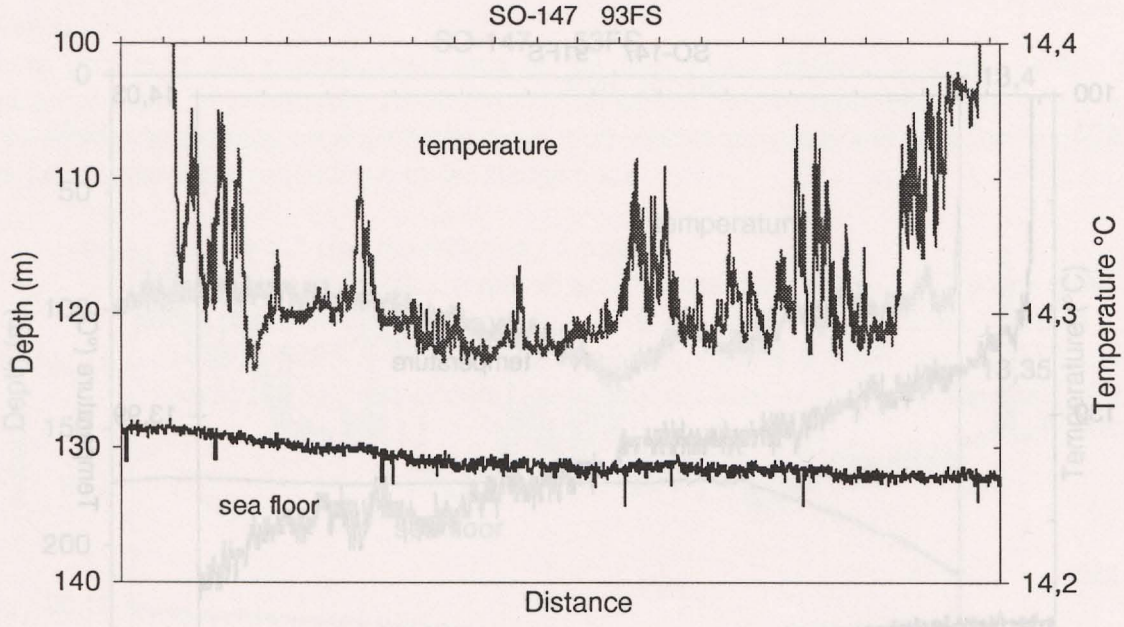
SO-147 93FS
100
110
120
130
140
Depth (m)
temperature
sea floor
14,4
14,3
14,2
Temperature °C
Distance

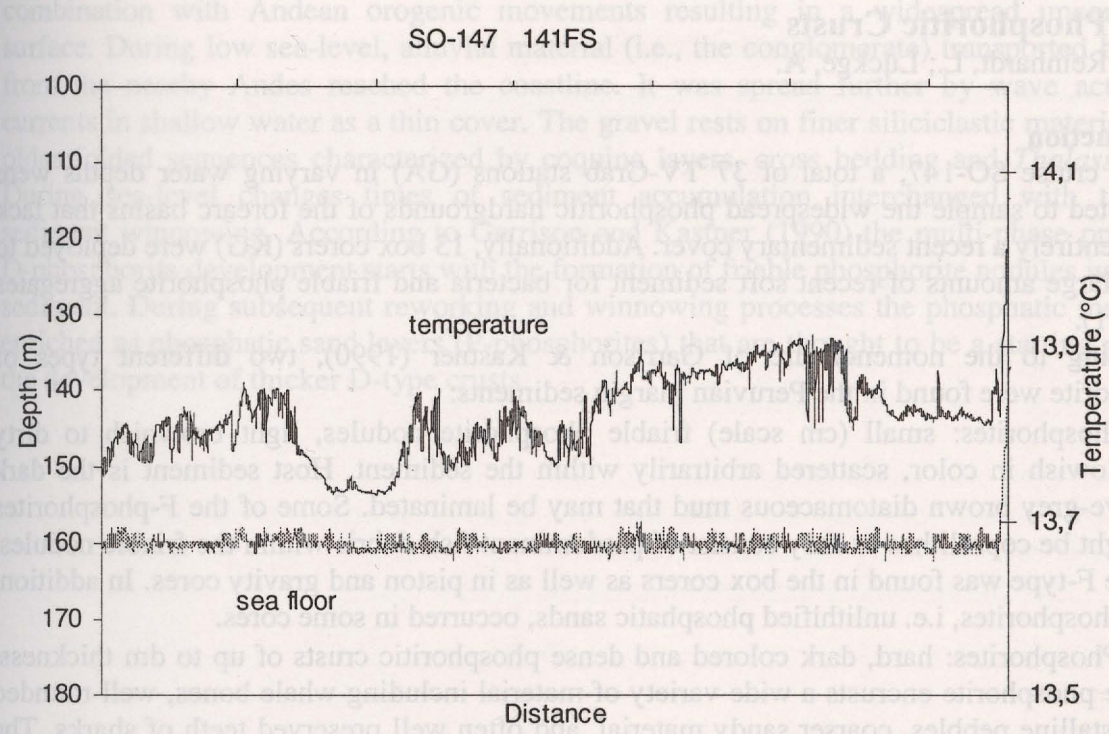
SO-147 141FS
100
110
120
130
140
150
160
170
180
Depth (m)
temperature
sea floor
Distance
14,1
13,9
13,7
13,5
Temperature (°C)

9. Phosphoritic Crusts

Reinhardt, L.; Lückge, A.

Introduction

During cruise SO-147, a total of 37 TV-Grab stations (GA) in varying water depths were completed to sample the widespread phosphoritic hardgrounds of the forearc basins that lack nearly entirely a recent sedimentary cover. Additionally, 13 box corers (KG) were deployed to obtain large amounts of recent soft sediment for bacteria and friable phosphorite aggregates (Fig. 9.1).

According to the nomenclature of Garrison & Kastner (1990), two different types of phosphorite were found in the Peruvian margin sediments:

- F-phosphorites: small (cm scale) friable phosphorite nodules, light brownish to dirty yellowish in color, scattered arbitrarily within the sediment. Host sediment is the dark olive-grey brown diatomaceous mud that may be laminated. Some of the F-phosphorites might be coprolithes as they consist of predominant fish-debris within the friable nodules. The F-type was found in the box corers as well as in piston and gravity cores. In addition, P-phosphorites, i.e. unlithified phosphatic sands, occurred in some cores.
- D-Phosphorites: hard, dark colored and dense phosphoritic crusts of up to dm thickness. The phosphorite encrusts a wide variety of material including whale bones, well-rounded crystalline pebbles, coarser sandy material, and often well preserved teeth of sharks. The surface of the crusts has regularly a metallic glance. Apart from that, it is often covered by a film of organic material. Some of the crusts are intensely perforated by boring-organisms. Sections reveal a layered structure of the crusts in the millimeter-scale. Frequent intraclasts are hints for repeated reworking of the crusts.

Idealized profile

An idealized profile was composed from the TV-Grab samples. It includes from top to base:

- The recent sedimentary cover of varying thickness (few mm to dm), typically a soft, dark olive-gray diatomaceous mud that may be laminated, frequently with abundant *Thioploca*-bacteria.
- Hard dense and dark phosphorite crust (see above) cementing a conglomerate layer (well-rounded crystalline/sedimentary components often > 10 cm, whale bones, shark teeth etc., sometimes graded).
- Lithified gray sand/silt (cement: dolomite?), occurrence of the trace fossil *Thalassinoides*, shows diffuse transition into:
- Gray fine sand/silt showing weak parting-lineation and sometimes cross-bedding, often dm-thick coquina layers are interbedded.

Preliminary interpretation

The three types of phosphate deposits differentiated by Garrison & Kastner (1990) represent an explicit time and energy spectrum: F-phosphates represent the youngest, least developed aggregates of phosphorite, i.e., CFA (Calcium-Fluor-Apatite) that grew within the sediment. The complex D-type phosphorites represent the other end-member. They are the result of long time intervals including repeated intervals of phosphate formation, burial by sediments and surface exposition, reworking and re-deposition.

Most TV-Grab stations assessed the hard reflectors of the widespread rugged unconformity surfaces. The recovered sediments consist of similar sequences: 1. recent sediment, 2. phosphorite crust, 3. lithified gray sand, and 4. unlithified gray sand. The D-type phosphorites formed as a lag deposit in areas affected by intense winnowing. A scenario for the formation of the phosphorite crust covering large areas of the platform off Chimbote is as follows: intense folding of Cenozoic sediments occurred during the Miocene/Pliocene in

combination with Andean orogenic movements resulting in a widespread unconformity surface. During low sea-level, alluvial material (i.e., the conglomerate) transported by rivers from the nearby Andes reached the coastline. It was spread further by wave action and currents in shallow water as a thin cover. The gravel rests on finer siliciclastic material of the older folded sequences characterized by coquina layers, cross bedding and *Thalassinoides*. During sea-level changes times of sediment accumulation interchanged with times of sediment winnowing. According to Garrison and Kastner (1990) the multi-phase process of D-phosphorite development starts with the formation of friable phosphorite nodules within the sediment. During subsequent reworking and winnowing processes the phosphatic material is enriched as phosphatic sand layers (P-phosphorites) that are thought to be a starting point for the development of thicker D-type crusts.

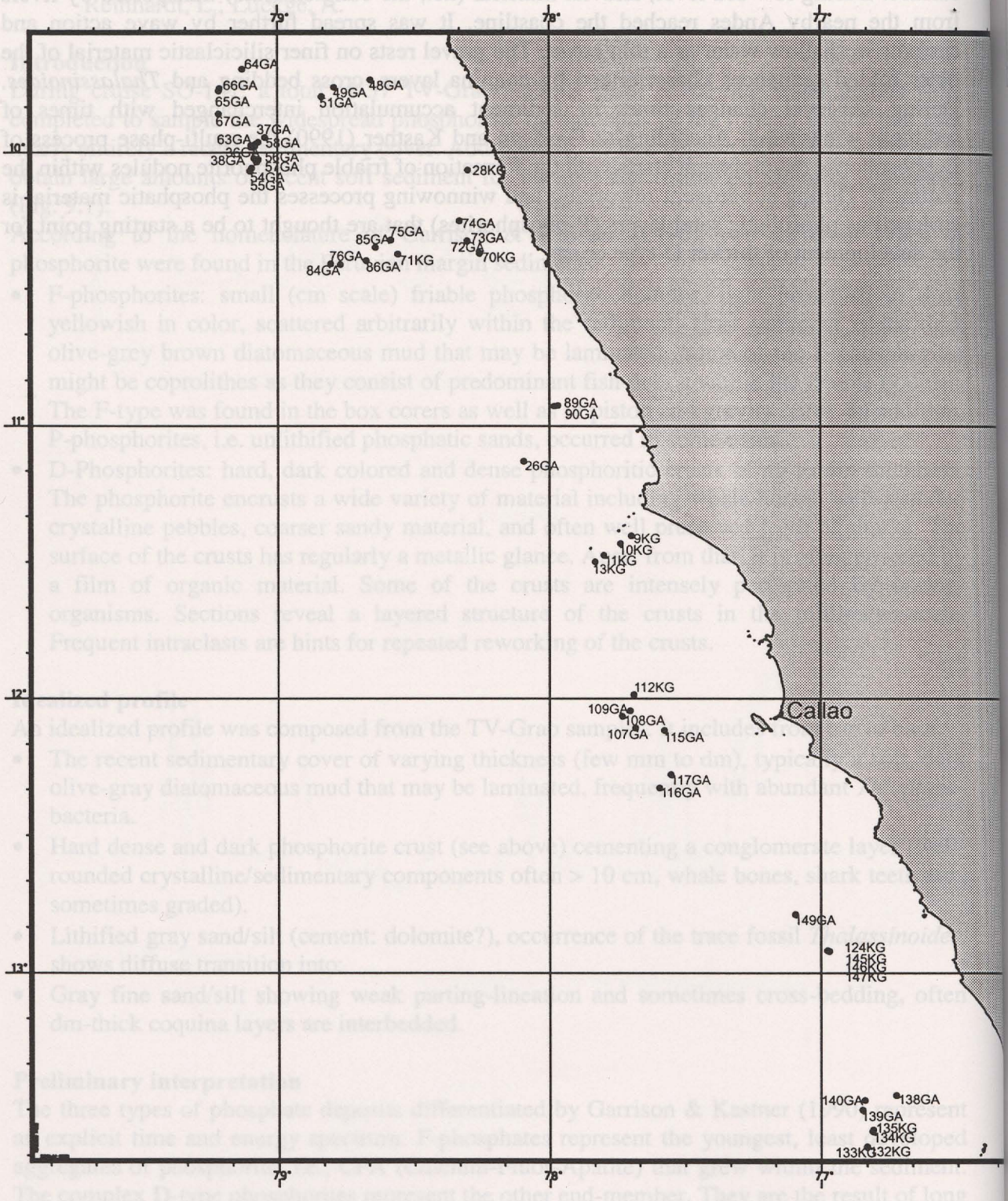

Fig. 9.1: Locations of TV-Grab (GA) and box corer (KG) stations.

10. Inorganic geochemical signatures of upwelling sediments

Straßburg, S. / Harazim, B
Schnetger, B. / Dellwig, O.

10.1. Introduction

The aim of the investigation is to decipher the early diagenetic processes concerning formation of phosphorites. The chemical composition of pore-water from marine sediments reflects diagenetic processes. To distinguish the geochemical signals in the Peruvian sediments which derive from the ocean/atmosphere system (intensity of upwelling, bioproduction) from that of secondary overprinting (formation of phosporites, sulfate reduction, opaline diagenesis) we carried out pore water analysis. Sea water samples from the same area were analysed for comparison.
Here we present the methods and results of the chemical analysis which have been carried out onboard. In addition, we also present the procedures to preserve samples for future investigations in the home labs. For some parameters, with no analytical facilities available on board, aliquots of the pore-waters have to be preserved for later analysis on shore.

10.2. Pore-water extraction

Two different systems were applied for pore water extraction and following handling of samples.

By BGR:

During Cruise SO 147 interstitial water samples were extracted from sediments with a newly designed "BGR pore-water press" [Cruise Report SO 139].
High density-PTFE sample vessels with a maximum volume of 125 ml, Tefzel LUER LOCK outlets for the sample-water and self-locking sea-waterproof V4A-stainless steel inertgas-valves guaranteed a contamination-free sample preparation procedure. Also a newly designed quick-lock support and a miniaturized pressure gas distribution-block improved the handling of great amounts of samples (670 pcs.).

For geochemical analyses the cores from the Multicorer were carried immediately to the cool lab (temperature about 4° C). There they were cut into slices of 0,5 cm up to 2 cm and transferred into the sample vessels of the pore-water press.
The piston and gravity cores were cut into 1 m-sections, sealed with caps and carried then immediately to the cold storage at a temperature around 4° C. After the whole core (up to 5 m) was cut into 1 m sections each section was split in half-core segments. One half was used for stratigraphic analyses. The other half was used for the extraction of pore-water. A maximal volume of 125 mL of sediment was filled into the sample vessels.
After covering the sample with parafilm and a NBR-rubbermat the vessels were mounted in the pore-water press stand. Extraction time was 15 minutes for Multicorer and 30 minutes for piston and gravity cores. A pressure of 4 to 8 bars (Argon) was applied. Depending on the composition of the sediment 20 ml up to 50 ml of pore water were gained. The sample was pressed through a "Sartorius" cellulose nitrate filter 0.45µm type 11306-100-N and directly collected in 25 ml argon-flushed storage containers.

By ICBM:

Interstitial water was removed from the sediments by a Macrolon pore-water press (Reeburgh squeezer) operating with argon for pressure filtration in a cool room at 4 °C. The interstitial water was split into four fractions. Supernatant water of the surface samples (Multicorer) was filtered through 0.45 µm filters and split in the same way like interstitial water.

For later H_2S determination one fraction of the interstitial water (1-2 ml) was immediately filled into Eppendorf cups, pre-filled with Zn-acetate. A second fraction was filtered (0.2 um filter) into HDPE vials and acidified with HNO_3 (suprapure, 1 % V/V). This fraction will be used for metal analysis (Mn, Fe, Ba). A third fraction was filled into glass ampoules and preserved with 0.1 % (v/v) H_3PO_4 for DOC (dissolved organic carbon) determination. The remaining solution was kept in HDPE vials without any precondition and will be used for the analysis of conservative major and minor elements by a XRF method (Wehausen et al. 1999). All interstitial water samples were kept cool at 4 °C until further treatment aboard or in the home laboratory.

10.3. Shipboard analyses

By BGR:

The instruments listed in table 10.1 were used for pore water on board ship analyses. Besides pore water samples, CTD-samples and bottom-near sea waters were analysed with same methods.

Table 10.1: Instruments for pore-water on board ship analyses and analysed parameters.

Instrument	Analysed parameters
SCHOTT pH-meter CG 837, temperature compensated Electrode SCHOTT Pt 61 (Pt-Ag/AgCl)	Redox-potential (Eh)
SCHOTT pH-meter CG 837, temperature compensated Electrode SCHOTT N 1042 A	pH
WTW Conductivity Meter LF 323 Electrode WTW Tetra Con 325 (851228041)	Conductivity, Salinity
AMT-Picoamperemeter with **H_2S-microsensor** for probe systems, in situ determination Electrode No. 17099804 - 3 mg/L Electrode No. 17099803 - 10 mg/L Electrode No. 17099801 - 50 mg/L ***see 10. 3.1***	H_2S, S^{2-}
AMT-Picoamperemeter with **O_2-microsensor** for probe systems, in situ determination Electrode No. 17099802 Static measuring process	O_2
WTW-OXI 96 Electrode. WTW EO 96 Dynamic measuring process	O_2
DIONEX Ion Chromatograph IC 20 Eluent-Generator EG 40 Thermal Column Compartment AS 50 Sample Preparation Module AS 50 ***see10. 3.2***	Acetate, Br^-, Cl^-, CO_3^{2-}, F^-, Formiate, NO_2^-, NO_3^-, PO_4^{3-}, Propionate, SO_4^{2-}, (S^{2-})

10.3.1 Shipboard analyses of Sulphide

By BGR:

The new amperometric microsensor has been developed for the in situ determination of dissolved H_2S /Sulphide in natural waters. Because of the partial pressure of the gaseous H_2S, the analyte is separated by penetration through the membrane. Inside the sensor the hydrogen sulfide reacts with a redox mediator. The reoxidation at the working electrode causes a current corresponding to the concentration of the dissolved molecular H_2S amount.
The sensor works highly selectively and there are no signal equivalents to CO, CO_2, H_2O-vapour, CH_4 nor NH_3. Both salt concentrations of up to 40 g/L and turbid or colored solutions do not interfere with the signal.
The pH of the original sample ranged from 7.2 to 8.5. To adjust the pH below pH 3, the sample was mixed in a reaction-coil of 1 m with 0.05 n-H_2SO_4 (1:1) and pumped through a closed measuring-cell (flow rate 1.8 ml/min.). Total sulfide was calculated with to following to terms:

$$C_{H^+} = 10^{-pH} \qquad \text{(eq. 1)}$$

$$C_{totalsulphide} = \frac{C_{H_2S} * \left[C_{H^+}^2 + \left(C_{H^+} * 1{,}205 * 10^{-7}\right) + 4{,}7861 * 10^{-21}\right]}{C_{H^+}^2} \qquad \text{(eq. 2)}$$

10.3.2 Shipboard analysis of anions in pore-water and seawater

By BGR:

Often anions like sulphide, sulphate, nitrate, chloride etc. are analysed photometrically or titrimetrically on board. Samples are also stabilised and analysed later on shore.

The ION-CHROMATOGRAPHY is an ideal tool to simplify analytical procedures, making results available within a reasonable time, avoiding deterioration of material and offering the chance of immediate response by scientific crew on board ship.

The anions mentioned in table 10.1 were directly analysed by ION-CHROMATOGRAPHY. Some like Acetate, Formiate or Propionate showed concentrations below the detection limit.

The used ION-CHROMATOGRAPH **"DIONEX IC 20"** with eluent generator **EG 40,** thermal column compartment **AS 50** and autosampler with sample preparation module **AS 50** and also the advanced chromatography software **PEAKNET-DIONEX** allows the determination of the above mentioned anions within 30 minutes per sample. Needed highly pure de-ionised water is prepared from pre-de-ionised water (3 $\mu S_{25°C}$) on board ship with a portable "MILLIPORE SIMPLYCITY 185" unit.

It is a great advantage to analyse these samples directly after the sampling procedure, because of the well known instability, not only of pore-water samples, but even of water samples in general (Schulz, H. D. 2000).

No manual pre-treatment of the samples, except the charging of the auto-sampler vials is required. The use of the sample preparation module and the invention of a new high-capacity-chromatography-column (AS11 HC) permits the analysis of the original pore-water sample without any further manipulation. The high-capacity analytical column allows to analyse in such a wide dynamic range, that all analytical components are analysed within one run. No

chemicals, e.g. for the stabilisation of single components are needed, which excludes any contamination especially while analysing traces.

Analytical procedure

After charging the sample-preparation-module with sealed 1,5 ml-vials the pore- or sea-water is diluted automatically 20 times. 10 µL of the prepared sample are injected into the sample loop.

Using a dynamic gradient eluent-programme (eluent: n mmol OH^-), the single components of the sample are separated by the analytical column. After a special process of suppressing the basic conductivity of the effluent, the anions are detected in a conductivity measuring cell. All analytical components are analysed within one run.

The above mentioned eluent is produced electro-chemically with an eluent generator (DIONEX EG 40) by using de-ionised water, conductivity 0,057 $\mu S_{25° C}$ (18,2 MΩ) as basic effluent.

The long-time-stability of the used working unit allows to run the analytical procedure 24 hours a day without interruption.

10.3.3 Shipboard analysis of Alkalinity, Ammonia, Phosphate, Silica and Chloride

By ICBM:

Alkalinity was measured with a spectroscopic method (Sarazin et al. 1999). The method neutralizes all the basic species causing the alkalinity. A weak acid (formic acid) mixed with a pH sensitive dye, bromo-phenol blue, is used which has a dissociation constant close to the one of formic acid. The neutralization reaction leads to a final mixture absorbing at 590 nm. The quantity of absorbance is a function of the original alkalinity of the sample. A second order polynomial fit was applied to the 5 calibration solutions. The calibration curve range from 0 - 5 mM. The method is slightly less precise than Gran's potentiometric method, but has the advantage to run small samples (1-2 ml) and is much faster.

The following methods are described in detail by Gieskes and Peretsman (1986) and will therefore not be described in detail. All spectroscopic methods use a simultaneous diode-array spectrophotometer with an spectral range of 320-900 nm (Specol 1100, Zeiss Jena) and a 1 cm micro-cell. A second order polynomial fit was applied for the calculation of all calibration curves.

Ammonia was transferred into a blue complex (reagents consist of phenol-alcohol, sodium nitroprusside, alkaline solution, sodium hypochlorite) and was measured at a wavelength of 640 nm. Calibration solutions range from 0 – 1.0 mM.

Phosphate was transferred into a blue complex with a mixed reagent (ammonium molybdate, sulfuric acid, ascorbic acid and potassium antimonyltartrate) and was measured at 715 nm. Calibration solutions range from 0 to 0.02 mM. Only a few phosphate values are available because samples with high H_2S concentrations could not be analysed colorimetrically owing to colour interference. Concentrations of phosphate decrease in all cases where H_2S is present (smell) (see: 1MC, 2MC, 5MC, 14MC, 18MC).

For Silica determination, samples were filtered with a 0.2 um filter. In the first step a yellow silicamolybdate complex was produced by adding ammonium paramolybdate to the sample. Then, this complex was reduced with a reagent (metol sulphite, oxalic acid and sulfuric acid) to give a blue colour. Measurement was carried out at 725 nm. Reduction of the yellow complex occurs in the first step if H_2S is present in the sample. In both cases the second reagent was given to the sample. The reduction by H_2S can be used as an indicator for significant amounts of H_2S in interstitial water. Calibration curves range from 0 – 0.7 mM.

Chloride determination was done by titration with a Gilmont micro-burette. A mixture of 0.1 ml interstitial water, 0.1 indicator solution (potassium chromate and potassium di-chromate), and 2 ml water (18 mΩ) with was titrated with silver nitrate (0.1 M) until a faintly reddish-brown color was observed (silver chromate). Accuracy and precision was done with IAPSO seawater standard. Accuracy is mostly better than 0.4 % (rel. 5 determinations) and precision is better than 1 % (rel.) (IAPSO: measured 559 mM, certified 558 mM).

10.3.4 Planned on shore analyses

By BGR:

Determination of following elements and parameters in the pore water:

- Fe
- Mn
- alkaline metals and earth alkaline metals } by ICP-OES
- heavy metals
- O_2-Isotopes by MS
- S-speciation by ion-chromatography

Determination of the following elements and parameters in the squeeze cakes:

- Fe
- Mn
- alkaline metals and earth alkaline metals } all by XRF
- heavy metals
- Trace elements by ICP-OES and ICP-MS
- Element-speciation (Tessier et al. 1979) by ICP-OES
- TOC (total organic carbon)
- Petrographic analysis

10.3.5 Comparison of results between ICBM and BGR

It is planned to compare the results of pore water and squeeze cakes analyses from multicorer cores in cases in which both groups obtained parallel cores from one multi corer.

10.4. Sampling

10.4.1 Seawater

By BGR:

Samples of seawater were taken from the stations shown in table 10.2.

Table 10.2: Multisonde-(CTD)-sampling sites for water analysis with deepest water depths in parenthesis.

Multisonde		
24MS (202 m)	50MS (165 m)	100MS (385 m)
32MS (1438 m)	59MS (353 m)	130MS (124 m)

At every sampling site 6 to 8 water samples were taken from different water depths. The deepest sample were taken five meters over the sediment surface. Oxygen was determined directly after boarding by sensor measuring technique (dynamic O_2-electrode, see table 10.1). Anions were analyzed by ion-chromatography (for instrument description see table 1).

10.4.2 Pore-water

By BGR:

Pore-water was gained from the following cores (table 10.3):

Table 10.3: Sampling stations for Multicorer, Gravity-core and Box-shaped gravity corer samples.

Multicorer					Gravity-core	Box-shaped gravity corer
1MC	17MC	45MC	81MC	111MC	4SL	118KA
2MC	21MC	47MC	82MC	119MC	40SL	123KA
5MC	29MC	67MC	88MC	121MC	80SL	128KA
7MC	33MC	71MC	98MC	125MC	96SL	
14MC	35MC	79MC	104MC	127MC		

By ICBM:

Interstitial water was sampled and analyzed from the following multicorer material onboard:
1MC, 2MC, 5MC, 14MC, 18MC, 29MC, 33MC, 35MC, 45MC, 71MC, 81MC, 104MC, 120MC, 122MC and 125MC.

Interstitial water was sampled and analyzed from the following box-shaped gravity cores and gravity cores onboard:
40SL, 80SL, 96SL, 118KA, 123KA.

The following multicorer material was sampled onboard:
1MC, 2MC, 5MC, 8MC, 14MC, 18MC, 29MC, 33MC, 35MC, 45MC, 71MC, 81MC, 79MC, 88MC, 104MC, 120MC, 122MC and 125MC.

The following heavy gravity cores were sampled onboard:
40SL, 80SL, 96SL.

10.4.3 Sampling strategy

By BGR:

Multicorer (MC):

Directly after boarding the MC-surface water was analyzed for O_2 (static measurement AMT-electrode, see table 1). A MC-surface water sample was taken for further analyses.

The core was immediately transferred to the cool lab. All cores were prepared for the pressing procedure in the following way.

Table 10.4: Sectional cutting of Multicorer cores.

Depth [cm]	Height of sample segment [cm]
0 – 1	½
1 – 10	1
10 – end of core (max. 50)	2

The outer parts of the "sample segment" were discharged, only the inner parts were used for the pressing procedure.

Gravity corer (SL):

Directly after boarding the five-meter-liners were end-capped and cut into one-meter-parts. The one-meter-pieces were sealed and stored at 4° C. Successively the above mentioned pieces were split into half core segments. Distance of the sampling points was 25 cm or 30 cm, thickness of the sample section was 5 cm, outer parts of the sample segment were discharged.

Box-shaped gravity corer (KA):

Directly after boarding the box was opened, surface was cleaned and samples were taken by inserting two syringes with cut tip of 50 ml for each sample in a distance of 30 cm. After removing the syringes from the core the open ends were covered with "para-film", the syringes were transferred to the cool lab and immediately pressed like above mentioned.

Table 10.5: Type and amount of samples treated by BGR group of Geochemistry during cruises SO 147.

Sampling technique	Sample type	Number of sample-sites	Number of samples	Number of samples analyzed on board
Multicorer	pore-water	25	572	572
Gravity core	pore-water	4	70	70
Box shaped gravity corer	pore-water	3	37	37
Squeeze cakes	Sediment	32	679	---
Bottom sea water	Seawater	24	24	24
Multisonde CTD	Seawater	6	45	45

By ICBM:

For pore water analysis surface cores (multicorer) were sampled in 1 or 2 cm intervals up to 10 cm, then in 5 cm distances usually. Longer cores (gravity core or box-shaped gravity core) were sampled every 30-40 cm.

The main target for ICBM was to obtain sediment samples from multicorer and gravity corer in high resolution. Sediments were sampled with a plunger and a micrometer device. With this technique, sediment discs down to 0.25 cm could be obtained. Sampling usually was done in 0.25 - 1 cm intervals, depending on the type of laminae present. Longer cores (gravity cores, box-shaped gravity cores) were sampled generally in 2 cm intervals. Some sections were sampled in more detail (transition pelagic sedimentation – turbidite, changes in color, laminae).

Remaining samples from pressure filtration of pore-waters (squeeze cakes) were stored for further investigations in home labs.

All samples were filled into PE bags and kept frozen or stored at 4 °C.

10.5. Results

The sampling strategy was coordinated with the aim to examine the process of the formation of phophorites. The process of the formation takes place in the first centimeters of the sediment, therefore Multi corer-samples, with a maximum core-depth of 50 cm, were the most important samples for pore-water extraction.

10.5.1 Ammonia

Decomposition of organic nitrogen components leads to the formation of ammonia in pore waters from continental margin sediments. If dissolved oxygen is lacking, ammonia does not undergo oxidation. Ammonia increases with sediment depth from seawater concentrations up to a maximum of 1.4 mM). Off Peru, ammonia profiles in pore water are similar to alkalinity profiles. The highest concentrations of both parameters are also found in interstitial waters from the upper shelf which are rich in H_2S. In contrast, cores from greater water depth show the lowest values due to a lack of metabolisable organic matter. Alkalinity and ammonia are well correlated (Fig. 1) with two exceptions. In the cores 118Ka and 5MC alkalinity in a certain depth remains constant downcore, whereas the concentration of ammonia still increases. Most possibly this is related to the presence of methane in the cores (see below).

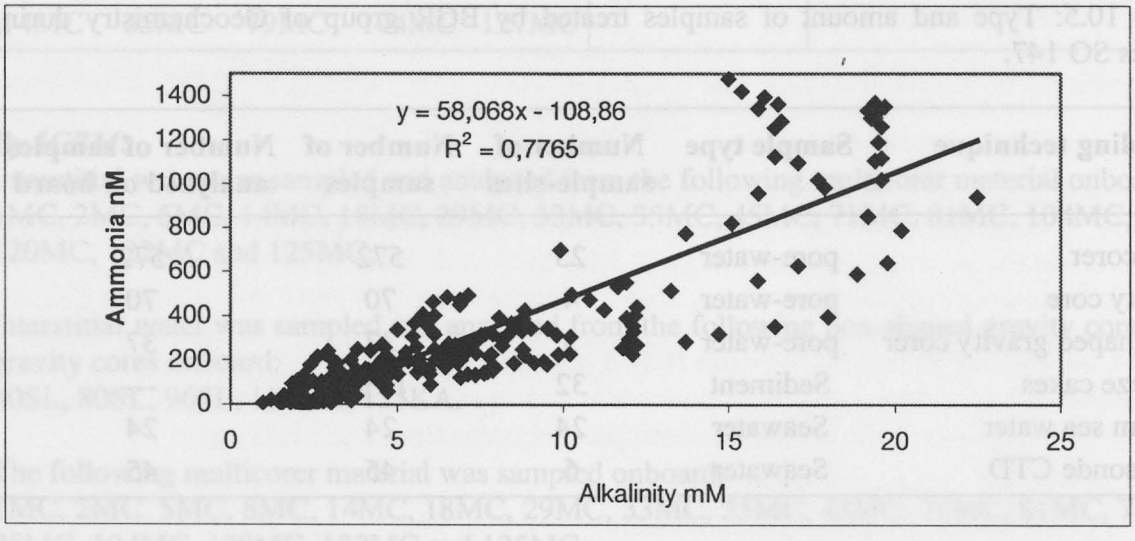

Fig. 10.1: Relationship between alkalinity and ammonia for all interstitial waters from sediments of the Peruvian margin.

10.5.2 Phosphate

Phosphate profiles of interstitial waters show maximum concentrations of 50 µM in a sediment depth of 5-10 cm. Below this reactive zone, the phosphate concentration decreases. Concentration of phosphate is high in interstitial waters from sediments up to 650 m water depth, (e.g. 35MC, 14MC) even in cores in which alkalinity and ammonia are close to seawater concentrations. In water depths greater than 650 m phosphate concentrations in pore water are below 30 µM. Generally, oxidative regeneration of phosphate from the organic matter under anoxic condition is coupled with microbiological mediated sulfate reduction processes. The investigations of Suess (1981) indicate that the high dissolved phosphate concentration in pore water can in some cases result also from the dissolution of fish debris. Dissolution of phosphoric fish debris represents a mechanism for remineralisation of phosphate comparable to that by oxidative regeneration of organically bound Phosphorus, or even larger in magnitude. Phosphate flux estimates, based on diffusion from the sediment, suggest that this mechanism may generate up to 10 % of the nutrient pool in the waters of the Peru undercurrent (Suess 1981). Possibly, the high flux of phosphate may also control widespread phosphorite formation in this area.

10.5.3 Silica

Silica shows almost constant concentrations in interstitial waters except in uppermost few sediment centimeters, which are influenced by seawater penetration. Except for longer cores and one surface core from 185 m water depth (104MC, mud hole) the saturation level with respect to opal solubility seems not to be reached (1.3 mM at 5 °C, Morey et al. 1964). The lowest silica concentrations are seen in sediments from deeper sites below 500 m water depth (Fig.2).

In regions of high productivity the dissolution of the siliceous tests will exceed the uptake capacity of the clays for silica, as a consequence very high interstitial water silica concentrations will be obtained (Fanning and Schink 1969). Diatoms form the most abundant opaline skeletal components found in the Peruvian upwelling region (Tiede 1981). Their abundance is highest in the neritic water mass (0-200 m water depth) affected by the coastal upwelling and decrease rapidly seaward by several orders of magnitude.

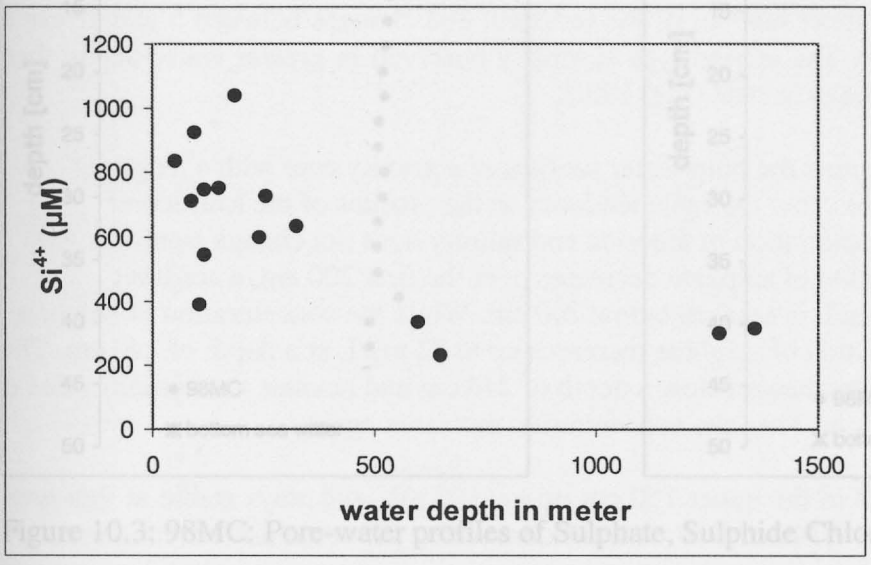

Fig. 10.2: Maximum concentrations of silica in interstitial waters in surface samples (multicorer material) from the Peruvian coast versus water depth.

10.5.4 Eh, pH, salinity, sulphate, sulphide

Figures 3 and 4 present typical pore-water profiles of a Multicorer, as we observed in the inspected area. Neither salinity nor chloride shows a special change in dependence on the sediment depth. The values are similar to that of seawater. The concentration of sulphate decreases with depth (from 2600 mg/L in seawater to 1700 mg/L in sediment depth of 48 cm), the concentration of sulphide increases with depth (<0,1 mg/L in seawater, 23 mg/L in sediment depth of 48 cm) due to the reduction of sulphate. The amount of sulphide in porewater is not equivalent to the amount of reduced sulphate, because generated sulphide precipitates as Pyrit in the sediment. The pore-waters of the top part of the core, down to 9 cm, are oxic, demonstrated by the Eh. At 9 cm of depth in the core the status changes from oxic to anoxic and the decrease of Eh continues. Within the first 2 cm the pH is slightly decreasing (three samples at 0,5 cm, 1 cm and 2 cm). A strong increase of pH is then observed between sediment depth of 5 to 10 cm (up to a value of 7,7).

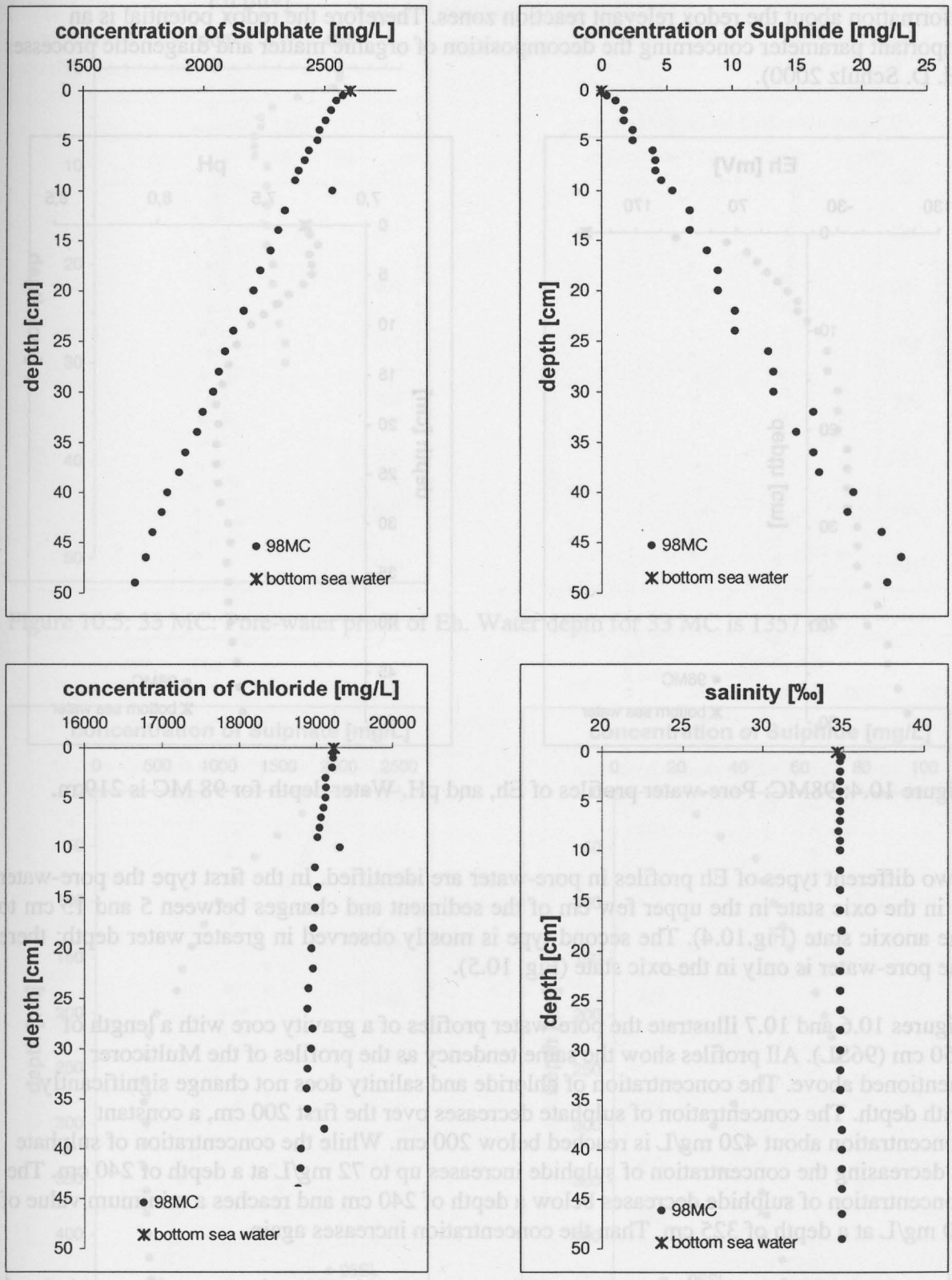

Figure 10.3: 98MC: Pore-water profiles of Sulphate, Sulphide Chloride and salinity.

The Eh-value characterizes the redox environment of the marine sediment and provides information about the redox relevant reaction zones. Therefore the redox potential is an important parameter concerning the decomposition of organic matter and diagenetic processes (H. D. Schulz 2000).

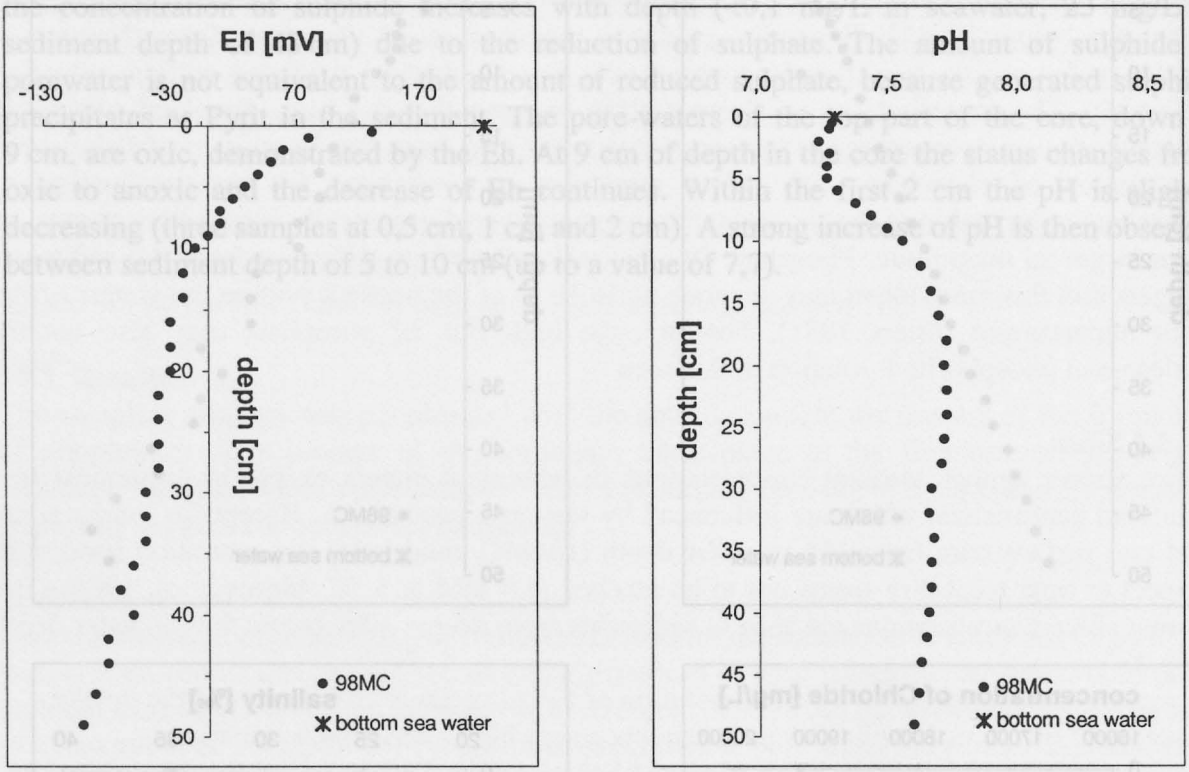

Figure 10.4: 98MC: Pore-water profiles of Eh, and pH. Water depth for 98 MC is 219 m.

Two different types of Eh profiles in pore-water are identified. In the first type the pore-water is in the oxic state in the upper few cm of the sediment and changes between 5 and 15 cm to the anoxic state (Fig.10.4). The second type is mostly observed in greater water depth: there the pore-water is only in the oxic state (Fig. 10.5).

Figures 10.6 and 10.7 illustrate the pore-water profiles of a gravity core with a length of 450 cm (96SL). All profiles show the same tendency as the profiles of the Multicorer mentioned above. The concentration of chloride and salinity does not change significantly with depth. The concentration of sulphate decreases over the first 200 cm, a constant concentration about 420 mg/L is reached below 200 cm. While the concentration of sulphate is decreasing the concentration of sulphide increases up to 72 mg/L at a depth of 240 cm. The concentration of sulphide decreases below a depth of 240 cm and reaches a minimum value of 20 mg/L at a depth of 325 cm. Than the concentration increases again.

The value of Eh decreases in the upper 150 cm up to -120 mV and stays stable at this level. The pH fluctuates between 7,74 and 7,49. A trend concerning pH could not be recognised.

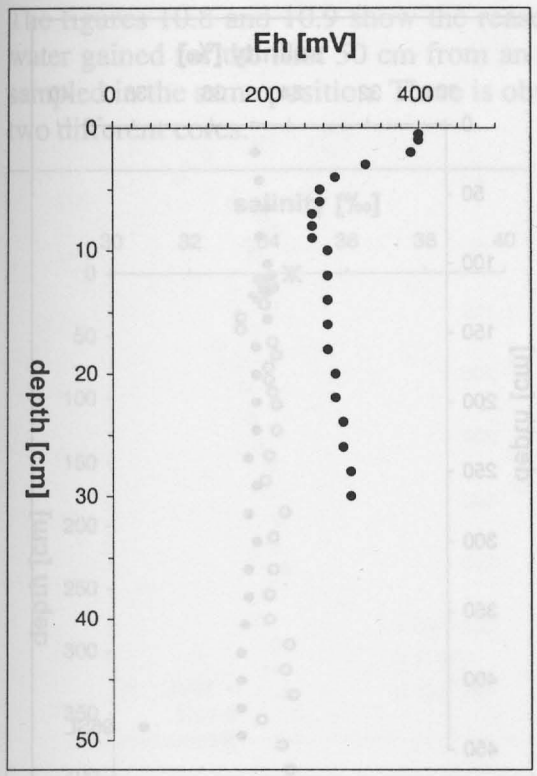

Figure 10.5: 33 MC: Pore-water profil of Eh. Water depth for 33 MC is 1357 m.

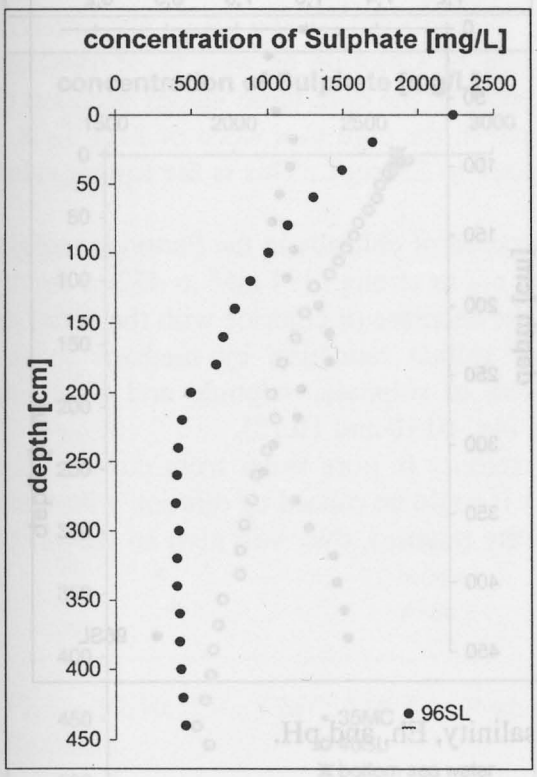

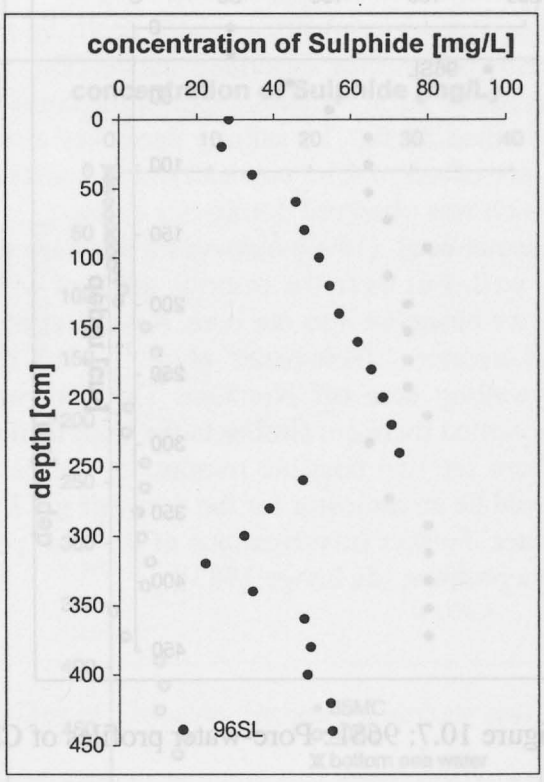

Figure 10.6: 96SL: Pore-water profiles of Sulphate and Sulphide.

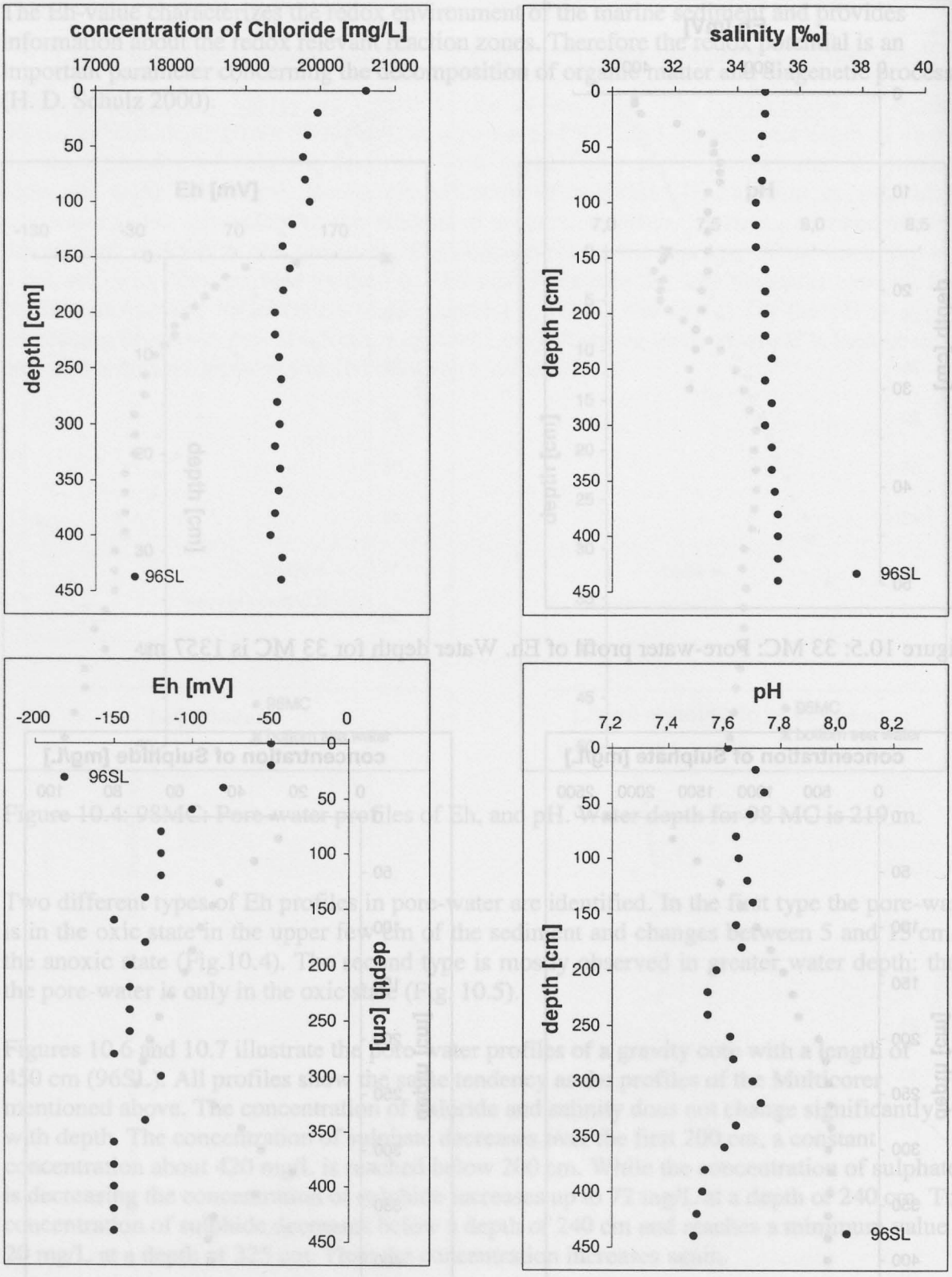

Figure 10.7: 96SL: Pore-water profiles of Chloride, salinity, Eh, and pH.

The figures 10.8 and 10.9 show the reasonable match between the measured values of pore-water gained for the first 50 cm from an Multicorer and in deeper parts from an gravity core sampled in the same position. There is obviously no significant break near the transition of the two different cores.

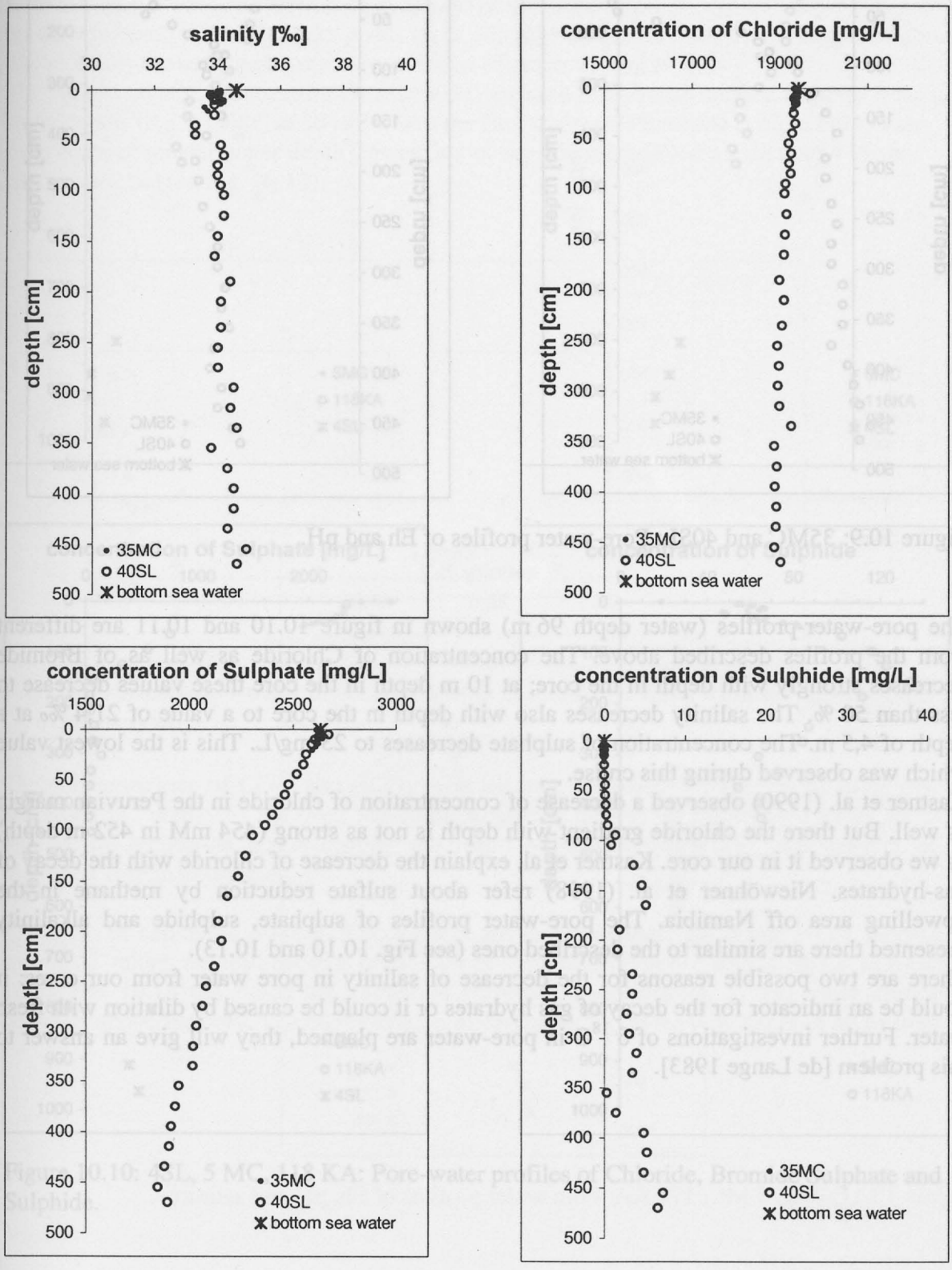

Figure 10.8: 35MC and 40SL: Pore-water profiles of salinity, Chloride, Sulphate and Sulphide.

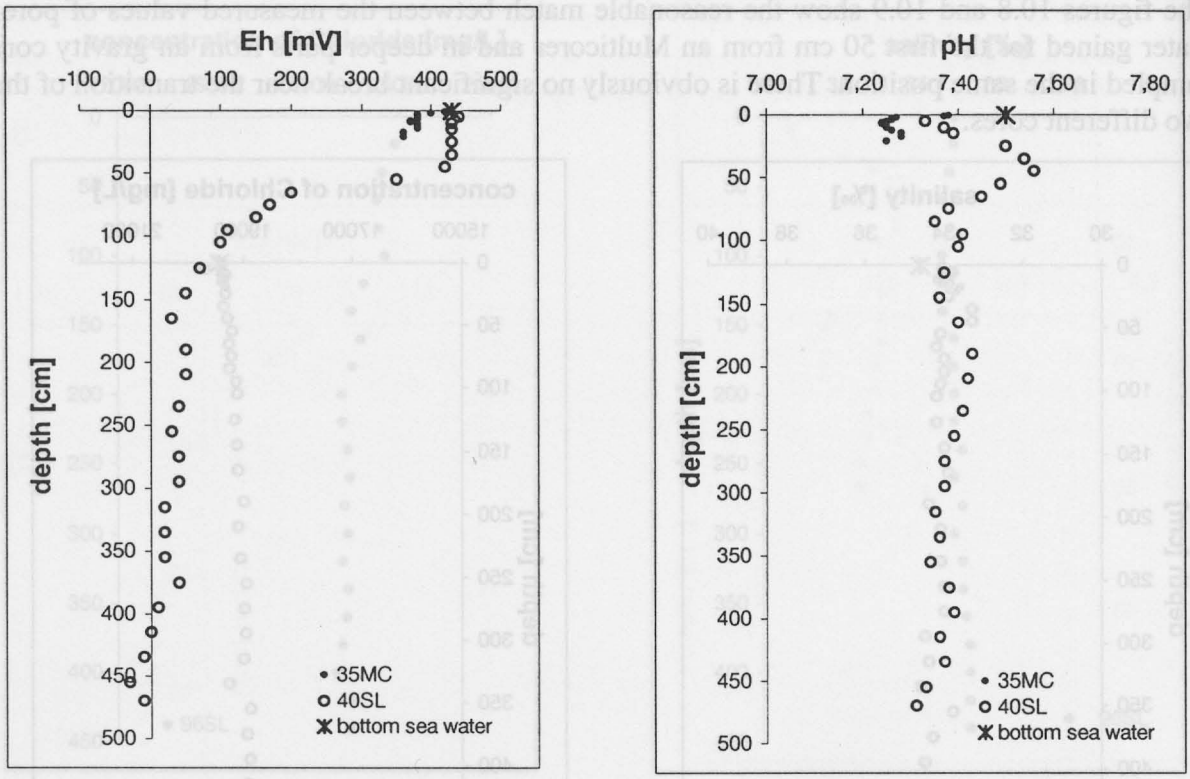

Figure 10.9: 35MC and 40SL: Pore-water profiles of Eh and pH.

The pore-water-profiles (water depth 96 m) shown in figure 10.10 and 10.11 are different from the profiles described above. The concentration of Chloride as well as of Bromide decreases strongly with depth in the core; at 10 m depth in the core these values decrease to less than 50 %. The salinity decreases also with depth in the core to a value of 21,4 ‰ at a depth of 4,5 m. The concentration of sulphate decreases to 23 mg/L. This is the lowest value which was observed during this cruise.

Kastner et al. (1990) observed a decrease of concentration of chloride in the Peruvian margin as well. But there the chloride gradient with depth is not as strong (454 mM in 452 m depth) as we observed it in our core. Kastner et al. explain the decrease of chloride with the decay of gas-hydrates. Niewöhner et al. (1998) refer about sulfate reduction by methane in the upwelling area off Namibia. The pore-water profiles of sulphate, sulphide and alkalinity presented there are similar to the described ones (see Fig. 10.10 and 10.13).

There are two possible reasons for the decrease of salinity in pore water from our cores: it could be an indicator for the decay of gas hydrates or it could be caused by dilution with fresh water. Further investigations of $\delta\ ^{18}O$ in pore-water are planned, they will give an answer to this problem [de Lange 1983].

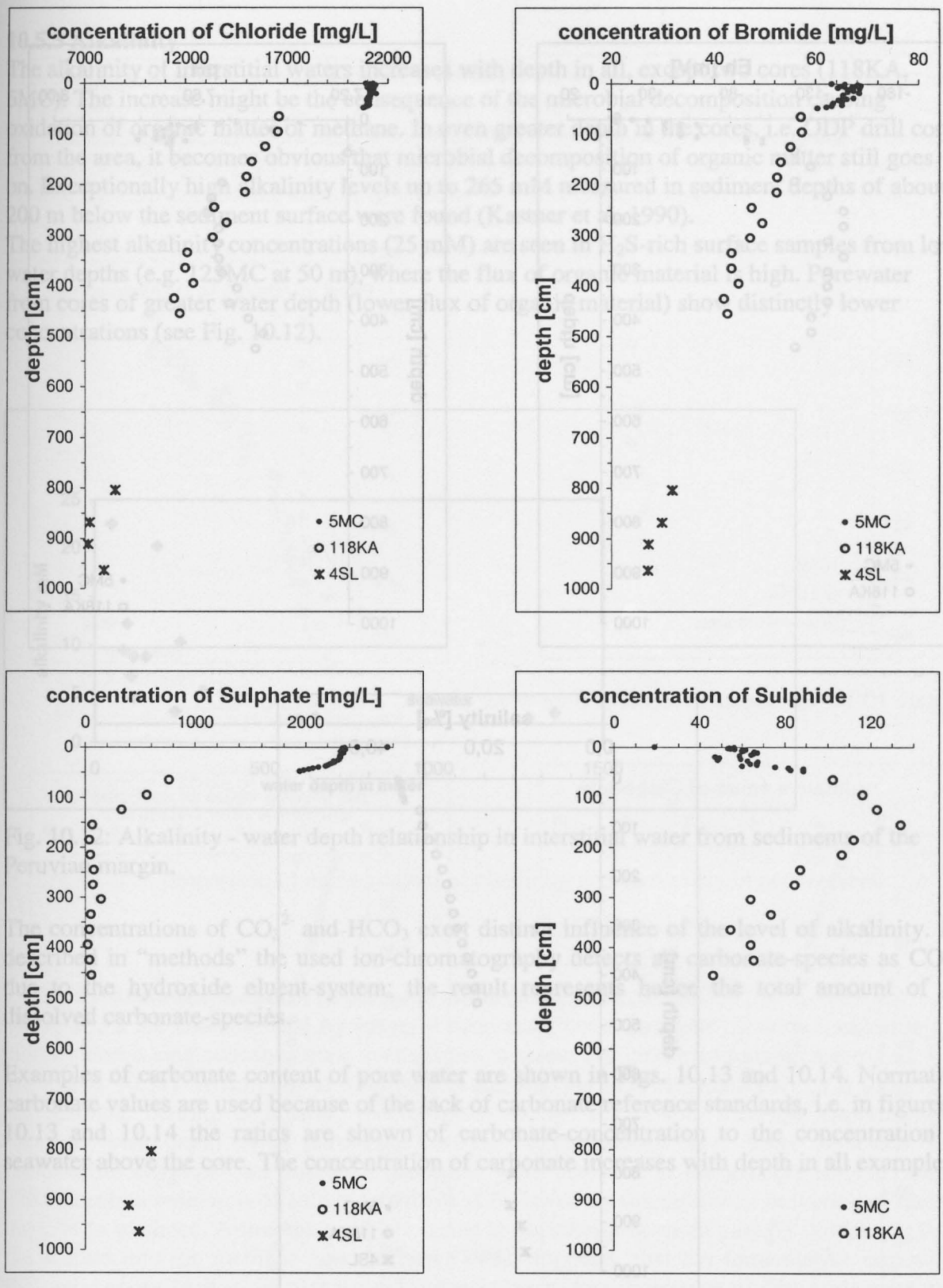

Figure 10.10: 4SL, 5 MC, 118 KA: Pore-water profiles of Chloride, Bromide Sulphate and Sulphide.

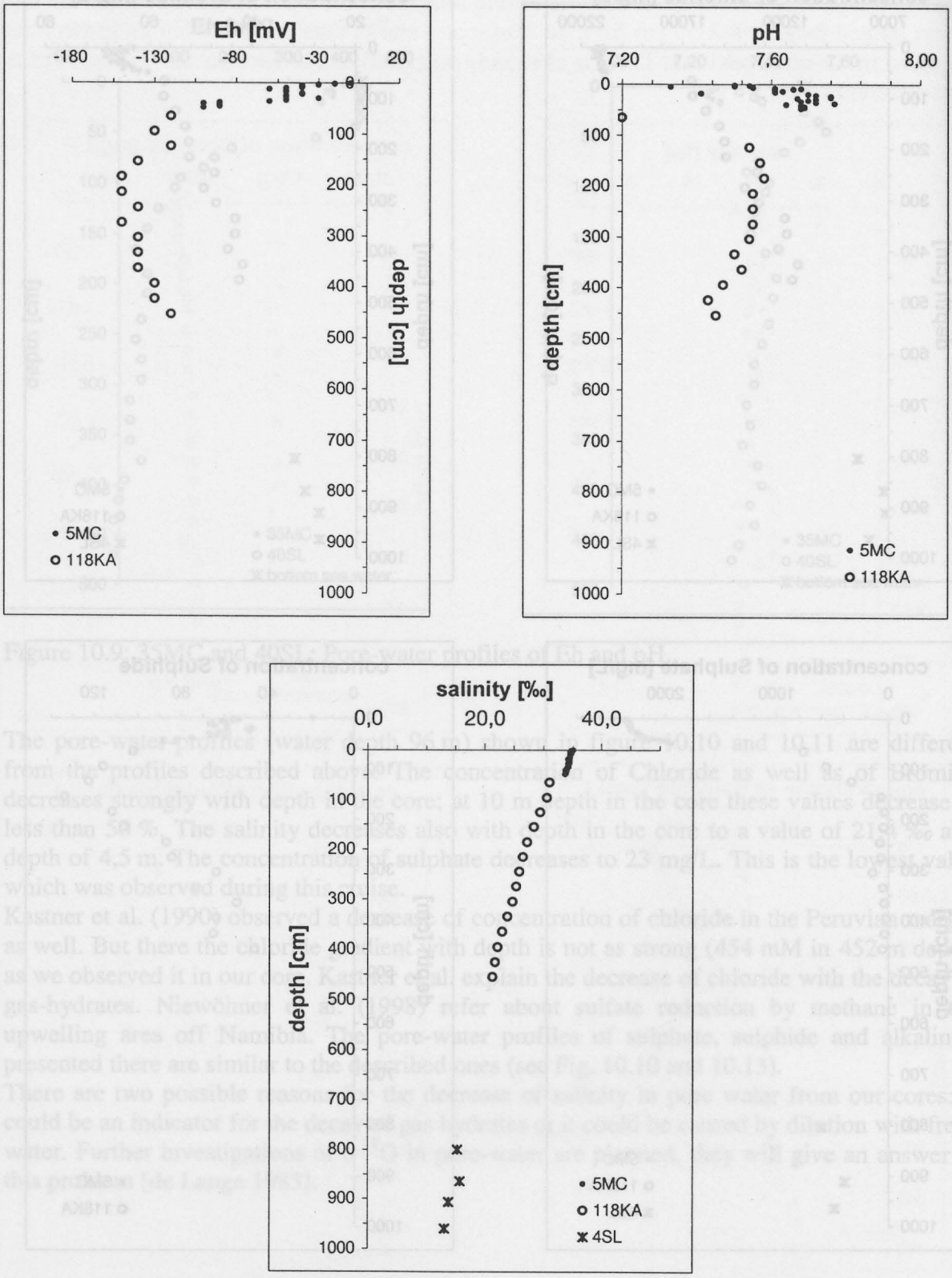

Figure 10.11: 4SL, 5 MC, 118 KA: Pore-water profiles of Eh, pH and salinity.

10.5.5 Alkalinity

The alkalinity of interstitial waters increases with depth in all, except two cores (118KA, 5MC). The increase might be the consequence of the microbial decomposition causing oxidation of organic matter or methane. In even greater depth in the cores, i.e. ODP drill cores from the area, it becomes obvious that microbial decomposition of organic matter still goes on. Exceptionally high alkalinity levels up to 265 mM measured in sediment depths of about 200 m below the sediment surface were found (Kastner et al. 1990).
The highest alkalinity concentrations (25 mM) are seen in H_2S-rich surface samples from low water depths (e.g. 125MC at 50 m), where the flux of organic material is high. Porewater from cores of greater water depth (lower flux of organic material) show distinctly lower concentrations (see Fig. 10.12).

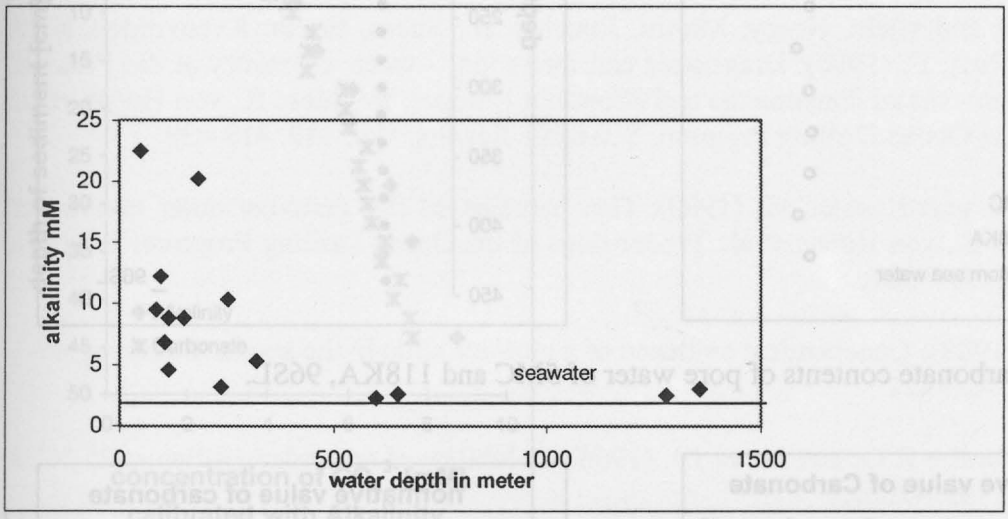

Fig. 10.12: Alkalinity - water depth relationship in interstitial water from sediments of the Peruvian margin.

The concentrations of CO_3^{2-} and HCO_3 exert distinct influence of the level of alkalinity. As described in "methods" the used ion-chromatography detects all carbonate-species as CO_3^{2-} due to the hydroxide eluent-system; the result represents hence the total amount of all dissolved carbonate-species.

Examples of carbonate content of pore water are shown in Figs. 10.13 and 10.14. Normative carbonate values are used because of the lack of carbonate reference standards, i.e. in figures 10.13 and 10.14 the ratios are shown of carbonate-concentration to the concentration in seawater above the core. The concentration of carbonate increases with depth in all examples.

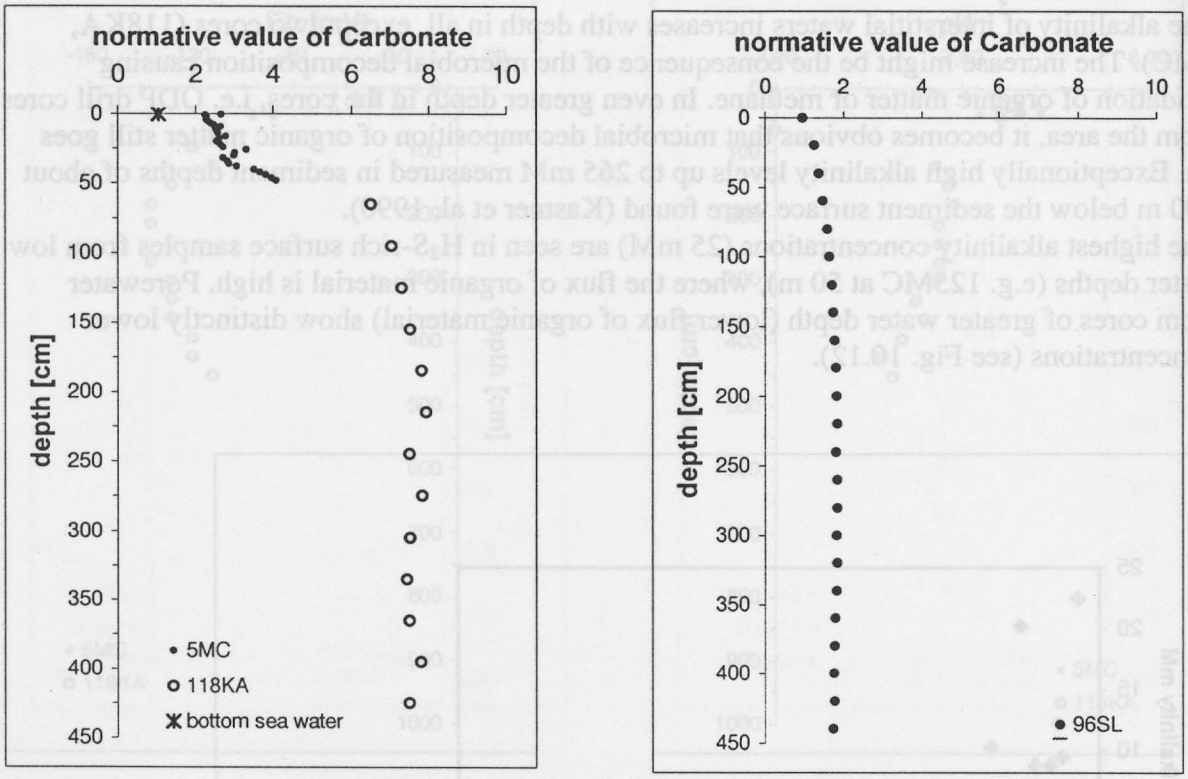

Figure 10.13: Carbonate contents of pore water of 5MC and 118KA, 96SL.

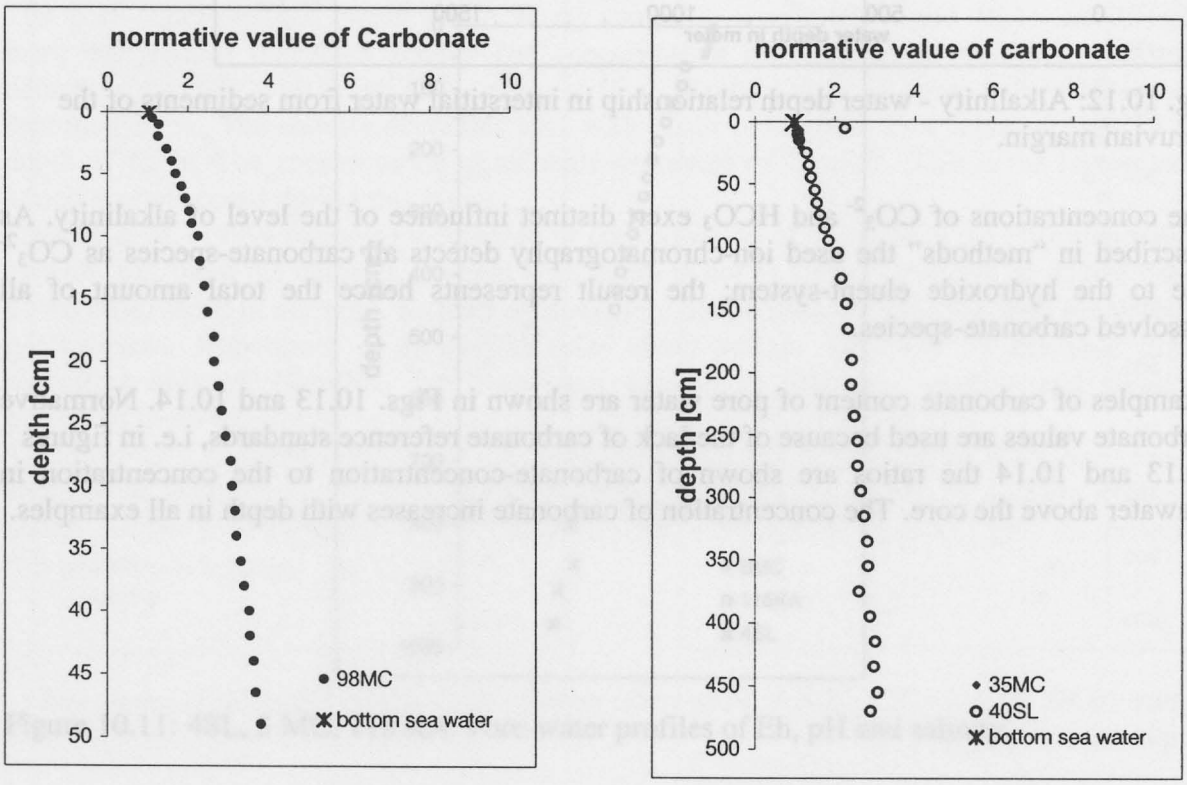

Figure 10.14: Carbonate contents of pore water of 98MC; 35MC and 40SL.

Figure 10.15 shows similarity of trends between alkalinity and carbonate amount for one typical pore water profile (45MC). This figure shows that the concentrations of HCO_3^- and CO_3^{2-} exert distinct influence on the level of alkalinity. We plan to perform the comparison between alkalinity and the value of CO_3^{2-} detected by ion-chromatography with the aim to replace the time consuming alkalinity titration with ion-chromatography.

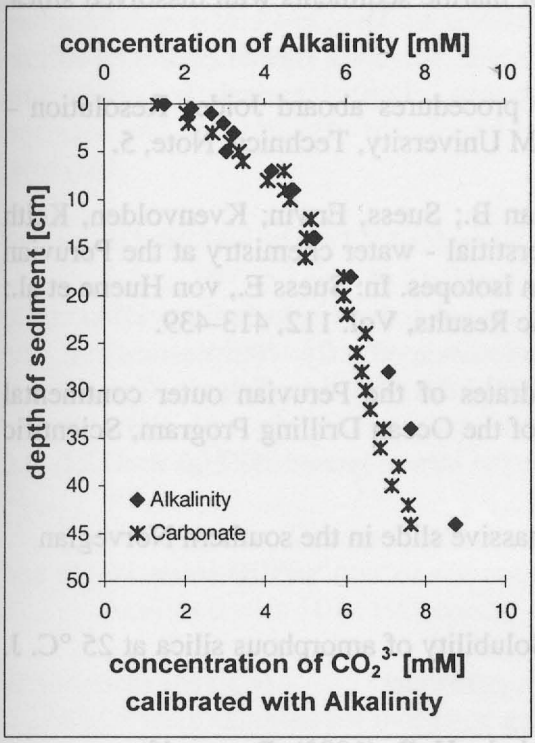

Figure 10.15: Comparison of measurement of alkalinity and Carbonate in pore-waters of 45 MC.

10.5.6 Evidence for methane in cores off Lima (4SL, 5MC, 118KA)

These cores are characterized by strongly decreasing concentrations of sulfate, chloride and slightly decreasing concentrations in alkalinity, whereas H_2S and ammonia increases (see Fig. 10.10 and 10.11). According to Kvenvolden and Kastner (1990) such a pattern is diagnostic for methane bearing sediments. Geochemical studies reveal that methane concentrations increase with depth after pore-water sulfate concentrations have been depleted. This relationship suggests that microbial processes were involved in the generation of methane. The microbial reduction of sulfate to sulfide is followed by the microbial reduction of carbon dioxide to methane. Ammonia production rate is not changing when passing downward from the sulfate into the methane zone. Berner (1980) suggests, that the fermentative organisms that decompose high molecular weight components to low molecular weight molecules used by the sulfate reducers are similar in both zones. Decreasing chloride contents in the interstitial water represent a dilution by fresh water, possibly released from the dissociation of gas hydrates.

10.6. References

Berner R.A. (1980): Early Diagenesis. A Theoretical Approach. Princeton University Press, Princeton, N.J.,pp. 241.

Cruise Report BMBF-Forschungsvorhaben 03G0139A SONNE-Fahrt-SO 139, BGR Archiv-Nr.: 118.878,1 Juni 1999

Fanning K.A. and Schink D.K. (1969): Interaction of marine sediments with dissolved silica. Limnol. Oceanogr. 14, 59-68.

Gieskes J., Peretsman G. (1986): Water chemistry procedures aboard Joides Resolution – some comments. Ocean Drilling Program Texas A&M University, Technical Note, 5.

Kastner, Miriam; Elderfield, Henry; Martin, Jonathan B.; Suess, Erwin; Kvenvolden, Keith A.; Garrison, Robert, E. (1990): Diagenesis and interstitial - water chemistry at the Peruvian continental margin - major constituents and strontium isotopes. In: Suess E., von Huene et al.: Proceedings of the Ocean Drilling Program, Scientific Results, Vol. 112, 413-439.

Kvenvolden K.A. and Kastner M. (1990): Gas hydrates of the Peruvian outer continental margin. In: Suess E., von Huene et al.: Proceedings of the Ocean Drilling Program, Scientific Results, Vol. 112, 517-527.

De Lange G. J. (1983): Geochemical evidence of a massive slide in the southern Norvegian Sea. Nature 305, 420-422

Morey G.W., Fournier R.O. and Rowe J.J. (1964): Solubility of amorphous silica at 25 °C. J. geophys.Res. 68, 1995-2002.

Niewöhner, C.; Hensen, C.; Kasten, S.; Zabel, M.; Schulz, H. D. (1983): Deep sulfate reduction completely mediated by anaerobic methane oxidation in sediments of the upwelling area off Namibia. Geochimica et Cosmochimica Acta 62, 455-464.

Sarazin G., Michard G., Prevot F. (1999): A rapid and accurate spectroscopic method for alkalinity measurements in sea water samples. Water Research 33, 290-294.

Schulz, H. D. (2000): Quantification of early diagenesis: Dissolved constituents in marine pore water, in: Schulz, H. D.; Zabel, M.; Marine Geochemistry, Springer Verlag, Berlin, Heidelberg.

Schulz H. D. (2000): Redox measurements in marine sediments, in: Schüring, J.; Schulz, H.D.; Fischer, W.R.; Böttcher, J.; Duijnisveld, W.H.M.: Redox, fundamental processes and applications, Springer Verlag, Berlin, Heidelberg

Suess E. (1981): Phosphate regeneration from sediments of the Peru continental margin by dissolution of fish debris. Geochimica et Cosmochimica Acta 45, 577-588.

Tessier, A.; Campell, P.G.C.; Bison, M. (1979): Sequentiell extraction procedure for the speciation of particulate trace metals, Anal. Chem. 51, 844-851.

Thiede J. (1981): Skeletal plancton and nekton in upwelling water masses off Northwestern South America and Northwest Africa. In Suess S. and Thiede J.: Coastal Upwelling, Its Sediment Record, Part A, 183-209. Plenum Press, New York.

Wehausen R., Schnetger B. Brumsack H.-J., De Lange, G.J. (1999): Determination of major and minor ions in brines by X-ray fluorescence spectrometry: comparison with other common analytical methods. X-Ray Sepctrometry. 28, 168-172.

11. Microbiology

11.1. Interaction between nitrate storing sulfur bacteria and sulfate reducing bacteria

Kallmeier, J., Klockgether, G.

Introduction

The interactions between nitrate storing sulfur bacteria and sulfate reducing bacteria were the main focus of the investigations of the MPI group. In order to develop a better understanding how such high productivity areas maintain conditions that prevent a flux of hydrogen sulfide from the sediment into the water column a variety of geochemical and biological investigations were performed.

Gravity and Piston cores.

A total of 3 gravity cores, each about 5 m long, were taken for MPI exclusively and processed on board. The numbers of the cores used are: SL 23, 39, 95.

The cores were not opened lengthwise like normally done in sedimentological work but cut in 1 m whole round core (wrc) pieces and the ends sealed immediately with plastic caps. The cores are then stored at 4^0 Celsius and processed within the next 2 to 3 days. Sampling is done with the core sitting vertically inside a custom made cutting rig with the sediment pushed out to the top of the liner. With this technique the loss of gasses like H_2S and CH_4 and the introduction of oxygen can be minimized.

Sampling was done in 10 or 20 cm resolution. Each sample section was 10 cm in length and had a distinct depth for each kind of subsample.

0-1 cm	discarded
1-7 cm	SRR, CH_4, porosity, org. geochemistry, porewater
7-9 cm	archive
9-10 cm	discarded

In case of sampling in 20 cm resolution, one 10 cm section was sampled, the next 10 cm were discarded completely.

Sulfate reduction rate measurements

5 ml glass tubes with a syringe plunger on the one end were introduced into the sediment, pulled out and the open end closed with black rubber stoppers immediately. It was tried to fill the glass tubes without trapping any air bubbles. 10 □l of $^{35}SO_4^{2-}$ radiotracer (about 200-400 kBq) was injected into each sample. The samples were incubated for 24 hours at 4^0 Celsius in the dark. Incubation is stopped by pushing the sediment into centrifuge tubes, filled with 20 ml of 20% zinc acetate.

The analysis will be done in Bremen. The sediment will be boiled in a reflux distillation in an acidic and reduced chrome $^{2+}$ solution. This will liberate all sulfides and elemental sulfur as Hydrogen Sulfide. The sulfide produced is then trapped in zinc acetate. By comparison of the radioactivity added as sulfate to the produced sulfide the bacterial activity can be calculated.

Porosity

Sediment is sampled in cut off 10 ml syringes. The syringes were closed with rubber stoppers and stored.

Methane

Sediment is sampled in cut off 5 ml syringes. Exactly 3 ml of sediment is transferred into a 20 ml crimp vial filled with 6 ml 2.5 % NaOH and sealed immediately. The vial is thoroughly shaken and stored cool upside down.

Analysis is done by headspace analysis with a gas chromatograph.

Archive
About 40 to 50 ml of sediment is transferred into a Zip Lock Bag and stored cool.

Porewater (PW)
2 Plexiglas cylinders (about 10 cm^2 each) are inserted into the sediment and either immediately transferred into the PW squeezer (KC equipment, Silkeborg, Denmark) or wrapped into SARAN foil (Dow), stored in the dark at 4^0 Celsius and processed within the next hour. WHATMAN GF/F FILTERS (0.45 □m) were used for filtration. For volatile fatty acid (VFA) analysis the filters were ignited before use. The PW was collected in glass syringes and subsequently transferred into different vials, depending on the substance to be analyzed.

SO_4/H_2S
3-5 ml PW in 1 ml 2% $ZnCl_2$ solution, stored frozen.
CO_2 (Alkalinity)
Ca. 1 ml PW with 60 ul saturated $HgCl_2$ sol. in 2 ml Zinsser Vial. PW has to filled up so there is no headspace left in the vial.
NH_4
Ca. 2 ml PW. Stored frozen
VFA
PW in ignited Zinsser Vials. Stored frozen.
Remaining PW
Acidified with 10 ul HCl conc.

Multicores (MUCs)
32 MUCs were sampled for inorganic geochemical analysis and SRR.
Analysis were performed on the following MUCs: MC 1, 2, 3, 5, 8, 14, 17, 18, 19, 21, 22, 30, 33, 35, 45, 47, 67, 71, 79, 81, 88, 98, 104, 119, 120, 121, 122, 123, 125, 126, 127, 129.

Subsampling
Because the sediment is much softer than in the gravity cores the subsampling strategy is different. Immediately upon arrival on deck, Plexiglas tubes with 26 or 36 mm diameter were carefully inserted into the MUC tube. In order not to disturb the surface that contained bacterial mats, the top 1 to 2 cm were cut with a scalpel around the tubes. After removal from the MUC the tubes were brought into the lab and either stored at 4^0 Celsius in the dark (for SRR) or processed immediately (for PW). Not all analysis described were performed on all cores.

Porewater
For PW pressing, one 36 mm tube was sliced into 1 cm sections down to 10 cm, below that in 2 cm sections down to 26 cm. The sediment was transferred immediately into the PW squeezer (KC equipment, Silkeborg, Denmark). The processing of the PW was identical to the one described for the gravity cores except VFAs, which were not measured on the MUC samples.

Sulfate reduction rate (SRR) measurements
For SRR measurements we used 26 mm diameter Plexiglas Tubes with small holes in 1 cm intervals that were closed with silicone rubber cement. Those tubes were inserted into the MUC immediately upon retrieval and brought into the lab. There they were stored for at least

a few hours at 4^0 Celsius in order to equilibrate. Into each hole that was in contact with the sediment 5□l of $^{35}SO_4^{2-}$ radiotracer (about 100-200 kBq) was injected. The core was then incubated for 24 hours at 4^0 Celsius in the dark. After that the sediment was sliced in 1 cm sections for the top 6 cm below that in 2 cm respectively and transferred into centrifuge tubes, filled with 20 ml of 20% zinc acetate. The analysis in Bremen is identical to the one described for the gravity cores.

Samples for organic geochemistry

For the determination of organic compounds the following samples were taken and stored frozen immediately.

Multicorer: 1, 2, 5, 7, 14, 17, 18, 20, 29, 32, 33, 35, 45, 47, 50, 67, 71, 79, 81, 88, 98, 99, 104, 111, 113, 119, 121, 125, 127, 129, 130, 142, 143

Multicorer were sampled as follows: the first 5 cm every cm, 5 to 10 cm every 2 nd centimeter, 10 to core end every 5 cm

Gravity corer: 23, 39, 95

Gravity corer were samples every 10 to 20 cm

11.2 Abundance of Nitrate-storing Sulfur Bacteria (*Thioploca* spp., *Beggiatoa* spp.) along the Coast of Peru and Microsensor Profiling

Riechmann, D., Wieringa, E.

Introduction

The aim of this study was a quantitative analysis of the population and species distribution of nitrate-storing sulfur bacteria in shelf sediments of the upwelling region along the Peruvian coast. During a cruise aboard R/V SONNE (SO 147) from 04. - 30. June 2000 sediment samples were taken by multicorer sampling between 9° and 14° south. Stations along OFOS transects were chosen between 86 m and 360 m water depth according to the visual presence of the filamentous, mat-forming sulfur bacteria. In the upper layers of the sediment cores the habitat was described by microsensor profiling.

These organisms couple the sedimentary sulfur and nitrogen cycle in a previously unknown manner. They are able to store both metabolites, sulfur and nitrate, up to 800 mM (Fossing *et al.*, 1995). They gain energy by oxidizing sulfide with nitrate as the electron acceptor. Hydrogen sulfide is produced by bacterial anaerobic sulfate reduction in the upwelling region across the Chilean and Peruvian shelf in high amounts (Ferdelman *et al.*, 1997). Nitrate is provided from the water column. *Thioploca*-filaments are motile by gliding. The mostly vertical orientated sheath is used as a tunnel-system in which they shuttle chemotactically between deeper parts of the sediment and the bottom water.

Material and Methods

Biomass

To measure the biomass of the filamentous *Thioploca* spp. and *Beggiatoa* spp. subcores were obtained from the multiple corer (MC) with plexiglas tubes (3.6 cm inner diameter, 30 cm length). The cores were stored at 4°C for up to three days. The sediment in each core was extruded from the tube and placed on a slightly tilted surface. The silt between the sheaths (bundles of *Thioploca*-trichomes) was then washed away carefully with seawater from a

squirt bottle, starting at the top of the core. After one centimeter of the sediment had been washed away, the number of exposed sheaths was counted using a stereolupe. At each depth 5 to 8 randomly chosen sheaths were cut of and inspected with a microscope. The number of sheaths per square centimeter multiplied by the average number of trichomes per sheath, the average diameter of trichomes (which is species dependent) and the average sheath length in the one centimeter interval gave the biovolume of trichomes per sediment volume at a given depth (Schulz *et al.*, 1996; Schulz *et al.*, in press). The average sheath length was calculated by a given factor depending on the orientation of the sheaths per sediment depth (Schulz *et al.*, 1996). The biomass of trichomes was calculated from the biovolume by assuming that the *Thioploca* trichomes have a density of 1 g cm^{-3}. The selected sheaths were prepared in 35‰ NaCl and 100% methanol for further investigations of intracellular nitrate and sulfur concentrations.

Microsensor measurements

Vertical profiles of oxygen, pH and redox signals were measured in the upper 3 cm of the sampled cores (Revsbech, 1989; Kühl *et al.*, 1998). Cores were incubated in 8°C seawater under a N_2/CO_2 (95:5) atmosphere to simulate *in situ* oxygen concentrations. Bottom water oxygen concentration was measured using Winkler titration (Grasshoff *et al.*, 1983). Mild magnetic stirring of the water layer above the sediment was used to reduce diffusive boundary layer disturbance. Glass electrodes (with tip diameters of 5 - 10 µm) were mounted on a motor driven micromanipulator. Profiles were recorded in 100 to 200 µm vertical steps, with 2 sec-15 sec intermittent stabilization time. Electrode outputs were recorded with a computer (program Insight by Roland Thar).

Results and Discussion

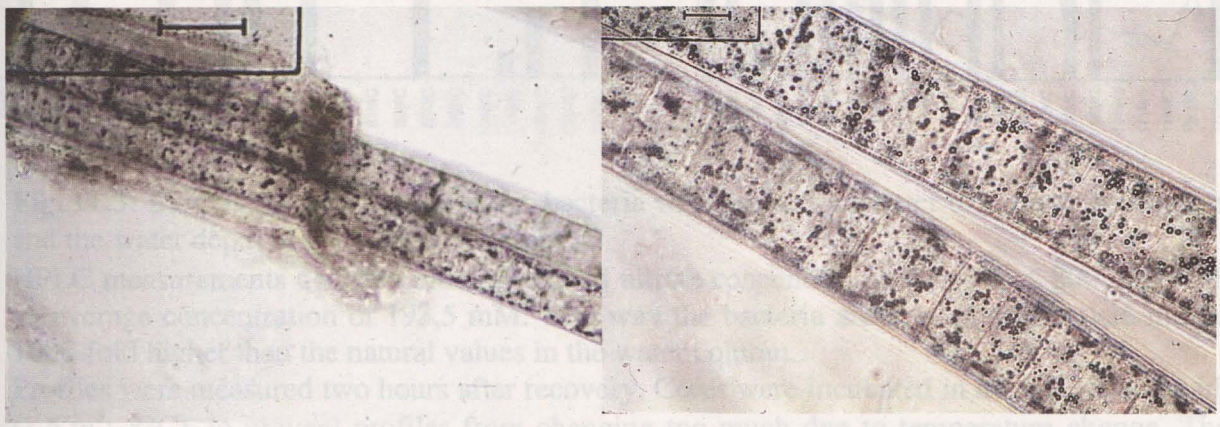

Fig. 11.1: Multicellular filaments (trichomes) of *Thioploca* spp. (left scale bar = 100 µm, right scale bar = 25 µm), with intracellular sulfur globules.

At 16 stations members of the genus *Thioploca* and *Beggiatoa* were abundant. The diameter frequency (Fig. 2) by which the different species are distinguished showed that the sediments on the Peruvian shelf are inhabited by all up to now known marine *Thioploca* species: *T. marina* (2.5 - 5 µm), *T. chileae* (12 -20 µm) and *T. araucae* (30 – 43 µm) and a larger species with a filament diameter between 50 and 80 µm (Fig. 11.1). This last diameter class remains to be proven as a new species by additional 16S rDNA sequencing. Sheathless *Beggiatoa* filaments inhabited at station MC 98 and MC 47 the sediment surface while *Thioploca* appeared in the sediment horizon underneath. A maximum length of *Thioploca*-sheaths up to 28 cm could be measured. Station MC45 showed the highest biomass of filamentous bacteria with 240 g/m^2 at 153 m water depth (Fig. 11.3).

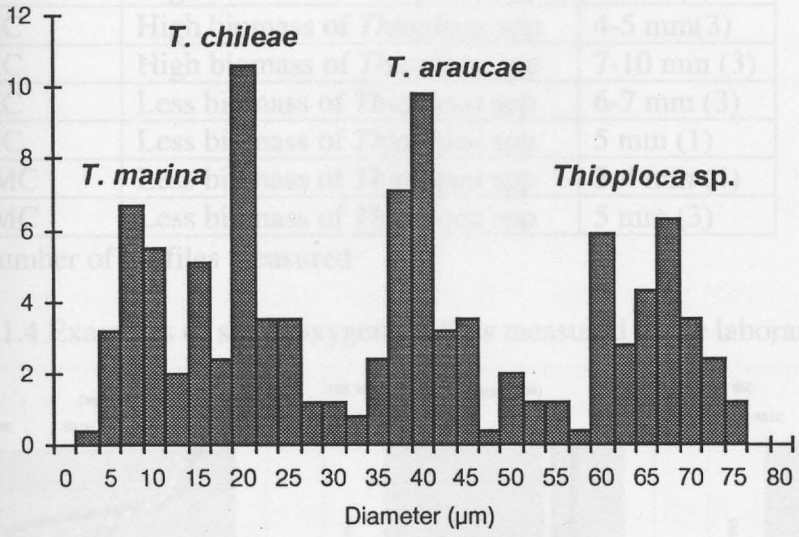

Fig. 11.2: Diameter frequency of 254 randomly chosen filaments.

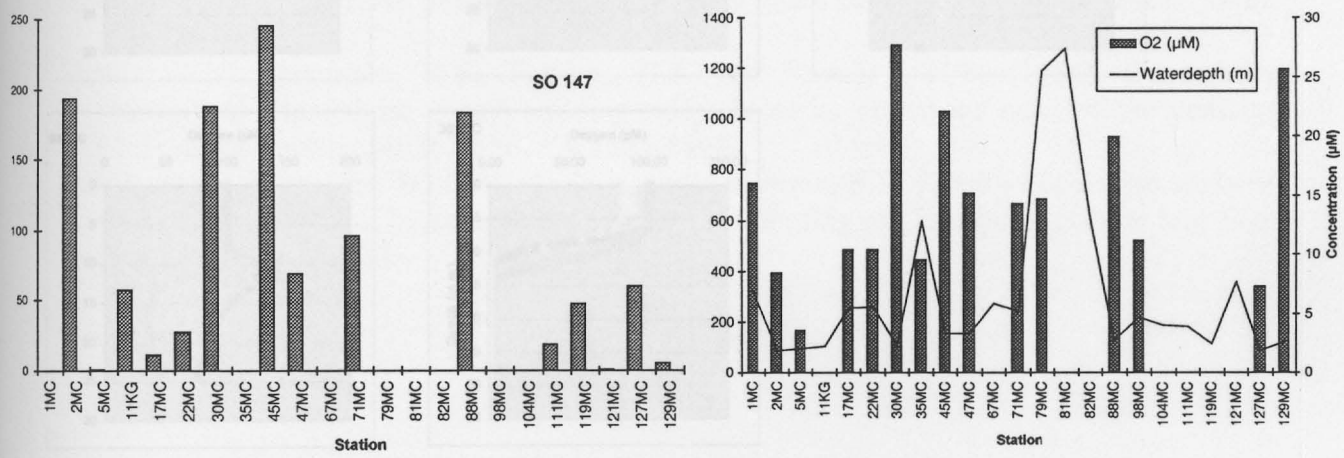

Fig. 11.3: Biomass of filamentous sulfur bacteria with the bottom water oxygen concentration and the water depth at the different stations.

HPLC measurements detected intravacuolated nitrate concentrations of up to ≤ 800 mM with an average concentration of 193,5 mM. This way the bacteria are able to accumulate nitrate 1000-fold higher than the natural values in the water column.

Profiles were measured two hours after recovery. Cores were incubated in a cooled water bath (1.5 m^3; 8°C), to prevent profiles from changing too much due to temperature change. The overlaying water of the cores had to be brought in contact with the water in the water bath, but this turned acidic upon contact with the sealing-kit (used because the bath was leaking). This disturbed the pH signal considerably and thus the redox profiles too. Sulfide profiles were not measured, while the electrical contact could not be established.

Table 11.1. Oxygen penetration depth (OPD) measured on board with microsensors in multicorer cores from different stations.

Station	Description	OPD (*)
14 MC	Deep	7 mm (2)
35 MC	Deep	6-10 mm (4)
125 MC	Above OMZ	8 mm (3)
47 MC	Feltish *Beggiatoa*	8 mm (3)
98 MC	Feltish *Beggiatoa*	5 mm (1)

30 MC	High biomass of *Thioploca* spp.	8 mm (3)
45 MC	High biomass of *Thioploca* spp	4-5 mm(3)
88 MC	High biomass of *Thioploca* spp	7-10 mm (3)
17 MC	Less biomass of *Thioploca* spp	6-7 mm (3)
71 MC	Less biomass of *Thioploca* spp	5 mm (1)
111 MC	Less biomass of *Thioploca* spp	2-4 mm (4)
129 MC	Less biomass of *Thioploca* spp	5 mm (3)

- number of profiles measured

Fig 11.4 Examples of some oxygen profiles measured in the laboratory aboard R/V SONNE.

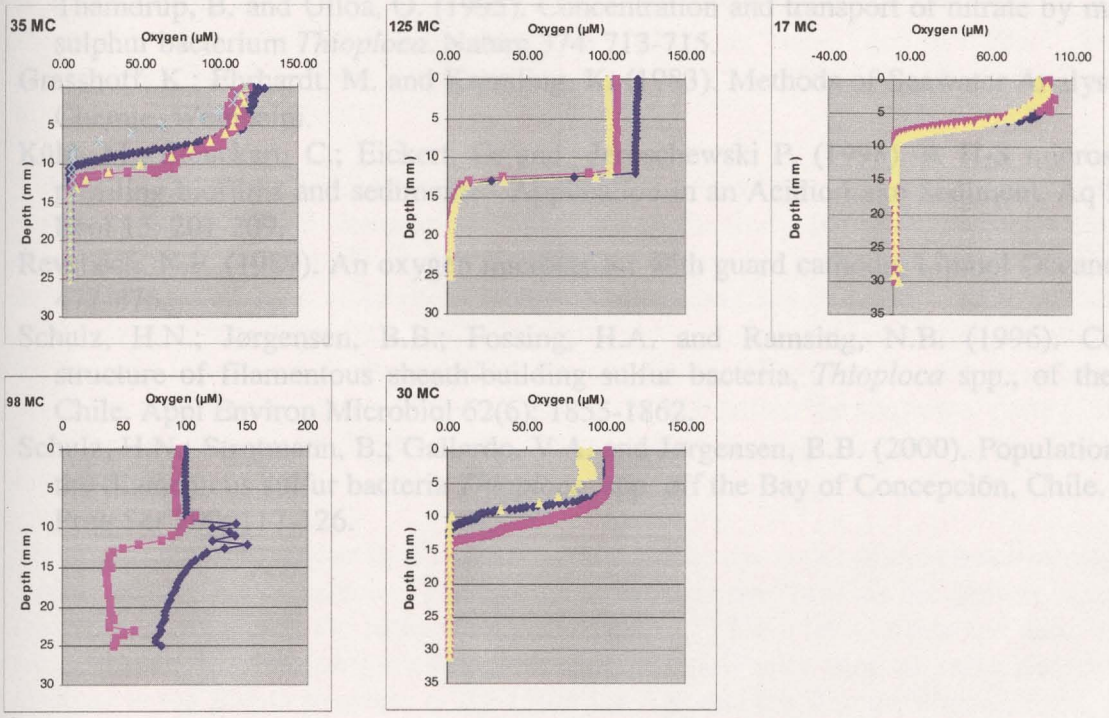

References

Braman, R.S. and Hendrix, S.A. (1989). Nanogram nitrite and nitrate determination in enviromental and biological materials by vanadium (III) reduction with chemiluminescence detection. Anal Chem. 61: 2715-2718.

Ferdelmann, T.G.; Lee,C.; Pantoja,S.; Harder, J.; Bebout, B.B. and Fossing, H. (1997). Sulfate reduction and methanogenesis in *Thioploca*-dominated sediment off the coast of Chile. Geochim. Cosmochim. Acta 61: 3065-3079.

Fossing, H.; Gallardo, V.A.; Jørgensen, B.B.; Hüttel, M.; Nielsen, L.P.; Schulz, H.; Canfield, D.E.; Forster, S.; Glud, R.N.; Gundersen, J.K.; Küver, J.; Ramsing, N.B.; Teske, A.; Thamdrup, B. and Ulloa, O. (1995). Concentration and transport of nitrate by matforming sulphur bacterium *Thioploca*. Nature 374: 713-715.

Grasshoff, K.; Ehrhardt, M. and Kremling, K. (1983). Methods of Seawater Analysis. Verlag Chemie, Weinheim.

Kühl, M.; Steuckart, C.; Eickert, G. and Jeroschewski P. (1998). A H_2S microsensor for profiling biofilms and sediments - Application in an Acidic Lake Sediment. Aq Microbiol Ecol 15: 201-209.

Revsbech, N.P. (1989). An oxygen microsensor with guard cathode. Limnol Oceanogr 34(2): 472-476.

Schulz, H.N.; Jørgensen, B.B.; Fossing, H.A. and Ramsing, N.B. (1996). Community structure of filamentous sheath-building sulfur bacteria, *Thioploca* spp., of the coast of Chile. Appl Environ Microbiol 62(6): 1855-1862.

Schulz, H.N.; Strotmann, B.; Gallardo, V.A. and Jørgensen, B.B. (2000). Population study of the filamentous sulfur bacteria *Thioploca* spp. off the Bay of Concepción, Chile. Mar Ecol Prog Ser 200: 117-126.

12. Core descriptions and reflectance spectra

Dullo,W. Chr., Rein, B., Wolf, A.; Biebow, N., Schaber, K., Sirocko, F.

Regional setting of the investigated area and objectives

The continental shelf offshore Peru is characterised by different forearc basins. The deepest basin is the Yaquina Basin in an upper continental slope setting off Chimbote. The outer shelf and middle slope basins which stretch in a NNW-SSE direction comprise the Lima Basin and the West Pisco Basin. These basins occur in present day water depth between 500 and 2000 m. The shallower basins in a coastal setting are the large Salaverry Basin and the East Pisco Basin (Fig. 12.1). They are separated by the Lima Platform, a structural high with almost no significant Holocene sediments. Between the Salaverry Basin in the north and the East Pisco Basin, there is a small depression, which we address as "Mud Lens of Callao", This lens is seawards encircled by the elevated structure of the Lima Platform. This mud lens contains thicker Holocene sediments.

The coastal basins occur in present day water depths between 100 m and 350 m. The surface waters above (50m) are characterised by a high productivity due to intense upwelling. Hence, these shallow basins are all characterised by a depositional environment fully exposed to the oxygen minimum zone and exhibit high sedimentation rates of up to 50cm/ky. The presence of the oxygen minimum zone results in distinctly stratified and laminated sediments, at least for specific time intervals during which the upwelling cell was active. Due to changes in sea level, the sedimentary record of the activity of the cell within the shallower parts (150 m - 180 m of present day water depth) of the coastal basins is almost limited to the Holocene and interglacials.

The major objective of our studies is to reconstruct the dynamics of the upwelling regime with respect to El Niño frequencies. The laminated sections may provide the archive to reconstruct these dynamics within the Holocene time. Apart of El Niño frequencies and their variability, we also want to focus on intra Holocene climatic variability such as early Holocene abrupt changes in the ENSO structure or the Little Ice Age and the Roman Warm Period, for which the stratigraphic record should provide the necessary resolution in time. In addition, we included aspects of glacial interglacial changes. Therefore, we concentrated our sampling on the coastal basins on the shallow shelf.

Hydroacoustic Profiles

In order to check for suitable coring sites, all study areas were first explored with two high resolution hydroacoustic systems (SEL 96 and SES 2000) provided by the University of Rostock. With its improved technique, it was possible to visualise strata thinner than 10cm even down the continental slope up to an overall sediment thickness of 30m. The major advantage of these systems is the resolution quality in shallow water settings in contrast to the installed parasound system.

We defined three study areas. The central Salaverry Basin offshore Chimbote, study area A, the southern Salaverry Basin NW offshore Callao including the Mud Lens, study Area B, and the East Pisco Basin, which is study area C. Within all selected areas we run 216 profiles ± perpendicular to the slope inclination and ± parallel to the slope covering about 6000 km. These profiles provided an excellent insight into the sedimentary geometries of the strata. The position of all profiles is given in Figs. 5.1, 5.2, 5.3

Sampling methods

We used gravity cores and piston cores 12,5 cm in Ø as well as box cores of 30 x 30 cm. To recover undisturbed surface sediments we used a multi coring device of 10 cm Ø. All in all we run 26 gravity cores, 6 piston cores, and 3 box cores. Total recovery is 155.63 m. In addition we run 39 multi cores for retrieving undisturbed surfaces. Fig 12.2 provides a location of all stations

All multicores were sampled immediately on board in cm intervals for dinoflagellate cyst analyses and sedimentological studies. Every five cm a syringe sample (5 ml) was taken for physical property analyses. All gravity cores and piston cores were scanned for magnetic susceptibility, gamma ray and sonic velocity. After this procedure they were opened for lithological description and sampling for radiographs. From selected sediment cores (see appendix III), reflectance spectra (Fig12.6 – 12.12) were acquired for a first screening of spectral features on fresh cores and spectral variability downcore. Onboard reflectance measurements were made every 5, 10 or 20 mm. The point spread of this device is 2mm, the spectral coverage ranges from 380 to 730 nm with a spectral resolution of 10 nm. Part of the cores were also colour scanned.

All box cores were opened on deck in order to avoid poisoning with the toxic H_2S gas. Subsampling was performed by 10 ml syringes in a distance of 5 cm. Three series of archive boxes (15 x 5 x 100 cm) were taken.

The central Salaverry Basin offshore Chimbote, study area A

The relative wide shelf area off Chimbote is characterised by sandy residual sediments typical for environments with stronger hydrodynamic conditions. Cross bedding and onlapping strata indicate varying currents, sometimes associated with small erosional features. Most of the core sections, however, are very homogenous due to intense bioturbation, except SL 40 and SL 41. In some sections burrows are visible. All cores are dominated by terrigenous input. In contrast to cores 40 SL, 41 SL, and 46 SL, cores 34 SL, 80 SL, and 83 SL exhibit coarser grains (Fig. 12.3).

Description of sites:

29 MC, 30 MC, 31 KL: This station is located on profile 45 in 102 m of present day water depth (pdwd). The profile runs from SW to NE and comprises a tectonically deformed "basement", which is overlain unconformably by younger sediments, which cover and seal all depressions. The unconformity is characterised by a strong reflector (red) and occurs 3 m below the sediment surface. The sediment surface is as well a strong reflector below which parallel strata of less acoustic reflectance are visible.

33 MC, 34 SL:The station is located on profile 51 in 1369 m pdwd. The profile runs from NE to SW and the subsurface geometry of the strata do not show much variety. All strata are parallel oriented and exhibit almost no inclination, part of the section shows wavy acoustic reflectors. Stronger reflectors occur only on the surface and 10m below the sediment surface.

35 MC, 39 SL, 40 SL, 41 SL: The stations are located on profile 67 in 590 m pdwd at the end of a steeply inclined slope. The slope inclination increases drastically between 430 m and 590 m pdwd. In the hydroacoustic records only the upper 75 cm of

sediment thickness are recorded as distinct reflectors (yellow green). They are parallel to each other.

44 SL, 45 MC, 46 KL: The stations are located on profile 65 in 154 m pdwd. The trend of the profile is SW-NE with no big change in water depth (155 - 150 m pdwd. The "basement" shows depression-like deformations, which all have been filled by younger sediments obscuring any morphology prior to the infill. The unconformity occurs 75 cm below the sediment surface above slightly folded strata of the "basement" at the station.

47 MC: The station is located on profile 65 in 155 m pdwd. The NE part of the profile shows older and inclined strata. The unconformity is a strong reflector (orange – red) and occurs 6 m below the sediment surface. The younger sediments, however, decrease in thickness near the station. Here the unconformity is only 1 m below the sediment surface. The younger sediments are characterised by blue to green reflectors. A prominent reflector is seen 6 m below the sediment surface.

67 MC: The station is located on profile 101 in 270 m pdwd. The sediment surface is almost horizontal and the young sediments show parallel reflectors. The sediment surface is characterised by a strong reflector. Other prominent reflectors occur 1.5, 3, 6, 11.5, 26 and 30 below the sediment surface.

71 MC: The station is located on profile 105 in 238 m pdwd. The Profile runs NW – SE and comprise a plain between 150 and 165 m, where the sea bottom drops down to 225 towards SE in a very short distance. Then follows a wavy surface (mud waves) between 225 m and 252 m pdwd. The sediment surface at the station is a strong reflector (red). Reflectors with less acoustic impedance occur 1, 2, 3, 4, 5, and 6m below the surface. The latter represents the unconformity between the parallel stratified younger sediments and the slightly deformed "basement". The overall record shows 30 m of sediments with prominent reflectors at 10, 15 and 21 m

78 SL, 79 SL, 80 SL, 81 MC, 83 SL: All these stations are located on profile 43. The whole section shows several levee structures of ancient turbidite systems. The channel morphology is almost obscured by younger sediments. Gravity core (SL 83) derives from 604 m pdwd penetrating into 10 m incised channel, which has been filled completely by younger sediments. Stations 78/79 SL derive from 1180 m pdwd while 80SL/81MC derive from 1278m pdwd.

The southern Salaverry Basin NW offshore Callao including the Mud Lens, study area B

The cores from the shelf off Callao derive from a water depth between 86 m and 654 m (Fig. 4). The cores show distinct differences in their development with respect to lithological facies:

The cores 4 SL and 97 SL from a water depth less than 300 m consist mainly of diatomaceous oozes and diatom bearing oozes, indicating their position within the active upwelling cell. The cores 97 SL and 106 KL show a distinct lamination consisting of light yellow and darker olive strata of 1 mm thickness and less. There are no signs of bioturbation, as one expects for a setting within the oxygen minimum zone. This zone has oxygen levels below 0,2 ml/l and is developed between 100 and 600 m of present day water depth.

Cores 101 SL and 103 SL are characterised by coarser sediments of terrigenous origin (sandy oozes), which show frequent foraminifera. There is rather a gradual transition between single strata than a sharp contact. The recovery was very poor due to the occurrence of these sandy strata.
Cores 110 KA and especially 118 KA from the Mud Lens of Callao displayed perfect laminations. However some of these laminae show a kind of cross bedding contacts and even erosional features indicating fluctuating hydrodynamic regimes. This rises the question whether the lamination seen in cores 97 SL and 106 KL are caused by changes in surface productivity or are of hydrodynamic origin as well. Part of the recovered section is bioturbated, indicating a sedimentary setting almost not influenced by the oxygen minimum zone. Foto sledge operations in this basin revealed partly benthic live by crabs. This means that the oxygen minimum zone is not fixed to a certain position but may vary within relatively short intervals in time and space.

Description of sites:

2 MC, 3 MC: The stations are located on profile 4 in 86 m of present day water depth (pdwd). The profile runs parallel to coast line in SE-NW direction. The water depth varies between 110 m and 85 m. The hydroacoustic records show three distinct horizons of strong reflectance (red), which follow parallel to the surface morphology down to a sediment thickness of 3 m.

5 MC, 4 SL, 110 KA, 118KA: Both stations are located on profile 4 in 96 m pdwd. The three distinct horizons seen at stations 2 MC and 3 MC are gently inclined towards SE and they can be traced down to a sediment thickness of 3 m. Box core 118 KA is slightly off the profile line in the order of 0.1 nautical mile.

6 KL, 7 MC, 8MC: The stations are located on profile 11 in 282 m pdwd. The profile runs from SW to NE. The slope drops quickly between 150 m and 275 m. Then follows an almost horizontal plain until the end of profile 11. The hydroacoustic records show a sediment thickness of 30 m, which are characterised by 24 parallel reflectors. The layer with highest acoustic reflector (orange) occurs 1 m below the sediment surface.

14MC: The station is located on profile 26 in 654 m pdwd. The trend of the profile is SSE to NNW. The record shows an ancient turbidite channel with distinct levee structures on both sides. The slope of the levees on the SW side drops from 480 m down to 815 m pdwd and rises up to 630 m on the NE side. The relief is perfectly displayed by a green reflector along the surface.

17 – 20 MC, 22 MC, 23 SL: This station is located at the crossroad of profile 33 and 34 in 252 m pdwd. The slope shows a gentle inclination towards S and SW. The hydroacoustic record shows a sediment thickness of 40 m. The strongest reflector (orange) occurs between 2,5 and 3 m below the sediment surface. Below this "unconformity" there are 8 distinct reflectors visible down to 20 m of the sediment column.

25 SL, 99 MC: The station is located on profile 24 in 202 m pdwd. The inclination of the slope varies between slightly inclined and steeper inclined values along with the variation in water depth (125 m - 380 m). At the end of the profile the slope drops drastically down to 770 m pdwd. The upper part of the hydroacoustic record shows parallel reflectors (blue green) down to an obvious erosional unconformity

2.5 m below the sediment surface. Distinct layers follow 5 m, 9 m, 12 m, 15 m, and 20 m below the sediment surface.

12, KL, 27KL, 101-103 SL: The station is located on profile 36 in 382 m pdwd. The N-S trending profile shows graben-like depressions of ancient turbidite channel with levee structures. The depressions are partly filled with younger sediments. The unconformity between the levee deposits and the younger sequence is perfectly displayed by the orange and red reflector. The station is located at the outside base of a levee, where the sediments of the younger sequence onlap.

87 SL, 88 MC, 94 SL, 95 SL: The stations are located at the beginning of profile 24 in 127 m pdwd. The profile runs NE – SW and drops continuously from 120 m pdwd down to 470 m. The water depth decreases abruptly at the end of the profile (770 m). The young sequence is characterised by parallel strata. Stronger reflectors occur 2.5 – 3m, 6m 8m and 12.5 m below the sediment surface.

97 SL, 98 MC: All stations are located on profile 22 in 215 m pdwd. The profile runs SW-NE and exhibits an almost continous deepening of the surface. The strata of the younger sediments follow parallel to the surface. There is a prominent double reflector (orange-red) 3.5 m below the sediment surface. Others occur at 6 m (orange red), 16 m (green yellow), 20 m (green blue) and at 24 m (blue). The reflector at 6 m is assumed to represent the Pleistocene-Holocene unconformity.

104 MC, 105 SL, 106 KL: These three stations are located within the Mud Lens of Callao on profile 10 in 185 m pwd. The profile exhibits perfectly the mud lens, which increases in thickness from NE to SW. The lens ends in 190 m pdwd at a structural high (150 m pdwd). There is a prominent double reflector at the station at 5m below the sediment surface. Other strong reflectors occur at 12m and 22m.

111 MC: The station is located on profile 176 in 179 m pdwd. The profile runs over a plain which exhibits partly a wavy surface. The whole sedimentary sequence recorded has parallel strata. Prominent reflectors occur at 3.5 m, 12m, 18m, 23m, and 28m below the sediment surface.

The East Pisco Basin, which is study area C

The cores recovered in study area C show similar facies pattern than in are B. Cores 136 SL and 137 SL derive from a setting within the oxygen minimum zone and are characterised by a fine distinct lamination (Fig. 12.5). Thin orange and yellow laminae, consisting predominantly of diatomaceous oozes, are very typical. However, it has to be noted that in the large box core 128 KA, onlap structures, slumping, small erosional features and a gently inclined cross bedding was visible.

119 MC, 120 MC: The stations are located on profile 191 in 115 m pdwd. Most parts of the profile show the outcropping erosional unconformity above slightly inclined strata. only around the station, there are younger sediments deposited above the unconformity, showing 2m of maximum thickness. The unconformity is a strong reflector (red).

121MC, 122 MC, 123 KL: The stations are located on profile 192 in 360 m pdwd. The profile runs from NE to SW. The NE part is characterised by an increasing water depth

from 120 m down to 380 m. During its SW course, the water depth decreases slightly to 320 m. The whole sedimentary sequence shows parallel strata. Stronger reflectors (erosional unconformities?) occur at 4 m, 6 m, 12.5 m, 15 m and 17 m below the sediment surface.

125 MC, 126 MC, 127 MC, 128 KA: The stations are located on profile 199 in 85m pdwd. The profile runs from WNW to ESE upslope from 140 m to 50 m. The strata run parallel to the sediment surface, however they thin out towards WNW. Two prominent reflectors (orange red) occur in shallow depth at 1.3 and 2.3 m below the sediment surface. Another prominent reflector (yellow green) is displayed at 6.5 m.

129 MC: This station is also located on profile 199 in 123 m pdwd. There is a slight tilt displayed of the strata below an erosional unconformity (red reflector) near the sediment surface. The overlaying younger sediments reach a thickness of 1m.

136 SL, 137 SL: The stations are located on profile 205. 136 SL derives from 282 m pdwd, while 137 SL derives from 196 pdwd. The profile covers a gently inclined slope from 140 m pdwd (E) down to 460 m pdwd (W). The sediment sequence within the upper 10 m exhibit parallel strata over an unconformity. Below the strata are slightly inclined and tilted. At station 137 there are stronger reflectors at 4.5 m (red), 7 m, 8m, and 10 m (yellow green - orange). At station 136, there is only one prominent reflector at 7.5 m below the surface. The younger sequence with soft, muddy and oozy sediments is thicker than at station 137.

1 MC, 148 MC: The station is located on profile 190 in 326 m pdwd. The profile covers a gently inclined slope from 150 m pdwd (E) down to 490 m pdwd (W). The whole sedimentary sequence exhibits parallel reflectors down to 30 m below the surface. Prominent reflectors occur at 2.5 m (red), 5 m (yellow – red).

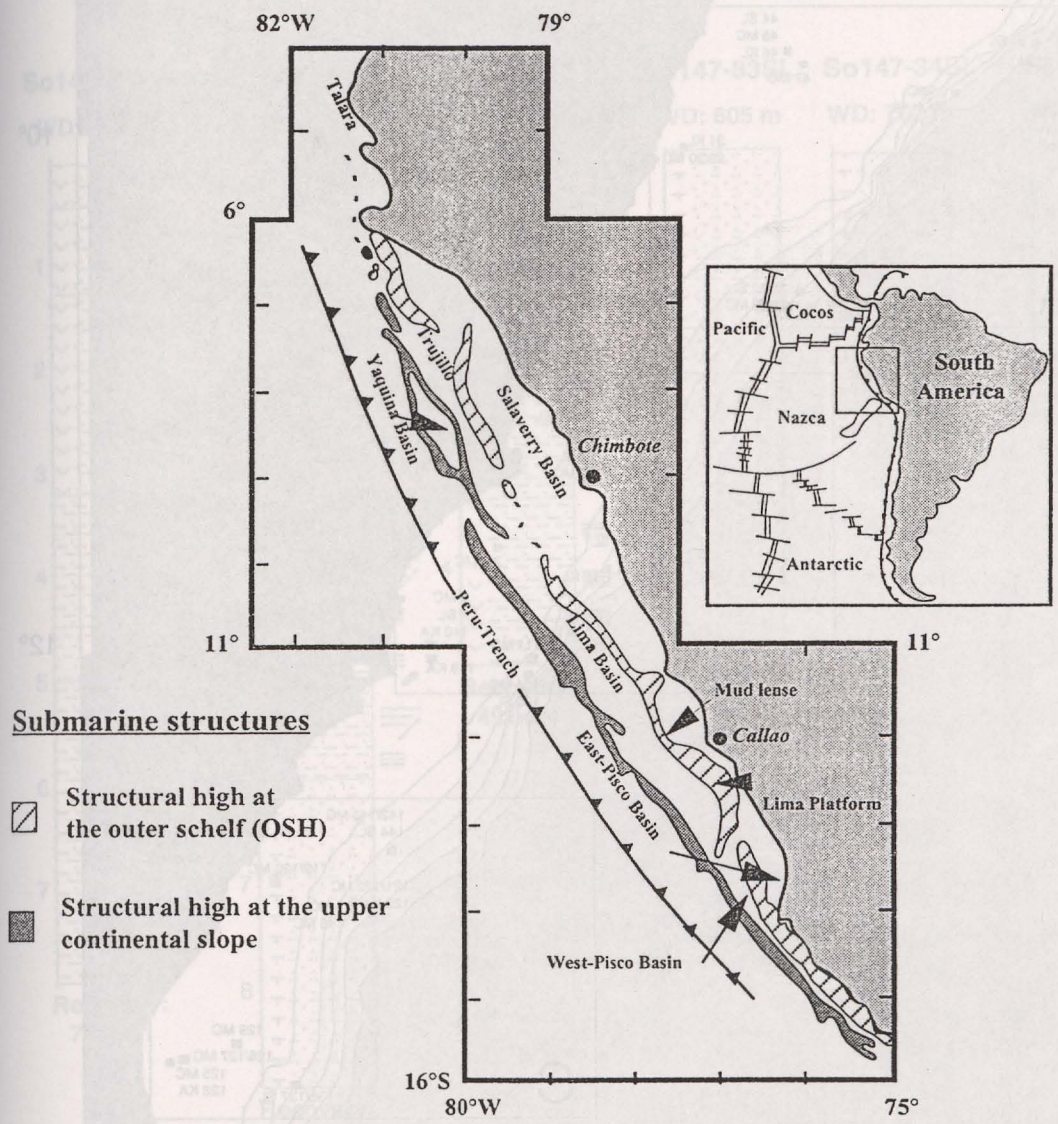

Fig. 12.1: Major forearc basins along the Peru Continental Margin.

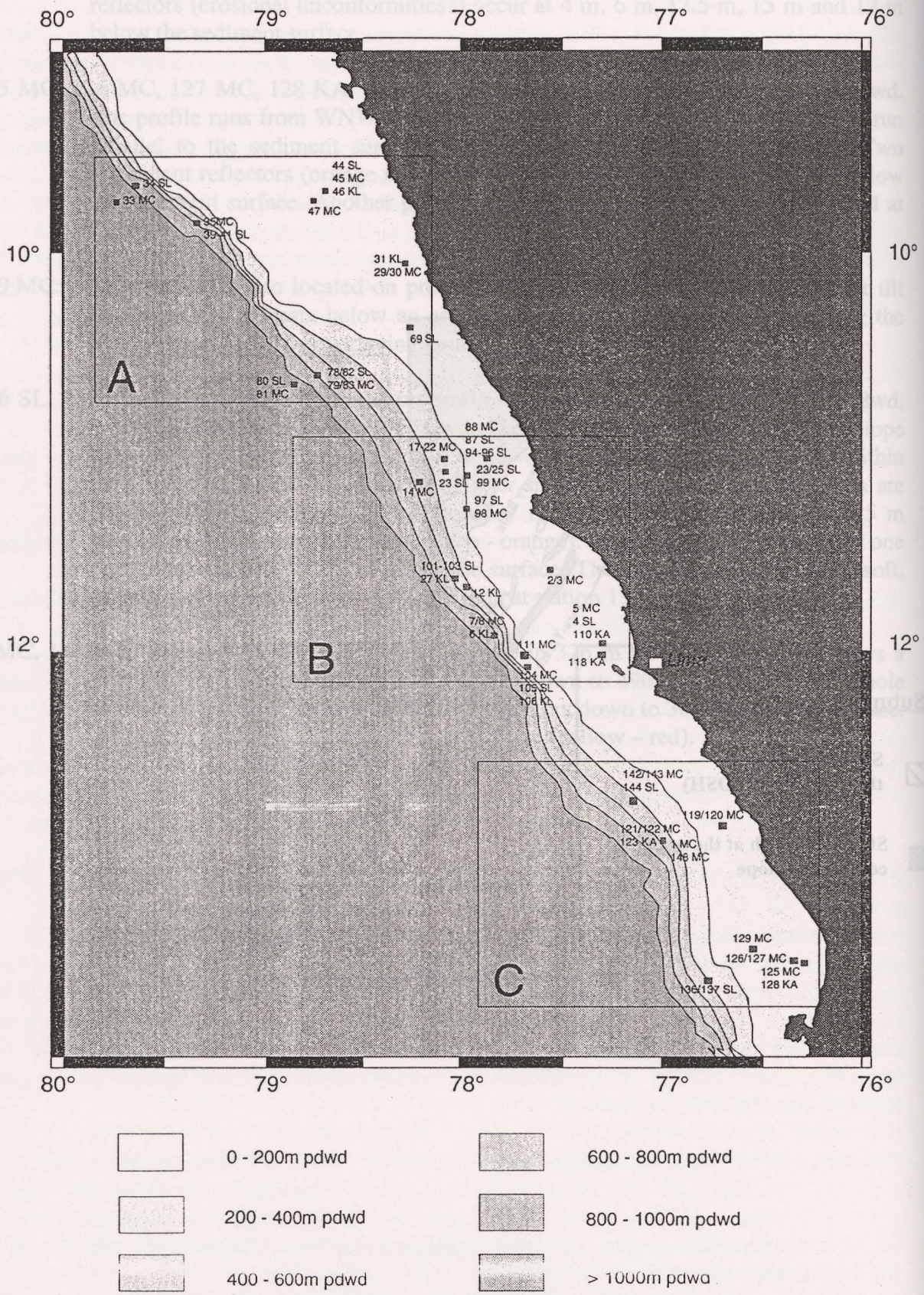

Fig. 12.2: Map of all coring stations sampled during So147-cruise.

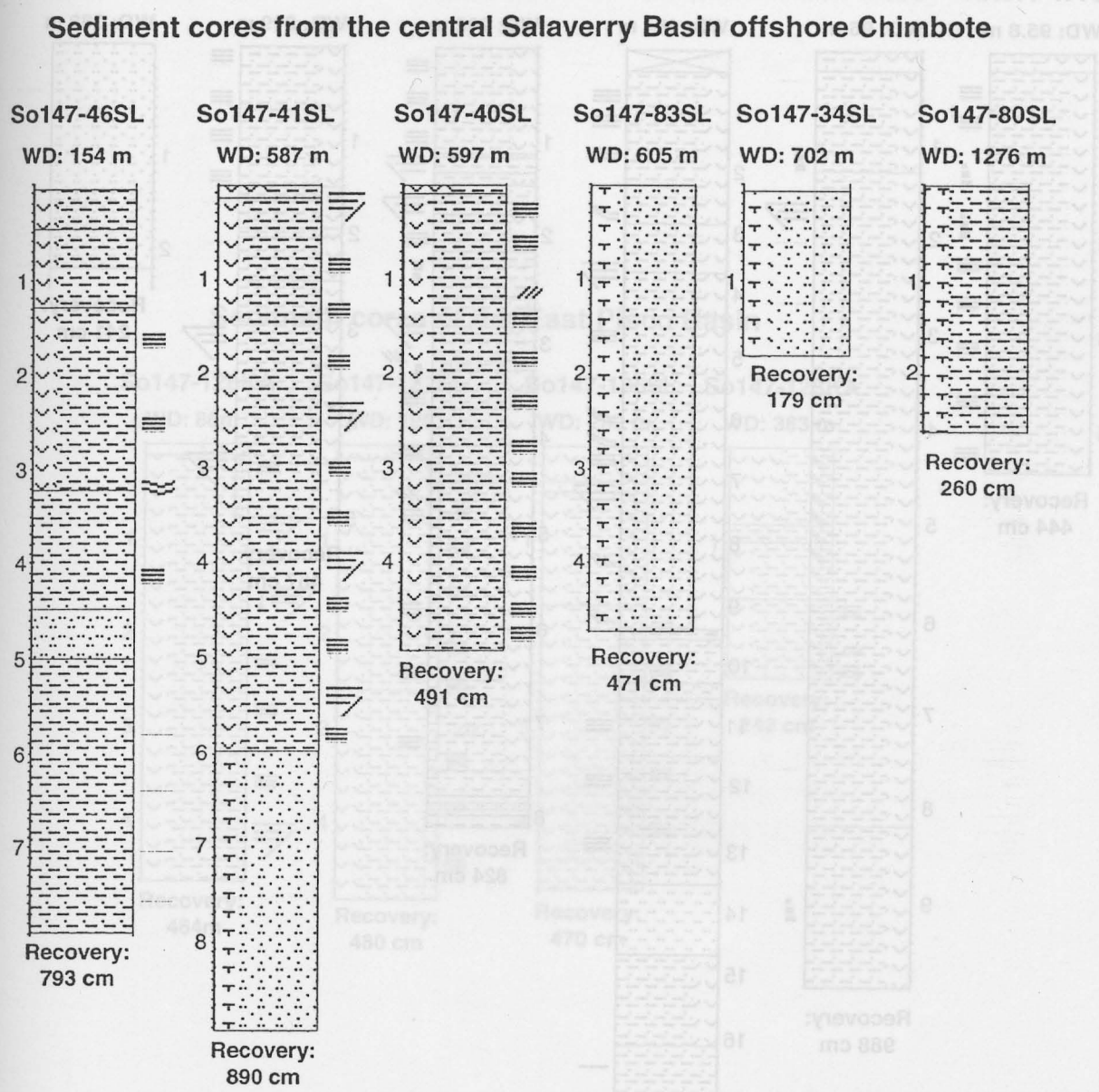

Fig. 12.3: Schematic diagram of recovered lithologies within study area A. The symbols used in the graphical core description are figured in Appendix III

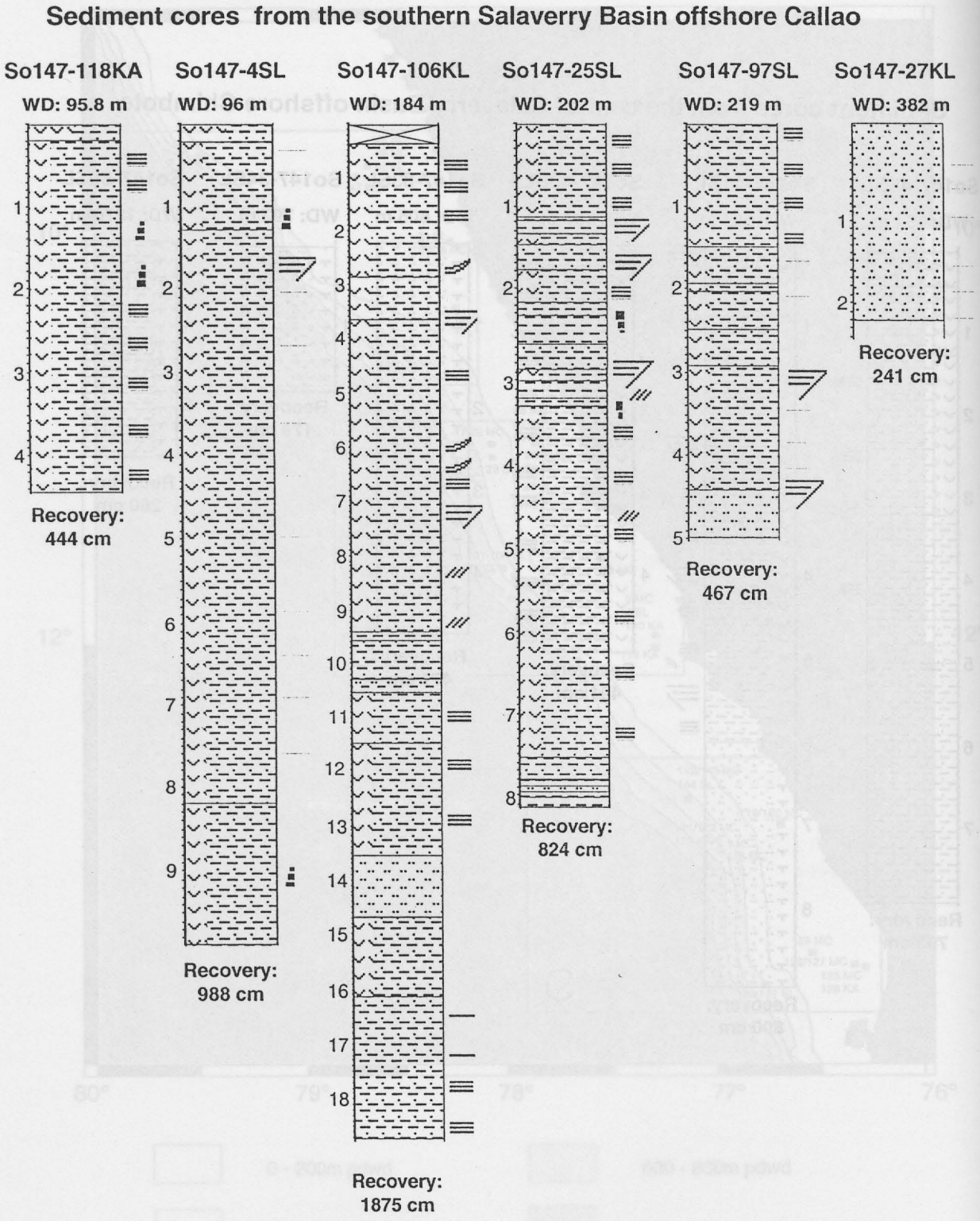

Fig. 12.4: Schematic diagram of recovered lithologies within study area B. Please not that core So147-106KL has a different scale. The symbols used in the graphical core description are figured in Appendix III.

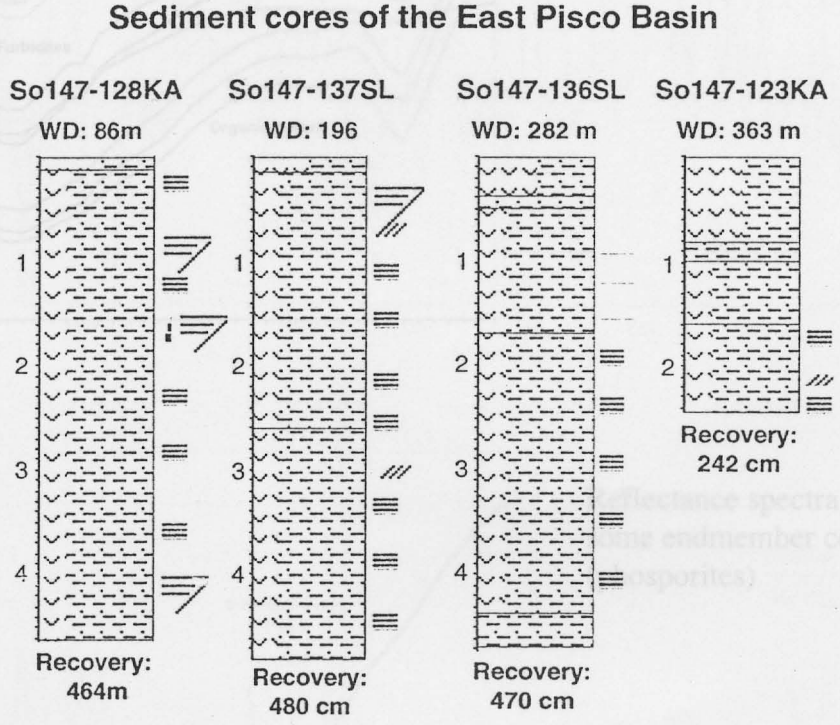

Fig. 12.5: Schematic diagram of recovered lithologies within study area C. The symbols used in the graphical core description are figured in Appendix III.

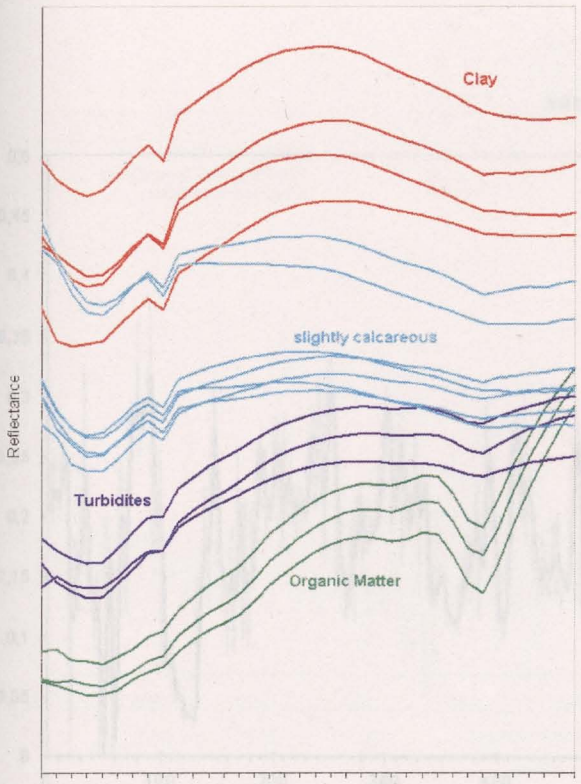

Reflectance spectra of
some endmember components
(component groups in the top figure
are offset for clarity)

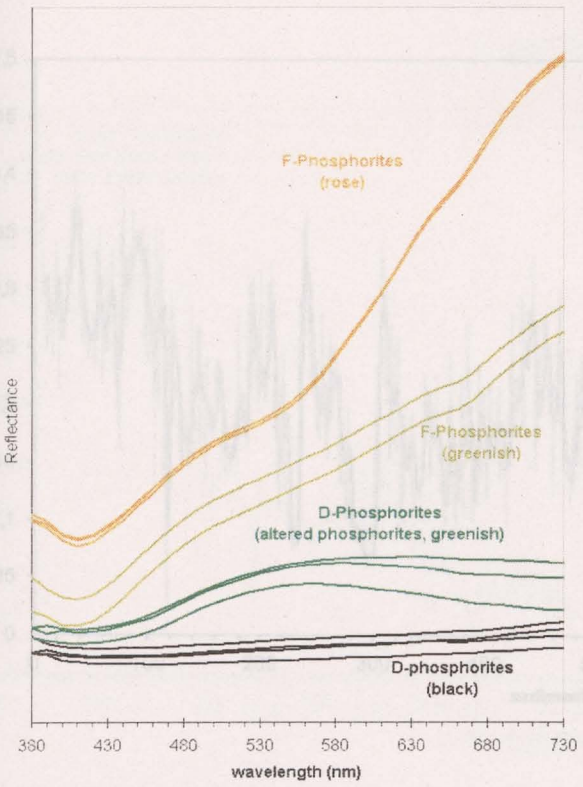

Reflectance spectra of
some endmember components
(phosporites)

Fig. 12.6

Fig. 12.7: Relative absorptionband depth at 670 nm in cores 4SL, 25SL

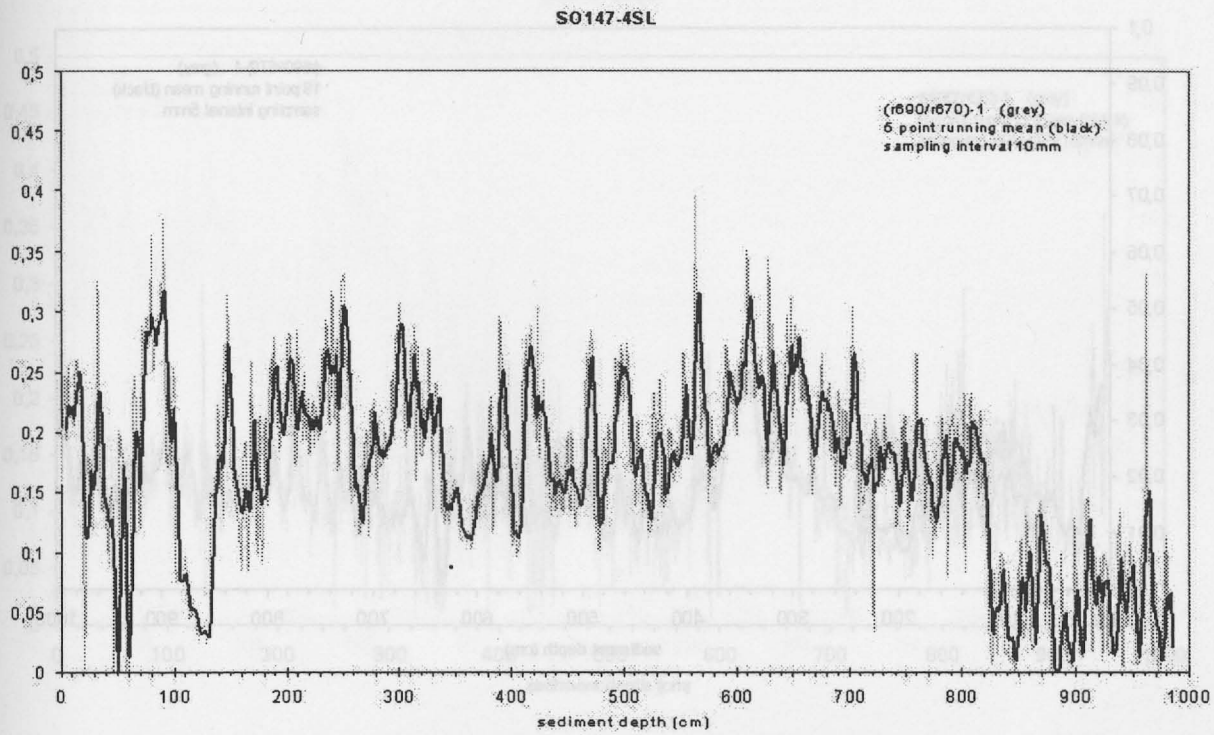

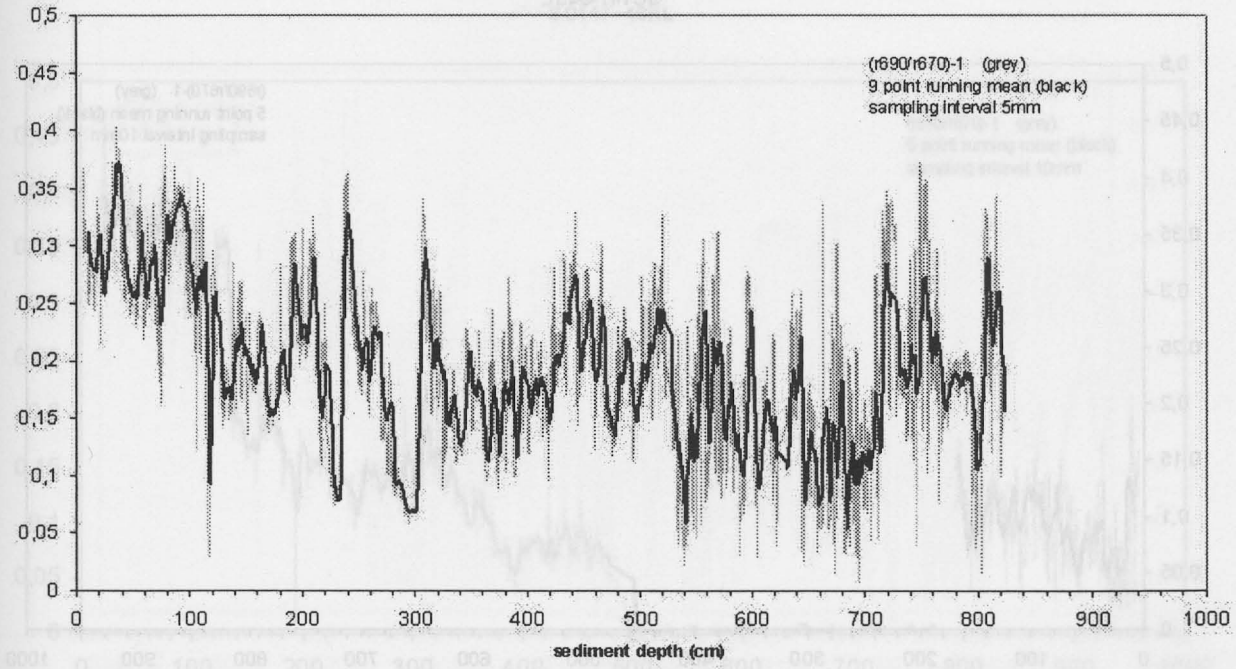

Fig. 12.8: Relative absorptionband depth at 670 nm in cores 27KL, 34SL

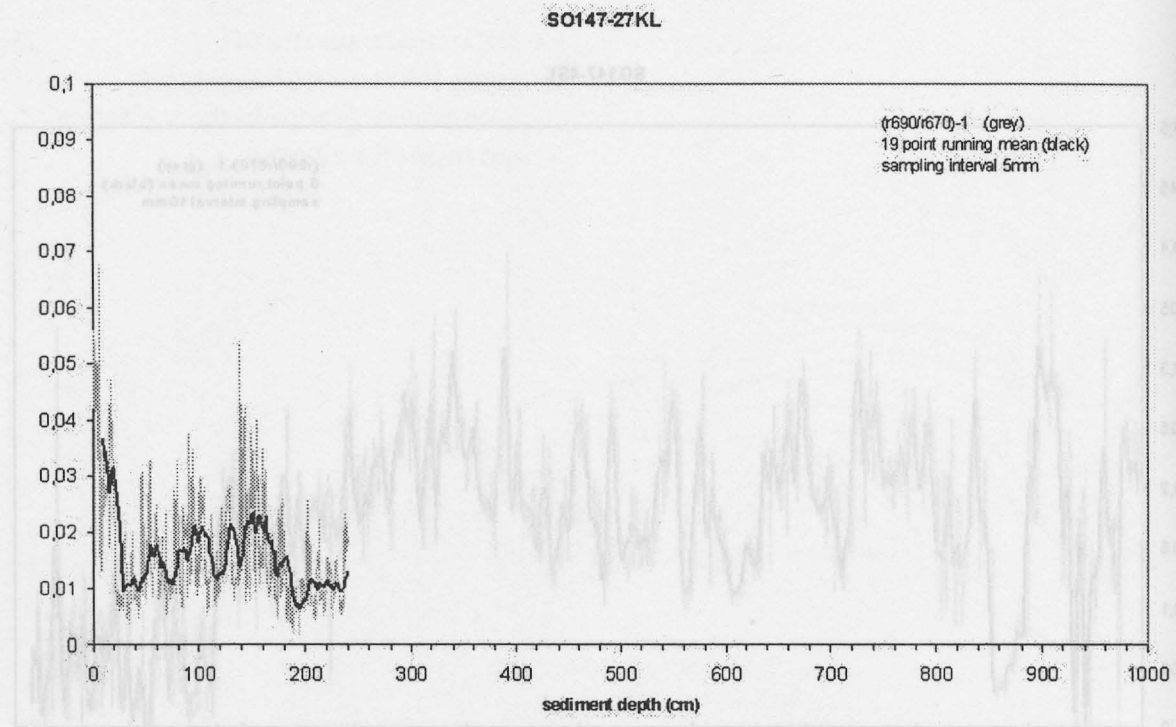

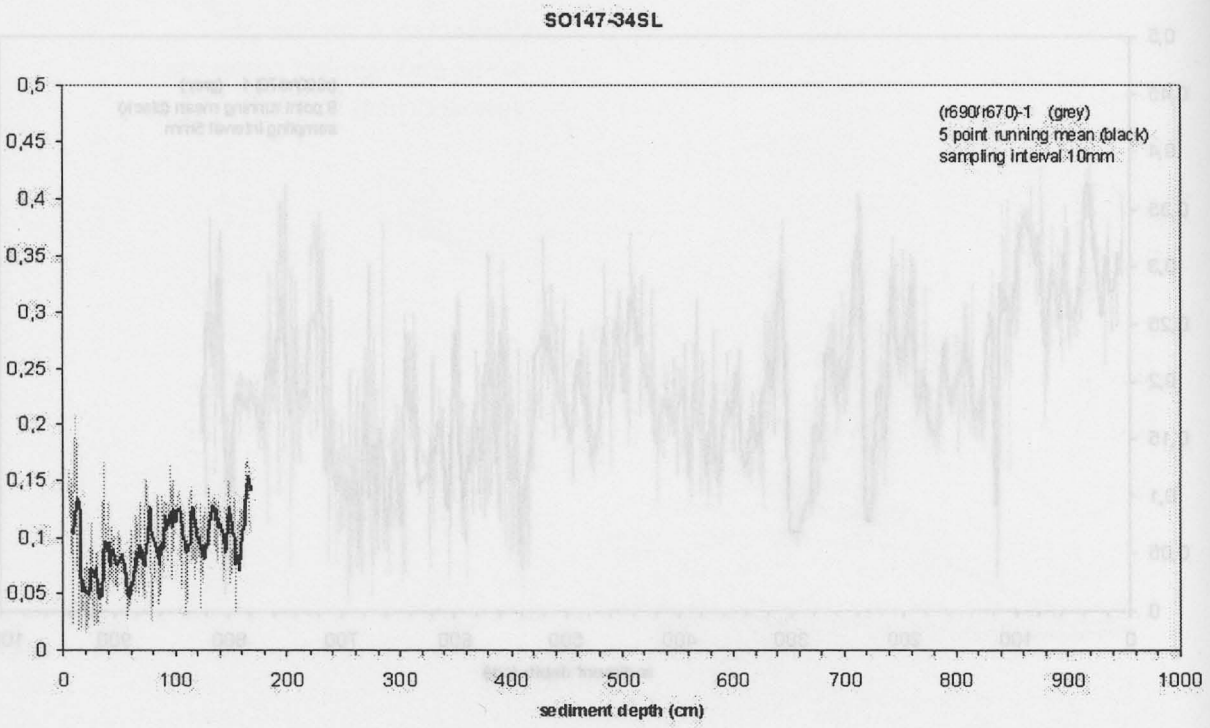

Fig. 12.9: Relative absorptionband depth at 670 nm in cores 41SL, 46KL

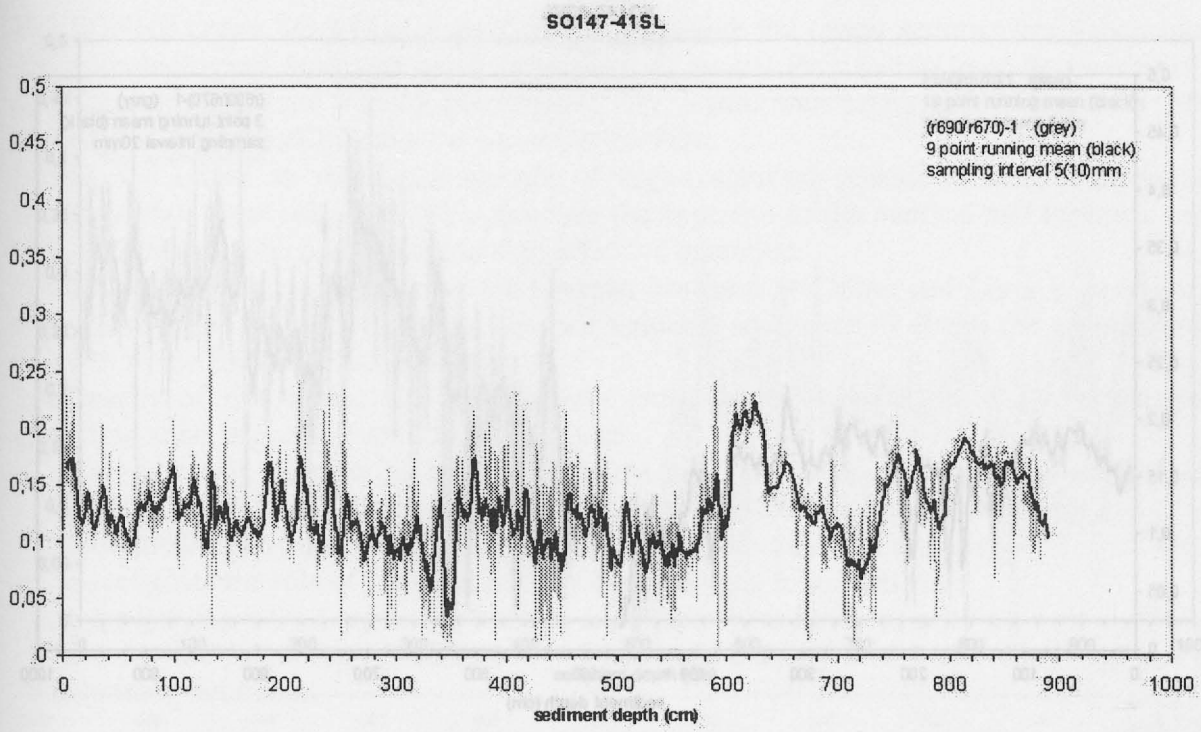

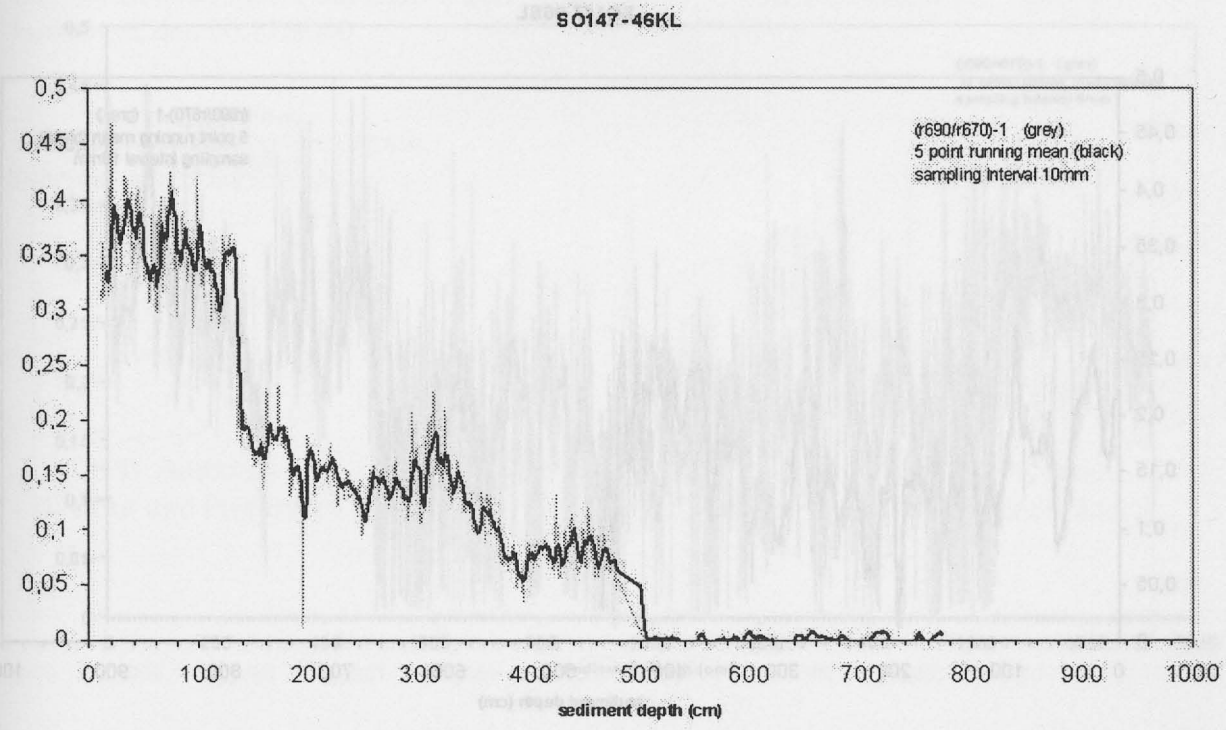

Fig. 12.10: Relative absorptionband depth at 670 nm in cores 83SL, 96SL

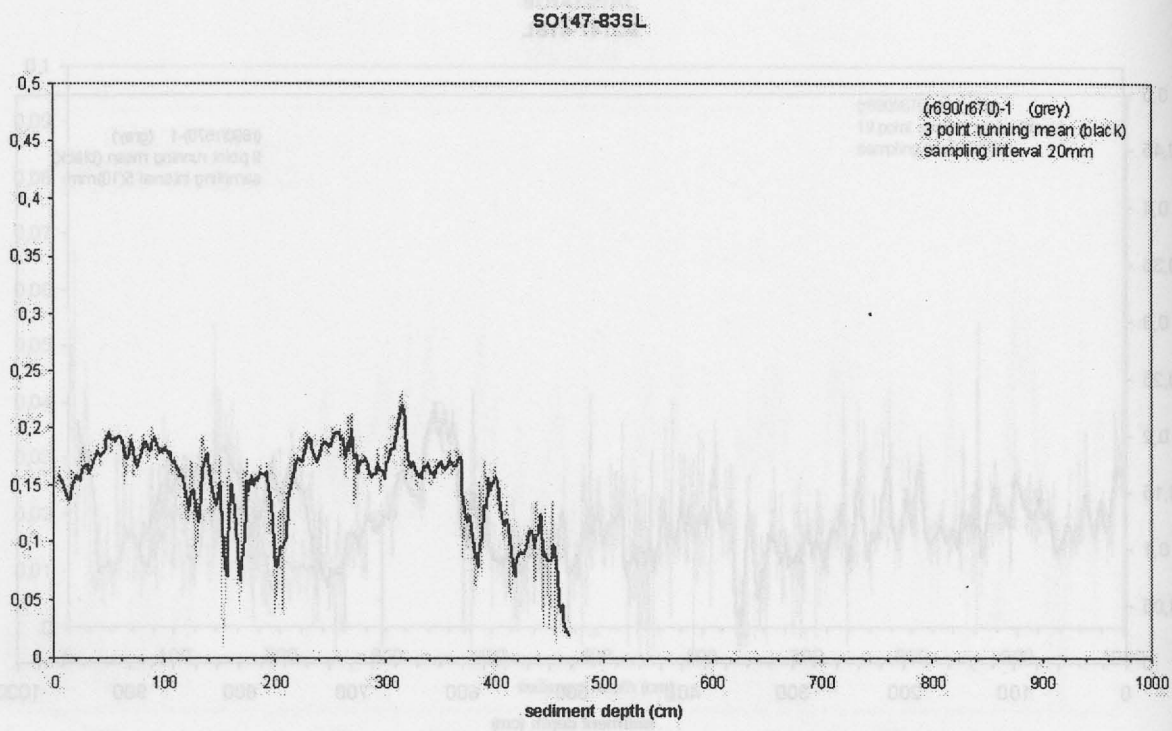

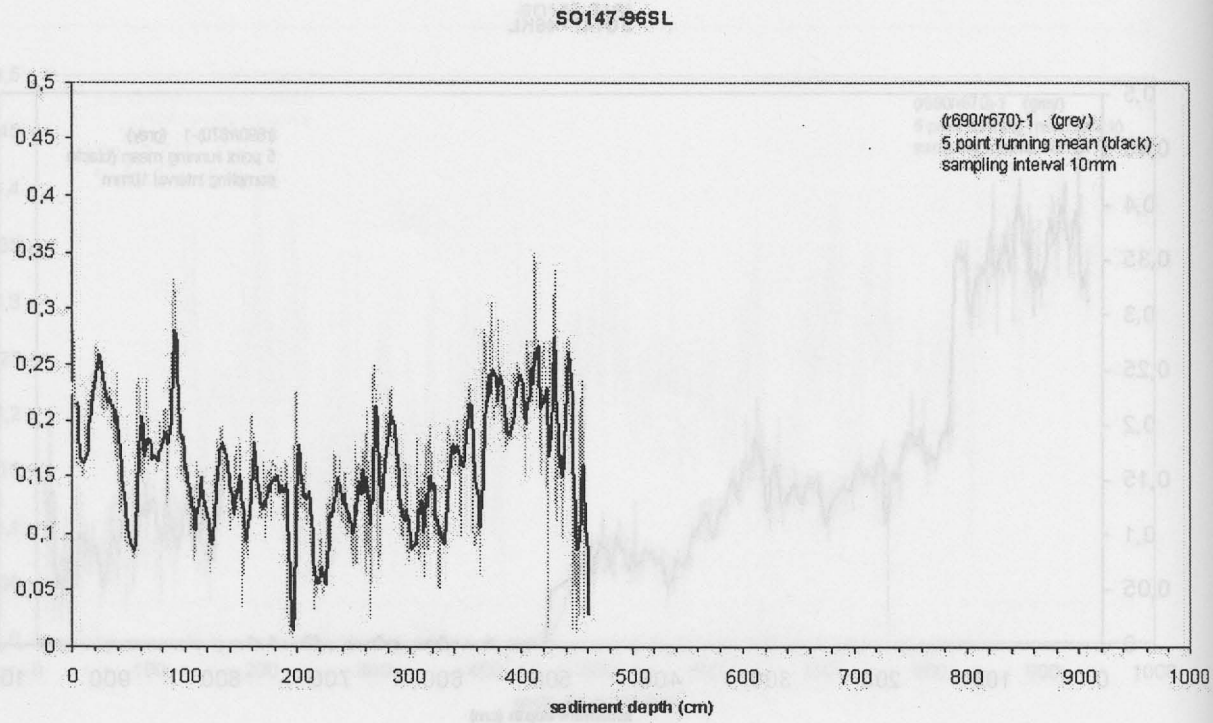

Fig. 12.11: Relative absorptionband depth at 670 nm in cores 97SL, 106KL

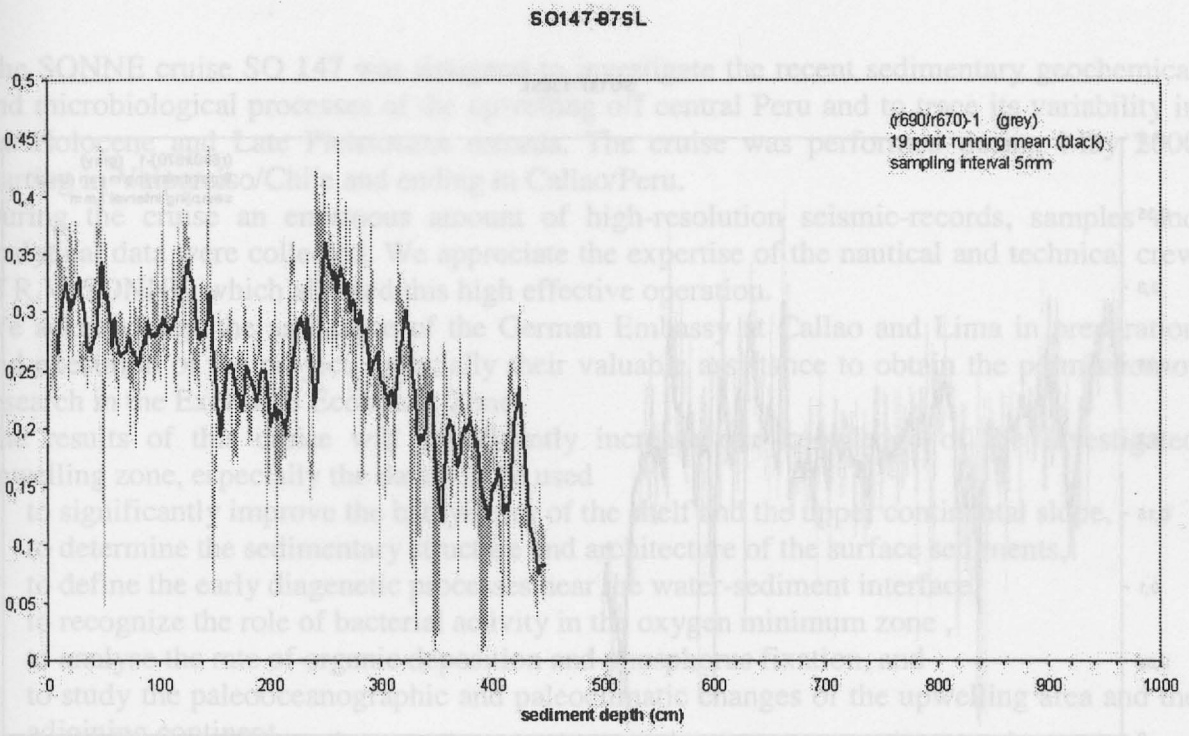

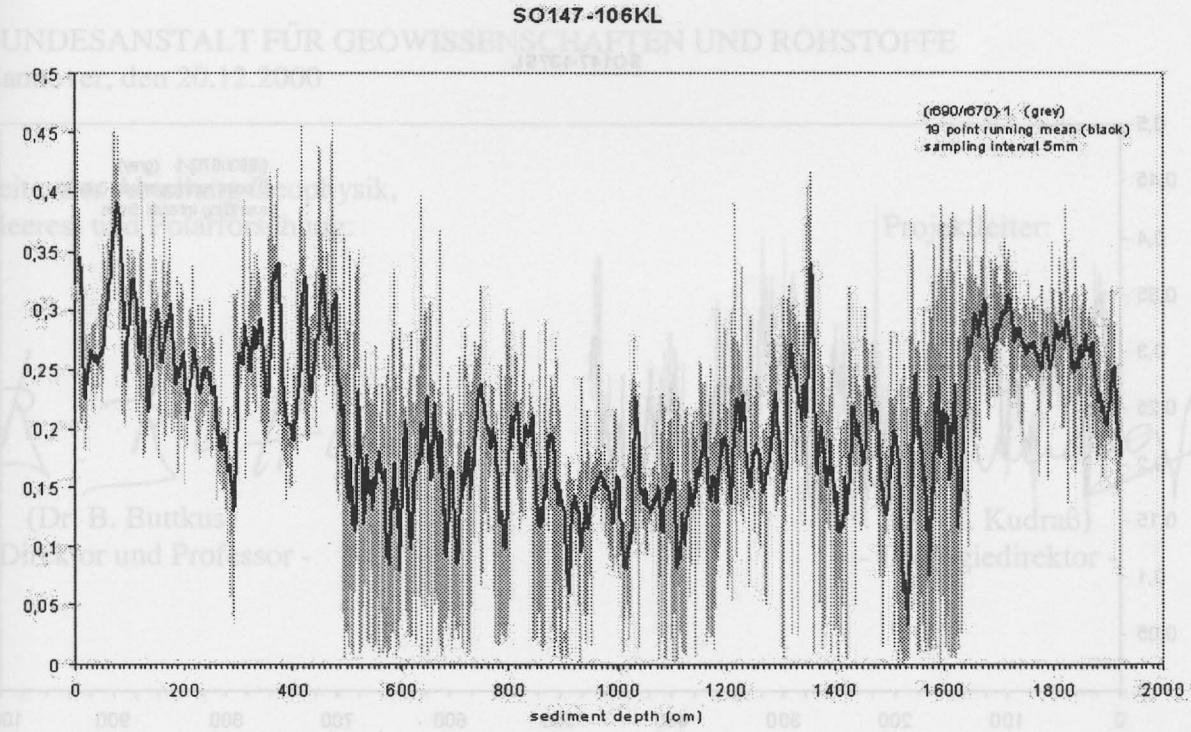

Fig. 12.12: Relative absorptionband depth at 670 nm in cores 136SL, 137SL

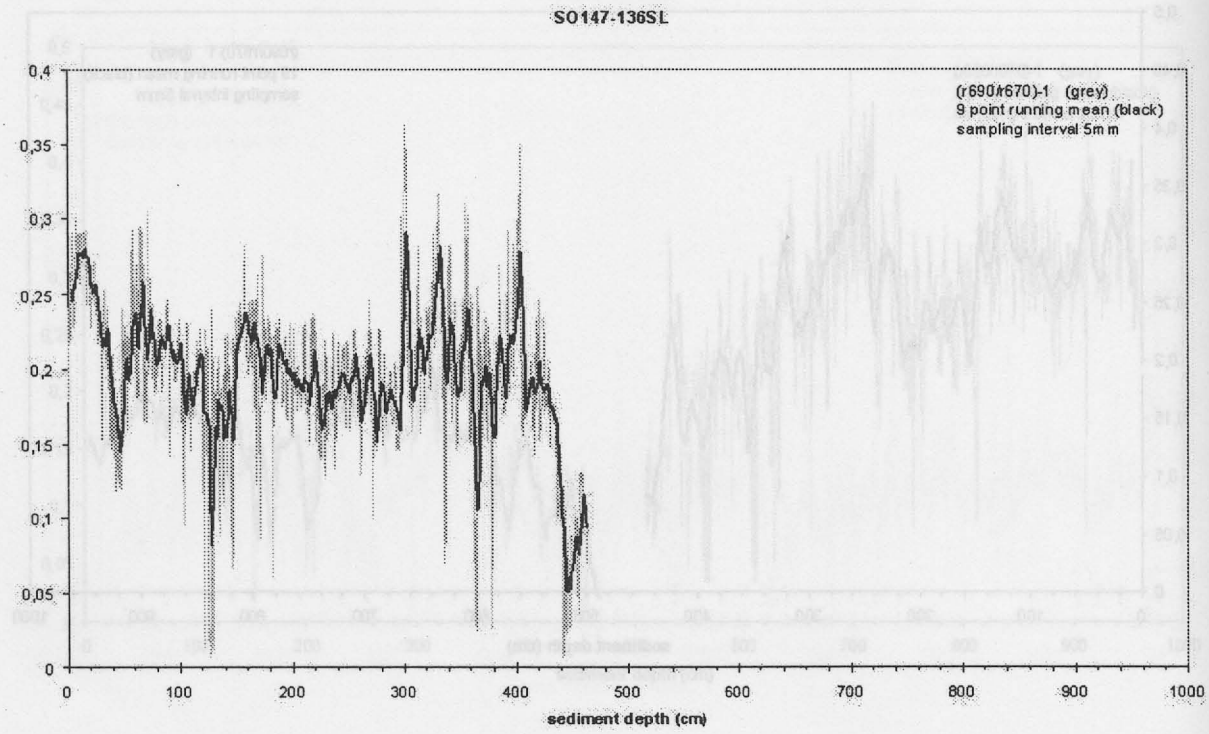

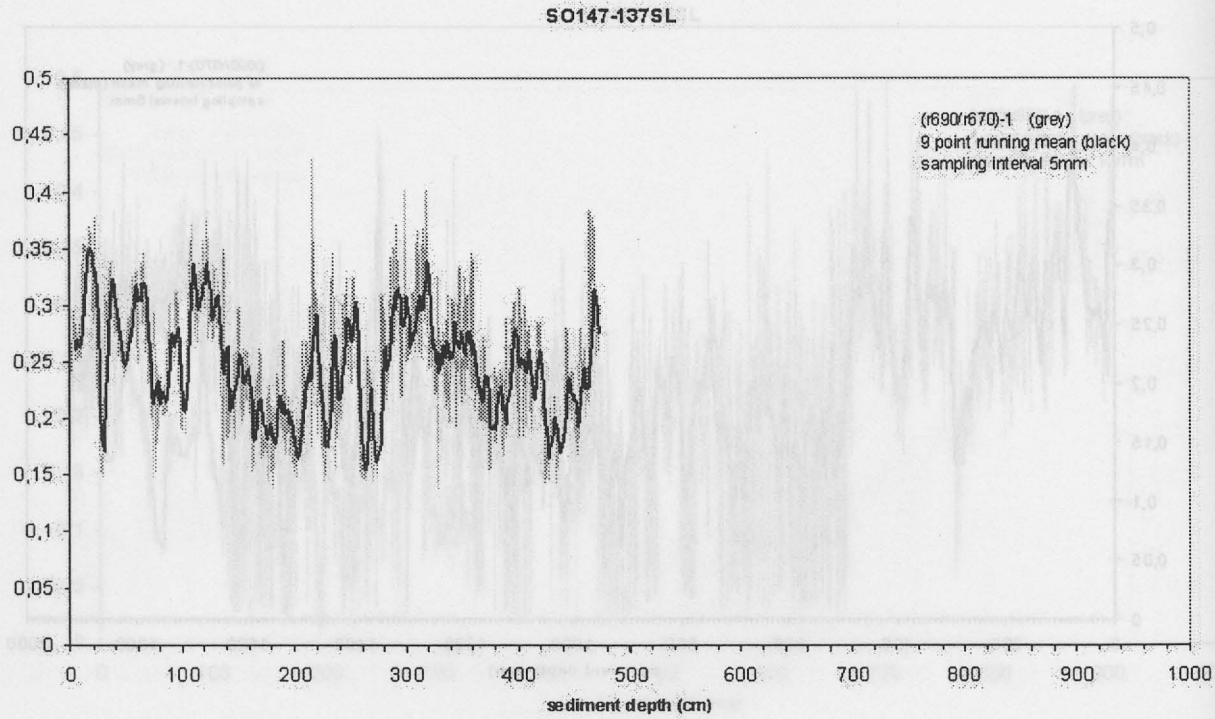

13. Concluding remarks

Kudrass, H. R.

The SONNE cruise SO 147 was designed to investigate the recent sedimentary geochemical and microbiological processes of the upwelling off central Peru and to trace its variability in the Holocene and Late Pleistocene records. The cruise was performed during May 2000 starting in Valparaiso/Chile and ending in Callao/Peru.

During the cruise an enormous amount of high-resolution seismic-records, samples and analytical data were collected. We appreciate the expertise of the nautical and technical crew of R.V. SONNE, which allowed this high effective operation.

We acknowledge the assistance of the German Embassy at Callao and Lima in preparation and execution of the project, especially their valuable assistance to obtain the permission of research in the Exclusive Economic Zone.

The results of this cruise will significantly increase our knowledge of the investigated upwelling zone, especially the data will be used

- to significantly improve the bathymetry of the shelf and the upper continental slope,
- to determine the sedimentary structure and architecture of the surface sediments,
- to define the early diagenetic processes near the water-sediment interface,
- to recognize the role of bacterial activity in the oxygen minimum zone ,
- to analyse the rate of organic deposition and phosphorus fixation, and
- to study the paleooceanographic and paleoclimatic changes of the upwelling area and the adjoining continent.

BUNDESANSTALT FÜR GEOWISSENSCHAFTEN UND ROHSTOFFE
Hannover, den 20.12.2000

Leiter der Abteilung Geophysik,
Meeres- und Polarforschung:

(Dr. B. Buttkus)
- Direktor und Professor -

Projektleiter:

(Dr. H. Kudraß)
- Geologiedirektor -

Appendix I

Station No.	Date	Time (UTC) from:	Time (UTC) to:	Position Latitude:	Position Longitude	Water depth / m	Remarks
1 MC	04.06.00	13:50		12°55,21 S	76°58,25 W	321	7 tubes filled
2 MC	06.06.00	00:12		11°34,97 S	77°33,08 W	86	8 tubes filled
3 MC	06.06.00	13:53		11°35,04 S	77°32,89 W	86	10 tubes filled
4 SL	06.06.00	18:15		11°56,95 S	77°18,03 W	96,3	9,75 m
5 MC	06.06.00	18:55		11°56,95 S	77°18,04 W	96	
6 KL	07.06.00	00:06		11°54,33 S	77°49,72 W	280	300 -1300 cm
7 MC	07.06.00	02:13		11°54,36 S	77°49,73 W	282	6 tubes filled
8 MC	07.06.00	02:56		11°54,39 S	77°49,70 W	282	10 tubes filled
9 KG	07.06.00	18:09		11°24,25 S	77°41,76 W	65	
10 KG	07.06.00	18:58		11°25,97 S	77°44,18 W	75	
11 KG	07.06.00	19:56		11°28,53 S	77°47,91 W	102	
12 KL	07.06.00	22:20		11°40,02 S	77°57,93 W	307	6,32 m
13 KG	08.06.00	01:08		11°29,94 S	77°49,86 W	115	
14 MC	08.06.00	14:56		11°08,00 S	78°21,33 W	654	12 tubes filled
15 FS	08.06.00	17:36		11°03,62 S	78°16,52 W	208	
			ca. 20:42	11°05 S	78.15 W	115	
16 FS	08.06.00	22:32		11°00,54 S	78°06,00 W	159	
			01:11	11°01,32 S	78°04,72 W	79	
17 MC	09.06.00	14:46		11°01,63 S	78°04,72 W	252	10 tubes filled
18 MC	09.06.00	15:19		11°01,82 S	78°04,83 W	255	6 tubes filled
19 MC	09.06.00	16:00		11°01,85 S	78°04,89 W	255	12 tubes filled
20 MC	09.06.00	17:25		11°01,87 S	78°04,98 W	258	10 tubes filled
21 MC	09.06.00	17:57		11°01,86 S	78°04,99 W	257	10 tubes filled
22 MC	09.06.00	18:29		11°01,87 S	78°05,00 W	258	8 tubes filled
23 SL	09.06.00	19:49		11°05,45 S	78°00,00 W	203	8,45 m
24 MS	09.06.00	20:10		11°05,75 S	77°59,86 W	202	
25 SL	09.06.00	21:26		11°05,47 S	78°00,01 W	202	8,24 m
26 GA	10.06.00	00:15		11°07,80 S	78°05,75 W	263	

Station No.	Date	Time (UTC) from:	Time (UTC) to:	Position Latitude:	Position Longitude	Water depth / m	Remarks
27 KL	10.06.00	16:42		11°36,96 S	78°02,02 W	382	2,41 m
28 KG	11.06.00	15:55		10°03,25 S	78°17,09 W	102	
29 MC	11.06.00	17:36		10°03,28 S	78°17,10 W	102	4 tubes filled
30 MC	11.06.00	17:59		10°03,24 S	78°17,10 W	102	4 tubes filled
31 KL	11.06.00	18:42		10°03,90 S	78°18,10 W	106	1,50 m
32 MS	12.06.00	17:26		9°45,80 S	79°45,49 W	1438	(OMZ 70 630m)
33 MC	12.06.00	21:02		9°44,56 S	79°44,22 W	1369	12 tubes filled
34 SL	12.06.00	23:33		9°39,55 S	79°38,43 W	707	1,79 m
35 MC	13.06.00	12:53		9°51,15 S	79°20,32 W	598	12 tubes filled
36 GA	13.06.00	17:15		9°58,45 S	79°05,74 W	203	salvage effort test-equipment
37 GA	13.06.00	20:30		9°57,83 S	79°04,74 W	172	
38 GA	14.06.00	01:17		9°58,84 S	79°05,58 W	202	salvage effort test-equipment
39 SL	14.06.00	12:38		9°51,12 S	79°20,30 W	594	4,62 m
40 SL	14.06.00	13:41		9°51,18 S	79°20,22 W	597	4,74 m
41 SL	14.06.00	14:56		9°51,08 S	79°20,31 W	587	8,90 m
42 KD	15.06.00	17:34		9°58,31 S	79°05,91 W	174	
			23:32	9°58,64 S	79°05,41 W	197	
43 KD	15.06.00	00:07		9°58,59 S	79°05,06 W	172	
			01:40	9°58,74 S	79°04,71 W		
44 SL	15.06.00	12:14		9°41,47 S	78°40,97 W	154	3,75 m
45 MC	15.06.00	12:45		9°41,47 S	78°40,99 W	153	12 tubes filled
46 KL	15.06.00	14:30		9°41,43 S	78°40,97 W	154	7,93 m
47 MC	15.06.00	16:02		9°44,36 S	78°45,10 W	155	8 tubes filled
48 GA	15.06.00	17:56		9°43,97 S	78°39,51 W	145	
49 GA	15.06.00	20:08		9°45,64 S	78°47,55 W	141	
50 MS	15.06.00	21:25		9°45,74 S	78°47,24 W	165	
51 GA	15.06.00	22:29		9°47,57 S	78°50,29 W	167	
52 FS	16.06.00	00:35		9°43,65 S	78°48,60 W	139	
			03:00	9°44,79 S	78°47,67 W	140	
53 FS	16.06.00	12:24		9°57,95 S	79°05,03 W	172	

Station No.	Date	Time (UTC) from:	to:	Position Latitude:	Longitude	Water depth / m	Remarks
			18:26	10°01,34 S	79°05,00 W	210	
54 GA	16.06.00	19:47		10°01,89 S	79°04,33 W	179	
55 GA	16.06.00	21:57		10°03,49 S	79°05,59 W	162	
56 GA	16.06.00	22:46		10°02,19 S	79°04,54 W	205	
57 GA	17.06.00	00:07		10°01,52 S	79°04,14 W	170	
58 GA	17.06.00	01:36		9°59,70 S	79°02,74 W	170	
59 MS	17.06.00	03:25		10°04,12 S	79°05,98 W	353	
60 GA	17.06.00	15:28		9°36,57 S	78°43,16 W	142	
61 GA	17.06.00	17:58		9°24,66 S	78°42,32 W	101	
62 GA	17.06.00	19:38		9°31,46 S	78°44,27 W	130	
63 GA	18.06.00	01:44		9°58,10 S	79°04,75 W	170	salvage test-equipment D
64 GA	18.06.00	15:25		9°41,60 S	79°07,67 W	157	
65 GA	18.06.00	17:35		9°46,43 S	79°12,74 W	171	
66 GA	18.06.00	18:34		9°45,42 S	79°12,74 W	155	
67 MC	18.06.00	21:22		9°51,52 S	79°12,74 W	270	
68 SL	19.06.00	18:15		10°21,59 S	78°20,71 W	190	
69 SL	19.06.00	19:27		10°22,23 S	78°15,43 W	136	
70 KG	19.06.00	21:09		10°22,29 S	78°15,49 W	136	
71 MC	20.06.00	00:53		10°23,42 S	78°33,51 W	239	
72 GA	20.06.00	13:30		10°19,46 S	78°18,25 W	150	
73 GA	20.06.00	14:44		10°19,57 S	78°18,21 W	151	
74 GA	20.06.00	16:06		10°15,05 S	78°19,96 W	144	
75 GA	20.06.00	19:25		10°19,16 S	78°35,25 W	160	
76 GA	20.06.00	22:24		10°25.33 S	78°45,71 W	172	
77 FS	20.06.00	23:48		10°24,74 S	78°46,17 W	154	
	21.06.00		03:14	10°27,32 S	78°45,05 W	182	
78 SL	21.06.00	12:34		10°39,16 S	78°51,17 W	1184	1,43 m
79 MC	21.06.00	13:35		10°39,17 S	78°51,17 W	1186	10 tubes filled
80 SL	21.06.00	14:46		10°40,04 S	78°51,15 W	1276	2,60 m
81 MC	21.06.00	15:50		10°40.04 S	78°51,15 W	1278	12 tubes filled
82 MC	21.06.00	17:37		10°36,52 S	78°44,02 W	605	
83 SL	21.06.00	18:14		10°36,52 S	78°44,02 W	605	4,71 m

Station No.	Date	Time (UTC) from:	Time (UTC) to:	Position Latitude:	Position Longitude	Water depth / m	Remarks
84 GA	21.06.00	21:13		10°24,57 S	78°48,29 W	177	
85 GA	21.06.00	23.51:00		10°20,97 S	78°38,43 W	153	
86 GA	22.06.00	02:00		10°23,87 S	78°40,43 W	177	
87 SL	22.06.00	13:45		11°01,52 S	77°52,35 W	127	
88 MC	22.06.00	14:12		11°01,56 S	77°52,35 W	127	
89 GA	22.06.00	15:00		10°55,46 S	77°58,19 W	228	
90 GA	22.06.00	17:44		10°55,48 S	77°58,20 W	257	salvage test-equipment B
91 FS	22.06.00	19:25		10°55,57 S	77°58,14 W	149	
			20:30	10°55,63 S	77°58,98 'W	155	
92 FS	22.06.00	21:47		10°57,60 S	77°50,23 W	100	
			22:05	10°57,62 S	77°50,23 W	100	
93 FS	23.06.00	00:20		10°44,58 S	77°59,93 W	132	
			02:01	10°44,61 S	78°00,92 W	132	
94 SL	23.06.00	12:07		11°01,56 S	77°52,48 W	128	2,60 m
95 SL	23.06.00	13:13		11°01,56 S	77°52,48 W	128	4,70 m
96 SL	23.06.00	13:59		11°01,52 S	77°52,41 W	127	3,75 m
97 SL	23.06.00	16:36		11°16,55 S	77°58,40 W	219	4,48 m
98 MC	23.06.00	17:30		11°16,50 S	77°58,40 W	218	6 tubes filled
99 MC	23.06.00	18:00		11°06,53 S	77°58,41 W	219	6 tubes filled
100 MS	23.06.00	22:00		11°36,56 S	78°01,99 W	385	
101 SL	23.06.00	23:02		11°36,82 S	78°02,00 W	375	10 cm sediment
102 SL	23.06.00	23:56		11°36,75 S	78°02,01 W	368	15 cm sediment
103 SL	24.06.00	01:05		11°37,05 S	78°04,23 W	435	20 cm sediment
104 MC	24.06.00	16:17		12°03,68 S	77°39,84 W	185	10 tubes filled
105 SL	24.06.00	16:50		12°02,99 S	77°39,87 W	185	8,31 m
106 KL	24.06.00	19:39		12°03,00 S	77°39,86 W	184	19,34 m
107 GA	24.06.00	22:14		12°06,40 S	77°40,86 W	178	
108 GA	25.06.00	00:54		12°03,86 S	77°43,79 W	171	
109 GA	25.06.00	02:24		12°02,67 S	77°42,04 W	142	
110 KA	25.06.00	17:13		11°57,00 S	77°18,04 W	97	
111 MC	25.06.00	20:30		12°00,55 S	77°40,70 W	179	10 tubes filled
112 KG	25.06.00	21:22		11°59,17 S	77°41,21 W	180	
113 MS	26.06.00	00:40		12°02,52 S	77°52,77 W	1063	

Station No.	Date	Time (UTC) from:	to:	Position Latitude:	Longitude	Water depth / m	Remarks
114 FS	26.06.00	02:35		11°59,11 S	77°41,22 W	146	
			03:56	11°59,83 S	77°40,89 W	168	
115 GA	26.06.00	12:13		12°06,93 S	77°34,65 W	172	
116 GA	26.06.00	16:46		12°19,60 S	77°35,66 W	427	
117 GA	26.06.00	18:13		12°16,68 S	77°33,16 W	276	
118 KA	26.06.00	23:36		11°56,90 S	77°18,03 W	96	4,44 m
119 MC	27.06.00	16:05		12°50,79 S	76°42.05 W	115	8 tubes filled
120 MC	27.06.00	16:33		12°50,77 S	76°42,06 W	115	6 tubes filled
121 MC	27.06.00	20:29		12°55,54 S	77°00,12 W	360	6 tubes filled
122 MC	27.06.00	21:02		12°55,54 S	77°00,15 W	364	8 tubes filled
123 KA	27.06.00	22:02		12°55,50 S	77°00,10 W	363	2,35 m
124 KG	27.06.00	23:24		12°55,14 S	76°58,24 W	322	
125 MC	28.06.00	14:31		13°32,19 S	76°16,97 W	50	
126 MC	28.06.00	15:22		13°30,86 S	76°21,03 W	85	6 tubes filled
127 MC	28.06.00	15:45		13°30,87 S	76°21,03 W	86	10 tubes filled
128 KA	28.06.00	16:09		13°30,85 S	76°21,02 W	86	
129 MC	28.06.00	17:56		13°28,05 S	76°33,13 W	123	
130 MS	28.06.00	18:42		13°27,61 S	76°33,11 W	124	
131 KD	28.06.00	20:30		13°27,18 S	76°46,06 W	197	
			21:28	13°27,13 S	76°45,73 W	197	
132 KG	29.06.00	12:14		13°37,98 S	76°50,01 W	400	
133 KG	29.06.00	13:34		13°38,08 S	76°49,98 W	399	
134 KG	29.06.00	14:38		13°34,69 S	76°48,80 W	514	
135 KG	29.06.00	15:23		13°34,34 S	76°48,69 W	312	
136 SL	29.06.00	16:29		13°36,85 S	76°45,86 W	282	
137 SL	29.06.00	18:12		13°36,36 S	76°40,62 W	196	
138 GA	29.06.00	20:35		13°26,77 S	76°43,60 W	170	
139 GA	29.06.00	22:07		13°27,99 S	76°50,98 W	157	
140 GA	30.06.00	00:02		13°27,84 S	76°50,50 W	184	
141 FS	30.06.00	02:29		13°32,67 S	76°37,83 W	178	
			03:35	13°33,27 S	76°37,47 W	176	
142 MC	30.06.00	12:58		12°43,67 S	77°08,52 W	365	12 tubes filled
143 MC	30.06.00	13:44		12°43,93 S	77°07,96 W	359	8 tubes filled

Station No.	Date	Time (UTC) from:	Time (UTC) to:	Position Latitude:	Position Longitude	Water depth / m	Remarks
144 SL	30.06.00	14:29		12°43,67 S	77°08,51 W	364	4,70 m
145 KG	30.06.00	18:15		12°55,02 S	76°58,57 W	326	
146 KG	30.06.00	19:00		12°55,02 S	76°58,65 W	328	
147 KG	30.06.00	19:34		12°54,99 S	76°58,60 W	327	
148 MC	30.06.00	20:20		12°55,03 S	76°58,55 W	326	
149 GA	30.06.00	22:29		12°47,18 S	77°05,60 W	357	

Appendix II

Profile No.	Date	Start (UTC)	End (UTC)	Position * Long.	Lat.	HS SEL-96	PS SES-2000	Remarks
1	04.06.00	08:45		76° 50,64' W	13° 43,02' S		X	without Paradigma
			15:25	76° 59,94' W	12° 45,12' S			Start Paradigma 11:40
2	04.06.00	15:25		76° 59,94' W	12° 45,12' S		X	PISCO
			20:46	77° 16,62' W	12° 05,34' S			
3	05.06.00	19:40		77° 18,00' W	11° 57,00' S			2 MC
			23:55	77° 32,7' W	11° 35,4' S			
4	06.06.00	00:34		77° 33,3' W	11° 34,62' S		X	
			02:13	77° 39,78' W	11° 22,8' S			
5	06.06.00	00:34		77° 39,78' W	11° 23,4' S		X	
			07:07	78° 12,72' W	11° 45,78' S			
6	06.06.00	07:07		78° 12,72' W	11° 45,78' S		X	
			08:44	78° 6,24' W	11° 56,64' S			
7	06.06.00	08:44		78° 6,24' W	11° 56,64' S		X	
			13:37	77° 33' W	11° 34,98' S			
8	06.06.00	14:16		77° 32,88' W	11° 34,92' S		X	
			15:00	77° 34,92' W	11° 40,08' S			
9	06.06.00	15:00		77° 34,92' W	11° 40,08' S		X	
			17:31	77° 23,1' W	11° 56,82' S			
transit to 3 SL							X	
			18:31	77° 18' W	11° 56,94' S			
10	06.06.00	19:17		77° 18,06' W	11° 57,18' S		X	
			22:21	77° 44,76' W	12° 3,9' S			
11	06.06.00	22:21		77° 44,76' W	12° 3,9' S		X	
			23:45	77° 49,68' W	11° 54,36' S			Station 6
12	07.06.00	02:52		77° 49,68' W	11° 54,48' S		X	
			04:41	77° 46,38' W	11° 43,2' S			
13	07.06.00	04:42		77° 46,38' W	11° 43,08' S		X	make way for fishery
			06:47	78° 2,82' W	11° 50,28' S			
14	07.06.00	07:16		78° 4,86' W	11° 47,28' S		X	
			07:31	78° 5,76' W	11° 45,36' S			
15	07.06.00	07:31		78° 5,76' W	11° 45,36' S		X	
			10:10	77° 45,78' W	11° 33,72' S			
16	07.06.00	10:10		77° 45,78' W	11° 33,72' S		X	
			11:38	77° 54,66' W	11° 26,4' S			
17	07.06.00	11:38		77° 54,66' W	11° 26,4' S		X	
			13:23	78° 8,04' W	11° 33,9' S			
18	07.06.00	13:23		78° 8,04' W	11° 33,9' S		X	
			14:13	78° 11,22' W	11° 27,24' S			
19	07.06.00	14:13		78° 11,22' W	11° 27,24' S		X	
			16:00	77° 56,46' W	11° 20,1' S			
20	07.06.00	16:00		77° 56,46' W	11° 20,1' S		X	
			17:46	77° 41,76' W	11° 24,24' S			
transit to 12KL	07.06.00						X	
			21:47	77° 58,02' W	11° 40,02' S			
transit to 13KG	07.06.00						X	
			23:00	77° 57,96' W	11° 40,02' S			
End of Parasound Profiling						**SEL-96**	**SES-2000**	
21	08.06.00	02:25		77° 50,22' W	11° 30,06' S	X	X	
			05:19	78° 13,8' W	11° 28,32' S			
22	08.06.00	05:19		78° 13,8' W	11° 28,32' S	X	X	

Profile No.	Date	Start (UTC)	End (UTC)	Position * Long.	Lat.	HS SEL-96	PS SES-2000	Remarks
			08:55	77° 48,24' W	11° 10,08' S			
23	08.06.00	08:55		77° 48,24' W	11° 10,08' S	X	X	
			09:55	77° 51,48' W	11° 1,56' S			
24	08.06.00	09:55		77° 51,48' W	11° 1,56' S	X	X	
			13:39	78° 21,3' W	11° 16,08' S			
25	08.06.00	13:39		78° 21,3' W	11° 16,08' S	X	X	
			14:24	78° 23,4' W	11° 9,3' S			
26	08.06.00	14:24		78° 23,4' W	11° 9,3' S	X	X	
27	08.06.00	21:37		78° 8,7' W	11° 3,3' S			
			22:10	78° 6,42' W	11° 0,9' S	X	X	
OFOS	08.06.00	22:30		78° 6' W	11° 0,6' S			
28	09.06.00	01:58		78° 4,5' W	11° 1,38' S	X	X	
			03:29	77° 54,6' W	10° 54' S			
29	09.06.00	03:29		77° 54,6' W	10° 54' S	X	X	
			04:41	77° 59,94' W	10° 44,76' S			
30	09.06.00	04:41		77° 59,94' W	10° 44,76' S	X	X	
			08:51	78° 33,6' W	10° 57,84' S			
31	09.06.00	08:51		78° 33,6' W	10° 57,84' S	X	X	
			09:55	78° 30,6' W	11° 5,22' S			
32	09.06.00	09:55		78° 30,6' W	11° 5,22' S	X	X	
			13:30	78° 0,78' W	10° 54,36' S			
33	09.06.00	13:30		78° 0,6' W	10° 54,36' S	X	X	
			14:26	78° 4,8' W	11° 1,5' S			
34	10.06.00	04:16		78° 4,26' W	11° 4,08' S	X	X	
			08:25	78° 4,26' W	11° 39,6' S			
transit to profile 35	10.06.00	08:25		78° 4,26' W	11° 39,6' S	X	X	
			08:55	78° 0' W	11° 39,66' S			
35	10.06.00	08:55		78° 0' W	11° 39,66' S	X	X	
			10:31	78° 0,06' W	11° 25,32' S			
	10.06.00	10:32		78° 0,12' W	11° 25,32' S	X	X	
			10:43	78° 1,68' W	11° 25,02' S			
36	10.06.00	10:44		78° 1,8' W	11° 25,08' S	X	X	
			10:44					
37	10.06.00	13:00		78° 1,98' W	11° 44,46' S	X	X	
			13:35	78° 6,96' W	11° 44,64' S			
38	10.06.00	13:36		78° 6,96' W	11° 44,58' S	X	X	
			14:50	78° 6,96' W	11° 32,46' S			
39	10.06.00	14:50		78° 6,96' W	11° 32,46' S	X	X	
			15:25	78° 1,32' W	11° 32,64' S			
40	10.06.00	15:25		78° 1,32' W	11° 32,64' S	X	X	
			15:52	78° 1,2' W	11° 36,9' S			
41	10.06.00	17:44		78° 2,16' W	11° 37,02' S	X	X	
			23:22	78° 0,96' W	10° 50,16' S			
42	10.06.00	23:22		78° 0,96' W	10° 50,16' S	X	X	course 338°
			02:50	78° 15,06' W	10° 22,08' S			
43	11.06.00	02:50		78° 15,06' W	10° 22,08' S	X	X	course 243°
			07:55	78° 54,9' W	10° 41,94' S			
44	11.06.00	07:55		78° 54,9' W	10° 41,94' S			course 334°
			09:43	79° 3,84' W	10° 27,96' S			

Profile No.	Date	Start (UTC)	End (UTC)	Position * Long.	Lat.	HS SEL-96	PS SES-2000	Remarks
45	11.06.00	09:43		79° 3,84' W	10° 27,96' S	X	X	from 13:25 SEL96 only
			15:39	78° 17,46' W	10° 3,54' S			course 28°
46	11.06.00	19:45		78° 18,18' W	10° 4,08' S	X	X	course 65°
			20:55	78° 15,18' W	10° 12,78' S			
47	11.06.00	20:55		78° 15,18' W	10° 12,78' S	X	X	course 240°
			22:52	78° 30,78' W	10° 20,04' S			
48	11.06.00	22:52		78° 30,78' W	10° 20,04' S	X	X	course 335°
			00:42	78° 38,46' W	10° 5,88' S			
49	12.06.00	00:42		78° 38,46' W	10° 5,88' S	X	X	from 01:16 SEL96 only
			02:04	78° 27,96' W	9° 59,94' S			course 23°
50	12.06.00	02:04		78° 27,96' W	9° 59,94' S	X	X	course 338°
			09:09	78° 52,44' W	9° 0,36' S			
51	12.06.00	09:09		78° 52,44' W	9° 0,36' S	X	X	course 230°
			17:30	78° 45,42' W	9° 45,78' S			
52	13.06.00	00:12		79° 38,52' W	9° 39,48' S	X	X	
			00:40	79° 40,74' W	9° 36,3' S			
53	13.06.00	00:41		79° 40,8' W	9° 36,18' S	X	X	
			01:43	79° 33,36' W	9° 30,3' S			
54	13.06.00	01:43		79° 33,36' W	9° 30,3' S	X		
			02:36	79° 29,04' W	9° 36,24' S			
55	13.06.00	02:38		79° 29,16' W	9° 36,48' S	X		
			04:40	79° 42,72' W	9° 46,8' S			
56	13.06.00	04:40		79° 42,72' W	9° 46,8' S	X		
			05:40	79° 37,62' W	9° 53,7' S			
57	13.06.00	05:40		79° 37,62' W	9° 53,7' S	X		
			08:00	79° 37,98' W	9° 41,16' S			
58	13.06.00	08:00		79° 37,98' W	9° 41,16' S	X		
			09:05	79° 13,92' W	9° 48,42' S			
59	13.06.00	09:05		79° 13,92' W	9° 48,42' S	X		
			11:08	79° 27,3' W	9° 59,82' S			
60	13.06.00	11:08		79° 27,3' W	9° 59,82' S	X		
			11:29	79° 27,3' W	9° 56,82' S			
61	13.06.00	11:29		79° 27,3' W	9° 56,82' S	X		
			12:30	79° 20,52' W	9° 51,06' S			
62	13.06.00	13:13		79° 20,1' W	9° 51,06' S	X		13:35 power failure
			13:35	79° 18,48' W	9° 51,36' S			
62	13.06.00	14:12		79° 18,18' W	9° 54,66' S	X		
			14:45	79° 18,18' W	9° 58,56' S			
63	13.06.00	14:45		79° 15,72' W	9° 58,56' S	X		
			15:50	79° 5,94' W	9° 58,02' S			
64	13.06.00	19:45		79° 5,7' W	9° 58,44' S	X		
			20:20	79° 4,74' W	9° 57,78' S			
65	14.06.00	02:20		79° 5,58' W	9° 59,22' S	X		
			05:55	78° 40,2' W	9° 39,54' S			
66	14.06.00	05:55		78° 40,2' W	9° 39,54' S	X		
			07:36	78° 43,5' W	9° 26,28' S			
67	14.06.00	07:36		78° 43,5' W	9° 26,28' S	X		
			12:09	79° 20,16' W	9° 51' S			
68	14.06.00	15:33		79° 20,16' W	9° 51,24' S		X	
			17:23	79° 5,88' W	9° 58,32' S			
transit to 43 KD	14.06.00	23:57		79° 5,1' W	9° 58,56' S	X		

Profile No.	Date	Start (UTC)	End (UTC)	Position * Long.	Lat.	HS SEL-96	PS SES-2000	Remarks
			02:18	79° 5,4' W	9° 58,92' S			
69	15.06.00	02:26		79° 5,7' W	9° 58,56' S	X		
			03:10	79° 0,18' W	9° 56,04' S			
70	15.06.00	03:11		79° 0,12' W	9° 56,1' S	X		
			04:53	79° 8,64' W	10° 8,52' S			
71	15.06.00	04:54		79° 8,52' W	10° 8,58' S	X		
			05:39	79° 3,54' W	10° 13,44' S			
72	15.06.00	05:39		79° 3,54' W	10° 13,44' S	X		07:17 make way for fishery
			09:35	78° 31,44' W	9° 57,24' S			back on course 07:44
72	15.06.00	09:35		78° 31,44' W	9° 57,24' S	X		
			11:35	78° 41,04' W	9° 41,46' S			
74	15.06.00	16:33		78° 45' W	9° 44,34' S	X	X	from 16:45 SES-2000
			17:18	78° 39,48' W	9° 43,92' S			
75	15.06.00	18:48		78° 40,02' W	9° 44,4' S	X	X	
			19:46	78° 47,58' W	9° 45,6' S			
76	15.06.00	21:33		78° 46,98' W	9° 46,08' S	X	X	
			22:05	78° 50,16' W	9° 48,24' S			
77	15.06.00	23:36		78° 50,88' W	9° 45,72' S		X	
			00:05	78° 48,6' W	9° 43,56' S			
OFOS	16.06.00	01:36		78° 48,42' W	9° 44,22' S		X	
			03:30	78° 47,52' W	9° 44,82' S			
78	16.06.00	03:33		78° 47,52' W	9° 44,82' S	X	X	
			05:43	78° 28,02' W	9° 43,74' S			
79	16.06.00	05:44		78° 27,96' W	9° 43,92' S	X	X	
			06:16	78° 27' W	9° 48,78' S			
80	16.06.00	06:17		78° 27,06' W	9° 48,9' S	X	X	
			10:22	78° 59,82' W	10° 8,4' S			
81	16.06.00	10:22		78° 59,22' W	10° 8,4' S	X	X	
			11:50	79° 5,04' W	9° 57,96' S			
OFOS	16.06.00	11:50		79° 5,04' W	9° 57,96' S	X	X	from 15:40 SES 2000 only
			18:15	79° 4,98' W	10° 1,2' S			
82	17.06.00	03:59		79° 6,12' W	10° 3,48' S	X		
			05:00	79° 7,56' W	9° 54,36' S			
83	17.06.00	05:00		79° 7,56' W	9° 54,36' S	X		
			09:31	78° 34,32' W	9° 29,94' S			
84	17.06.00	09:31		78° 34,32' W	9° 29,94' S	X		
			10:18	78° 41,04' W	9° 28,08' S			
85	17.06.00	10:18		78° 41,04' W	9° 28,08' S	X		
			12:11	78° 51,96' W	9° 35,94' S			
86	17.06.00	12:43		78° 51,72' W	9° 36,24' S	X		
			13:38	78° 43,5' W	9° 36,54' S			
87	17.06.00	16:11		78° 42,6' W	9° 36,84' S	X		
			17:40	78° 42,24' W	9° 24,54' S			
88	17.06.00	18:30		78° 42,36' W	9° 24,9' S	X		
			19:24	78° 44,22' W	9° 31,44' S			
89	17.06.00	20:38		78° 44,64' W	9° 32,04' S	X		
			23:33	79° 5,94' W	9° 47,28' S			
90	17.06.00	23:33		79° 5,94' W	9° 47,28' S	X		
	18.06.00		00:50	79° 4,8' W	9° 57,96' S			
91	18.06.00	01:10		79° 4,86' W	9° 57,96' S	X		
			01:38	79° 4,74' W	9° 58,14' S			

Profile No.	Date	Start (UTC)	End (UTC)	Position * Long.	Lat.	HS SEL-96	PS SES-2000	Remarks
92	18.06.00	03:34		79° 4,68' W	9° 58,2' S	X	X	
			04:36	79° 11,88' W	10° 3,18' S			
93	18.06.00	04:36		79° 11,88' W	10° 3,18' S	X	X	
			05:24	79° 5,82' W	10° 6,54' S			
94	18.06.00	05:24		79° 5,82' W	10° 6,54' S	X	X	
			06:20	78° 58,74' W	10° 1,92' S			
95	18.06.00	08:28		79° 7,74' W	9° 44,82' S	X	X	
			09:17	79° 1,62' W	9° 40,2' S			
96	18.06.00	09:18		79° 1,56' W	9° 40,2' S	X	X	
			11:24	78° 52,26' W	9° 57,12' S			
97	18.06.00	11:25		78° 52,32' W	9° 57,24' S	X	X	
			11:45	78° 54,78' W	9° 58,8' S			
98	18.06.00	11:46		78° 54,78' W	9° 58,8' S	X	X	
			13:51	79° 4,5' W	9° 43,08' S			
99	18.06.00	16:15		79° 7,68' W	9° 53,7' S	(X)	X	
			17:15	79° 12,72' W	9° 46,38' S			
100	18.06.00	19:50		79° 12,6' W	9° 45,9' S	(X)	X	
			20:40	79° 12,54' W	9° 52,74' S			
101	18.06.00	22:04		79° 12,54' W	9° 51,6' S	X	X	
			03:43	78° 41,82' W	10° 30,24' S			
102	19.06.00	03:43		78° 41,82' W	10° 30,24' S	X	X	
			04:16	78° 37,26' W	10° 29,16' S			
103	19.06.00	04:16		78° 37,26' W	10° 29,16' S	X	X	
			07:11	78° 51,84' W	10° 6,78' S			
104	19.06.00	07:11		78° 51,84' W	10° 6,78' S	X	X	
			08:00	78° 46,02' W	10° 2,16' S			
105	19.06.00	08:00		78° 46,02' W	10° 2,16' S	X	X	
			11:08	78° 30,12' W	10° 25,62' S			
106	19.06.00	11:08		78° 30,12' W	10° 25,62' S	X	X	
			12:32	78° 20,28' W	10° 19,74' S			
107	19.06.00	12:32		78° 20,28' W	10° 19,74' S	X	X	
			14:13	78° 27,96' W	10° 6,84' S			
108	19.06.00	14:13		78° 27,96' W	10° 6,84' S	X	X	
			15:12	78° 22,2' W	10° 0,42' S			
109	19.06.00	15:12		78° 22,2' W	10° 0,42' S	X	X	
			17:15	78° 16,26' W	10° 16,26' S			
110	19.06.00	17:15		78° 16,26' W	10° 16,26' S	X	X	
			18:00	78° 20,7' W	10° 21,48' S			
111	19.06.00	21:14		78° 15,54' W	10° 22,32' S	X	X	
			21:30	78° 13,62' W	10° 21,12' S			
112	19.06.00	21:30		78° 13,62' W	10° 21,12' S	X	X	
			22:08	78° 15,42' W	10° 15,96' S			
113	19.06.00	22:08		78° 15,42' W	10° 15,96' S	X	X	
	20.06.00		00:07	78° 30,9' W	10° 24' S			
114	20.06.00	01:57		78° 33,48' W	10° 23,46' S	X	X	
			03:46	78° 47,4' W	10° 31,38' S			
115	20.06.00	03:46		78° 47,4' W	10° 31,38' S	X	X	
			03:57	78° 46,86' W	10° 32,76' S			
116	20.06.00	03:57		78° 46,86' W	10° 32,76' S	X	X	
			05:35	78° 33,9' W	10° 25,92' S			
117	20.06.00	05:35		78° 33,9' W	10° 25,92' S	X	X	

Profile No.	Date	Start (UTC)	End (UTC)	Position * Long.	Lat.	HS SEL-96	PS SES-2000	Remarks
			06:03	78° 36' W	10° 22,68' S			
118	20.06.00	06:04		78° 36,06' W	10° 22,68' S	X	X	
			07:37	78° 48,6' W	10° 29,82' S			
119	20.06.00	07:37		78° 48,6' W	10° 29,82' S	X	X	
			08:07	78° 50,76' W	10° 25,92' S			
120	20.06.00	08:08		78° 50,64' W	10° 25,8' S	X	X	
			11:42	78° 21,36' W	10° 10,2' S			
121	20.06.00	11:42		78° 21,36' W	10° 10,2' S	X	X	
			12:55	78° 18,06' W	10° 20,1' S			
122	20.06.00	17:30		78° 18,72' W	10° 13,14' S	X	X	
			19:15	78° 35,22' W	10° 19,08' S			
123	20.06.00	20:10		78° 35,4' W	10° 19,2' S	X	X	
			21:36	78° 46,8' W	10° 25,56' S			
OFOS	20.06.00	23:15		78°46,32' W	10°24,66' S	X	X	
			04:04	78°44,58' W	10°27,48' S			
124	21.06.00	05:52		78° 44,34' W	10° 25,44' S	X	X	
			07:10	78° 37,86' W	10° 35,46' S			
125	21.06.00	07:10		78° 37,86' W	10° 35,46' S	X	X	
			07:26	78° 35,76' W	10° 34,44' S			
126	21.06.00	07:26		78° 35,76' W	10° 34,44' S	X	X	
			08:37	78° 41,76' W	10° 24,9' S			
127	21.06.00	08:37		78° 41,76' W	10° 24,9' S	X	X	
			09:07	78° 45,72' W	10° 26,88' S			
128	21.06.00	09:07		78° 45,72' W	10° 26,88' S	X	X	
			10:24	78° 40,08' W	10° 36,84' S			
129	21.06.00	10:24		78° 40,08' W	10° 36,84' S	X	X	
			11:31	78° 48,78' W	10° 41,94' S			
130	21.06.00	11:31		78° 48,78' W	10° 41,94' S	X	X	
			11:55	78° 51,06' W	10° 39,3' S			
131	21.06.00	18:48		78° 44,04' W	10° 36,6' S	X	X	
			19:00	78° 44,82' W	10° 35,4' S			
132	21.06.00	19:00		78° 44,82' W	10° 35,4' S	X	X	
			19:32	78° 41,1' W	10° 33' S			
133	21.06.00	19:37		78° 41,52' W	10° 32,34' S	X	X	
			20:40	78° 46,44' W	10° 24,06' S			
134	21.06.00	22:20		78° 45,06' W	10° 23,34' S	X	X	
			23:02	78° 38,76' W	10° 21,12' S			
135	22.06.00	02:38		78° 38,58' W	10° 24,9' S	X	X	
			05.05	78° 16,56' W	10° 28,98' S			
136	22.06.00	05:05		78° 16,56' W	10° 28,98' S	X	X	
			09:40	77° 53,88' W	11° 4,5' S			
137	22.06.00	09:40		77° 53,88' W	11° 4,5' S	X	X	
			10:41	78° 1,14' W	11° 10,08' S			
138	22.06.00	10:41		78° 1,14' W	11° 10,08' S	X	X	
			11:27	78° 5,88' W	11° 4,86' S			
139	22.06.00	11:28		78° 5,88' W	11° 4,74' S	X	X	
			13:00	77° 54,42' W	11° 56,7' S			
140	22.06.00	13:00		77° 54,42' W	10° 56,7' S	X	X	
			13:35	77° 52,38' W	11° 1,38' S			
141	22.06.00	22:22		77° 50,46' W	10° 57,3' S	X	X	
			00:00	77° 59,4' W	10° 45,36' S			

Profile No.	Date	Start (UTC)	End (UTC)	Position * Long.	Lat.	HS SEL-96	PS SES-2000	Remarks
142	23.06.00	03:27		77° 58,08' W	10° 47,52' S	X	X	
			06:07	78° 20,64' W	10° 57,12' S			
143	23.06.00	06:07		78° 20,64' W	10° 57,12' S	X	X	
			06:50	78° 17,7' W	11° 3,18' S			
144	23.06.00	06:50		78° 17,7' W	11° 3,18' S	X	X	
			09:22	77° 55,8' W	10° 54,06' S			
145	23.06.00	09:22		77° 55,8' W	10° 54,06' S	X	X	
			09:38	77° 54,72' W	10° 56,22' S			
146	23.06.00	09:38		77° 54,72' W	10° 56,22' S	X	X	
			10:33	78° 0,9' W	11° 2,04' S			
147	23.06.00	10:33		78° 0,9' W	11° 2,04' S	X	X	
			10:42	78° 0' W	11° 3' S			
148	23.06.00	10:42		78° 0' W	11° 3' S	X	X	
			11:37	77° 52,8' W	11° 59,16' S			
149	23.06.00	14:21		77° 52,38' W	11° 1,74' S		X	
			15:00	77° 52,2' W	11° 7,32' S			
150	23.06.00	15:00		77° 52,2' W	11° 7,32' S		X	
			16:12	77° 58,32' W	11° 16,38' S			
151	23.06.00	18:16		77° 58,26' W	11° 16,5' S		X	
			20:54	77° 58,56' W	11° 39,9' S			
152	24.06.00	01:34		78° 4,08' W	11° 37,02' S		X	
			01:54	78° 4,2' W	11° 34,2' S			
153	24.06.00	02:36		78° 4,38' W	11° 33,06' S		X	
			03:10	78° 5,7' W	11° 37,56' S			
154	24.06.00	03:10		78° 5,7' W	11° 37,56' S		X	
			03:40	78° 5,88' W	11° 33,18' S			
155	24.06.00	03:46		78° 5,4' W	11° 33' S		X	
			04:19	78° 5,22' W	11° 37,86' S			
156	24.06.00	04:28		78° 6,06' W	11° 37,98' S		X	
			05:03	78° 6,24' W	11° 33' S			
transit to 157	24.06.00	05:03		78° 6,24' W	11° 33' S		X	
			05:07	78° 5,7' W	11° 33' S			
157	24.06.00	05:07		78° 3,3' W	11° 33' S		X	
			05:46	78° 5,46' W	11° 38,88' S			
transit to 158	24.06.00	05:46		78° 5,46' W	11° 38,88' S		X	
			05:55	78° 6,48' W	11° 38,88' S			
158	24.06.00	05:56		78° 6,48' W	11° 38,82' S		X	
			06:36	78° 6,48' W	11° 33,06' S			
transit to 159	24.06.00	06:36		78° 6,48' W	11° 33,06' S		X	
			06:41	78° 7,02' W	11° 33,12' S			
159	24.06.00	06:41		78° 7,02' W	11° 33,12' S		X	
			07:24	78° 6,78' W	11° 39,9' S			
transit to 160	24.06.00	07:24		78° 6,78' W	11° 39,9' S		X	
			07:31	78° 7,62' W	11° 39,96' S			
160	24.06.00	07:31		78° 7,62' W	11° 39,96' S		X	
			08:15	78° 7,68' W	11° 33' S			
transit to 161	24.06.00	08:15		78° 7,68' W	11° 33' S		X	
			08:19	78° 7,26' W	11° 33,18' S			
161	24.06.00	08:19		78° 7,26' W	11° 33,18' S		X	
			09:11	78° 7,02' W	11° 41,22' S			
162	24.06.00	09:11		78° 7,02' W	11° 41,22' S		X	

Profile No.	Date	Start (UTC)	End (UTC)	Position * Long.	Lat.	HS SEL-96	PS SES-2000	Remarks
			12:13	77° 42,48' W	11° 55,56' S			
163	24.06.00	12:14		77° 42,42' W	11° 55,62' S		X	
			14:00	77° 38,16' W	12° 10,14' S			
164	24.06.00	14:00		77° 38,16' W	12° 10,14' S		X	
			14:09	77° 39,42' W	12° 10,38' S			
165	24.06.00	14:09		77° 39,42' W	12° 10,38' S		X	
			15:30	77° 42,9' W	12° 0,36' S			
166	24.06.00	15:30		77° 42,9' W	12° 0,36' S		X	
			16:00	77° 40,2' W	12° 2,64' S			
167	25.06.00	03:00		77° 41,82' W	12° 3' S		X	
			03:34	77° 36,96' W	12° 5,04' S			
168	25.06.00	03:34		77° 36,96' W	12° 5,04' S	X	X	
			04:58	77° 26,76' W	12° 12,66' S			
169	25.06.00	04:58		77° 26,76' W	12° 12,84' S	X	X	
			07:22	77° 38,94' W	12° 31,02' S			
170	25.06.00	07:22		77° 38,94' W	12° 31,02' S	X	X	
			08:30	77° 29,88' W	12° 35,76' S			
171	25.06.00	08:30		77° 29,88' W	12° 35,76' S	X	X	
			10:50	77° 16,02' W	12° 19,02' S			
172	25.06.00	10:50		77° 16,02' W	12° 19,02' S	X		
			11:53	77° 15' W	12° 10,14' S			
transit to 110KA	25.06.00	16:25		77° 16,2' W	11° 59,64' S	X	X	
			16:54	77° 18' W	11° 57' S			
173	25.06.00	18:07		77° 18,3' W	11° 57,06' S	X	X	
			19:18	77° 32,94' W	11° 55,02' S			
174	25.06.00	19:18		77° 32,94' W	11° 55,02' S	X	X	
			20:21	77° 40,74' W	12° 0,54' S			
175	25.06.00	22:00		77° 41,1' W	11° 59,34' S	X	X	
			23:15	77° 52,74' W	12° 2,52' S			
176	26.06.00	04:45		77° 40,62' W	12° 0,48' S	X	X	
			06:03	77° 31,2' W	12° 7,44' S			
177	26.06.00	06:03		77° 31,2' W	12° 7,44' S	X	X	
			07:38	77° 39,96' W	12° 18,96' S			
178	26.06.00	07:38		77° 39,96' W	12° 18,96' S	X	X	
			08:18	77° 39,9' W	12° 24,72' S			
179	26.06.00	08:18		77° 39,9' W	12° 24,72' S	X	X	
			10:37	77° 26,1' W	12° 7,98' S			
180	26.06.00	10:38		77° 26,22' W	12° 7,92' S	X	X	
			11:32	77° 33,9' W	12° 6,9' S			
181	26.06.00	13:52		77° 35,1' W	12° 7,74' S	X	X	
			15:15	77° 35,58' W	12° 19,38' S			
182	26.06.00	19:00		77° 30,78' W	12° 16,44' S	X	X	
			19:58	77° 22,86' W	12° 7,38' S			
183	26.06.00	19:58		77° 22,86' W	12° 7,38' S	X	X	
			20:25	77° 22,86' W	12° 5,34' S			
transit to 118 KA	26.06.00	23:05		77° 16,86' W	11° 58,74' S	X	X	
	27.06.00		00:14	77° 18,12' W	11° 57,24' S			
184	27.06.00	00:14		77° 18,12' W	11° 57,24' S	X	X	
			01:36	77° 23,46' W	12° 4,68' S			
185	27.06.00	01:36		77° 23,46' W	12° 4,68' S	X	X	
			05:23	77° 21,36' W	12° 38,52' S			

Profile No.	Date	Start (UTC)	End (UTC)	Position * Long.	Lat.	HS SEL-96	PS SES-2000	Remarks
186	27.06.00	05:23		77° 21,36' W	12° 38,52' S	X	X	
			07:54	76° 58,98' W	12° 47,46' S			
187	27.06.00	07:54		76° 58,98' W	12° 47,46' S	X	X	
			09:15	76° 47,7' W	12° 41,4' S			
188	27.06.00	09:15		76° 47,7' W	12° 41,4' S	X	X	
			09:34	76° 46,62' W	12° 43,98' S			
189	27.06.00	09:34		76° 46,62' W	12° 43,98' S	X	X	
			12:05	77° 6,54' W	12° 55,62' S			
190	27.06.00	12:05		77° 6,54' W	12° 55,62' S	X	X	
			13:55	76° 50,1' W	12° 55,02' S			
191	27.06.00	13:55		76° 50,1' W	12° 55,02' S	X	X	
			17:06	76° 43,56' W	12° 48' S			
192	27.06.00	17:06		76° 43,56' W	12° 48' S	X	X	
			19:13	77° 01,49' W	12° 54,85' S			
193	27.06.00	23:55		76° 58,46' W	12° 55,54' S	X	X	
			00:47	77° 03,81' W	13° 00,08' S			
194	28.06.00			77° 03,81' W	13° 00,08' S	X	X	
			03:28	76° 54,84' W	12° 43,2' S			
195	28.06.00	03:28		76° 54,84' W	12° 43,2' S	X	X	
			07:46	76° 48,12' W	13° 21,06' S			
196	28.06.00	07:46		76° 48,12' W	13° 21,06' S	X	X	
			08:55	76° 57,78' W	13° 25,92' S			
197	28.06.00	08:55		76° 57,78' W	13° 25,92' S	X	X	
			09:15	76° 57,12' W	13° 28,62' S			
198	28.06.00	09:15		76° 57,12' W	13° 28,62' S	X	X	
			11:15	76° 38,82' W	13° 26,04' S			
199	28.06.00	11:15		76° 38,82' W	13° 26,04' S	X	X	
			13:41	76° 16,98' W	13° 31,98' S			
transit to 131KD	28.06.00	19:04		76° 35,22' W	13° 27,66' S	X	X	Profile 200
			20:17	76° 46,08' W	13° 27,18' S			
201	28.06.00	22:20		76° 45,96' W	13° 27' S	X	X	
			00:56	76° 27,18' W	13° 11,82' S			
202	29.06.00	00:56		76° 27,18' W	13° 11,82' S	X	X	
			01:34	76° 30,9' W	13° 7,2' S			
203	29.06.00	01:34		76° 30,9' W	13° 7,2' S	X	X	
			04:35	76° 54,96' W	13° 20,7' S			
204	29.06.00	04:35		76° 54,96' W	13° 20,7' S	X	X	
			06:35	76° 53,76' W	13° 29,1' S			
205	29.06.00	06:35		76° 53,76' W	13° 29,1' S	X	X	
			08:34	76° 34,14' W	13° 35,88' S			
206	29.06.00	08:34		76° 34,14' W	13° 35,88' S	X	X	
			10:11	76° 45,96' W	13° 27,42' S			
207	29.06.00	10:11		76° 45,96' W	13° 27,42' S	X	X	
			11:38	76° 49,92' W	13° 37,8' S			
208	29.06.00	18:58		76° 40,68' W	13° 36,36' S		X	
			20:06	76° 43,68' W	13° 27' S			
209	30.06.00	04:22		76° 38,16' W	13° 32,81' S	X	X	
			04:41	76° 40,87' W	13° 33,40' S	X	X	
210	30.06.00	04:41		76° 40,87' W	13° 33,40' S	X	X	
			10:26	76° 51,20' W	12°42,16' S			
211	30.06.00	10:26		76° 51,20' W	12°42,16' S	X	X	

Profile No.	Date	Start (UTC)	End (UTC)	Position * Long.	Lat.	HS SEL-96	PS SES-2000	Remarks
			12:13	77° 07,52' W	12° 42,96' S			
212							X	
								missing, no data
213							X	
								missing, no data
214	30.06.00	16:35		77° 07,19' W	12° 45,32' S	X	X	
			18:04	76° 58,56' W	12° 54,97' S			
215	30.06.00	20:33		76° 58,22' W	12° 54,79' S	X	X	
			20:43	76° 57,47' W	12° 54,14' S			
216	30.06.00	20:43		76° 57,47' W	12° 54,14' S	X	X	
			21:57	77° 04,26' W	12° 46,50' S			
217	30.06.00	23:42		77° 05,62' W	12° 47,46' S	X	X	
			06:02	77° 39,84' W	12° 2,04' S			
218	01.07.00	06:02		77° 39,84' W	12° 2,04' S	X	X	
			06:25	77° 37,08' W	11° 59,94' S			
219	01.07.00	06:25		77° 37,08' W	11° 59,94' S	X	X	
			07:20	77° 40,2' W	11° 52,5' S			
220	01.07.00	07:20		77° 40,2' W	11° 52,5' S	X	X	
			09:53	78° 0,12' W	11° 40,68' S			
221	01.07.00	09:53		78° 0,12' W	11° 40,62' S	X	X	
			10:23	78° 4,56' W	11° 40,26' S			
222	01.07.00	10:23		78° 4,56' W	11° 40,26' S	X	X	
			11:09	78° 4,5' W	11° 33,36' S			
223	01.07.00	11:14		78° 3,84' W	11° 33,24' S	X	X	
			11:56	78° 3,66' W	11° 39,78' S			
224	01.07.00	12:01		78° 4,14' W	11° 40,02' S	X		
			12:18	78° 4,26' W	11° 37,62' S			
225	01.07.00	12:35		78° 3,18' W	11° 36,12' S	X		
			12:55	78° 3,06' W	11° 33,3' S			
226	01.07.00	12:56		78° 2,94' W	11° 33,3' S	X		
			14:25	77° 55,02' W	11° 39,96' S			

Appendix III

Smear-slide information of selected gravity and piston cores

SO 147 - 4SL

12cm: Diatomaceous ooze, small amount of coccoliths, silicoflagellates, benthic foraminifera. many spicules (sponges?), almost no terrigenous material, amorph Si, C_{org}.

47cm: terrigenous ooze, small amount of diatoms, small amount of foraminifera, plenty of quarz glaukonite

213cm: Foraminifera bearing ooze, benthics as well as planktonics.

243cm Diatom bearing ooze, spicules (sponges?), high amount of quarz, glaukonit, ash layer??

408cm: Diatomaceous ooze, spicules (sponges?), amoprh Si, C_{org}.

457cm: Diatomaceous ooze, spicules (sponges?) small amount of coccoliths, amorph Si, C_{org}.

913cm: Diatom bearing ooze and silt, spicules (sponges?), terrigenous ooze is common, quarz dominates,

SO 147 - 25SL

24cm: Diatom bearing ooze, silicoflagellates, spicules (sponges?), subordinate quarz, C_{org}

37cm: Diatomaceous ooze, many spicules (sponges?), silicoflagellates, *Protoperidinium* spp., many coccoliths, no terrigenous input, C_{org}

124cm: Diatom bearing anbd spicule baring- ooze, silicoflagellates, terrigenous input common with quarz, no coccoliths, C_{org}

234cm: terrigenous ooze and silt, clasts of diatoms, few spicules (sponges?), no coccoliths

251cm: terrigenous ooze, few diatoms, no coccoliths, small amount of quarz but frequent feldspars, glaukonite

280cm: terrigenous ooze and silt, quarz, very few diatoms, no coccoliths, no spicules

418cm: Diatomaceous ooze, coccoliths abundant, many spicules (sponges?), almost no quarz

739cm: Coccolith ooze, diatoms abundant, many spicules (sponges?)

770cm: Terrigenous silt and ooze with few diatoms, no coccoliths, C_{org}, glaukonite

795cm: Terrigenous ooze, many needle like crystals, phosphorite, glaukonite, benthic foraminifera (dominant biserial).

SO 147 - 41SL

42cm: Diatomaceous ooze, few coccoliths, radiolarians, no terrigenous input, silicoflagellates common, spicules (sponges?), C_{org}.

67cm: Diatom bearing ooze, few coccoliths, benthic foraminifera, spicules (sponges?), terrigenous input with quarz,

234cm: Diatomaceous ooze, coccoliths frequent, *Protoperidinium* spp. spicules (sponges?), C_{org}, almost no terrigenous input, calcite common.

596cm: Diatomaceous ooze, coccoliths common, few spicules (sponges?), little amount of terrigenous input with quarz but frequent calcite (bioclasts of foraminifera?), C_{org}

598cm: Diatom bearing ooze, diatoms significantly reduced in comparison to 596cm, reduced amount of coccoliths, spicules (sponges?), few terrigenous quarz but frequent calcite (bioclasts of foraminifera?)

604cm: Foraminifera bearing ooze, more silty, radiolarians, high amount of coccoliths, diatoms only as clasts, frequent calcite (bioclasts of foraminifera?), glaukonite, C_{org}

SO 147 - 46KL

25cm: Diatom bearing ooze, silicoflagellates, coccoliths common, *Protoperidinium* spp., little terrigenous input with quarz

74cm: Diatomaceous ooze, benthic foraminifera frequent, coccoliths, radiolorians and dinoflagellates, few C_{org}, spicules (sponges?)

98cm: Diatom bearing ooze, dinoflagellates, coccoliths, C_{org}, little amount of terrigenous input with quarz, spicules (sponges?)

139cm: Diatomaceous ooze with benthic foraminifera (many biseriale tests), high amount of terrigenous input with quarz, few coccoliths, C_{org}.

250cm: Diatom bearing ooze with benthic foraminifera and bioclasts of planctonics, coccoliths abundant. High amount of terrigenous input with quarz

311cm: Diatomaceous ooze, C_{org}, high amount of terrigenous silt with quarz, little calcite (bioclasts?), benthic foraminifera, many spicules (sponges?), coccoliths absent

479cm: Terrigenous ooze and silt with benthic Foraminifera. Few diatoms, coccolithen absent, few spicules (sponges?), little C_{org}, glaukonite.

513cm: Diatom bearing ooze and silt with benthic Foraminifera, coccoliths and spicules absent. Dark spherules (phosphorite? or pyrite?). High amount calcite (bioclasts?) and of terrigenous input with quarz, glaukonite

List of foraminfera from: So 147 14 MC

Planctonics:
Globigerinoides ruber
Globigerinoides bulloides
Globigerina quinqueloba
Globigerinita glutinata
Neogloboquadrina pachyderma
Neogloboquadrina dutertrei
Orbulina universa

Benthic:
? *Angulogerina carinata*
Bolivina costata
Bolivinella humilis
Cancris sp.
Cassidulina sp.
Cibicidoides sp.
? *Elphidium* sp.
Epistomella afueraensis
Nonionella sp.
Parabolivina peruensis

Ratio planctonics:benthics = 1:0784

List of foraminfera from So 147 34 SL

Planctonics:
Globigerinoides ruber
Globigerinoides bulloides
Globigerina quinqueloba
Globigerinita glutinata
Neogloboquadrina pachyderma
Neogloboquadrina dutertrei
Orbulina universa

Benthonics:
? *Angulogerina carinata*
Bolivina costata
Bolivinella humilis
Brizalina interjecta
Cancris caramensis
Cancris sp.
Cassidulina sp.
Cibicidoides sp.
? *Elphidium* sp.
Epistomella afueraensis
Nonionella sp
Parabolivina peruensis

Ratio planctonics:benthics = 1:0.77

Symbols used in graphical core description

Lithology:


mud


silty mud


silt


sand


sandy silt


diatomaceous mud


diatom bearing mud


foraminifera bearing mud


foraminifera bearing sand


lost core

Texture:

stratification

lamination

cross bedding

undulating bedding

flaser bedding


erosional contact

fining upward sequence


mollusk debris

fish debris

bone fragments

burrow

carapax

phosphorite nodules

mud lense

pyrite nodule


slight bioturbation


moderate bioturbation

So147-4SL

11°56.959´S, 77°18.034´W
Water depth: 96 m
Recovery: 988 cm

METRES | LITHOLOGY | BIOTURBATION INTENSITY | PHYSICAL STRUCTURES | REMARKS

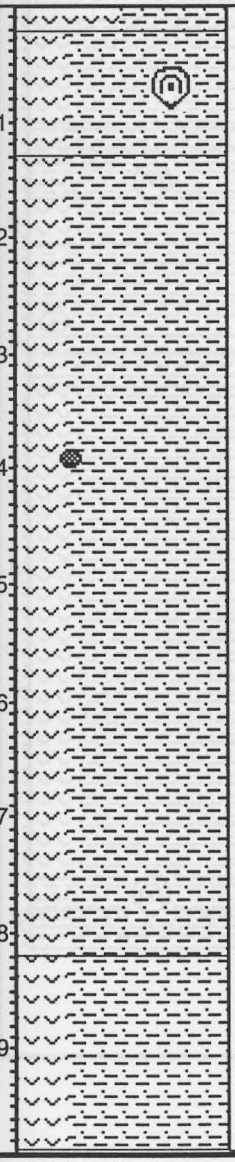

0-25 cm: diatomaceous mud, greenish black

25-133 cm: diatom bearing mud, dark greenish gray, strafified, mud, light gray with sharp contacts at bottom and top at: 16.5-17.5, 23.5-24, 42-48, 57-60 cm
27.5 and 90 cm: greenish brown silty layers
72-75 cm: shell debris
102.5-133 cm: fining upward sequence, dark greenish gray

133-822 cm: diatom bearing mud, dark greenish gray, stratified, with frequent erosive contacts
173-177 cm: silty mud, light gray, erosive contact at the bottom
diatomaceous layers, yellowish brown, with abundant foraminifers at:
214, 302, 317, 337, 389-389.5, 391.5-392, 503, 527, 573.5. 621 cm
390 cm: pebble ø 6 cm

822-988 cm: diatom bearing mud, dark greenish gray, intercalated mica bearing mud layers, grayish and yellowish brown, higher content of carbonate
878-887.5 and 901-907.5 cm: mica bearing silt, dark gray, fining upward sequence
912-950 cm: foraminifera bearing mud layers, light gray

So147-25SL

11°05.469´S, 78°00.009´W
Water Depth: 202 m
Recovery: 824 cm

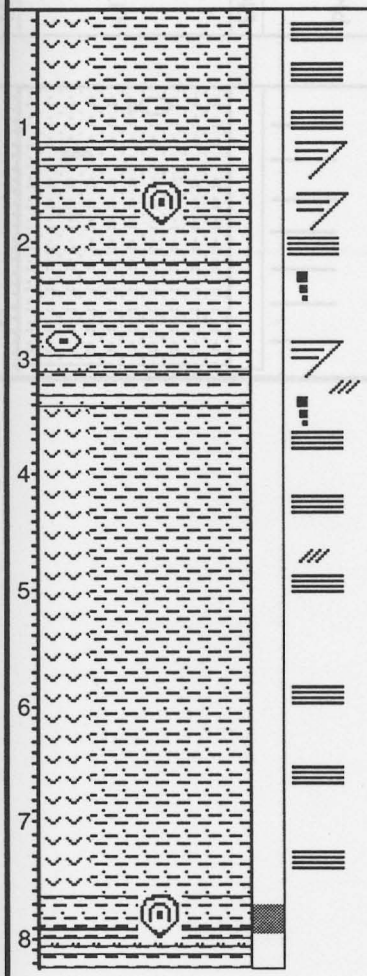

REMARKS

0-6 cm: void

6-117 cm: diatom bearing mud, dark olive-gray, distinct lamination, diatomaceous layers, yellowish brown, with abundant foraminifera at: 9-11, 35-38, 55-57, 63-64, 79-80, 82-83, 85-86, 110-111, 113-114, 116-117 cm

117-121 cm: mud, gray, silty at the base

121-138 cm: mud, very dark gray, homogenous

138-152 cm: diatom bearing mud, dark olive-gray, distinct lamination, diatomaceous layers, yellowish brown, with abundant foraminifera at: 139, 144-145, 146-147, 150, 151-152 cm

152-181 cm: silty mud, dark brown, between 152-165 cm mollusk fragments
165-181 cm: olive-brown

181-220 cm: diatom bearing mud, dark olive-gray, distinct lamination, diatomaceous layers, yellow brown, with abundant foraminifera at: 181-183, 191-192, 195, 207-213 cm

220-235 cm: silty mud, dark grayish green, sandy at the base

235-270 cm: mud, very dark brown, homogenous

270-302 cm: silty mud, dark brown, sandy at the base, phosphorite concretions at the base

302-314 cm: diatom bearing mud, olive-gray, diatomaceous layer, yellowish brown, with abundant foraminifera at 308-310 cm, cross bedded

314-335 cm: mud, dark brown, homogenous

335-342 cm: silty mud, dark gray, lighter gray at the base

342-765 cm: diatom bearing mud, dark olive-gray, distinct lamination, diatomaceous layers, yellowish brown, with abundant foraminifera at. 351, 370, 384, 385, 388, 442-443, 549, 552-553, 554-558, 565-566, 569-571, 576, 596-599, 602, 636-639, 668-669, 674, 708-709 cm
469-472 cm: cross bedding
460 cm: light gray layers, 0.5 cm thick

765-794 cm: silty mud, dark olive-gray, bioturbation, mollusk fragments at 778 cm

794-803 cm: mud, dark brown, homogenous

803-809 cm: silty to sandy mud, yellowish brown

809-814 cm: mud, dark brown, homogenous

814-815 cm: silty mud, yellowish brown

815-824 cm: mud, dark brown, homogenous

So147-27KL

11°36.96´S, 78°02.021´W
Water depth: 382 m
Recovery: 241 cm

METRES | LITHOLOGY | BIOTURBATION INTENSITY | PHYSICAL STRUCTURES | REMARKS

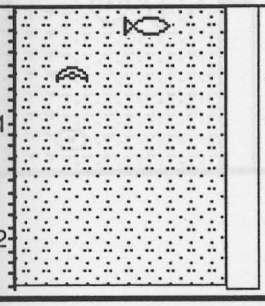

0-241 cm: fine grained sand, gray, with mica, foraminifera, stratification, intercalated olive coloured sections, finer grained
18 cm: fish bone (2 mm)
56 cm: carapax (4 mm)
87-98 cm: regular cm-spaced stratification
181 cm: thin layer with amorphous organic pellets
several lighter medium gray, silty clayey layers at 177, 187, 196 cm

So147-34SL

9°39.548´S, 79°38.426´W
Water depth: 702 m
Recovery: 179 cm

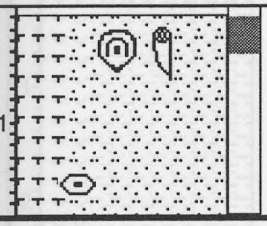

METRES	LITHOLOGY	BIOTURBATION INTENSITY	PHYSICAL STRUCTURES	REMARKS
1				**0-10 cm:** void **10-179 cm:** foraminifera bearing sand with mud and organic material, dark olive-gray 23-30 cm: escape structure 38-42 cm: sand filled clams, open burrows 104-110 cm: black, mm-scale chips of reworked phosphorite 152 cm: phosphorite pebble

So147-40SL

9°51.177´S, 79°20.221´W
Water Depth: 597 m
Recovery: 491 cm

METRES	LITHOLOGY	BIOTURBATION INTENSITY	PHYSICAL STRUCTURES	REMARKS
1 2 3 4				**0-13 cm:** diatomaceous mud, olive-green, homogenous **13-491 cm:** diatom bearing mud, olive-green, distinct lamination, diatomaceous layers, yellowish brown, with abundant foraminifera at: 20, 63, 110-112, 115, 138, 142, 163, 164, 167, 214, 215, 224-227, 231, 234, 235, 238, 244, 253, 257, 270, 278, 294, 295, 328 (4mm thick), 333, 380, 398, 401 (4mm thick), 419, 457 cm 110-112 cm: cross bedding 464-465 cm: dark olive brown laminae

So147-41SL

9°51.088´S, 79°20.312´W
Water depth: 587 m
Recovery: 890 cm

METRES | LITHOLOGY | BIOTURBATION INTENSITY | PHYSICAL STRUCTURES | REMARKS

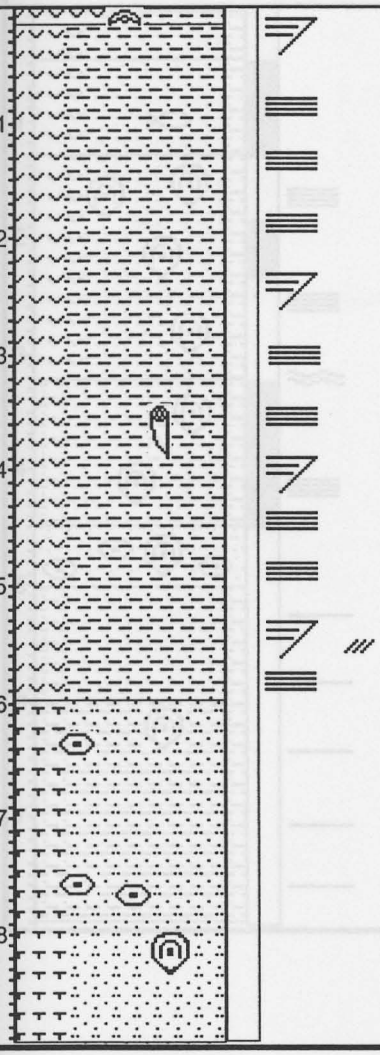

0-18 cm: diatomaceous mud, olive green, homogenous, diatomaceous layers, yellowish brown, with abundant foraminifera at: 4 and 8 cm,
12 cm: carapax

18-599 cm: diatom bearing mud, olive-green, distinct lamination, diatomaceous silty layers, yellowish brown, with abundant foramnifera at: 41, 123, 133-134 (3 layers), 227, 253, 254-254.5, 289, 293, 298, 410, 415, 429, 431, 448, 476, 488 cm
erosional contact at: 23-25 cm, 244-245 cm, 400-401 cm, 543-545 cm
364-367 cm: burrow (hole) ,1.5 cm broad
540-560 cm: cross bedding
598-599 cm: silty mud, dark olive-green, transition zone from muddy to sandy

598-890 cm: foraminfera bearing sand, olive-green, homogenous
634-635, 753, 763-764 cm: phosphorite concretions
812-820 cm: clam with phosphorite cover

So147-46SL

9°41.428´S, 78°40.965´W
Water depth: 154 m
Recovery: 793 cm

METRES | LITHOLOGY | BIOTURBATION INTENSITY | PHYSICAL STRUCTURES | REMARKS

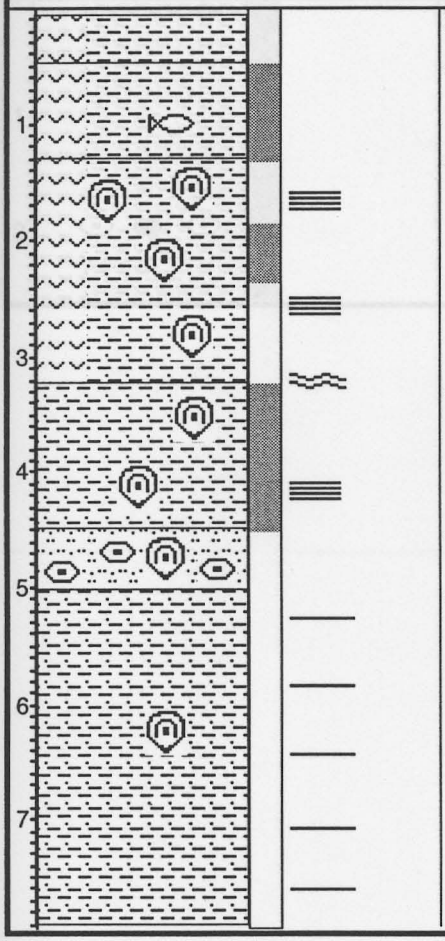

0-11 cm: void

11-50 cm: diatom bearing mud, dark brown, homogenous

50-133 cm: diatom bearing mud, dark brown to olive-brown, slight bioturbation
diatomaceous mud with abundant foraminifera, yellow to greenish yellow at 74-74.5, 106, 133 (diffuse) cm,
101-104 cm fish debris
sharp boundary at the base

133-327 cm: diatom bearing silty mud, olive-green, alternated bedding of homogenous, slightly bioturbated and laminated horizons,
mollusk debris at 141, 164-165, 175, 180, 237, 280 cm
289-298 cm, silty mud, yellowish brown
321 cm: undulating bedding

327-450 cm: silty mud, olive-grayish green, slight bioturbation
349-353 cm: clam in situ
393-397 cm: yellowish brown streaks
421-422 cm: lamination, yellowish brown layers
434-440 cm: yellowish to olive-grayish green layer
427-33 cm: mollusk debris

450-504 cm: sandy silt, olive-gray, sandy at the base, abundant phosphorite concretions and mollusk debris
462-469 cm: layer of mollusk debris
480-504 cm: mollusk debris and phosphorite concretions, very abundant

504-793 cm: silty mud, slight stratification
600-622 cm: mollusk debris
775-793 cm: strongly indurated

So147-80SL

10°40.036´S, 78°51.150´W
Water depth: 1276 m
Recovery: 260 cm

METRES	LITHOLOGY	BIOTURBATION INTENSITY	PHYSICAL STRUCTURES	REMARKS
1	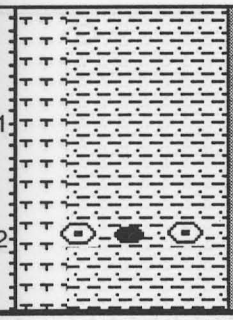			**0-260 cm:** foraminifera bearing mud, light olive-green, with phosphorite sand, moderate bioturbation 117 cm: sand lense, dark olive green, 0.5 cm thick 172-174 cm and 185-186 cm, dark olive-green, higher sand content 185 -186 cm: diatomaceous mud layer, yellowish brown, with abundant foraminifera 195 cm: pyrite nodule, transported 193 - 196.5 cm: two phosphorite concretions, ø 3-4 cm 199-260 cm: several lenses of diatomaceous mud, yellowish brown with abundant foraminifera 260 cm: black phosphorite crust, 0.5 cm thick, within olive coloured diatomaceous mud
2				

So147-83SL

10°36.515´S, 78°44.019´W
Water depth: 605 m
Recovery: 471 cm

METRES	LITHOLOGY	BIOTURBATION INTENSITY	PHYSICAL STRUCTURES	REMARKS
1 2 3 4	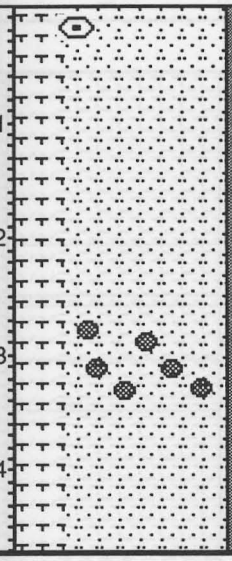			**0-471 cm**: foraminifera bearing sand, olive-green, bioturbated 0-3 cm: phophorite nodules layers enriched in foraminera at: 0-3, 71-90, 95-100, 109-116, 299-306, 420-425, 434-448 cm muddy layers at: 9-26, 90-96, 100-108, 115-119, 124-129, 131-134, 135-136, 139-154, 157-171, 182-211, 396-413, 417-420, 425-431, 448-471 cm 155-157 cm: silty layer, yellowish green mud clasts, dark green, at: 271-299, 306-316, 323-331 cm

So147-97SL

11°16.552´S, 77°58.404´W
Water depth: 219 m
Recovery: 467 cm

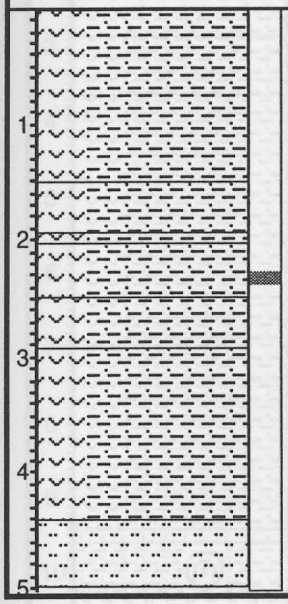

0-153 cm: diatom bearing mud, dark olive-brown, distinct lamination, lighter laminae at: 14, 23, 38, 46, 51, 68, 75, 76, 77, 108, 120, 129 132 cm

153-196 cm: diatom bearing mud, dark olive-brown, stratification in the upper part

196-205 cm: diatom bearing mud, alternated bedding of dark brown and yellowish brown layers

205-251 cm: diatom bearing silty mud, dark olive-brown, distinct stratification in the upper part, between 226-236 cm: moderate bioturbation

251-295 cm: diatom bearing mud, alternated bedding of dark brown and yellowish brown layers

295-443 cm: diatom bearing mud, dark olive-brown, cm-thick stratification, 312-313 and 442-443 cm : silty mud, yellowish brown, laminated, with erosional contacts

443-467 cm: silt, dark olive-brown, homogenous
456-461 cm: yellowish brown sandy layer, with erosional contact

So147-106KL

12°03.002´S, 77°39.862´W
Water depth: 184 m
Recovery: 1875 cm

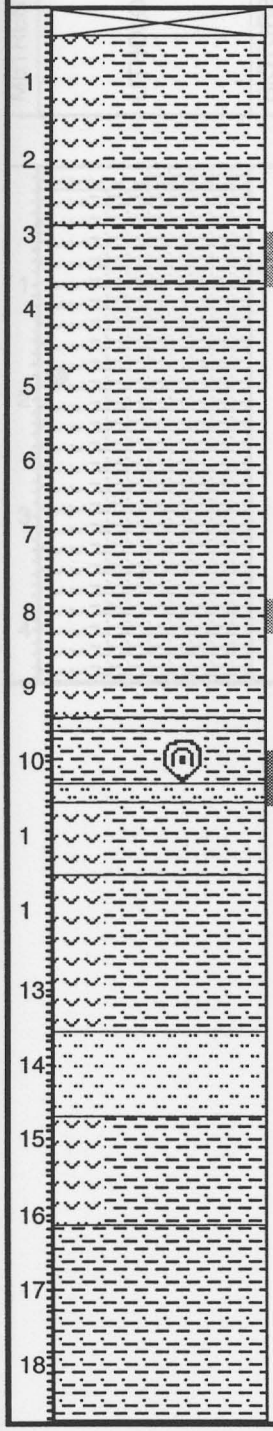

REMARKS

0-46 cm: pipe broken, core not opened

46-298 cm: diatom bearing mud, alternated bedding of homogenous and laminated horizons,
diatomaceous mud, yellowish brown, with abundant foraminifera at: 72-81, 97-105, 118-133, 144-173, 190-194, 264-264 cm (flaser beddding)

298-371 cm: diatom bearing mud, slightly bioturbated, at 371 cm erosional contact

371-943 cm: diatom bearing mud, dark brown, alternated bedding of homogenous and laminated horizons, distinct lamination at 373-381, 406-438, 457-464 cm
473-478 cm: diatomaceous mud, yellowish brown, with abundant foraminifera
521-522 cm: yellowish brown streaks
594-595, 597-598 and 630-631 cm: yellowish brown silty layers, very hard, flaser bedding
665-666, 708-709, 743 cm: diatomaceous mud, yellowish brown, with abundant foraminifera
731-735 cm: erosinal contact
789-832 cm: slight bioturbation
823-824, 915, 917, 935-936 cm: diatomaceous mud, yellowish brown, with abundant foraminifera, cross bedded

943-963 cm: silty mud, olive-green, homogenous

963-972 cm: silty mud, dark gray, between 964-967 cm mollusk debris

972-989 cm: diatom bearing mud, olive-brown, stratification, yellowish brown laminae at 980, 985-986 cm

989-1036 cm: muddy silt, dark gray, bioturbated,
1032-1036 cm: mud, light gray

1036-1059 cm: muddy silt, dark gray, bioturbated

1059-1150 cm: diatom bearing silty mud, olive-green, dark olive-green laminae at: 1068-1071, 1073-1076, 1077-1085, 1093-1096, 1104-1106, 1124-1126, 1129-1132, 1148-1150 cm

1150-1357 cm: diatom bearing mud, olive-green, alternated bedding with dark olive green layers,
diatomaceous mud, yellowish brown, with abundant foraminifera at: 1152-1153, 1162, 1164, 1169, 1172, 1238, 1273, 1296, 1303-1309, 1321-1322, 1345-1346 cm
1320-1357 cm: diffuse bedding

1357-1470 cm: silt, dark brown to olive-brown, sandy at its base, intercalated muddy layers, yellowish brown at 1431-1433 and 1464-1465 cm

1470-1614 cm: diatom bearing, silty mud, alternated bedding between olive-green and dark olive-brown layers,
diatomaceous mud, yellowish brown, with abundant foraminifera at: 1485-1487, 1495-1497, 1499-1500, 1517-1542, 1548-1552, 1558-1572, 1587-1593, 1601-1603, 1613-1614 cm

1614-1875 cm: silty mud, olive-green, slight stratification,
1740 cm: foraminifera bearing layer
1753-to bottom: distinct lamination

So147-118KA

11°56.900´S, 77°18.033´W
Water depth: 95.8 m
Recovery: 444 cm

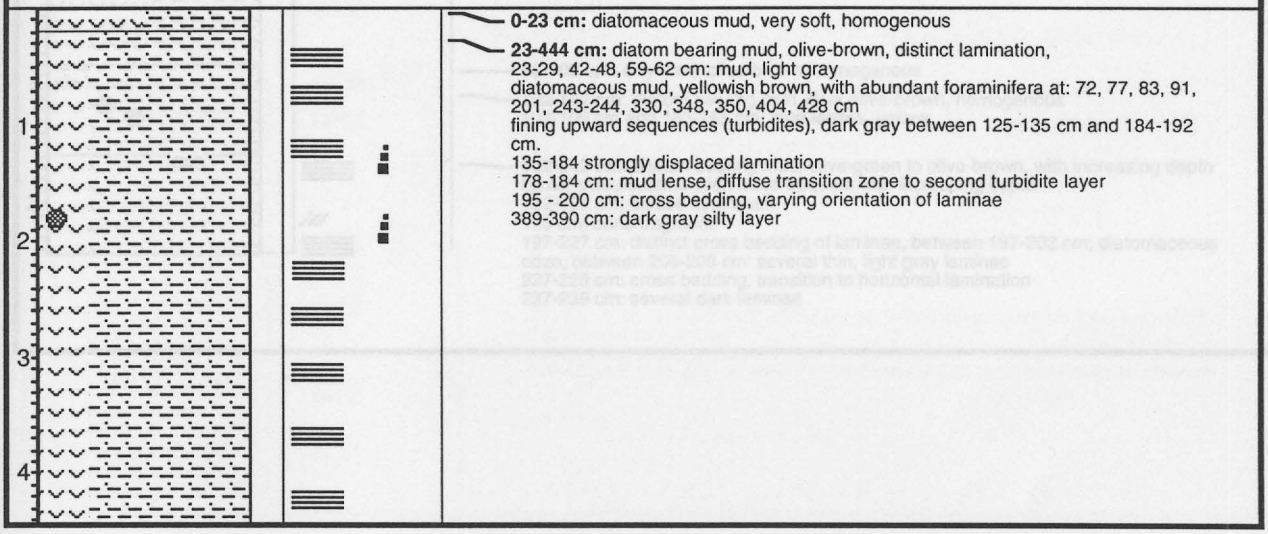

0-23 cm: diatomaceous mud, very soft, homogenous

23-444 cm: diatom bearing mud, olive-brown, distinct lamination,
23-29, 42-48, 59-62 cm: mud, light gray
diatomaceous mud, yellowish brown, with abundant foraminifera at: 72, 77, 83, 91, 201, 243-244, 330, 348, 350, 404, 428 cm
fining upward sequences (turbidites), dark gray between 125-135 cm and 184-192 cm.
135-184 strongly displaced lamination
178-184 cm: mud lense, diffuse transition zone to second turbidite layer
195 - 200 cm: cross bedding, varying orientation of laminae
389-390 cm: dark gray silty layer

So147-123KA

12°55.519´S, 77°00.133´W
Water depth: 363 m
Recovery: 242 cm

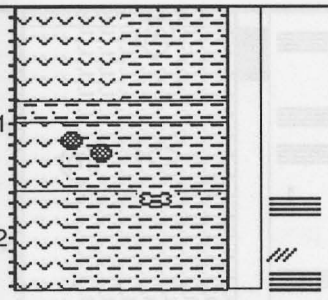

REMARKS

0-82 cm: diatomaceous mud, dark brown, homogenous

82-102 cm: silty mud, olive-brown, homogenous

102-162 cm: diatom bearing mud, dark olive-brown, homogenous
107-109 cm and 153-155 cm: mud lenses, yellow

162-242 cm: diatom bearing mud, olive-green to olive-brown, with increasing depth lighter colours, lamination more frequent with increasing depth
162-167 cm: diffuse lamination
165 cm: bone fragment
197-227 cm: distinct cross bedding of laminae, between 197-202 cm; diatomaceous ooze, between 206-208 cm: several thin, light gray laminae
227-229 cm: cross bedding, transition to horizontal lamination
237-239 cm: several dark laminae

So147-128KA

13°30.849´S, 76°21.022´ W
Water depth: 86m
Recovery: 464m

METRES | LITHOLOGY | BIOTURBATION INTENSITY | PHYSICAL STRUCTURES | REMARKS

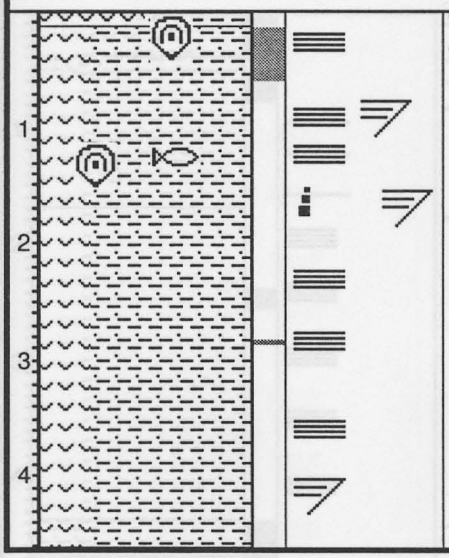

0-15 cm: diatomaceous mud, olive-greenish gray, with abundant *Thioploca* and mollusk fragments

15-464 cm: diatom bearing mud, olive-green to olive-greenish brown, distinct lamination, with intercalated layers of
1) silty to sandy turbidite layers, dark gray
2) diatomaceus mud, yellowish brown, with abundant foraminifera
3) slump structures

15-60 cm: slight bioturbation
60-66 cm: silt, dark gray, abundant mica
88-90 cm: mud layer, light gray, erosive base
102-144 cm: silty mud, dark gray, abundant mica
126 cm: fish debris
130 cm: mollusk fragments
162-169 cm: silty mud to sandy silt, dark gray, fining upward sequence, mollusk fragments at the base
177-183 cm: silty to sandy mud, gray, fining upward sequence
191-193 cm: mud, light gray
212 cm: diatomaceous mud, yellow brown, with abundant foraminifera, 2mm thick
283-284 cm: bioturbated
348-373 cm: slump structure
416-422 cm: mud, gray, erosional contacts at top and base, water escape structure

So147-136SL

13°36.244´S, 76°45.859´W
Water depth: 282 m
Recovery: 470 cm

METRES | LITHOLOGY | BIOTURBATION INTENSITY | PHYSICAL STRUCTURES | REMARKS

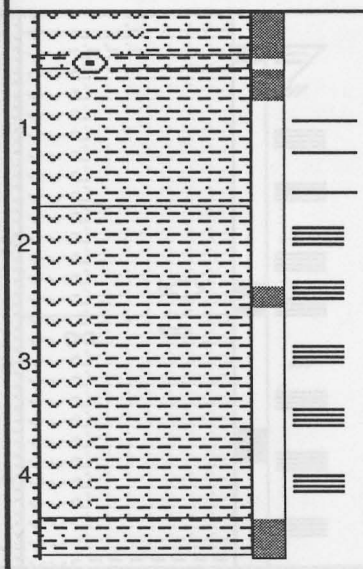

0-41 cm: diatomaceous mud, dark brown to dark greenish brown, moderate bioturbation

41-51 cm: silty mud, dark olive-green, with abundant phophorite concretions

51-78 cm: diatom bearing mud, dark olive-green, moderate bioturbation

78-170 cm: diatom bearing mud, dark olive-green, moderate stratification

170-438 cm: diatom bearing mud, olive-green, distinct lamination
237-254 cm: moderate bioturbation
267-271 cm: diatomaceous mud, yellow
297-301 cm: diatomaceous mud, yellowish brown, slump structure
311-332 cm, 356-359 cm, 385-405 cm: several laminae of diatomaceous mud, yellowish brown with abundant formainifera

438-470 cm: silty mud, olive-greenish gray, abundant mica, moderate bioturbation

So147-137SL

13°36.357´S, 76°40.618´W
Water Depth: 196
Recovery: 480 cm

METRES | LITHOLOGY | BIOTURBATION INTENSITY | PHYSICAL STRUCTURES | REMARKS

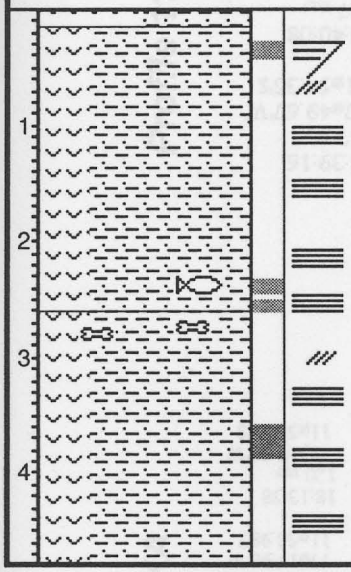

0-18 cm: diatomaceous mud, dark brown to dark olive-brown, homogenous

18-264 cm: diatom bearing mud, dark olive-green, distinct lamination,
22-28 cm: olive-gray mud, homogenous, erosional contact at the base,
28-43(49) cm: olive-greenish brown mud, homogenous, erosional contact at the base, slight bioturbation,
64 cm: cross bedding,
80-89 cm: homogenous layer, slight bioturbation,
111-125 cm: dark layer, homogenous,
137-140 cm: mud lense, olive-green,
156-163 cm: dark layer, homogenous,
221-232 cm: several diatomaceous layers, yellowish brown, abundant foraminifera
232-245 cm, 252-259 cm: dark layer, homogenous, moderate bioturbation
237 cm: fish debris

264-480 cm: diatom bearing mud, olive-green, distinct lamination,
267 cm: bone fragment
272 cm: diatomaceous mud, light yellow
276 cm: bone fragment
301 cm: diatomaceous mud, light yellow, 1 cm thick
309-317 cm: cross bedding
360-386 cm: moderate bioturbation
469-470 cm: three thin laminae of diatomaceous mud, light yellow

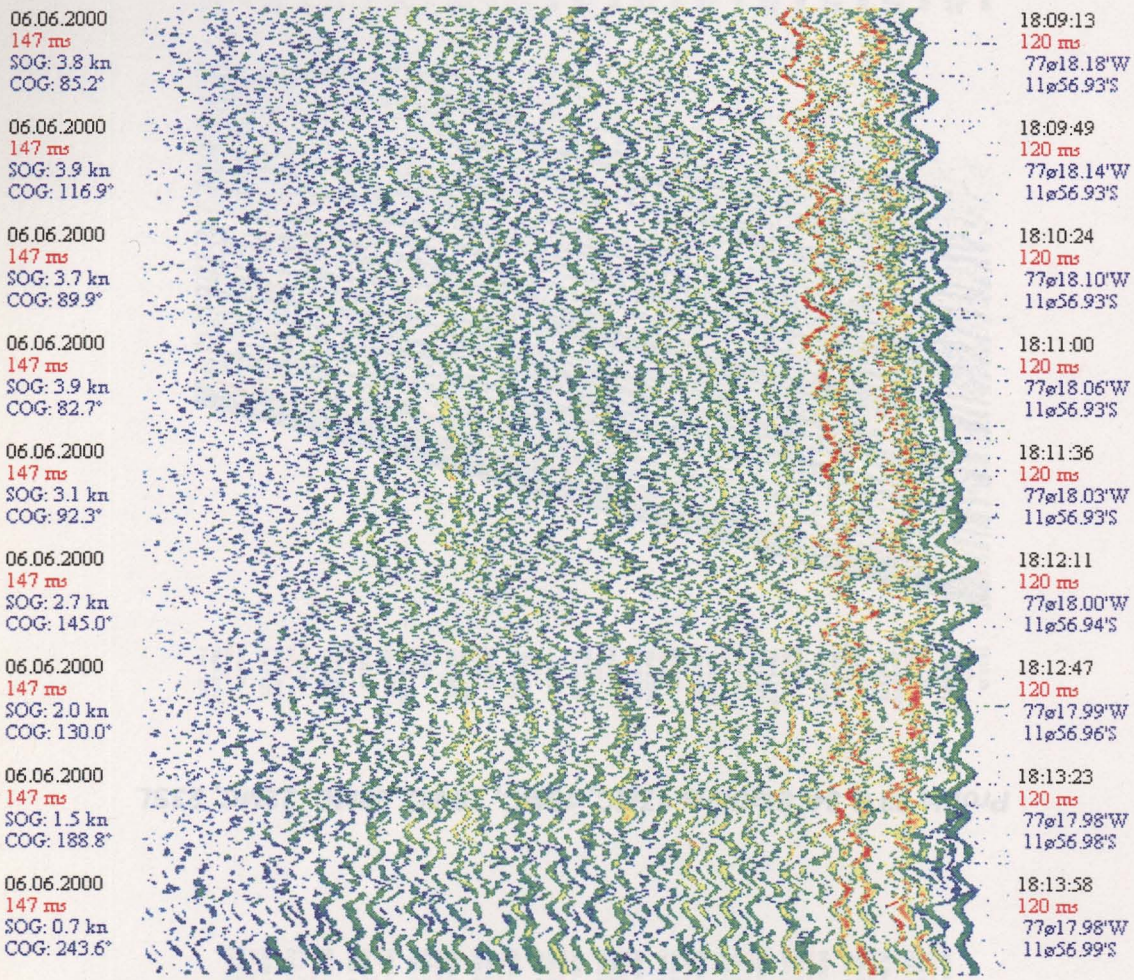

Profile 4, stations 4SL, 5MC, 110KA, 118KA

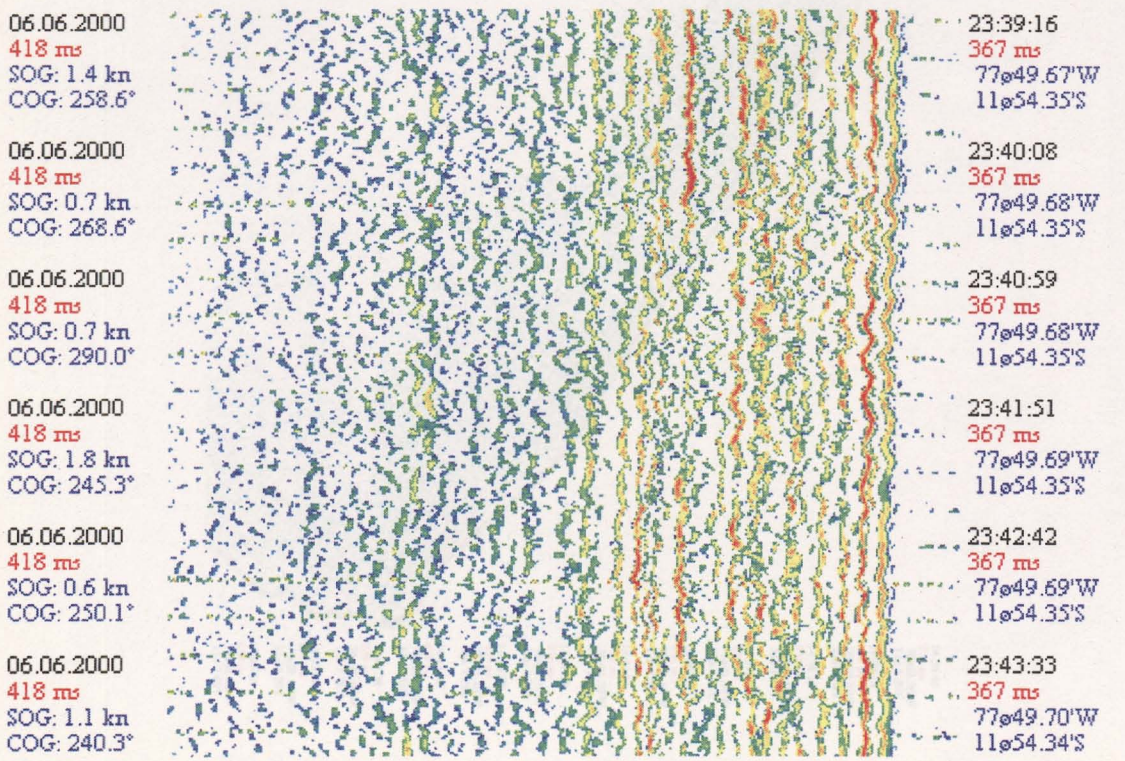

Profile 11, stations 6KL, 7MC, 8MC

Profile 26, station 14MC

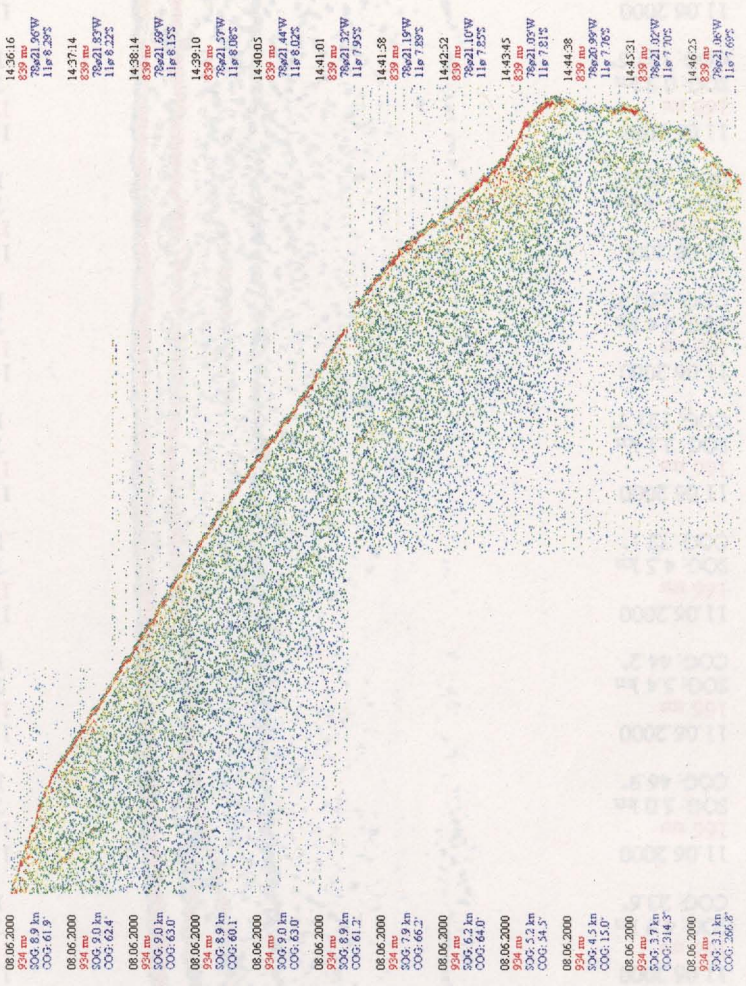

Profile 33 & 34, Stations 17MC, 18MC, 19MC, 20MC, 22MC, 23SL

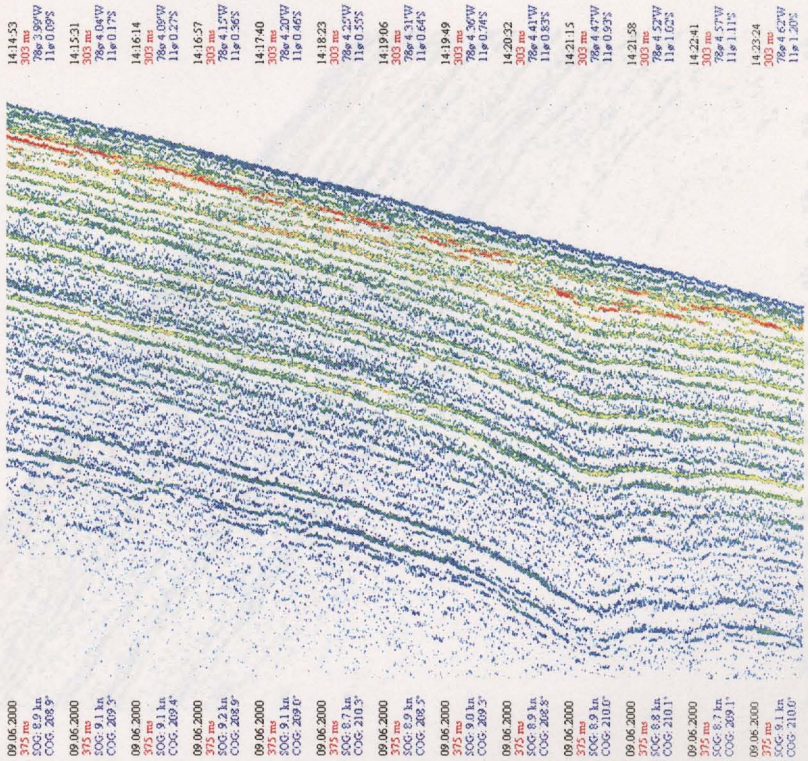

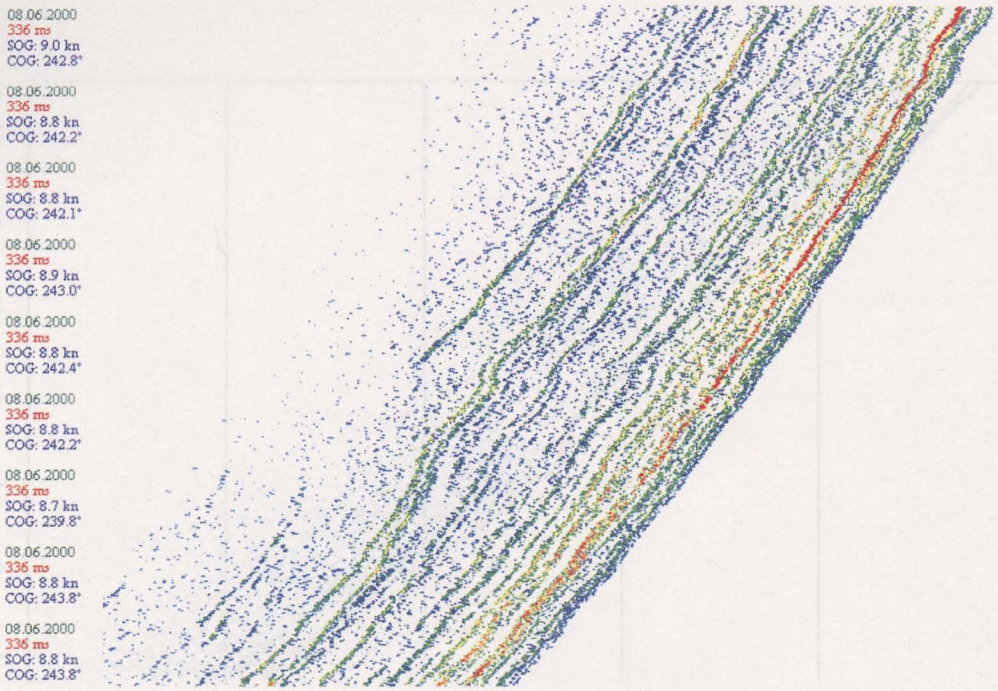

Profile 24, stations 25SL, 99 MC

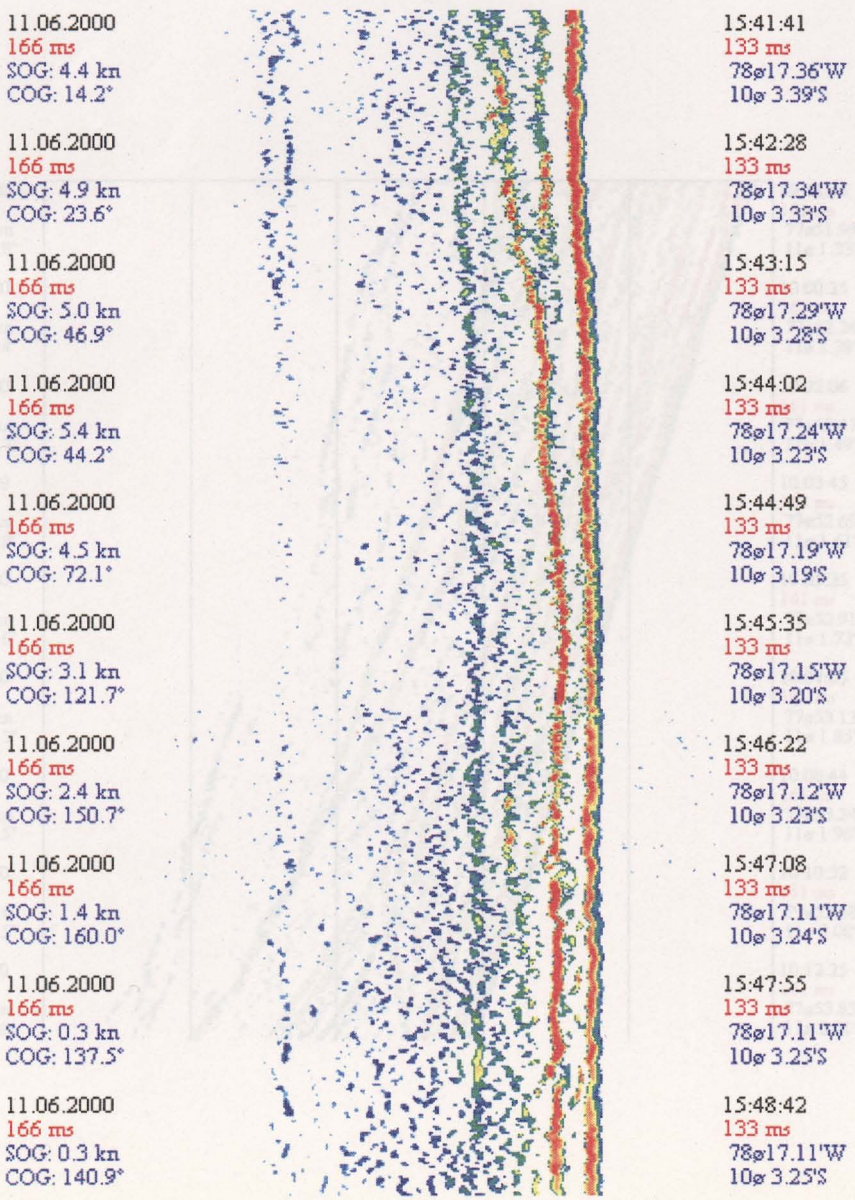

Profile 45, stations 29MC, 30MC, 31KL

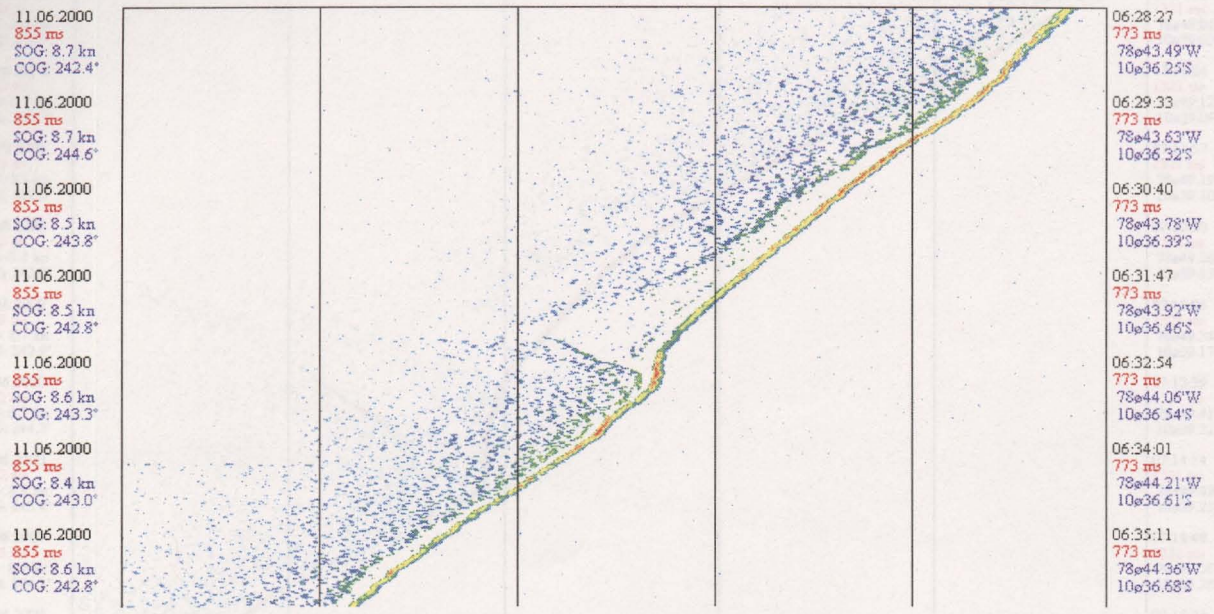

Profile 43, station 83SL

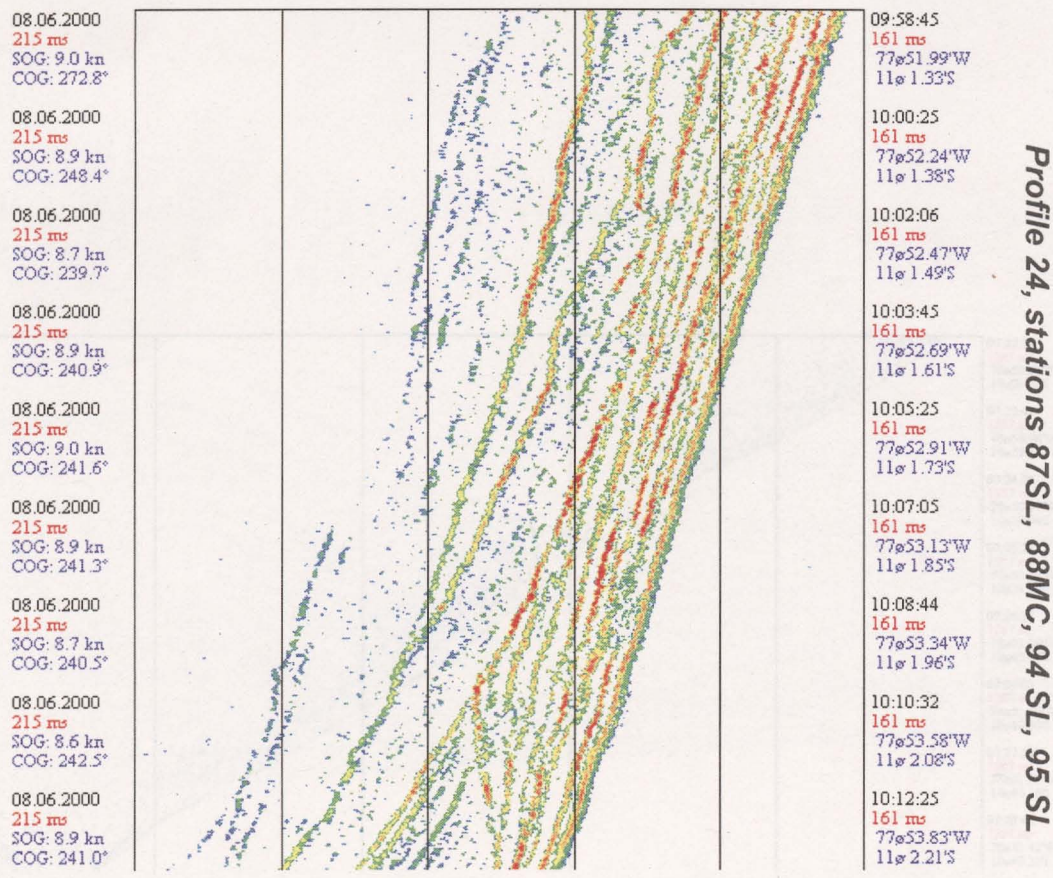

Profile 24, stations 87SL, 88MC, 94 SL, 95 SL

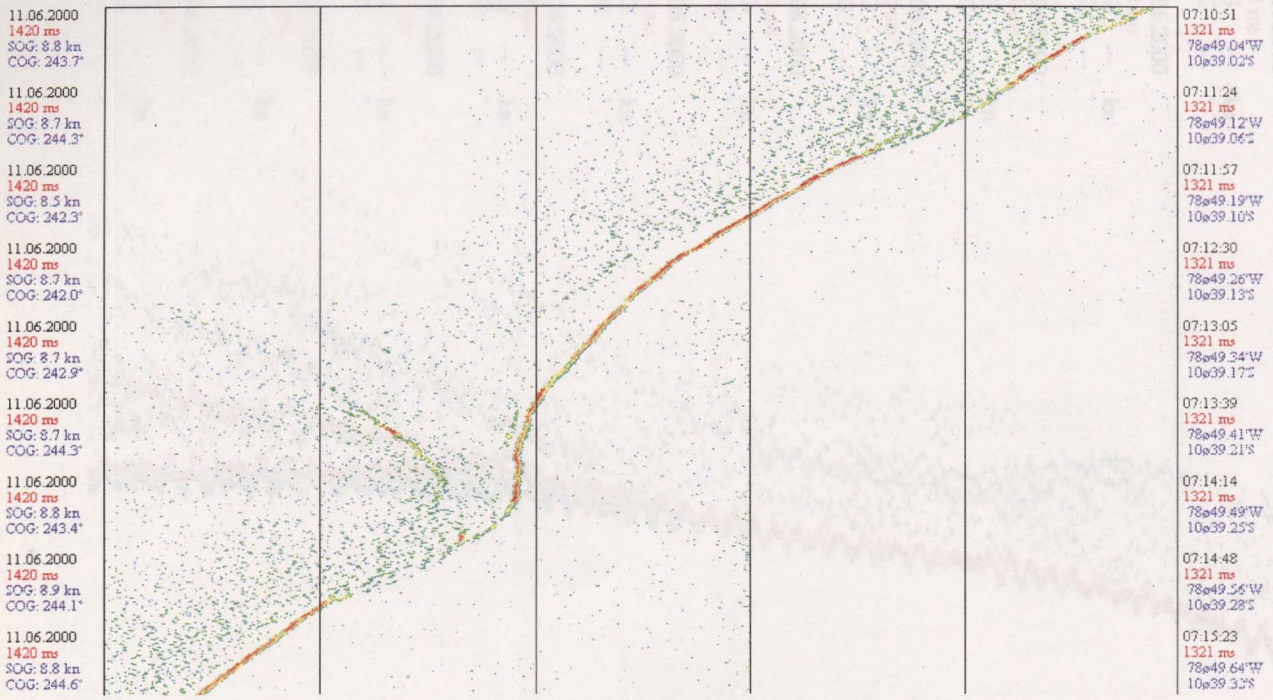

Profile 43, stations 78SL, 79SL, 80SL

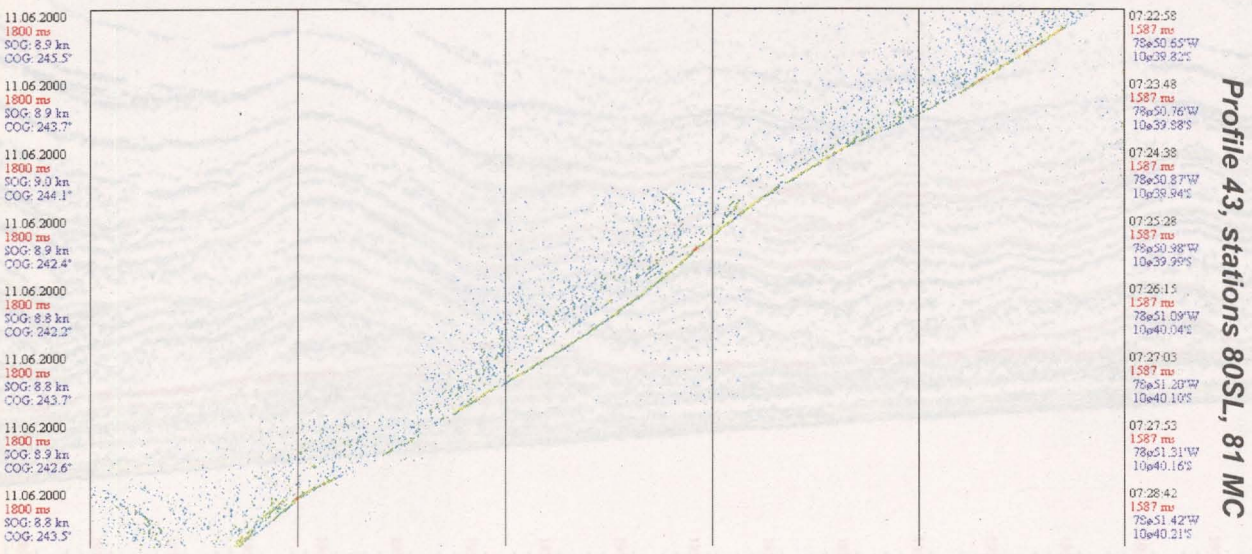

Profile 43, stations 80SL, 81 MC

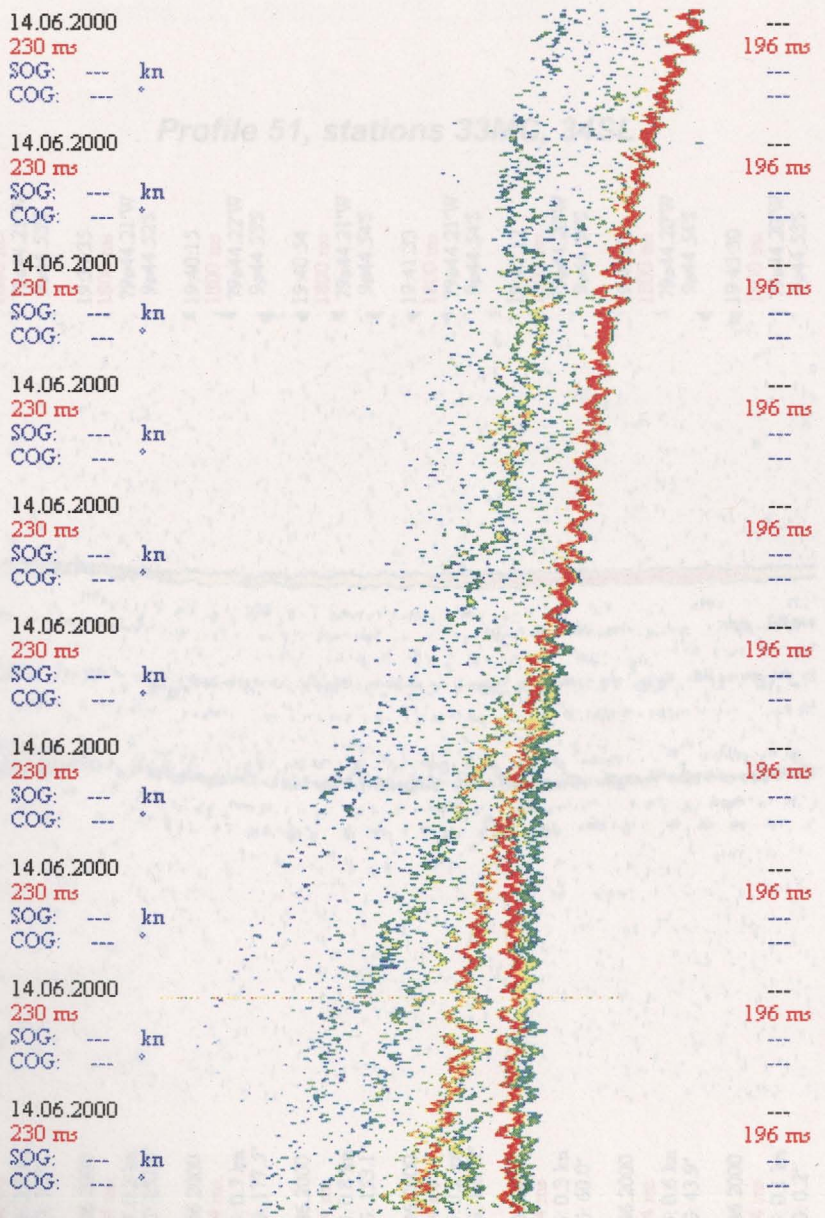

Profile 65, station 47MC

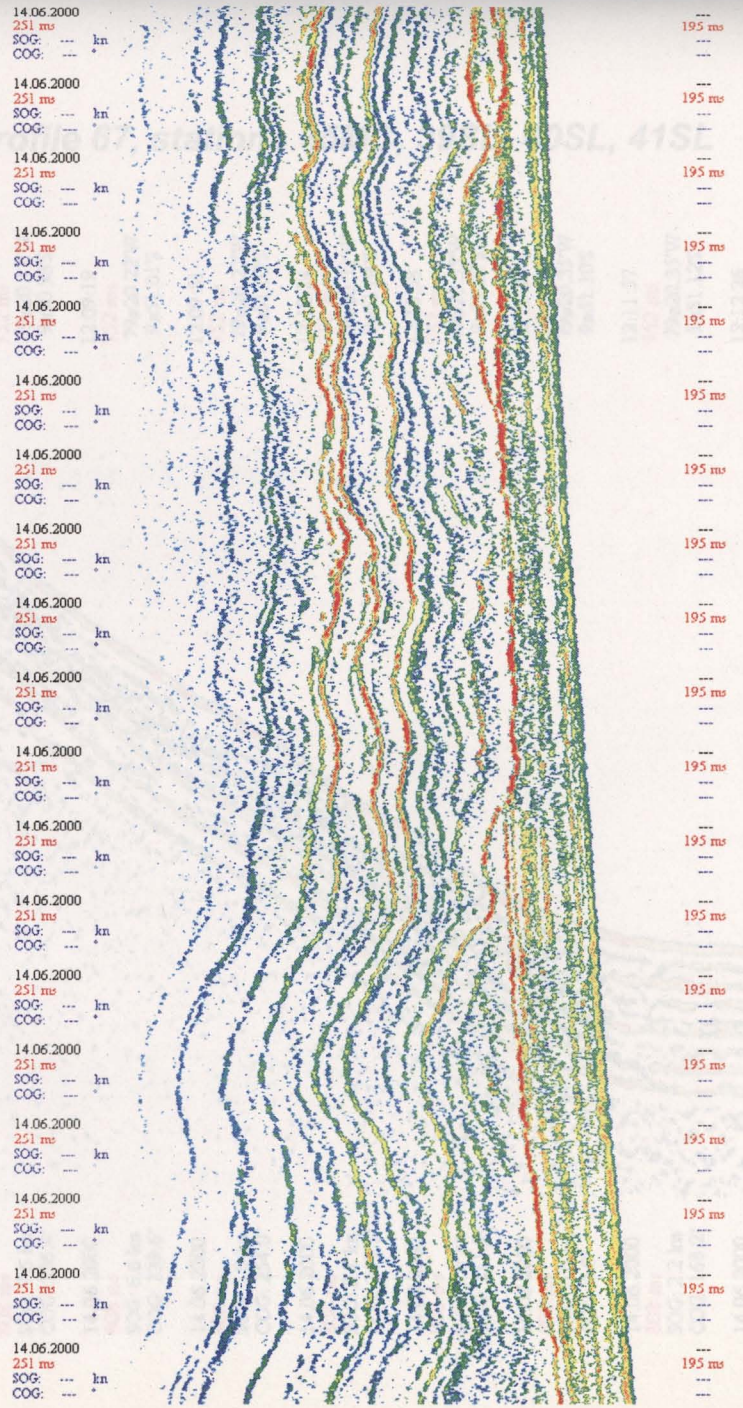

Profile 65, stations 44SL, 45MC, 46KL

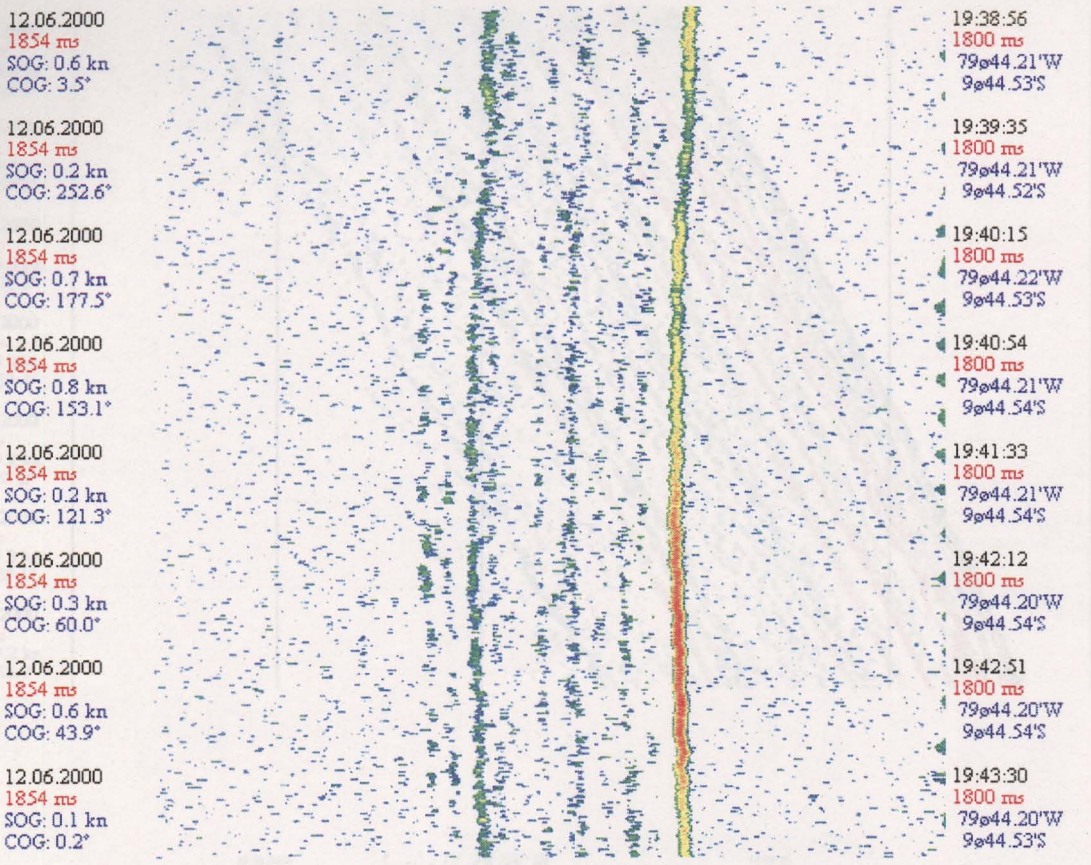

Profile 51, stations 33MC, 34SL

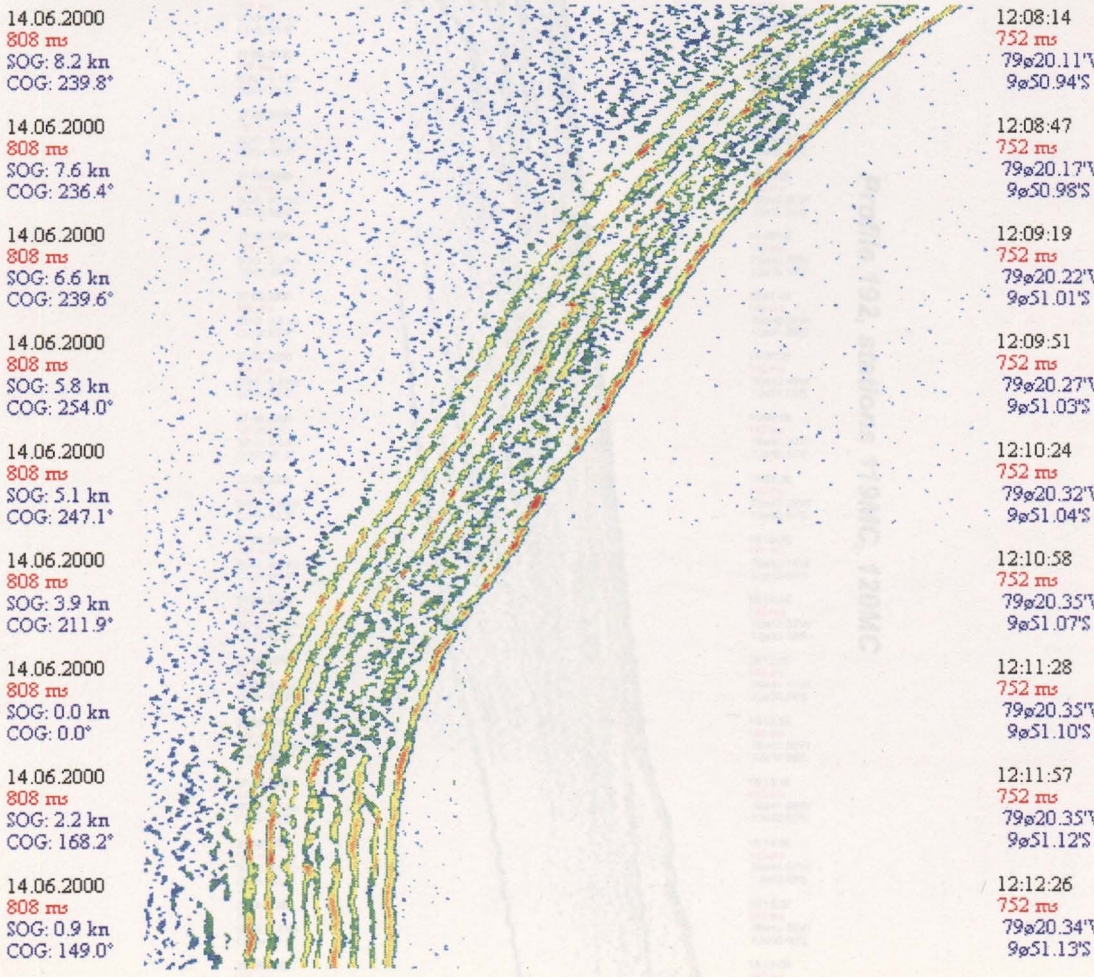

Profile 67, stations 35MC, 39SL, 40SL, 41SL

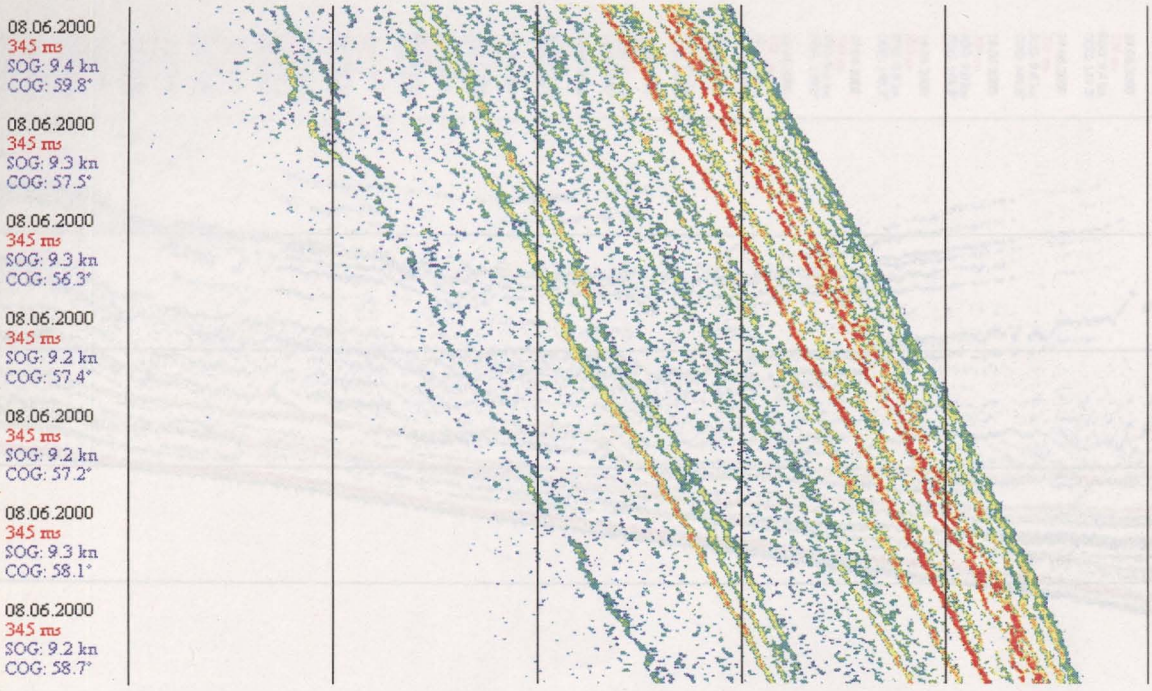

Profile 22, stations 97SL, 98MC

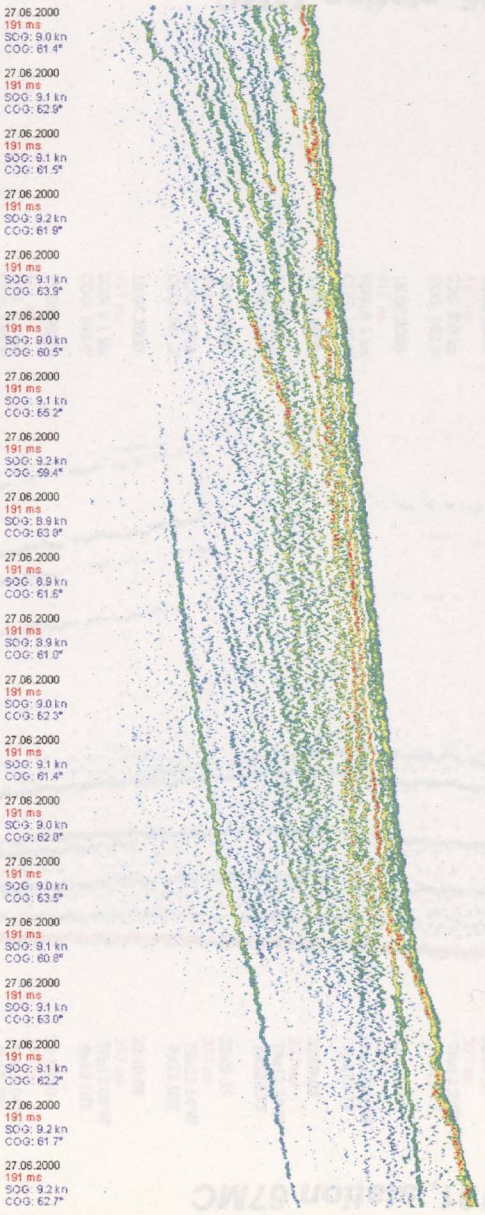

Profile 192, stations 119MC, 120MC

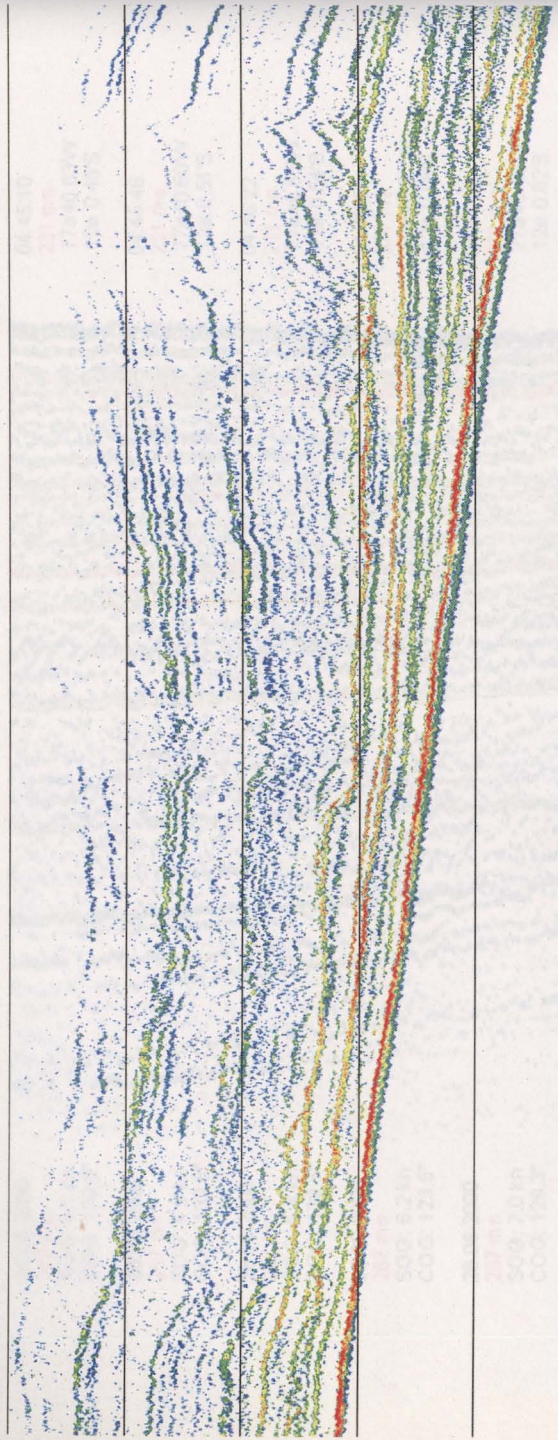

19.06.2000
359 ms
SOG: 9.2 kn
COG: 147.5°

19.06.2000
359 ms
SOG: 9.3 kn
COG: 148.6°

19.06.2000
359 ms
SOG: 9.1 kn
COG: 147.6°

19.06.2000
359 ms
SOG: 9.3 kn
COG: 148.8°

19.06.2000
359 ms
SOG: 9.4 kn
COG: 147.7°

19.06.2000
359 ms
SOG: 9.6 kn
COG: 146.6°

19.06.2000
359 ms
SOG: 9.0 kn
COG: 148.8°

19.06.2000
359 ms
SOG: 8.9 kn
COG: 148.7°

19.06.2000
359 ms
SOG: 9.1 kn
COG: 149.3°

19.06.2000
359 ms
SOG: 9.5 kn
COG: 148.7°

19.06.2000
359 ms
SOG: 9.1 kn
COG: 148.9°

19.06.2000
359 ms
SOG: 9.1 kn
COG: 148.7°

19.06.2000
359 ms
SOG: 9.1 kn
COG: 148.3°

19.06.2000
359 ms
SOG: 9.3 kn
COG: 150.0°

19.06.2000
359 ms
SOG: 8.8 kn
COG: 147.9°

19.06.2000
359 ms
SOG: 9.0 kn
COG: 146.8°

19.06.2000
359 ms
SOG: 9.3 kn
COG: 149.9°

19.06.2000
359 ms
SOG: 9.2 kn
COG: 148.7°

19.06.2000
359 ms
SOG: 9.3 kn
COG: 149.0°

19.06.2000
359 ms
SOG: 9.4 kn
COG: 148.8°

19.06.2000
359 ms
SOG: 9.6 kn
COG: 147.5°

10:28:27
298 ms
78ø33.86'W
10ø21.42'S

10:29:24
298 ms
78ø33.78'W
10ø21.55'S

10:30:20
298 ms
78ø33.70'W
10ø21.67'S

10:31:17
298 ms
78ø33.63'W
10ø21.79'S

10:32:14
298 ms
78ø33.55'W
10ø21.92'S

10:33:11
298 ms
78ø33.47'W
10ø22.05'S

10:34:08
298 ms
78ø33.39'W
10ø22.17'S

10:35:05
298 ms
78ø33.31'W
10ø22.29'S

10:36:02
298 ms
78ø33.24'W
10ø22.42'S

10:36:58
298 ms
78ø33.16'W
10ø22.54'S

10:37:55
298 ms
78ø33.08'W
10ø22.67'S

10:38:52
298 ms
78ø33.01'W
10ø22.79'S

10:39:49
298 ms
78ø32.93'W
10ø22.92'S

10:40:46
298 ms
78ø32.85'W
10ø23.04'S

10:41:46
298 ms
78ø32.77'W
10ø23.17'S

10:42:44
298 ms
78ø32.70'W
10ø23.29'S

10:43:44
298 ms
78ø32.62'W
10ø23.42'S

10:44:43
298 ms
78ø32.53'W
10ø23.55'S

10:45:42
298 ms
78ø32.45'W
10ø23.68'S

10:46:41
298 ms
78ø32.37'W
10ø23.81'S

10:47:40
298 ms
78ø32.29'W
10ø23.94'S

Profile 105, station 71MC

18.06.2000
411 ms
SOG: 5.4 kn
COG: 128.5°

18.06.2000
411 ms
SOG: 5.9 kn
COG: 138.9°

18.06.2000
411 ms
SOG: 6.5 kn
COG: 143.1°

18.06.2000
411 ms
SOG: 7.2 kn
COG: 145.3°

18.06.2000
411 ms
SOG: 8.0 kn
COG: 142.3°

18.06.2000
411 ms
SOG: 8.5 kn
COG: 140.3°

18.06.2000
411 ms
SOG: 8.8 kn
COG: 142.1°

18.06.2000
411 ms
SOG: 9.0 kn
COG: 141.2°

18.06.2000
411 ms
SOG: 9.1 kn
COG: 140.6°

18.06.2000
411 ms
SOG: 8.9 kn
COG: 140.8°

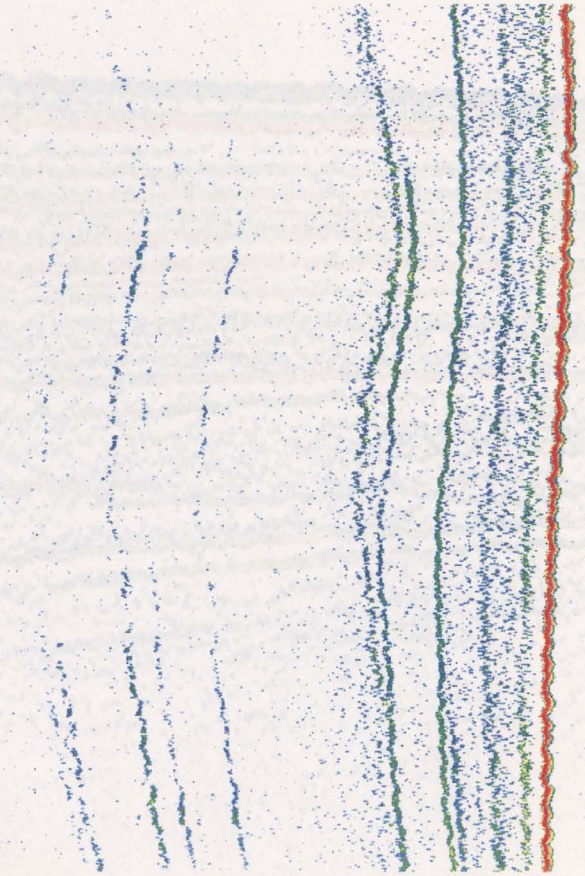

22:05:47
357 ms
79ø12.44'W
9ø51.72'S

22:06:19
357 ms
79ø12.40'W
9ø51.76'S

22:06:52
357 ms
79ø12.36'W
9ø51.80'S

22:07:25
357 ms
79ø12.33'W
9ø51.85'S

22:07:57
357 ms
79ø12.29'W
9ø51.91'S

22:08:30
357 ms
79ø12.24'W
9ø51.97'S

22:09:03
357 ms
79ø12.19'W
9ø52.03'S

22:09:35
357 ms
79ø12.14'W
9ø52.10'S

22:10:08
357 ms
79ø12.09'W
9ø52.16'S

22:10:40
357 ms
79ø12.04'W
9ø52.23'S

Profile 101, station 67MC

Profile 176, station 111 MC

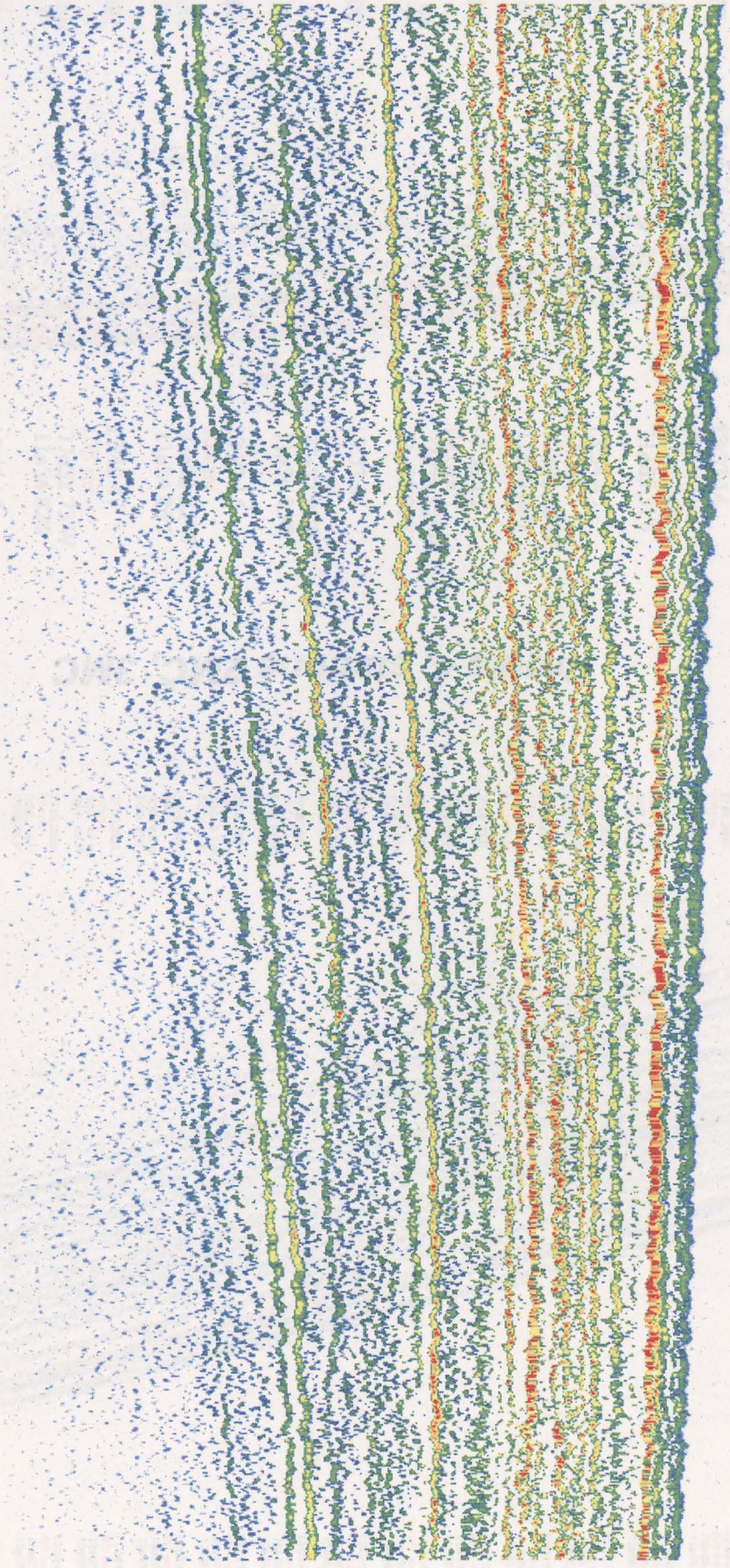

26.06.2000 287 ms SOG: 4.1 kn COG: 130.6°		04:45:10 231 ms 77ø40.63'W 12ø 0.48'S
26.06.2000 287 ms SOG: 4.9 kn COG: 132.6°		04:45:46 231 ms 77ø40.60'W 12ø 0.51'S
26.06.2000 287 ms SOG: 5.4 kn COG: 129.5°		04:46:22 231 ms 77ø40.56'W 12ø 0.54'S
26.06.2000 287 ms SOG: 6.2 kn COG: 123.5°		04:46:59 231 ms 77ø40.51'W 12ø 0.58'S
26.06.2000 287 ms SOG: 7.0 kn COG: 129.3°		04:47:35 231 ms 77ø40.45'W 12ø 0.62'S
26.06.2000 287 ms SOG: 7.6 kn COG: 126.0°		04:48:11 231 ms 77ø40.39'W 12ø 0.66'S
26.06.2000 287 ms SOG: 7.9 kn COG: 118.9°		04:48:47 231 ms 77ø40.32'W 12ø 0.70'S
26.06.2000 287 ms SOG: 8.0 kn COG: 117.9°		04:49:23 231 ms 77ø40.25'W 12ø 0.74'S
26.06.2000 287 ms SOG: 8.3 kn COG: 122.5°		04:50:00 231 ms 77ø40.18'W 12ø 0.78'S
26.06.2000 287 ms SOG: 8.5 kn COG: 115.4°		04:50:36 231 ms 77ø40.10'W 12ø 0.82'S
26.06.2000 287 ms SOG: 8.5 kn COG: 117.1°		04:51:12 231 ms 77ø40.03'W 12ø 0.86'S
26.06.2000 287 ms SOG: 8.8 kn COG: 117.1°		04:51:48 231 ms 77ø39.95'W 12ø 0.91'S
26.06.2000 287 ms SOG: 8.8 kn COG: 120.4°		04:52:24 231 ms 77ø39.87'W 12ø 0.95'S
26.06.2000 287 ms SOG: 8.9 kn COG: 119.3°		04:53:00 231 ms 77ø39.79'W 12ø 0.99'S
26.06.2000 287 ms SOG: 8.9 kn COG: 118.1°		04:53:36 231 ms 77ø39.71'W 12ø 1.04'S
26.06.2000 287 ms SOG: 9.0 kn COG: 119.0°		04:54:13 231 ms 77ø39.63'W 12ø 1.08'S

Profile 4, stations 2MC, 3MC

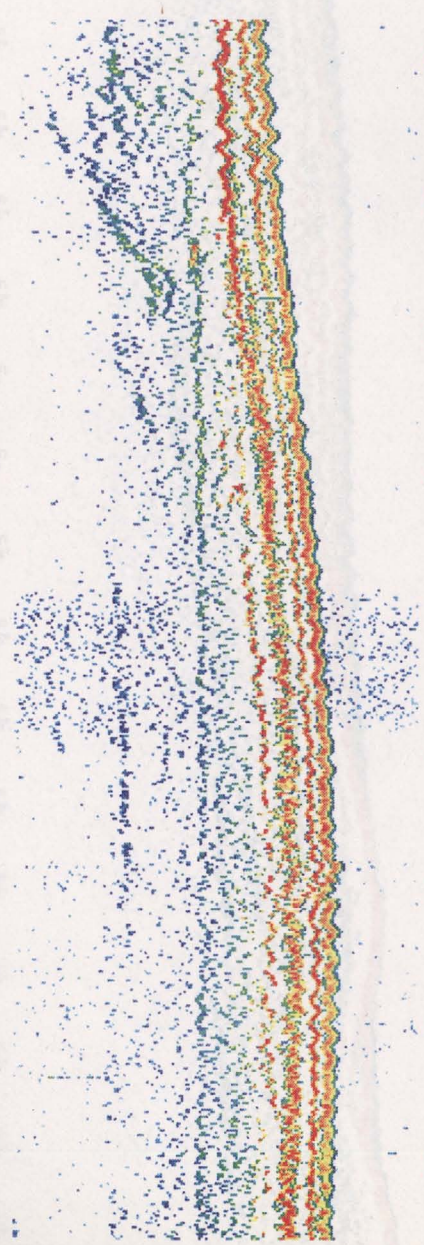

06.06.2000	137 ms	13:31:44
SOG: 8.6 kn	COG: 53.1°	108 ms
		77ø33.63'W
		11ø35.42'S
06.06.2000	137 ms	13:33:14
SOG: 8.5 kn	COG: 55.6°	108 ms
		77ø33.46'W
		11ø35.31'S
06.06.2000	137 ms	13:34:45
SOG: 8.3 kn	COG: 50.6°	108 ms
		77ø33.28'W
		11ø35.20'S
06.06.2000	137 ms	13:36:15
SOG: 8.5 kn	COG: 48.2°	108 ms
		77ø33.12'W
		11ø35.07'S
06.06.2000	137 ms	13:37:46
SOG: 7.8 kn	COG: 53.3°	108 ms
		77ø32.95'W
		11ø34.95'S
06.06.2000	137 ms	13:39:16
SOG: 4.8 kn	COG: 61.9°	108 ms
		77ø32.82'W
		11ø34.86'S
06.06.2000	137 ms	13:40:47
SOG: 3.6 kn	COG: 79.7°	108 ms
		77ø32.73'W
		11ø34.82'S
06.06.2000	137 ms	13:42:17
SOG: 2.6 kn	COG: 119.4°	108 ms
		77ø32.65'W
		11ø34.83'S
06.06.2000	137 ms	13:43:48
SOG: 2.0 kn	COG: 204.3°	108 ms
		77ø32.64'W
		11ø34.88'S

Profile 190, stations 1MC, 148MC

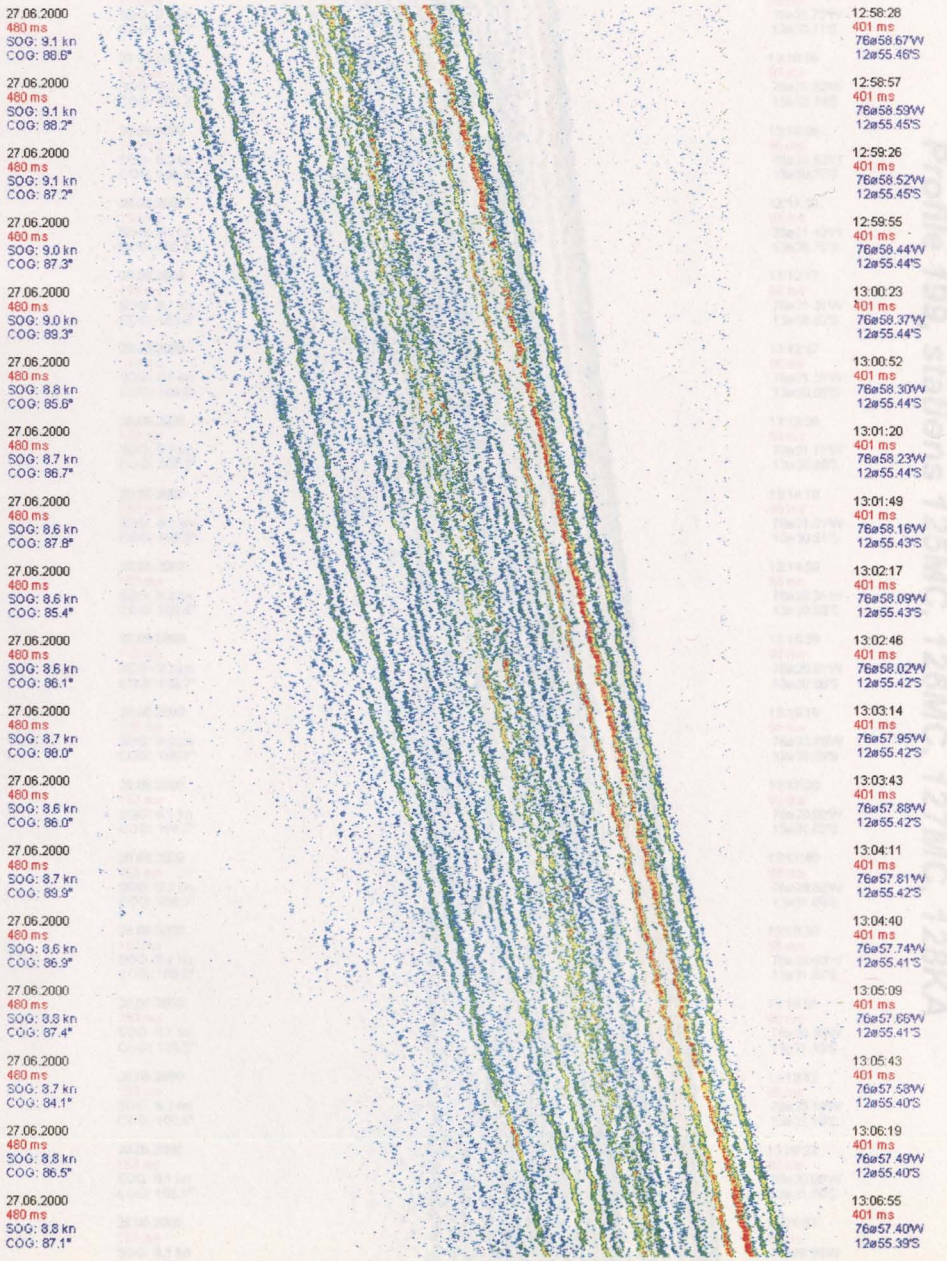

27.06.2000	480 ms	12:58:28
SOG: 9.1 kn	COG: 88.6°	401 ms
		76ø58.67'W
		12ø55.46'S
27.06.2000	480 ms	12:58:57
SOG: 9.1 kn	COG: 88.2°	401 ms
		76ø58.59'W
		12ø55.45'S
27.06.2000	480 ms	12:59:26
SOG: 9.1 kn	COG: 87.2°	401 ms
		76ø58.52'W
		12ø55.45'S
27.06.2000	480 ms	12:59:55
SOG: 9.0 kn	COG: 87.3°	401 ms
		76ø58.44'W
		12ø55.44'S
27.06.2000	480 ms	13:00:23
SOG: 9.0 kn	COG: 89.3°	401 ms
		76ø58.37'W
		12ø55.44'S
27.06.2000	480 ms	13:00:52
SOG: 8.8 kn	COG: 85.6°	401 ms
		76ø58.30'W
		12ø55.44'S
27.06.2000	480 ms	13:01:20
SOG: 8.7 kn	COG: 86.7°	401 ms
		76ø58.23'W
		12ø55.44'S
27.06.2000	480 ms	13:01:49
SOG: 8.6 kn	COG: 87.8°	401 ms
		76ø58.16'W
		12ø55.43'S
27.06.2000	480 ms	13:02:17
SOG: 8.6 kn	COG: 85.4°	401 ms
		76ø58.09'W
		12ø55.43'S
27.06.2000	480 ms	13:02:46
SOG: 8.6 kn	COG: 86.1°	401 ms
		76ø58.02'W
		12ø55.42'S
27.06.2000	480 ms	13:03:14
SOG: 8.7 kn	COG: 88.0°	401 ms
		76ø57.95'W
		12ø55.42'S
27.06.2000	480 ms	13:03:43
SOG: 8.6 kn	COG: 86.0°	401 ms
		76ø57.88'W
		12ø55.42'S
27.06.2000	480 ms	13:04:11
SOG: 8.7 kn	COG: 89.9°	401 ms
		76ø57.81'W
		12ø55.42'S
27.06.2000	480 ms	13:04:40
SOG: 8.6 kn	COG: 86.9°	401 ms
		76ø57.74'W
		12ø55.41'S
27.06.2000	480 ms	13:05:09
SOG: 8.8 kn	COG: 87.4°	401 ms
		76ø57.66'W
		12ø55.41'S
27.06.2000	480 ms	13:05:43
SOG: 8.7 kn	COG: 84.1°	401 ms
		76ø57.58'W
		12ø55.40'S
27.06.2000	480 ms	13:06:19
SOG: 8.8 kn	COG: 86.5°	401 ms
		76ø57.49'W
		12ø55.40'S
27.06.2000	480 ms	13:06:55
SOG: 8.8 kn	COG: 87.1°	401 ms
		76ø57.40'W
		12ø55.39'S

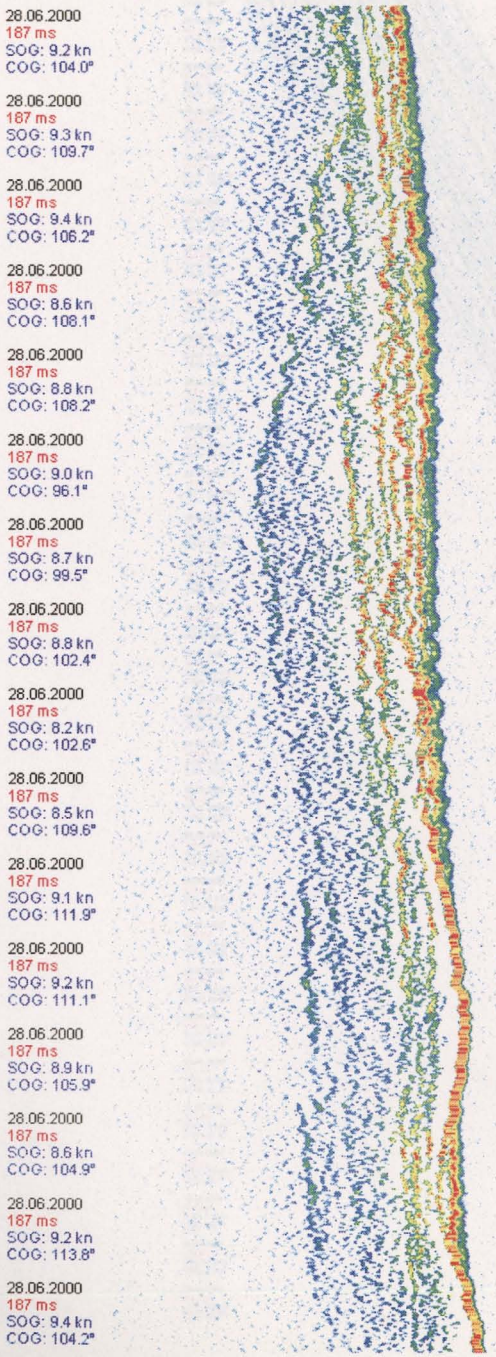

Profile 199, station 129MC

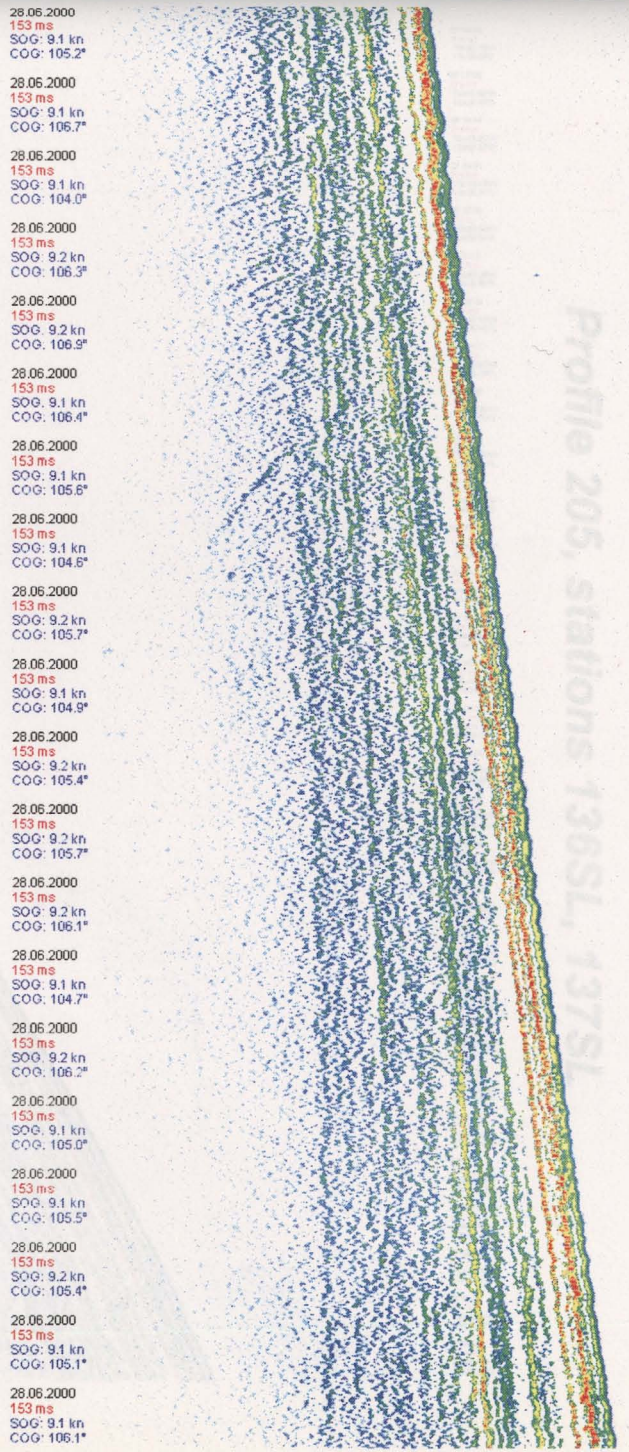

Profile 199, stations 125MC, 126MC, 127MC, 128KA

Profile 205, stations 136SL, 137SL

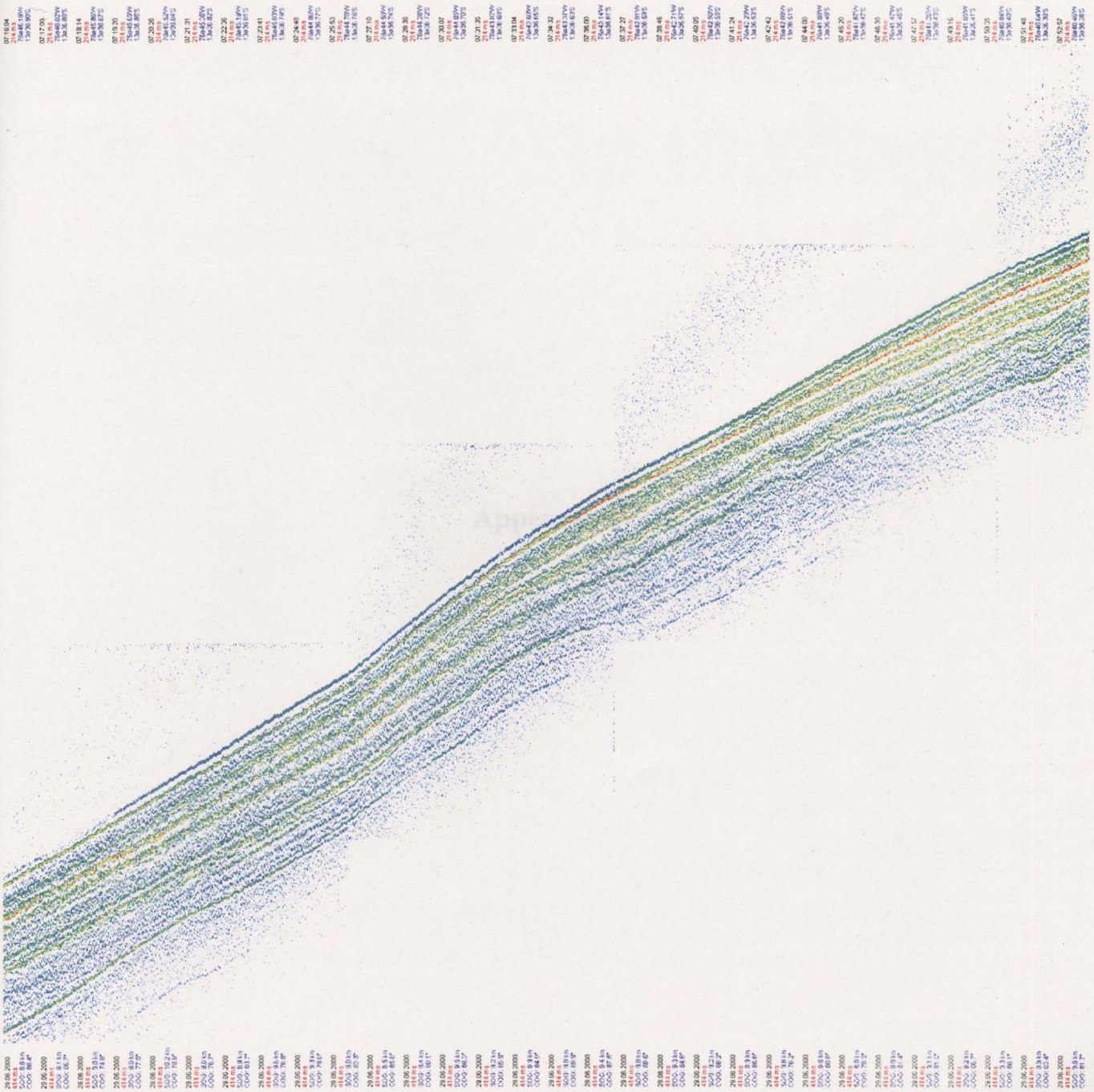

Appendix IV

Neue Presse 22.06.2000

Forscher aus Hannover vor Perus Küste unterwegs

Auf der Suche nach Phosphat und den Spuren El Niños

AN BORD: Auf dem Schiff werden Daten ausgewertet. Foto: BGR

Deutsche Wissenschaftler erforschen den Südpazifik vor der Küste Perus – angeführt von Experten der Bundesanstalt für Geowissenschaften und Rohstoffe in Hannover.

HANNOVER/LIMA. Seit zwei Wochen sind die Meereswissenschaftler mit dem deutschen Forschungsschiff Sonne unterwegs. In einem einzigartigen Gebiet: Die Gewässer vor der Küste Perus gehören zu den nährstoffreichsten Meeresbereichen der Erde.

In solchen Gebieten bilden sich unter noch weitgehend unbekannten Bedingungen phosphathaltige Körnchen, die in großen Lagerstätten auf dem Festland Perus abgebaut und zum Beispiel zu Düngemitteln verarbeitet werden.

Ziel der aktuellen Expedition ist es, neue Phosphatlagerstätten im Meer aufzuspüren und heraus zu bekommen, wie sie sich bilden. Außerdem wollen die Forscher die Klimaschwankungen untersuchen, die durch das Wetterphänomen El Niño im pazifischen Raum entstehen.

El Niño („das Christkind") wird durch eine große Erwärmung der Oberfläche des tropischen Pazifiks verursacht, die durchschnittlich etwa alle vier Jahre zur Weihnachtszeit auftritt. Sie führt zu Dürren in Südostasien und Australien sowie zu Überschwemmungen im westlichen Südamerika – zum Teil mit katastrophalen Folgen. In den Schichten des Meeresschlamms vor der Küste Perus lässt sich El Niños Geschichte ablesen.

Die Forschungsarbeiten werden von der Bundesanstalt koordiniert. Mit zehn Teilnehmern stellt sie den größten Teil der 25 Wissenschaftler aus sechs Institutionen in Oldenburg, Bremen, Kiel, Mainz und Rostock.

P. HERZIG

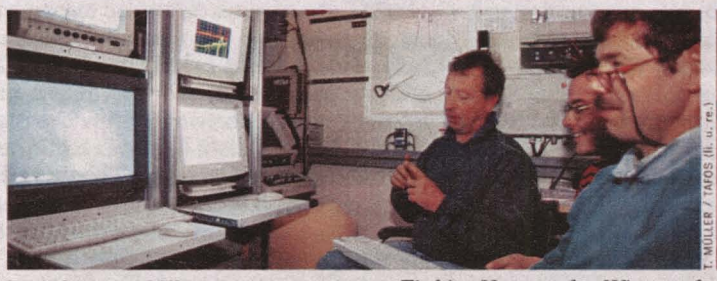

T. MÜLLER / TAFOS (li. u. re.)

Forschungsschiff „Sonne", Forscher* *„Tief im Herzen des Wissenschaftlers sitzende, lustgetriebene Neugier"*

MEERESFORSCHUNG

Riesen in der Todeszone

Das deutsche Forschungsschiff „Sonne" erkundete vor Peru, wie unter Bakterienwäldern und Walfriedhöfen die Ölfelder der Zukunft entstehen könnten.

Forscherglück auf 77 Grad westlicher Länge und 11 Grad südlicher Breite: „Soeben treibt das Schiff mit der Tiefseekamera über große weiße Matten von Bakterien." Der Meeresgeologe Hermann Kudrass, der über Bordvideo den Pazifikgrund vor Peru observiert, mag es kaum glauben.

Scheinbar endlos wandert das Scheinwerferfeld über eine geballte Biomasse. Es sind paradoxe Wesen – Riesenbakterien der Gattung Thioploca, zu faserigen Strängen gebündelt, die nahezu 30 Zentimeter lang werden. Sie wachsen aus dem Meeresboden und wabern wie Seegras im Strom; hingerissen mailt der Forscher nach Deutschland: „Die Bilder waren so faszinierend, dass ich das Abendessen verpasst habe."

Aber es gibt nicht nur Volltreffer auf dem Bremer Forschungsschiff „Sonne", das mit zwei Dutzend deutschen Meeres-Wissenschaftlern an der südamerikanischen Westküste kreuzt.

Gerade wird eine defekte Kastensonde geborgen. Beim Einrammen des Blechkörpers in den Bodenschlamm muss wieder mal ein Stein im Weg gewesen sein, jedenfalls ist die Sonde nun abgeknickt und krumm gebogen. So gewinnt die Bordwette ein Oldenburger Geochemiker, der in den Umlaufbogen mit den Ergebnisprognosen für dieses Experiment „Banane" eingetragen hat. Eigentlich hätte jetzt ein zehn Meter langer Sedimentkern mit den Ablagerungsmarken mehrerer Jahrtausende offen liegen müssen; aufs Deck ergießt sich stattdessen nur stinkender Matsch.

Ein dicht am Schiff vorüberschnaufender Großwal rettet die Stimmung der frustrierten Forscher. „Schwund gibt es überall", tröstet sich Kudrass.

An Land dient der 57-jährige Wissenschaftler als Referatsleiter bei der Bundesanstalt für Geowissenschaften und Rohstoffe in Hannover, an Bord von „FS Sonne" präsidiert Hermann Kudrass einer bunt gemixten Truppe von Meeresforschern verschiedener Fachrichtungen.

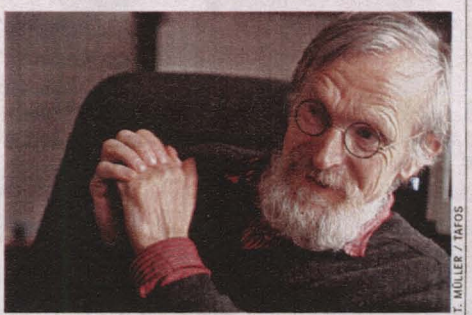

T. MÜLLER / TAFOS

Geologe Kudrass
„Schwund gibt es überall"

Sie schippern auf einem Gefährt, das 1969 als Fischtrawler die Werft verließ. 1977 ist die „Sonne" umgerüstet worden und gehört jetzt der Bremer RF-Reedereigemeinschaft Forschungsschiffahrt GmbH. In deren Flotte fahren auch weit modernere Bauten wie das Vorzeigeschiff „Meteor"; doch die „Sonne" ist mit ihrer vielseitigen Hightech-Ausrüstung auf Forschungsprojekte technisch wie personell spezialisiert und sehr gefragt. Gut ausgebucht, kreuzt sie zum Charterpreis zwischen 50 000 bis 60 000 Mark pro Tag zwischen Polarmeeren und Tropen.

In diesem Jahr fuhr „FS Sonne" mit Geologen, Chemikern und Biologen aus sechs deutschen Forschungsinstituten vor der südamerikanischen Westküste. Erkundet wurde das örtliche

* Bei Videobeobachtung des Meeresgrundes, bei Probenentnahme.

„Auftriebsgebiet", eine Meereszone besonderer Art.

Dass hier nährstoffreiches Tiefenwasser aus der Antarktis emporsteigt, beweisen schon die Horden von Pelikanen und Tölpeln, die sich auf Fischschwärme dicht unter den Wellen stürzen. In den tieferen Schichten fahnden seit langem ganze Flotten von Forschungsschiffen nach der eigenartigen Fauna und Flora. Meeresforscher lieben das Meer vor Peru mit seiner „3-D-Zone" („deep, dark and dirty") als lehrreichen Themenpark.

Ständig rieseln abgestorbene Kleinorganismen herab und schaffen riesige Flächen ohne Sauerstoff („Minimumzone"). Kaum erforschte Schwefelbakterien wie Thioploca, die vermutlich das im Wasser gelöste Kohlendioxid binden können, leben dort. Im Bodensediment türmen sich die Skelettreste von Mikrowesen zu Schichten voller Mineralien und Metallspuren, denn im Heruntersinken hatte das tote Plankton gelöste Wasserbestandteile „wie ein Staubtuch" (Kudrass) aufgesaugt.

Dann und wann schwebt durch die naturtrübe Todeszone eine Wolke aus sauerstoffhaltigem Wasser, Krebse und Fische wie ein wanderndes Aquarium umschließend.

Ganze Friedhöfe versteinerter Walknochen und millionenjähriger Riesenhaizähne gibt es, dazwischen die weißen Wiesen der Riesenbakterie Thioploca, die aus der Mikroskopwelt ihrer Verwandtschaft derart bizarr herausragt, dass es auch Meeresforscher anhaltend verblüfft. Diese Bakterienmasse kann bis zu einem Kilogramm pro Quadratmeter betragen. Geologe Andreas Lückge aus Hannover staunt: „Man kann sie mit der Hand herauspicken."

Neben lauter Wunderwesen bergen die Peru-Gewässer viel Nährstoff für Theorien und wissenschaftliche Spekulationen. Deshalb mögen Meeresgeologen Exkursionen hierher auch nicht als erdgeschichtlichen Museumsgang verkannt wissen.

Grundlagenforschung als teurer Spaß – Wolf-Christian Dullo, Direktor des Geomar-Instituts der Universität Kiel, weiß das zu begründen: Ohne Forschungsmittel keine Erfüllung der „tief im Herzen des Wissenschaftlers sitzenden lustgetriebenen Neugier" – und ergo auch keine Resultate im „angewandten Bereich".

Die Probe aufs Exempel bietet das Fahrgebiet vor Peru. Aus ihren Bodenproben erfahren die „Sonne"-Forscher die Zeitabstände, in denen der kalte Strom von der Antarktis nachlässt, das Meerwasser sich erwärmt und dadurch die Luft aufheizt. Dann stirbt unter dem Meeresspiegel das turbulente Ozeanleben ab und oben drüber nimmt „El Niño" Anlauf zu neuen, oft verheerenden Wetterexzessen.

Das Wüten dieses Klimaphänomens können die Leute auf der „FS Sonne" aus ihren Sedimentkernen buchstäblich riechen. Wie eine mehrere Meter lange Messlatte liegt der behutsam herausgelöste Inhalt der Sonde auf dem Labortisch und spiegelt die Abläufe von Zeit und von Naturprozessen: Stinkende dunkle Schichten aus zerfallenen Organismen markieren Abschnitte reichen Lebens.

Dann folgen alle paar Zentimeter geruchlose und auffallend helle Streifen. Das ist ein Sand-Ton-Gemisch, das besagt: In dieser Phase hat „El Niño" das Meer aufgewärmt und verödet, gleichzeitig Regenfluten an Land verursacht und zermahlenes Geröll in die See gespült.

Niño-Zeiten, wie sie in den letzten Jahren Perus Behelfssiedlungen in Schlammwüsten verwandelten und die Menschen mit Erdrutschen bedrohten, quälten die Bewohner der südamerikanischen Westküste schon immer. Wahrscheinlich ließen die Unwetterphasen im Lauf der Geschichte ganze Völker untergehen, beispielsweise die im achten Jahrhundert nach Christus praktisch über Nacht verschwundene Vor-Inka-Kultur der Moche. In Bohrkernen deuten „mächtige graue Tonschichten" (Kudrass) auf extreme Niederschläge in jenem Zeitraum, als die Moche-Kultur ausgelöscht wurde.

BGR

D. STEINMANN / BGR

Bakterien, „Thioploca"-Kolonie*
Wie Seegras am Meeresgrund

„Die Meeresgegend ist ein gutes Archiv", erläutert Geomar-Chef Dullo. Schließlich sind hier auch solche erdgeschichtlichen Rückgriffe, die ein paar Millionen Jahre umspannen, voll überraschender Aspekte für die Gegenwart. Womöglich gibt die „schneebedeckte Welt" (Dullo) der Bakterienwälder, die sich 2700 Kilometer weit die Pazifikküste entlangziehen, sogar Hinweise auf bisher unbekannte Entstehungsweisen – und Lagerstätten – von Erdöl wie Methan.

Deren Hauptbestandteil Kohlenstoff bildet sich aus einem ständigen chemischen Veränderungsprozess der Biomasse – ein Vorgang, „der sich immer so am Sterbepunkt entlangmogeln muss" (Dullo): Eine Spur zu schnell, und die Kohlenstoffproduktion erstickt im Organismenregen wie im Bodenschlamm eines Gartenteichs. Die Verwertungsgesellschaft der Kleinstorganismen auf dem Meeresgrund braucht jeweils so viel Nachschub, dass sie gerade noch am Leben bleibt.

Dieser für die Meere lebenswichtige und für das Entstehen der fossilen Energiereserven einst ausschlaggebende Prozess lässt sich im jüngsten Kreuzungsgebiet des Forschungsschiffes gut studieren.

Auf dem Achterdeck stapelt Wissenschaftler Andreas Lückge große Platten aus schwärzlichem Phosphorit. Womöglich, vermutet er, ist das glasierte Gemenge aus versteinerten Walknochen, Haizähnen und Muschelvölkern ein „Vorläufer der klassischen Muttergesteine", die den Ort von Öl- und Gaslagern anzeigen können.

Auf dem peruanischen Schelf hat er Parallelen zum Ölgebiet an Kaliforniens Küste festgestellt, wo einst auch eine Auftriebszone gewesen sein könnte. Darauf lassen ein paar Ähnlichkeiten schließen – bei den Rückständen winziger Pflanzen und Tiere, beim hohen Kohlenstoffgehalt, bei der Menge an Schwefelbakterien.

Und Öl? Noch liegt Thioplocas kolossaler Bakterienteppich höchst geheimnisvoll über den Schichten des Sediments. Aber, fragt Geologe Lückge, „wer weiß, was inzwischen da unten abgeht"? CHRISTIAN HABBE

Meeresforscher, Baggergut vom Küstenschelf: *„Man kann sie mit der Hand herauspicken"*

T. MÜLLER / TAFOS

* Auf dem Meeresgrund, bei der Vermessung.

Document Control Sheet

1. ISBN or ISSN	2. Type of Report cruise report
3a. Report Title Peru Uwelling, Cruise Report , SONNE Cruise SO 147	
3b. Title of Publication	
4a. Author(s) of the Report (Family Name, First Name(s)) Kudrass, H. R., et al	5. End of Project 30.06.2002
	6. Publication Date December 2000
4b. Author(s) of the Publication (Family Name, First Name(s))	7. Form of Publication
8. Performing Organization(s) (Name, Address) Federal Institute for Geosciences and Natural Resources, Stilleweg 2, 30655 Hannover	9. Originator´s Report No. Archiv Nr.: 0120607
	10. Reference No. 03G0147A
	11a. No. of Pages Report
	11b. No. of Pages Publication
13. Sponsoring Agency (Name, Address) Bundesministerium für Bildung, Wissenschaft, Forschung und Technologie (BMBF) 53170 Bonn	12. No. of References
	14. No. of Tables 21
	15. No. of Figures 120
16. Supplementary Notes	
17. Presented at (Title, Place, Date)	

18. Abstract

The PERU UPWELLING project (PERU AUFTRIEB) consists of interfaced subprojects which are supported and carried out by six partners (BGR/Hannover, GEOMAR/Kiel, IfG/Mainz, ICBM/Oldenburg, MPI Mikrobiologie/Bremen, INI/Rostock). The combined multidisciplinary approach aims to establish a comprehensive model of the microbiological, sedimentary, and geochemical processes forming the sediments of the high-productivity zone of the Peru upwelling.

The SONNE expedition started at the 29 of May 2000 in Valparaiso/Chile and ended at the 3 of July 2000 in Callao/Peru. The investigations on the shelf and upper slope off central Peru focussed on the bacterial controlled geochemical processes at the oxic/anoxic water-sediment-interface, on the early diagenetic modification of the organic material and on the fluxes of methane, sulphur, and phosphor. The understanding of the presently active processes and the resulting sedimentary products will be used to interpret the variations of the sedimentary upwelling record during the Last Glacial and the Holocene. Especially, the El-Nino variability will be traced in different time intervals using seismic, sedimentological, geochemical and micropaleontological methods. The terrigenous input related to extreme La-Nina conditions will be used to correlate the marine record with the continental climatic variation.

The new echosounders from the University Rostock were used to survey 6000 km-long profiles. 143 appropriate sites chosen on the online processed seismic records were sampled by piston and gravity corers, multicorer and the TV-guided hydraulic grab. The 35 coring stations yielded a total length of 155 m. Off Callao a 19 m-long core consists of laminated diatomeous ooze. 700 samples of porewater were recovered and immediately analysed. Phosphoritic crusts mainly occur at the exposed discordance of the broad shelf off Chimbote.

19. Keywords

Peru, upwelling, paleoceanography, Holocene, phosphorite

20. Publisher BGR	21. Price

Berichtsblatt

1. ISBN or ISSN	2. Berichtsart Fahrtbericht

3a. Titel des Berichts
Peru-Auftrieb, SONNE-Fahrt SO147 -Fahrtbericht -

3b. Titel der Publikation

4a. Autoren des Berichts (Name, Vorname(n))
Kudrass, H.R. et al.

4b. Autoren der Publikation (Name, Vorname(n))

8. Durchführende Institution(en) (Name, Adresse)
Bundesanstalt für Geowissenschaften und Rohstoffe, Stilleweg 2, 30655 Hannover

13. Fördernde Institution (Name, Adresse)
Bundesministerium für Bildung, Wissenschaft, Forschung und Technologie (BMBF)

53170 Bonn

5. Abschlußdatum des Vorhabens	30.06.2002
6. Veröffentlichungsdatum	Dezember 2000
7. Form der Publikation	Broschüre
9. Ber.Nr. Durchführende Institution	Archiv Nr.: 0120607
10. Förderkennzeichen *)	03G0147A
11a. Seitenzahl Bericht	120
11b. Seitenzahl Publikation	
12. Literaturangaben	
14. Tabellen	21
15. Abbildungen	120

16. Zusätzliche Angaben

17. Vorgelegt bei (Titel, Ort, Datum)

18. Kurzfassung
Das Projekt Peru-Auftrieb besteht aus Teilprojekten mehrerer mariner Forschungsgruppen (BGR/Hannover, Geomar/Kiel, IfG/Mainz, INI/Rostock, ICBM/Oldenburg, MPI Mikrobiologie/Bremen), die über vielfältige methodische Ansätze eng miteinander verbunden sind. Die multidisziplinären Untersuchungen ergänzen sich so, dass ein umfassendes Bild der Variabilität des Auftriebs vor Peru in Zeit und Raum erarbeitet werden kann. Der Schwerpunkt der gemeinsamen Untersuchungen zielt darauf ab, die bakteriell gesteuerten geochemischen Prozesse in der anoxisch/suboxischen Wasser-Sediment-Grenzschicht zu verstehen, den Abbau und die Veränderung der organischen Substanzen zu untersuchen, die daraus resultierenden Flüsse von Methan, Schwefel und Phosphat unter in-situ Bedingungen und Langzeitexperimenten zu erfassen.
Die Kenntnis der rezenten Auftriebsprozesse und deren Auswirkungen auf das Sediment, wird es in einem zweiten Schritt erlauben, die zeitliche und räumliche Variabilität des Auftriebs seit dem letzten Hochglazial paläoklimatisch zu deuten. Dabei soll der multi-disziplinäre Ansatz mit seismischen, sedimentologischen, geochemischen und mikropaläontologischen Methoden dazu dienen, eine möglichst hoch aufgelöste Zeitreihe der Akkumulationsmuster, des terrigenen Eintrages, der Fixierung von Corg, Opal, Karbonat und Phosphat zu erhalten, um letztlich zu rekonstruieren, wie der Auftrieb vor Peru auf global klimatische Veränderungen reagiert hat .
Die Fahrt begann am 29.Mai 2000 in Valparaiso/Chile und endete am 3.Juli in Callao/Peru. Insgesamt 6000 km wurden mit den neuen Sedimentecholoten der Universität Rostock vermessen. Auf 143 Stationen konnten Sedimentproben mit Multicorer, Kastenlot, Kolbenlot und dem TV-kontrollierten Hydraulikgreifer gewonnen werden. Aus 155 insgesamt gewonnenen Kernmetern wurden über 700 Porenwasserproben an Bord abgepreßt und analysiert. Die Bakterienbesiedlung in der Sauerstoffminimum-Zone wurde bestimmt, quantifiziert und in Experimenten untersucht.

19. Schlagwörter
Peru, Auftrieb, Bakterien, Holozän, Phosphorit, Paläoozeanographie, El Nino

20. Verlag	21. Preis
BGR	

*) Auf das Förderkennzeichen des BMBF soll auch in der Veröffentlichung hingewiesen werden.